

New York State Energy Research and Development Authority

---

# Use of Waste and CO<sub>2</sub> Compression Heat to Reduce Penalty Due to Post-Combustion CO<sub>2</sub> Capture

Final Report  
March 2012

No. 12-11

# NYSERDA's Promise to New Yorkers:

New Yorkers can count on NYSERDA for objective, reliable, energy-related solutions delivered by accessible, dedicated professionals.

**Our Mission:** Advance innovative energy solutions in ways that improve New York's economy and environment.

**Our Vision:** Serve as a catalyst—advancing energy innovation and technology, transforming New York's economy, and empowering people to choose clean and efficient energy as part of their everyday lives.

**Our Core Values:** Objectivity, integrity, public service, and innovation.

## Our Portfolios

NYSERDA programs are organized into five portfolios, each representing a complementary group of offerings with common areas of energy-related focus and objectives.

### Energy Efficiency & Renewable Programs

Helping New York to achieve its aggressive clean energy goals – including programs for consumers (commercial, municipal, institutional, industrial, residential, and transportation), renewable power suppliers, and programs designed to support market transformation.

### Energy Technology Innovation & Business Development

Helping to stimulate a vibrant innovation ecosystem and a clean energy economy in New York – including programs to support product research, development, and demonstrations, clean-energy business development, and the knowledge-based community at the Saratoga Technology + Energy Park®.

### Energy Education and Workforce Development

Helping to build a generation of New Yorkers ready to lead and work in a clean energy economy – including consumer behavior, youth education, and workforce development and training programs for existing and emerging technologies.

### Energy and the Environment

Helping to assess and mitigate the environmental impacts of energy production and use – including environmental research and development, regional initiatives to improve environmental sustainability, and West Valley Site Management.

### Energy Data, Planning and Policy

Helping to ensure that policy-makers and consumers have objective and reliable information to make informed energy decisions – including State Energy Planning, policy analysis to support the Regional Greenhouse Gas Initiative, and other energy initiatives; and a range of energy data reporting including *Patterns and Trends*.

**USE OF WASTE AND CO<sub>2</sub> COMPRESSION HEAT TO  
REDUCE PENALTY DUE TO POST-COMBUSTION CO<sub>2</sub> CAPTURE**

Final Report

Prepared for the  
**NEW YORK STATE  
ENERGY RESEARCH AND  
DEVELOPMENT AUTHORITY**



Albany, NY  
[nyserda.ny.gov](http://nyserda.ny.gov)

Barry N. Liebowitz  
Senior Project Manager, Environmental Research

Prepared by:

**ENERGY RESEARCH CENTER**  
Nenad Sarunac  
Carlos E. Romero

and

**AES EASTERN ENERGY, L.P.**  
Thomas Jesikiewicz

## **NOTICE**

This report was prepared by the Energy Research Center in the course of performing work contracted for and sponsored by the New York State Energy Research and Development Authority (hereafter the “Sponsor”). The opinions expressed in this report do not necessarily reflect those of the Sponsor or the State of New York, and reference to any specific product, service, process, or method does not constitute an implied or expressed recommendation or endorsement of it. Further, the Sponsor and the State of New York, make no warranties or expressions, expressed or implied, as to the fitness for particulate purpose or merchantability of any product, apparatus, or service, or the usefulness, completeness, or accuracy of any process, methods, or other information contained, described, disclosed, or reflected to in this report. The Sponsor, the State of New York, and the contractor make no representation that the use of any product, apparatus, process, method or any information will not infringe privately owned rights and will assume no liability for any loss, injury, or damage resulting from, or occurring in connection with, the use of information contained, described, disclosed, or referred to in this report.

## ABSTRACT

This project was performed with funding from the New York State Energy Research and Development Authority to determine efficiency improvements that could be achieved for existing coal-fired power plants electing to adopt partial post-combustion CO<sub>2</sub> capture for carbon sequestration through thermal and cycle integration. Reduction of performance and capacity penalties that would be incurred by the retrofit or implementation of the mono-ethanol amine (MEA) post-combustion CO<sub>2</sub> capture technology was the main goal of the study. Optimization of the CO<sub>2</sub> capture process was performed to minimize performance penalties associated with the process. Thermal integration options analyzed in the study included thermal integration of the CO<sub>2</sub> capture process and turbine cycle with the boiler and CO<sub>2</sub> compression train, and integration of the Rankine and Brayton cycles. Analysis was performed by assuming 90% CO<sub>2</sub> capture. Economic analysis, i.e. implementation cost of various thermal integration options was outside of the project scope.

A model of the CO<sub>2</sub> capture process was developed and used to optimize operating parameters of the process. A model of the Rankine cycle and heat exchange equipment needed for thermal integration was developed and used to determine effects of various thermal integration options on plant performance and capacity. The model was expanded to include the Brayton cycle and determine effects of cycle integration.

The results of the study show that thermal integration and use of heat recovered from the flue gas and CO<sub>2</sub> compression could offset part of the performance and capacity penalty associated with the retrofit or implementation of the post-combustion CO<sub>2</sub> capture technology. It is recommended that thermal integration be applied at existing power plants to allow their operation in a carbon-constrained world. Thermal integration needs to be incorporated into design of the newly built power plants as well.

Cycle integration has a significant positive effect on performance and capacity. Capacity losses could be eliminated and performance losses halved if hydrogen-fueled and biogas-fueled Brayton cycles were considered. The cost of this option is significantly higher compared to the thermal integration, but lower compared to a Greenfield (newly built) combined cycle.

In addition to analyzing thermal integration options based on 90% CO<sub>2</sub> capture: partial CO<sub>2</sub> capture, involving treatment of 20 to 100% of the flue gas leaving the plant; and modular design of the CO<sub>2</sub> scrubbing systems was also investigated. Partial CO<sub>2</sub> capture could be the first step toward reducing CO<sub>2</sub> emissions from existing power plants expected to speed up deployment of the post-combustion CO<sub>2</sub> capture because of lower initial capital investment and associated risk. Partial capture could, also, be implemented at smaller power plants to reduce CO<sub>2</sub> emissions with a moderate loss of performance and capacity.

The authors hope that project results will advance use of innovative strategies to improve plant performance and reduce CO<sub>2</sub> emissions, and support early implementation of CO<sub>2</sub> reduction technologies at coal-fired power plants. The adoption of these innovative strategies will help improve ambient air quality and foster business and technology development in the New York State.

Keywords: CO<sub>2</sub> Emissions, Post-Combustion CO<sub>2</sub> Capture, Thermal Integration, Partial CO<sub>2</sub> Capture

## TABLE OF CONTENTS

<u>Section</u>	<u>Page</u>
SUMMARY .....	S-1
BACKGROUND.....	S-1
PROJECT RESULTS.....	S-2
1 INTRODUCTION .....	1-1
PROJECT GOALS.....	1-2
PROJECT OBJECTIVES .....	1-3
2 DESCRIPTION OF THE HOST UNIT .....	2-1
3 TECHNICAL APPROACH FOR CYCLE MODELING .....	3-1
4 POST-COMBUSTION CO <sub>2</sub> CAPTURE.....	4-1
Mono-Ethanol-Amine (MEA) -BASED CO <sub>2</sub> CAPTURE SYSTEM.....	4-2
CONVENTIONAL THERMAL INTEGRATION OF POST-COMBUSTION CO <sub>2</sub> CAPTURE PROCESS.....	4-3
ADVANCED THERMAL INTEGRATION OF POST-COMBUSTION CO <sub>2</sub> CAPTURE PROCESS.....	4-9
5 POST-COMBUSTION CO <sub>2</sub> CAPTURE AND PROCESS MODELING.....	5-1
STATUS OF DEVELOPMENT .....	5-1
MEA PROCESS MODELING .....	5-2
PARAMETRIC STUDY – DESIGN OPTIMIZATION.....	5-6
6 BOILER-TURBINE CYCLE INTEGRATION .....	6-1
OPTIMAL USE OF HEAT RECOVERED FROM THE FLUE GAS .....	6-2
7 THERMAL INTEGRATION OF THE CO <sub>2</sub> STRIPPER WITH PLANT HEAT SOURCES.....	7-1
THERMAL INTEGRATION OF THE TURBINE CYCLE WITH PLANT HEAT SOURCES AND CO <sub>2</sub> COMPRESSION HEAT.....	7-1
THERMAL INTEGRATION OF THE CO <sub>2</sub> STRIPPER AND TURBINE CYCLE WITH PLANT HEAT SOURCES AND COMPRESSION HEAT .....	7-7

8	PARTIAL CO <sub>2</sub> CAPTURE .....	8-1
9	RANKINE-BRAYTON CYCLE INTEGRATION.....	9-1
	HYDROGEN-FUELED BRAYTON CYCLE .....	9-3
	Rankine Cycle.....	9-5
	Combined Cycle .....	9-8
	BIOMASS GASIFICATION SYNGAS-FUELED BRAYTON CYCLE.....	9-12
	Rankine Cycle.....	9-14
	Combined Cycle .....	9-17
10	CONCLUSIONS AND RECOMMENDATIONS .....	10-1
	GENERAL.....	10-1
	BOILER-TURBINE CYCLE INTEGRATION.....	10-2
	OPTIMIZATION OF MEA-BASED POST-COMBUSTION CO <sub>2</sub> CAPTURE PROCESS.....	10-2
	THERMAL INTEGRATION OF THE TURBINE CYCLE AND CO <sub>2</sub> STRIPPER	
	WITH PLANT HEAT SOURCES .....	10-4
	PARTIAL CO <sub>2</sub> CAPTURE.....	10-5
	RANKINE-BRAYTON CYCLE INTEGRATION .....	10-6
11	REFERENCES .....	11-1
	APPENDIX A: OPTIMAL USE OF HEAT RECOVERED FROM THE FLUE GAS .....	A-1
	STEAM AIR PREHEATING (SAH).....	A-2
	ADVANCED AIR PREHEATING.....	A-5
	ADVANCED AIR PREHEATING AND FEEDWATER HEATING .....	A-8
	COMPARISON OF STEAM AIR PREHEATING, AND ADVANCED AIR PREHEATING	
	WITH OR WITHOUT FEEDWATER HEATING .....	A-12
	APPENDIX B: CO <sub>2</sub> COMPRESSION AND COMPRESSION HEAT .....	B-1
	APPENDIX C: THERMAL INTEGRATION OF THE TURBINE CYCLE AND CO <sub>2</sub> STRIPPER	
	WITH PLANT HEAT SOURCES: RESULTS .....	C-1

## LIST OF FIGURES

<u>Figure</u>		<u>Page</u>
2-1	Side Elevation of Somerset Unit 1 .....	2-2
2-2	Schematic Diagram of Boiler and Turbine Cycle: Somerset Unit 1. ....	2-5
2-3	Heat Balance Diagram of Steam Turbine Cycle: Somerset Unit 1. ....	2-5
3-1	PEPSE Model of Turbine Cycle: Somerset Unit 1.....	3-2
3-2	Spreadsheet-Based Mass and Energy Balance Model of Somerset Unit 1: Detail.....	3-3
4-1	Schematic Diagram of a Typical Post-Combustion Capture System. ....	4-1
4-2	Conventional Thermal Integration of the Post-Combustion CO <sub>2</sub> Capture Process. ....	4-4
4-3	Reduction in Total Gross Power Output due to Conventional CO <sub>2</sub> Capture Relative to Baseline.....	4-6
4-4	Steam Extraction for the Reboiler and LP Turbine Exhaust Flow as Functions of Reboiler Thermal Duty. ....	4-6
4-5	Increase in Turbine Cycle Heat Rate due to Conventional CO <sub>2</sub> Capture Relative to Baseline.....	4-7
4-6	Decrease in Turbine Cycle Efficiency due to Conventional CO <sub>2</sub> Capture Relative to Baseline.....	4-8
4-7	Increase in Net Unit Heat Rate due to Conventional CO <sub>2</sub> Capture Relative to Baseline. ....	4-8
4-8	Decrease in Net Unit Heat Rate due to Conventional CO <sub>2</sub> Capture Relative to Baseline.....	4-9
4-9	Advanced Thermal Integration of Post-Combustion CO <sub>2</sub> Capture Process. ....	4-10
4-10	Steam Extraction for the Deaerator: Conventional and Advanced Thermal Integration....	4-11
4-11	Increase in Total Gross Power Output Relative to Baseline. ....	4-12
4-12	Increase in Turbine Cycle Heat Rate Relative to Baseline.....	4-13
4-13	Improvement in Turbine Cycle Efficiency Relative to Baseline.....	4-13
4-14	Increase in Net Unit Heat Rate Relative to Baseline.....	4-14
4-15	Decrease in Net Unit Efficiency Relative to Baseline.....	4-14
5-1	ASPEN Model Diagram of the MEA-CO <sub>2</sub> Capture System. ....	5-5
5-2	Effect of Stripper Pressure on Reboiler Duty.....	5-7
5-3	Effect of Solvent Mass Flow on Reboiler Duty. ....	5-8
5-4	Effect of MEA Concentration in Solvent on Reboiler Duty. ....	5-9
5-5	Effect of CO <sub>2</sub> Removal on Reboiler Duty.....	5-10
5-6	Effect of Absorber Inlet Flue Gas Temperature on Reboiler Duty. ....	5-11
5-7	Effect of CO <sub>2</sub> Concentration in the Flue Gas on Reboiler Duty and Thermal Energy.....	5-12
5-8	Effect of Flue Gas Flow Rate on Reboiler Duty. ....	5-12
6-1	Schematic Representation of Air Preheating and Condensate Heating.....	6-3
6-2	Change in Turbine Cycle Heat Rate: SAH Air Preheating, Advanced Air Preheating, and Advanced Air Preheating Combined with the Condensate Heating .....	6-4

6-3	Change in Net Unit Heat Rate: SAH Air Preheating, Advanced Air Preheating, and Advanced Air Preheating Combined with the Condensate Heating.....	6-5
6-4	Optimal Use of Heat Recovered From the Flue Gas.....	6-6
7-1	Advanced Thermal Integration of Post-Combustion CO <sub>2</sub> Capture: Modification A.....	7-2
7-2	Advanced Thermal Integration of Post-Combustion CO <sub>2</sub> Capture: Modifications B. ....	7-4
7-3	Advanced Thermal Integration of Post-Combustion CO <sub>2</sub> Capture: Modification C.....	7-6
7-4	Advanced Thermal Integration of Post-Combustion CO <sub>2</sub> Capture: Modification D.....	7-9
7-5	Advanced Thermal Integration of Post-Combustion CO <sub>2</sub> Capture: Modification E. ....	7-11
7-6	Advanced Thermal Integration of Post-Combustion CO <sub>2</sub> Capture: Modification F. ....	7-12
7-7	Reduction in Gross Power Output Relative to Baseline (no CO <sub>2</sub> capture) vs. q <sub>Reb</sub> .....	7-14
7-8	Improvement in Gross Power Output Relative to Conventional Thermal Integration vs. q <sub>Reb</sub> .....	7-14
7-9	Decrease in Net Unit Efficiency Relative to Baseline vs. q <sub>Reb</sub> .....	7-15
7-10	Improvement in Net Unit Efficiency Relative to Conventional Thermal Integration vs. q <sub>Reb</sub> .....	7-16
8-1	Reboiler Steam Flow as a Function of Percentage of CO <sub>2</sub> Capture. ....	8-2
8-2	LP Turbine Inlet Steam Flow as a Function of Percentage of CO <sub>2</sub> Capture. ....	8-2
8-3	Improvement in Gross Power Output as a Function of Percentage of CO <sub>2</sub> Capture and q <sub>Reb</sub> .....	8-3
8-4	Improvement in Gross Power Output as a Function of Percentage of CO <sub>2</sub> Capture. ....	8-4
8-5	Improvement in Turbine Cycle Heat Rate as a Function of Percentage of CO <sub>2</sub> Capture. ....	8-4
8-6	Improvement in Turbine Cycle Efficiency as a Function of Percentage of CO <sub>2</sub> Capture. ....	8-5
8-7	Improvement in Net Unit Heat Rate as a Function of Percentage of CO <sub>2</sub> Capture.....	8-6
8-8	Improvement in Net Unit Efficiency as a Function of Percentage of CO <sub>2</sub> Capture. ....	8-6
9-1	Thermal Integration of Rankine and Brayton Cycles.....	9-2
9-2	Increase in Combined Cycle Heat Rate Relative to the Case Where Full HRSG Thermal Duty is Supplied to the HP FWH.....	9-3
9-3	Reduction in Power Output of the Rankine Cycle Relative to the Baseline (no CO <sub>2</sub> capture) as Function of q <sub>Reb</sub> , Cycle Integration, and Thermal Integration of the Post-Combustion MEA CO <sub>2</sub> Capture. ....	9-6
9-4	Improvement in Power Output of the Rankine Cycle Relative to the Conventional MEA as Function of q <sub>Reb</sub> , Cycle Integration, and Thermal Integration of the Post-Combustion MEA CO <sub>2</sub> Capture. ....	9-6
9-5	Decrease in Net Efficiency of the Rankine Cycle Relative to the Baseline (no CO <sub>2</sub> capture) as Function of q <sub>Reb</sub> , Cycle Integration, and Thermal Integration of the Post-Combustion MEA CO <sub>2</sub> Capture.....	9-7
9-6	Improvement in Net Efficiency of the Rankine Cycle Relative to the Conventional MEA as Function of q <sub>Reb</sub> , Cycle Integration, and Thermal Integration of the Post-Combustion MEA CO <sub>2</sub> Capture. ....	9-7
9-7	Change in Power Output of the Combined Cycle Relative to the Baseline (no CO <sub>2</sub> capture) Without Cycle Integration as Function of q <sub>Reb</sub> , Cycle Integration, and Thermal Integration of the Post-Combustion MEA CO <sub>2</sub> Capture. ....	9-8

9-8	Improvement in Power Output of the Combined Cycle Relative to the Conventional MEA Without Cycle Integration as Function of $q_{reb}$ , Cycle Integration, and Thermal Integration of the Post-Combustion MEA CO <sub>2</sub> Capture. ....	9-9
9-9	Decrease in Net Unit Efficiency of the Combined Cycle Relative to the Baseline (no CO <sub>2</sub> capture) Without Cycle Integration as Function of $q_{reb}$ , Cycle Integration, and Thermal Integration of the Post-Combustion MEA CO <sub>2</sub> Capture. ....	9-10
9-10	Improvement in Net Unit Efficiency of the Combined Cycle Relative to the Conventional MEA Without Cycle Integration as Function of $q_{reb}$ , Cycle Integration, and Thermal Integration of the Post-Combustion MEA CO <sub>2</sub> Capture. ....	9-11
9-11	Schematic of Rankine and Biomass-Fueled Brayton Cycles: Advanced MEA Integration. ....	9-13
9-12	Reduction in Power Output of the Rankine Cycle Relative to the Baseline(No CO <sub>2</sub> Capture, No Cycle Integration) as Function of $Q_{reb}$ , Cycle Integration, and Thermal Integration of the Post-Combustion MEA CO <sub>2</sub> Capture. ....	9-15
9-13	Improvement in Power Output of the Rankine Cycle Relative to the Conventional MEA as Function of $q_{reb}$ , Cycle Integration, and Integration of the Post Combustion MEA CO <sub>2</sub> Capture. ....	9-15
9-14	Decrease in Net Efficiency of the Rankine Cycle Relative to the Baseline (no CO <sub>2</sub> capture) as Function of $q_{reb}$ , Cycle Integration, and Thermal Integration of the Post-Combustion MEA CO <sub>2</sub> Capture. ....	9-16
9-15	Improvement in Net Efficiency of the Rankine Cycle Relative to the Conventional MEA as Function of $q_{reb}$ , Cycle Integration, and Thermal Integration of the Post-Combustion MEA CO <sub>2</sub> Capture. ....	9-17
9-16	Change in Power Output of the Combined Cycle Relative to the Baseline (no CO <sub>2</sub> capture, no cycle integration) as Function of $q_{reb}$ , Cycle Integration, and Thermal Integration of the Post-Combustion MEA CO <sub>2</sub> Capture.....	9-18
9-17	Improvement in Power Output of the Combined Cycle Relative to the Conventional MEA Without Cycle Integration as Function of $q_{reb}$ , Cycle Integration, and Thermal Integration of the Post-Combustion MEA CO <sub>2</sub> Capture.....	9-18
9-18	Decrease in Net Unit Efficiency of the Combined Cycle Relative to the Baseline (no CO <sub>2</sub> capture, no cycle integration) as Function of $q_{reb}$ , Cycle Integration, and Thermal Integration of the Post-Combustion MEA CO <sub>2</sub> Capture.....	9-19
9-19	Improvement in Net Unit Efficiency of the Combined Cycle Relative to the Conventional MEA Without Cycle Integration as Function of $q_{reb}$ , Cycle Integration, and Thermal Integration of the Post-Combustion MEA CO <sub>2</sub> Capture. ....	9-20
10-1	Optimal Use of Heat Recovered From the Flue Gas.....	10-2
A-1	Schematic Representation of Air Preheating and Condensate Heating.....	A-3
A-2	Total Heat Input to the SAH. ....	A-4
A-3	Change in Turbine Cycle Heat Rate Due to Steam Extraction for SAH. ....	A-5
A-4	Change in Net Unit Heat Rate Due to Steam Extraction for SAH. ....	A-5
A-5	Change in Boiler Efficiency due to Air Preheating by SAH. ....	A-6
A-6	Heat Transferred to Combustion Air by the FGC <sub>APH</sub> . ....	A-7
A-7	Temperature of the Flue Gas Leaving the FGC <sub>APH</sub> . ....	A-8
A-8	Change in Net Unit Heat Rate Due to Heat Recovery from Flue Gas for Air Preheating.....	A-8
A-9	Change in Boiler Efficiency Due to Advanced Air Preheating.....	A-9

A-10	Effect of External Heat Input to the LP Feedwater Heaters on Turbine Cycle Heat Rate. ...A-10
A-11	Heat Recovered from Flue Gas Available for LP Feedwater Heaters.....A-11
A-12	Change in Turbine Cycle Heat Rate: Advanced Air Preheating and Condensate Flow Heating.....A-11
A-13	Change in Net Unit Heat Rate: Advanced Air Preheating and Condensate Flow Heating. A-12
A-14	Change in Boiler Efficiency: Advanced Air Preheating and Condensate Flow Heating. ...A-13
A-15	Change in Turbine Cycle Heat Rate: SAH, Advanced Air Preheating, and Advanced Air Preheating Combined with Condensate Flow Heating. ....A-14
A-16	Change in Net Unit Heat Rate: SAH Air Preheating, Advanced Air Preheating, and Advanced Air Preheating Combined with Condensate Flow Heating. ....A-15
A-17	Optimal Use of Heat Recovered from the Flue Gas.....A-16
A-18	Change in Boiler Efficiency: SAH Air Preheating, Advanced Air Preheating, and Advanced Air Preheating Combined with Condensate Flow Heating. ....A-17
B-1	Schematic Representation of Heat Recovery from a Three-Stage Inline CO <sub>2</sub> Compressor. ...B-2
B-2	$\kappa$ as a Function of Gas Temperature: Carbon Dioxide.....B-3
B-3	Schematic Representation of Heat Recovery for Condensate Heating From a Two-Stage Ramgen CO <sub>2</sub> Compressor. ....B-3
B-4	Schematic Representation of Heat Recovery for Solvent Regeneration and Condensate Heating from a Two-Stage Ramgen CO <sub>2</sub> Compressor.....B-5
C-1	Reduction in Gross Power Output Relative to Baseline (no CO <sub>2</sub> capture) vs. $q_{Reb}$ .....C-1
C-2	Improvement in Gross Power Output Relative to Conventional Thermal Integration vs. $q_{Reb}$ .....C-2
C-3	Increase in Turbine Cycle Heat Rate Relative to Baseline vs. $q_{Reb}$ .....C-3
C-4	Improvement in Turbine Cycle Heat Rate Relative to Conventional Thermal Integration vs. $q_{Reb}$ .....C-4
C-5	Decrease in Turbine Cycle Efficiency Relative to Baseline(no CO <sub>2</sub> capture) vs. $q_{Reb}$ .....C-5
C-6	Improvement in Turbine Cycle Efficiency Relative to Conventional Thermal Integration vs. $q_{Reb}$ . ....C-6
C-7	Increase in Net Unit Heat Rate Relative to Baseline (no CO <sub>2</sub> capture) vs. $q_{Reb}$ . ....C-7
C-8	Improvement in Net Unit Heat Rate Relative to Conventional Thermal Integration vs. $q_{Reb}$ .....C-8
C-9	Decrease in Net Unit Efficiency Relative to Baseline vs. $q_{Reb}$ .....C-9
C-10	Improvement in Net Unit Efficiency Relative to Conventional Thermal Integration vs. $q_{Reb}$ .....C-10

## LIST OF TABLES

<u>Table</u>		<u>Page</u>
2-1	Average Composition and HHV: Pittsburgh No. 8.....	2-1
3-1	Comparison of Predicted and Design Turbine Cycle Performance: Somerset Unit 1.....	3-1
4-1	Values of Reboiler Thermal Duty Used in the Analysis. ....	4-5
5-1	Flue Gas Conditions and Composition.....	5-3
5-2	Optimal and Worst MEA System Operating Points.....	5-13
7-1	Condensate Flow to LP FWH, Sensible Heat Recovered from Flue Gas, Condensate Temperature Leaving BP HXE, and Bypassed LP FWHs as Functions of Reboiler Thermal Duty: Modification A.....	7-3
7-2	Condensate Flow Entering LP FWH, Condensate Temperature Leaving BP HXE, and Bypassed LP FWHs as Functions of Reboiler Thermal Duty: Modification B – Inline CO <sub>2</sub> Compressor. ....	7-5
7-3	Condensate Flow Entering LP FWH, Condensate Temperature Leaving BP HXE, and Bypassed LP FWHs as Functions of Reboiler Thermal Duty: Modification B-R – Ramgen CO <sub>2</sub> Compressor. ....	7-5
7-4	Condensate Flow Entering LP FWH, Condensate Temperature Leaving BP HXE 1 and 2, and Bypassed LP FWHs as Functions of Reboiler Thermal Duty: Modification C – Inline CO <sub>2</sub> Compressor. ....	7-7
7-5	Condensate Flow Entering LP FWH, Condensate Temperature Leaving BP HXE 1 and 2, and Bypassed LP FWHs as Functions of Reboiler Thermal Duty: Modification C-R – Ramgen CO <sub>2</sub> Compressor.....	7-7
7-6	Condensate Flow Entering LP FWH, Condensate Temperature Leaving the BP HXE and Bypassed LP FWHs as Functions of Reboiler Thermal Duty: Modification D – Inline CO <sub>2</sub> Compressor. ....	7-8
7-7	Condensate Flow Entering LP FWH, Condensate Temperature Leaving the BP HXE, and Bypassed LP FWHs as Functions of Reboiler Thermal Duty: Modification E – Ramgen CO <sub>2</sub> Compressor. ....	7-10
7-8	Condensate Flow Entering LP FWH, Condensate Temperature Leaving BP HXE and Bypassed LP FWHs as Functions of Reboiler Thermal Duty: Modification F – Ramgen CO <sub>2</sub> Compressor. ....	7-13
7-9	Basic Features of Analyzed Thermal Integrations Options.....	7-16
7-10	Effect of Thermal Integration on Unit Performance: State-of-the-Art Amines.....	7-17
9-1	Rankine-Brayton Cycle Integration: Hydrogen-Fired Turbine, FWHs A and B.....	9-10
9-2	Rankine-Brayton Cycle Integration: Hydrogen-Fired Turbine, FWH A.....	9-11
9-3	Rankine-Brayton Cycle Integration: Biogas-Fired Turbine. ....	9-20
10-1	Optimal and Worst MEA System Operating Points.....	10-3
10-2	Basic Features of Analyzed Thermal Integrations Options.....	10-4
10-3	Effect of Thermal Integration on Unit Performance: State-of-the-art amines.....	10-5
10-4	Rankine-Brayton Cycle Integration: Hydrogen-Fired Turbine, FWHs A and B.....	10-7
10-5	Rankine-Brayton Cycle Integration: Hydrogen-Fired Turbine, FWH A.....	10-7

10-6	Rankine-Brayton Cycle Integration: Biogas-Fired Turbine .....	10-8
C-1	Reduction in Gross Power Output Relative to Baseline (no CO <sub>2</sub> capture) vs. q <sub>Reb</sub> .....	C-2
C-2	Improvement in Gross Power Output Relative to Conventional Thermal Integration vs. q <sub>Reb</sub> .....	C-2
C-3	Reduction in Turbine Cycle Heat Rate Relative to Baseline (no CO <sub>2</sub> capture) vs. q <sub>Reb</sub> .....	C-3
C-4	Improvement in Gross Power Output Relative to Conventional Thermal Integration vs. q <sub>Reb</sub> .....	C-4
C-5	Reduction in Turbine Cycle Heat Rate Relative to Baseline (no CO <sub>2</sub> capture) vs. q <sub>Reb</sub> .....	C-5
C-6	Improvement in Turbine Cycle Efficiency Relative to Conventional Thermal Integration vs. q <sub>Reb</sub> .....	C-6
C-7	Increase in Net Unit Heat Rate Relative to Baseline (no CO <sub>2</sub> capture) vs. q <sub>Reb</sub> .....	C-7
C-8	Improvement in Net Unit Heat Rate Relative to Conventional Thermal Integration vs. q <sub>Reb</sub> .....	C-8
C-9	Decrease in Net Unit Efficiency Relative to Baseline vs. q <sub>Reb</sub> .....	C-9
C-10	Improvement in Net Unit Efficiency Relative to Conventional Thermal Integration vs. q <sub>Re</sub> .....	C-10

## LIST OF ABBREVIATIONS

AEP	American Electric Power
APH	Air Preheater
ASME	American Association of Mechanical Engineers
ATS	DOE Advanced Turbine System Program
B	Boiler Credits as Defined by ASME PTC4.1
BIGCC	Biomass Integrated Gasification Combined-Cycle
BP HXE	Bypass Heat Exchanger
BFP	Boiler Feed Pump
B&W	Babcock & Wilcox
CE	Combustion Engineering, Cold End
CEAT	Cold End Average Temperature, °C, °F
CH <sub>4</sub>	Methane, %
CO <sub>2</sub>	Carbon Dioxide, %
COS	Carbon Oxysulfide
CS <sub>2</sub>	Carbon Disulfide
DOE	Department of Energy
EIA	Energy Information Administration
EERE	DOE Office of Energy Efficiency and Renewable Energy
ERC	Energy Research Center
FE	DOE Office of Fossil Energy
FGC	Flue Gas Cooler
FGC <sub>APH</sub>	FGC Recovering Heat for Air Preheating
FGC <sub>FWH</sub>	FGC Recovering Heat for Feedwater Heating
FGD	Flue Gas Desulfurization
FGRHT	Flue Gas Reheat
FW	Feedwater
FWH	Feedwater Heater
GE	General Electric
GHG	Green House Gas
H <sub>2</sub>	Hydrogen, %
H <sub>2</sub> O	Water or Water Vapor, %
HHV	Higher Heating Value kJ/Kg, Btu/lb
HP	High Pressure
HR	Heat Rate, kJ/kWh, Btu/kWh
HR <sub>cycle</sub>	Turbine Cycle Heat Rate, kJ/kWh, Btu/kWh
HR <sub>cycle, gross</sub>	Gross Turbine Cycle Heat Rate, kJ/kWh, Btu/kWh
HR <sub>cycle, net</sub>	Net Turbine Cycle Heat Rate, kJ/kWh, Btu/kWh
HR <sub>net</sub>	Net Unit Heat Rate, kJ/kWh, Btu/kWh
HRSR	Heat Recovery Steam Generator
HTHR	High Temperature Heat Recovery Exchanger
HXE	Heat Exchanger
IGCC	Integrated Gasification Combined-Cycle
IP	Intermediate Pressure
LP	Low Pressure
LTHR	Low Temperature Heat Recovery Exchanger
LSTG	Let-down Steam Turbine Generator
M <sub>coal</sub>	Flow Rate of Coal, kg/s, kg/hr, klb/hr
M <sub>MST</sub>	Main Steam Flow Rate, kg/s, kg/hr, klb/hr
MEA	Mono-ethanol Amine
NEMS	National Energy Modeling System
N <sub>2</sub>	Nitrogen, %
NH <sub>3</sub>	Ammonia
NE	DOE Office of Nuclear Energy

NO <sub>x</sub>	Nitrogen Oxides, ppm
NTU	Number of Transfer Units
NYS	New York State
NYSERDA	New York State Energy Research and Development Authority
OCDO	Ohio Coal Development Office
PA	Primary Air
PAPH	Primary Air Preheater
PCEAT	Primary Air CEAT, °C, °F
P <sub>BFP</sub>	Boiler Feed Pump Power, MW
P <sub>G</sub>	Gross Power Output, MW, MW <sub>el</sub>
P <sub>SS</sub>	Station Service Power, MW
PR	Pressure Ratio
PSAH	Primary Steam Air Heater
q <sub>Reb</sub>	Reboiler Thermal Duty, GJ/tonne CO <sub>2</sub> , Btu/lb CO <sub>2</sub>
Q <sub>Reb</sub>	Total Reboiler Thermal Duty, MW <sub>th</sub> , MBtu/hr
RNH <sub>2</sub>	Primary Amines
PRB	Powder River Basin
RPM	Revolutions per Minute
SA	Secondary Air
SAPH	Secondary Air Preheater
SAH	Steam Air Heater
SCEAT	Secondary Air CEAT, °C, °F
SCR	Selective Catalytic Reactor
SSAH	Secondary Steam Heater
SO <sub>2</sub>	Sulfur Dioxide, %
Q <sub>FGC,MAX</sub>	Maximum Amount of Heat that can be Recovered from Flue Gas
Q <sub>T</sub>	Thermal Energy Transferred Steam in the Boiler, MW <sub>th</sub> , MBtu/hr
T <sub>APH,ai</sub>	Temperature of Air Entering APH, °C, °F
T <sub>APH,go</sub>	Temperature of Flue Gas leaving APH, °C, °F
T <sub>fg,min</sub>	Minimum Temperature of Flue Gas, °C, °F
TIT	Turbine Inlet Temperature, °C, °F
TOT	Turbine Outlet Temperature, °C, °F
T <sub>sah,out</sub>	Air temperature Leaving SAH, °C, °F
η	Efficiency, %
η <sub>B</sub>	Boiler Efficiency, %
η <sub>B,ASME</sub>	Boiler Efficiency as Defined by ASME PTC4.1
η <sub>net</sub>	Net Unit Efficiency, %
ε	Thermal Effectiveness

## SUMMARY

### BACKGROUND

Atmospheric levels of carbon dioxide (CO<sub>2</sub>) have increased over the last 150 years from around 280 to 360 ppm. Carbon dioxide is a greenhouse gas that is considered as a most likely cause of a global temperature increase. Concerns about the effect of anthropogenic emissions of CO<sub>2</sub> on global climate will undoubtedly result in regulations restricting CO<sub>2</sub> emissions from existing and newly built emitting sources. The required level of reduction in CO<sub>2</sub> emissions and the development status of affordable CO<sub>2</sub> abatement technologies will have a major impact on the commercial options and economics of newly built coal-fired power plants. Early reduction in anthropogenic CO<sub>2</sub> emissions is of utmost importance; the sooner CO<sub>2</sub> emissions are curtailed, the smaller the future reduction and lower the cost to stabilize CO<sub>2</sub> concentration in the atmosphere at desired level.

Electric power generation in the U.S. represents one of the largest sources of carbon-based emissions (approximately one-third of the man-made CO<sub>2</sub> emissions). A major issue is the fact that over 50% of total electric power generation capacity in the U.S. is based on coal. New York State (NYS) has 10 pulverized coal-fired power stations with a total nameplate capacity of 3,645 MW, and 11 oil-fired power stations with capacity of 6,497 MW. In 2005, coal-fired power stations emitted a total of 30 million tons of carbon dioxide (CO<sub>2</sub>) or 46% of NYS emissions from electric power generation.

Most of the existing coal-based power plant capacity in the U.S. is pulverized coal-fired boilers that are 25-35 years old (commissioned from 1965 to 1975) and in the 200-600 MW<sub>e</sub> unit size range, with subcritical single-reheat steam cycles. These conventional pulverized coal-fired power plants have the highest CO<sub>2</sub> emissions rate of any power systems; yet, are the lowest cost generators of electricity. A typical subcritical coal-fired power plant produces approximately 850 kg of CO<sub>2</sub> for every MWh of power produced [Narula, 2002]. The typical quantity of CO<sub>2</sub> to be captured from a 600 MW<sub>e</sub> plant is of the order of approximately 800,000 kg/h [Elwell and Grant, 2005]. The high CO<sub>2</sub> emissions are due to the use of carbon-intensive fuel and the relatively low thermal efficiency (less than 30%) of the older coal-fired power plants.

The authors expect CO<sub>2</sub> emissions regulations will require existing coal-fired power plants to reduce their carbon footprints in the future. While oxy-fuel, integrated gasification combined-cycle (IGCC), and post-combustion carbon capture and sequestration (CCS) technologies are viable options for the newly built power plants, it is very likely that a significant percentage of existing power plants will be retrofitted with post-combustion CCS technology. The major barriers to implementation of this technology are high cost, significant reduction in power plant output, and high performance penalty.

Although, the technical challenges of CO<sub>2</sub> emissions control for the existing fossil-fired power generation fleet appear to be similar to those that the power industry successfully overcame in controlling sulfur dioxide (SO<sub>2</sub>) and nitrogen oxide (NO<sub>x</sub>) emissions, the scale, the scope and economic impact of CO<sub>2</sub> emissions reduction are by several orders of magnitude larger. The option of retiring older and less efficient plants and replacing them with high-efficiency supercritical or, preferably, ultra supercritical units equipped with CCS to reduce CO<sub>2</sub> emissions is not practical for three main reasons. First, it is logistically impossible to rebuild about one half of coal-fired power generation fleet in next 10-20 years, second, the initial investment in excess of \$250 billion would be required, and third, commercialization and significant market penetration of advanced or alternative power generation and CCS technologies is expected to take at least 10 to 20 years.

Considering time required for commercialization and significant market penetration of advanced or alternative power generation and CCS technologies, the most effective and commercially available approach for reducing CO<sub>2</sub> emissions from existing coal-fired plants is efficiency improvement. Higher efficiency will lower fuel use, which will reduce emissions and will offset part of the efficiency and capacity losses that will be incurred by the retrofit of post-combustion CO<sub>2</sub> capture and other CCS technologies to existing units [Sarunac, 2009].

This report presents results of the project funded by the New York State Energy Research and Development Authority (NYSERDA) concerning efficiency improvements that can be achieved at existing power plants by optimizing performance of the mono-ethanol amine (MEA) post-combustion CO<sub>2</sub> capture process to minimize reboiler thermal duty, thermal integration of the reboiler, steam turbine cycle, boiler, and CO<sub>2</sub> compression train, and integration of the Rankine and Brayton cycles to improve plant performance and partially offset efficiency and capacity penalties to be incurred by the retrofit or implementation of post-combustion CO<sub>2</sub> capture.

## **PROJECT RESULTS**

### **Boiler-Turbine Cycle Integration**

Thermal integration of the boiler and turbine cycle, analyzed in this study, involves recovery of heat from the flue gas in a flue gas cooler (FGC) and its use for air preheating (advanced air preheating) and condensate heating. The optimal use of recovered heat was determined by considering effects of air preheating and associated cold end average temperature (CEAT) constraints and condensate heating on the turbine cycle and net unit heat rate. Air preheating (conventional air preheating) via a steam air heater (SAH) was used as a benchmark.

For a given CEAT, the optimal split of heat used for air preheating and condensate heating depends on the ambient temperature. For Somerset and design value of ambient temperature of 29.4°C (85°F) and empirically determined values of CEAT for the secondary APH (SCEAT) of 104°C (220°F) and the primary APH (PCEAT) of 87.8°C (190°F), best performance is achieved when approximately 70% of heat recovered from the flue gas is used for condensate heating. For lower ambient temperature more heat is required for air preheating; for ambient temperature of -15°C best performance is achieved when 12% of recovered heat is used for condensate heating and 88% for air preheating.

At design value of the ambient temperature and operating conditions satisfying the secondary CEAT (SCEAT) and primary (PCEAT) set points, use of heat recovered from the flue gas results in approximately 1.6%-points<sup>1</sup> lower turbine cycle and net unit heat rate compared to the SAH air preheating. This difference increases as ambient temperature decreases. At the ambient temperature of -15°C turbine cycle and net unit heat rate is approximately 2.45%-points lower compared to the SAH air preheating.

### **Optimization of MEA-Based Post-Combustion CO<sub>2</sub> Capture Process**

Modeling of the CO<sub>2</sub> absorption/scrubbing process by aqueous Monoethylamine (MEA) for Somerset's power plant configuration was performed using ASPEN Plus version 2006.5 [Aspen Technology, 2006]. The process model was used to determine optimal combination of key operating parameters (stripper operating pressure, solvent circulation rate/the CO<sub>2</sub> lean solvent loading (mol CO<sub>2</sub>/mol MEA), MEA weight percentage in the absorption solvent, CO<sub>2</sub> removal percentage, and flue gas/lean solvent temperature) resulting in lowest energy requirements for CO<sub>2</sub> capture. The set of optimal operating parameters, presented in Table 5-2, results in 20.8% reduction in reboiler thermal duty from design conditions, and 26% from the non-optimal case.

### **Thermal Integration of the Turbine Cycle and CO<sub>2</sub> Stripper with Plant Heat Sources**

Owing to the steam extraction from intermediate pressure (IP) turbine exhaust for a reboiler, post-combustion CO<sub>2</sub> capture has a significant negative effect on plant performance (efficiency) and capacity (power output). Thermal integration of the steam turbine cycle with boiler and CO<sub>2</sub> compression train reduces steam extractions from the turbine for condensate and feedwater heating, increases turbine power output, improves cycle and plant performance and offsets, in part, negative effects of post-combustion CO<sub>2</sub> capture.

A number of thermal integration options were developed and analyzed in the study, including Advanced MEA and Modifications A to F to the Advanced MEA. Basic features of these thermal integration options are summarized in Table 7-9. Thermal integration of two types of the CO<sub>2</sub> compressors was also

---

<sup>1</sup> For a host unit, 1% improvement in net unit heat rate results in annual savings of \$1,500,000.

investigated: a conventional multi-stage inline compressor; and the advanced two-stage shock-wave Ramgen Power Systems compressor.

The effect of investigated thermal integration options on gross power output<sup>2</sup> and net unit efficiency for the state-of-the-art amines is summarized in Table 7-10. The results are compared to the baseline case (no CO<sub>2</sub> capture) and to the conventional and advanced thermal integration. The comparison relative to the baseline is a measure of the penalty that would be incurred by retrofit or implementation of the post-combustion CO<sub>2</sub> capture process, while comparison relative to the conventional MEA integration represents improvement achievable by thermal integration. The reduction in unit performance and capacity relative to the baseline is lowest and the improvement relative to Conventional MEA is highest for Modifications F and C-R.

Thermal integration should be considered for the existing and newly built plants. The best analyzed thermal integration option (Modification F) improves gross power output by 5% and net unit efficiency by 1.57%-points, relative to the Conventional MEA.

Also, when evaluating different thermal integration options, the cost of heat exchange and associated equipment has to be considered in addition to the performance improvement. For example, the cost of a FGC operating below acid dewpoint is approximately 10 times higher compared to the finned tube heat exchanger operating above the acid dewpoint.

### **Partial CO<sub>2</sub> Capture**

Partial CO<sub>2</sub> capture involves treatment of 20 to 100% of the flue gas leaving the plant, and involves modular design of the CO<sub>2</sub> scrubbing system. Partial CO<sub>2</sub> capture could be the first step toward reducing CO<sub>2</sub> emissions from the existing power plants, which is expected to speed up deployment of the post-combustion CO<sub>2</sub> capture because of the lower initial capital investment and associated risk.

Other reasons for considering partial CO<sub>2</sub> capture include: gathering operating experience on a smaller and easier-to-operate and maintain system and implementing design changes and improvements on subsequent CO<sub>2</sub> capture modules. Also, partial CO<sub>2</sub> capture could be implemented on smaller and older power plants to reduce CO<sub>2</sub> emissions with moderate performance penalty and significantly lower initial capital investment.

---

<sup>2</sup> In the case of comparisons of *gross power output, turbine cycle heat rate, turbine cycle efficiency, and boiler efficiency* of thermal integration options investigated in this study, *only thermally-related effects are accounted for* in these analyses. Hence, parasitic electrical loads associated with CO<sub>2</sub> compression are not accounted for in these metrics. Parasitic electrical loads, however, are taken into account in *net heat rate and net unit efficiency comparisons*.

The effect of partial CO<sub>2</sub> capture on plant performance was investigated for the conventional and advanced MEA integrations, and Modifications A, B, C and D to the advanced MEA integration, for reboiler thermal duty ( $q_{\text{Reb}}$ ) values of 3.95 and 4.65 GJ/tonne CO<sub>2</sub> (1,700 and 2,000 Btu/lb CO<sub>2</sub>).

As the percentage of CO<sub>2</sub> capture decreases, the amount of heat that needs to be supplied to the reboiler and steam flow to the reboiler decrease, because the flue gas flow rate that needs to be treated is lower resulting in a lower amount of CO<sub>2</sub> that needs to be captured. The reduced steam extraction to the reboiler increases steam flow through the low pressure (LP) turbine, which increases turbine power output. The improvement in cycle and plant performance varies linearly with the percentage of CO<sub>2</sub> capture and increases as percentage of CO<sub>2</sub> capture decreases and  $q_{\text{Reb}}$  increases.

For example, operating with 40% CO<sub>2</sub> capture increases gross power output by 11.6 to 14% (depending on the thermal integration option), relative to the conventional MEA integration and 90% CO<sub>2</sub> capture. This increase in power output improves turbine cycle heat rate by 10.4 to 12.2%, turbine cycle efficiency by 4.1 to 5%-points, net unit heat rate by 17.8 to 19.7%, and net unit efficiency by 5.5 to 6.2%-points, relative to the conventional thermal integration and 90% CO<sub>2</sub> capture. The improvement in net unit performance is larger compared to the improvement in turbine cycle performance because of the CO<sub>2</sub> compression work, which is also reduced by partial CO<sub>2</sub> capture.

### **Rankine-Brayton Cycle Integration**

Integration of the Rankine and Brayton cycles was analyzed to determine efficiency (heat rate) improvements that could be achieved at existing power plants by using heat recovered from the Brayton's cycle hot effluent to increase steam flow through the steam turbine and offset power loss due to reboiler steam extraction. The ultimate goal of the Rankine-Brayton cycle integration is efficiency improvement of the Rankine cycle and reduction of the capacity penalty which would be incurred by implementation of the post-combustion CO<sub>2</sub> capture technology. Cycle integration can be applied to existing larger coal-fired power plants that would be retrofitted by the post-combustion CO<sub>2</sub> capture, enabling them to continue operation in a carbon-constrained world.

The fueling options considered for the Brayton cycle included hydrogen- and biogas-fired turbine. In the latter case, biogas (syngas) is produced by gasification of biomass in a fluidized bed gasifier, while the leftover char is burned in the boiler. In these analyses, both fueling options result in zero CO<sub>2</sub> emissions from the Brayton cycle when energy for transportation and storage of biomass or hydrogen is excluded as transportation and storage energy requirements are site specific. In addition, hydrogen is assumed to be produced by renewable or nuclear sources off-peak. Based on these assumptions, the power output and

heat provided to the Rankine cycle through thermal integration do not contribute to the plant CO<sub>2</sub> emissions.

Optimal integration of the Rankine and Brayton cycles was determined by parametrically varying heat provided by the Brayton cycle for the high pressure (HP) feedwater heating (FWH) and for reboiler. The best Rankine and combined cycle performance is achieved when 100% of the heat is used for the HP feedwater heating. This is because the steam extracted from the steam turbine cycle for the HP FWH is of higher quality compared to the reboiler steam extracted from the IP turbine exhaust. Also, as steam extractions for the HP FWH are decreased and eliminated, the steam flow through the turbine increases, resulting in higher power output of the steam turbine cycle.

For the hydrogen-fired turbine option, the Brayton cycle was sized to provide sufficient amount of heat to replace steam extractions for the HP FWHs A and B (top two high pressure FWHs – Figure 2.2). This resulted in the power output of the hydrogen-fired turbine of 140.5 MW<sub>el</sub>. Cycle integration has a large positive effect on performance of the combined cycle. In addition to increasing the plant gross power output by approximately 20%, reduction in net plant efficiency relative to the baseline (Rankine cycle, no CO<sub>2</sub> capture) is decreased by approximately factor of two, i.e. from 8.67 to 4.38 % for advanced MEA integration and from 7.71% to 3.77% for Modification D (see Tables 7-10 and 9-10).

The analysis was extended to the case where the Brayton cycle was sized to provide sufficient amount of heat to replace steam extraction for the HP FWH A only. This decreased power output of the hydrogen-fired turbine to approximately 95 MW<sub>el</sub>. The performance improvement, although being smaller compared to the case where steam extractions for both HP FWHs are eliminated, is still significant; approximately 9.5% increase in gross power output, and 60% decrease in net unit efficiency relative to the baseline.

For the biogas-fired turbine option, in order to keep the amount of biomass needed manageable, economically harvestable and sustainable, Brayton cycle was sized to provide sufficient amount of heat to replace steam extraction for the HP FWH A and partially for the HP FWH B. This resulted in a power output of the biogas-fired turbine of approximately 33 MW<sub>el</sub>. Due to low turbine inlet temperature (TIT) and compressor pressure ratio (PR), calculations were performed by using a Brayton cycle efficiency of 16.83%. Performance improvement, compared to the baseline, is lower compared to the hydrogen-fired option mainly because of the low calorific value of biogas which adversely affects efficiency of the Brayton cycle due to low TIT. Increasing the size of the Brayton cycle to provide heat for both HP FWHs would help improve performance of the combined cycle provided sufficient amount of biomass is available and a sustainable harvest is possible.

Cycle integration has a significant positive effect on performance and capacity. Capacity losses could be eliminated and performance losses halved. The cost of this option is significantly higher compared to the thermal integration, but significantly lower compared to a Greenfield (newly built) combined cycle.

In summary, results of the study show that thermal integration and use of heat recovered from the flue gas and CO<sub>2</sub> compression can improve efficiency and increase power output of power plants that are equipped with the post-combustion CO<sub>2</sub> capture technology, and offset, in part, performance penalty associated with the retrofit or implementation of the technology. The best thermal integration option analyzed in this study would improve gross power output by 5% and net unit efficiency by 1.57%-points, relative to the conventional MEA. It is highly recommended thermal integration be applied at existing power plants to allow their operation in a carbon-constrained world. Additionally, thermal integration needs to be incorporated into design of the newly built power plants to improve efficiency.

The authors hope the project results will advance use of innovative strategies for superior plant performance and CO<sub>2</sub> emissions reduction, and support early implementation of CO<sub>2</sub> reduction technologies at coal-fired power plants. This will help improve ambient air quality and foster business and technology development in New York State.



## Section 1

### INTRODUCTION

Atmospheric levels of carbon dioxide (CO<sub>2</sub>) have increased over the last 150 years from around 280 to 360 ppm. Carbon dioxide is a greenhouse gas that is considered as a most likely cause of a global temperature increase. Concerns about the effect of anthropogenic emissions of CO<sub>2</sub> on global climate will undoubtedly result in regulations restricting CO<sub>2</sub> emissions from existing and newly built emitting sources. Early reduction in anthropogenic CO<sub>2</sub> emissions is of utmost importance; the sooner CO<sub>2</sub> emissions are curtailed, the smaller the future reduction and lower the cost to stabilize CO<sub>2</sub> concentration in the atmosphere at desired level.

Electric power generation in the U.S. represents one of the largest sources of carbon-based emissions (approximately one-third of the man-made CO<sub>2</sub> emissions). A major issue is the fact that over 50% of total electric power generation capacity in the U.S. is based on coal. New York State (NYS) has 10 pulverized coal-fired power stations with a total nameplate capacity of 3,645 MW, and 11 oil-fired power stations with capacity of 6,497 MW. In 2005, coal-fired power stations emitted a total of 30 million tons of carbon dioxide (CO<sub>2</sub>) or 46% of NYS emissions from electric power generation.

Most of the existing coal-based power plant capacity in the U.S. is pulverized coal-fired boilers that are 25-35 years old (commissioned from 1965 to 1975) and in the 200-600 MW<sub>el</sub> unit size range, with subcritical single-reheat steam cycles. These conventional pulverized coal-fired power plants have the highest CO<sub>2</sub> emissions rate of any power systems; yet, are the lowest cost generators of electricity. A typical subcritical coal-fired power plant produces approximately 850 kg of CO<sub>2</sub> for every MWh of power produced [Narula, 2002]. The typical quantity of CO<sub>2</sub> to be captured from a 600 MW<sub>e</sub> plant is of the order of approximately 800,000 kg/h [Elwell and Grant, 2005]. The high CO<sub>2</sub> emissions are due to the use of carbon-intensive fuel and the relatively low thermal efficiency (less than 30%) of the older coal-fired power plants.

CO<sub>2</sub> emissions regulations in the future are expected to require existing coal-fired power plants to reduce their carbon footprints in the future. While oxy-fuel, integrated gasification combined-cycle (IGCC), and post-combustion carbon capture and sequestration (CCS) technologies are viable options for the newly built power plants, it is very likely that a significant percentage of existing power plants will be retrofitted with post-combustion CCS technology. The major barriers to implementation of this technology are high cost, significant reduction in power plant output, and high performance penalty.

Although, the technical challenges of CO<sub>2</sub> emissions control for the existing fossil-fired power generation fleet appear to be similar to those that the power industry successfully overcame in controlling sulfur

dioxide (SO<sub>2</sub>) and nitrogen oxide (NO<sub>x</sub>) emissions, the scale, the scope and economic impact of CO<sub>2</sub> emissions reduction are by several orders of magnitude larger. The option of retiring older and less efficient plants and replacing them with high-efficiency supercritical or, preferably, ultra supercritical units equipped with CCS to reduce CO<sub>2</sub> emissions is not practical for three main reasons. First, it is logistically impossible to rebuild about one half of coal-fired power generation fleet in next 10-20 years, second, the initial investment in excess of \$250 billion would be required, and third, commercialization and significant market penetration of advanced or alternative power generation and CCS technologies is expected to take at least 10 to 20 years.

Considering time required for commercialization and significant market penetration of advanced or alternative power generation and CCS technologies, the most effective and commercially available approach for reducing CO<sub>2</sub> emissions from existing coal-fired plants is efficiency improvement. Higher efficiency will lower fuel use, which will reduce emissions and will offset part of the efficiency and capacity losses that will be incurred by the retrofit of post-combustion CO<sub>2</sub> capture and other CCS technologies to existing units [Sarunac, 2009].

This report presents results of the project funded by the New York State Energy Research and Development Authority (NYSERDA) concerning efficiency improvements that can be achieved at existing power plants by optimizing performance of the mono-ethanol amine (MEA) post-combustion CO<sub>2</sub> capture process to minimize reboiler thermal duty, thermal integration of the boiler, steam turbine cycle, boiler, and CO<sub>2</sub> compression train. It also includes integration of the Rankine and Brayton cycles to improve plant performance and partially offset efficiency and capacity penalties to be incurred by the retrofit or implementation of post-combustion CO<sub>2</sub> capture.

Partial CO<sub>2</sub> capture, involving treatment of 20 to 100% of the flue gas leaving the plant and modular design of the CO<sub>2</sub> scrubbing system, was also investigated. Partial CO<sub>2</sub> capture could be the first step toward reducing CO<sub>2</sub> emissions from the existing power plants expected to speed up deployment of the post-combustion CO<sub>2</sub> capture because of lower initial capital investment and associated risk. Also, it could be implemented at smaller power plants to reduce CO<sub>2</sub> emissions with a moderate loss of performance and capacity.

## **PROJECT GOALS**

Determine efficiency improvements that could be achieved at existing power plants by thermal integration of the steam turbine cycle, boiler, CO<sub>2</sub> compression train and post-combustion CO<sub>2</sub> capture process. Evaluate the integration of Rankine and Brayton cycles fueled by biomass and hydrogen, respectively to determine efficiency improvements that can be achieved by using heat recovered from the Brayton cycle to

increase steam flow through the steam turbine and offset efficiency and capacity losses due to MEA-reboiler steam extraction.

## **PROJECT OBJECTIVES**

Project objectives include:

- Determine the optimal use of heat recovered from the flue gas by exploring tradeoffs between air preheating, condensate flow heating and CO<sub>2</sub> scrubbing.
- Optimize the MEA-based CO<sub>2</sub> post-combustion process to reduce energy requirements for CO<sub>2</sub> capture.
- Investigate and evaluate partial CO<sub>2</sub> capture approach and determination of its characteristics in terms of overall energy requirements and associated performance and capacity penalties.
- Assess the integration of the CO<sub>2</sub> stripper with the power plant waste heat sources and quantification of reduction in process heat requirements for solvent regeneration and overall energy requirements for the CO<sub>2</sub> capture.
- Assess the integration of the CO<sub>2</sub> compression process with turbine cycle and a reboiler to allow use of compression heat for condensate flow heating and quantification of reduction in process heat to the MEA-reboiler.
- Assess the efficiency gains from the integration of Rankine and hydrogen- or biogas-fueled Brayton cycles to increase steam flow through the steam turbine and quantification of reduction in efficiency and capacity penalties to be incurred by implementation of post-combustion CO<sub>2</sub> capture.



Section 2

**DESCRIPTION OF THE HOST UNIT**

The analysis and calculations performed in this study were conducted for the host unit: AES Somerset Unit 1. The 640 MW<sub>el</sub> (nominal) rated coal-fired power plant is located in town of Somerset in Niagara County, NY on the shore of Lake Ontario. The boiler is balanced draft, radiant, natural circulation, opposed wall pulverized coal-fired, manufactured by Babcock & Wilcox (B&W). Steam conditions are 2,450 psig, 1,005°F and 1,005°F. The boiler is equipped with six Combustion Engineering (CE) bowl type mills, providing pulverized coal to 48 burners. A side elevation of the boiler is also presented in Figure 2-1.

The combustion air is heated in two Ljungstrom-type Secondary Air Preheaters (SAPHs), while the primary air is heated in two Ljungstrom-type Primary Air Preheaters (PAPHs), Figure 2-2. Prior to entering the PAPH and SAPH, primary and secondary air streams are preheated in the Primary Steam Air Heater (PSAH) and Secondary Steam Air Preheater (SSAH), to maintain air temperature into a PAPH and SAPH above an empirically determined value and maintain acceptable deposition rate of sulfuric acid and manageable fouling in the cold end (CE) layers of the PAPH and SAPH. Heat for the PSAH and SSAH is provided by steam extracted from the steam turbine.

The unit burns a variety of bituminous coals (Illinois No. 6, Central Appalachian, Pittsburgh No. 8), and sub-bituminous coals (Powder River Basin, PRB), and Petcoke. Calculations in this study were performed for the Pittsburgh No. 8 coal. The average composition and Higher Heating Value (HHV) of the Pittsburgh No. 8 coal are given in Table 2-1.

**Table 2-1. Average Composition and HHV: Pittsburgh No. 8.**

COAL COMPOSITION		
Constituent	% wet	
Carbon	71.33	
Hydrogen	4.82	
Nitrogen	1.32	
Sulfur	3.03	
Oxygen	6.62	
Moisture	5.40	
Ash	7.47	
HHV	13,176	BTU/lb



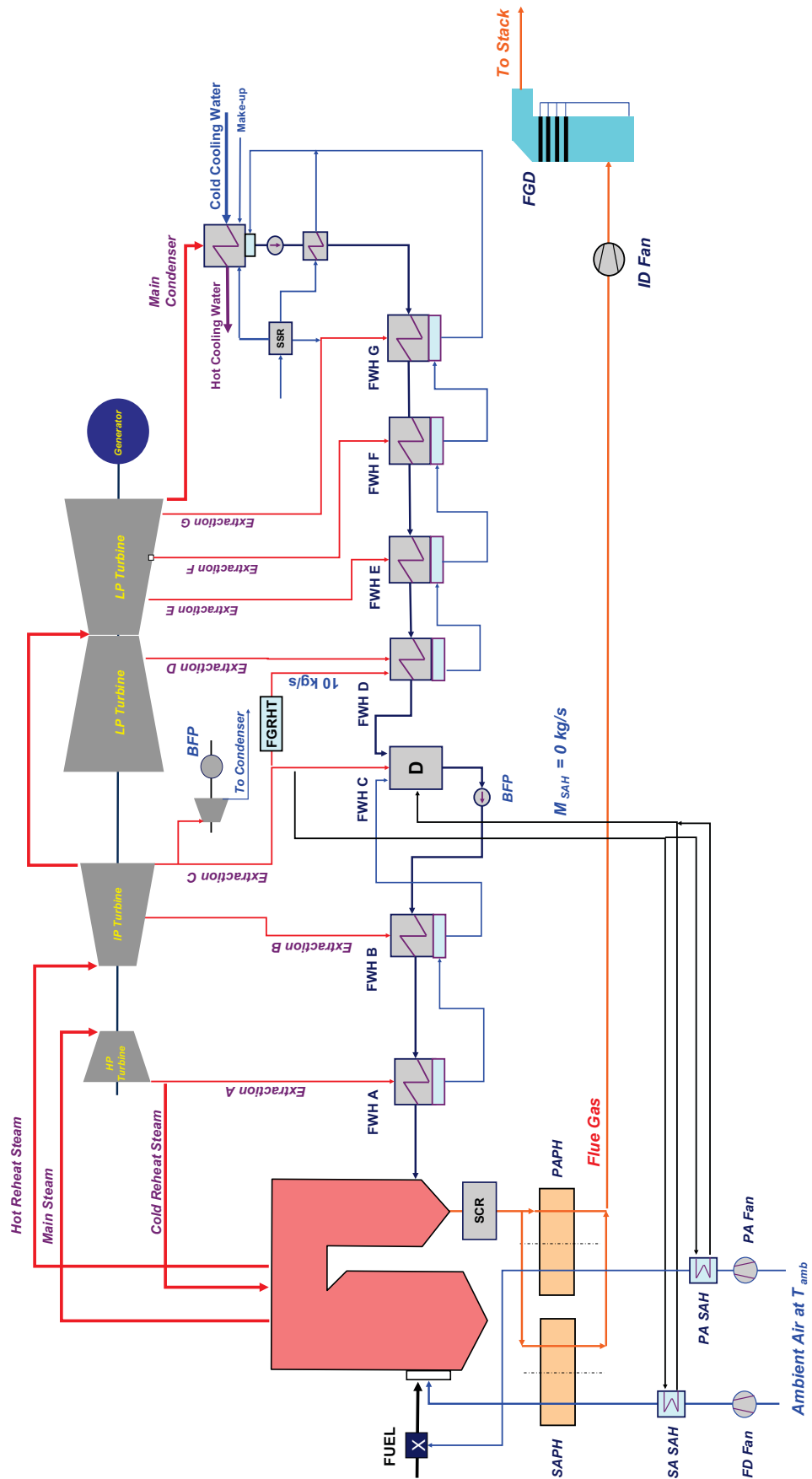


Figure 2-2. Schematic Diagram of Boiler and Turbine Cycle: Somerset Unit 1.

The unit was retrofitted with a Selective Catalytic Reduction (SCR) system containing three layers of catalyst. The SCR system is designed to reduce NO<sub>x</sub> emissions by 90%. Sulfur dioxide (SO<sub>2</sub>) emissions are controlled by a high-efficiency Flue Gas Desulphurization (FGD) system. The FGD system is a wet scrubbing process utilizing limestone as primary agent. The limestone is ground in a wet grinding process to produce slurry. SO<sub>2</sub> removal is accomplished by bringing the flue gas into contact with the limestone slurry. The SO<sub>2</sub> is absorbed by the slurry producing calcium sulfite. The FGD is designed to remove more than 95% of SO<sub>2</sub> from the flue gas.

The steam turbine is 3,600 RPM, 2,400 psig, 1000°F, 1,000°F 643 MW tandem compound reheat unit, comprised of a High Pressure (HP) turbine section, Intermediate Pressure (IP) turbine section, and double exit Low Pressure (LP) turbine sections, manufactured by General Electric (GE). The turbine cycle employs a seven-stage regenerative feedwater heating train comprised of two high pressure feedwater heaters (HP FWHs) A and B, deaerator (D), and four low pressure feedwater (condensate) heaters (LP FWHs) D, E, F and G. the FWHs are horizontal, two-pass, U-tube, closed design manufactured by Struthers Wells. The deaerator is of a horizontal design, manufactured by Chicago Heater Company. Heat for the FWHs is supplied by steam extracted from the steam turbine, Figure 2-2. The electric generator is hydrogen-cooled, 3-phase, 730 MVA, manufactured by GE. The main steam condenser is a single-pass two-shell, transverse surface design manufactured by Foster Wheeler.

The heat balance diagram of the steam turbine cycle, provided by the manufacturer, is presented in Figure 2-3. The design value of the gross turbine cycle heat rate ( $HR_{\text{Cycle,gross}}$ ) is 8,285 kJ/kWh (7,853 Btu/kWh), while the net turbine cycle heat rate ( $HR_{\text{Cycle,net}}$ ) is 8,476 kJ/kWh (8,034 Btu/kWh) at 634.95 MW, condenser back pressure of 2.5" Hg absolute, no steam extraction for the PAPH and secondary APH, and 10.06 kg/s (80,000 lb/hr) steam extraction for flue gas reheat (FGRHT). The gross turbine cycle heat rate accounts for the Boiler Feed Pump (BFP) power (14.62 MW), while the net turbine cycle heat rate does not.

LEGEND: Calculations based on  
 1967 ASME Steam Tables  
 H, h - Enthalpy - Btu/Lb.  
 # - Flow - Lb/Hr.  
 P - Pressure, Psia  
 F - Temperature, F degrees

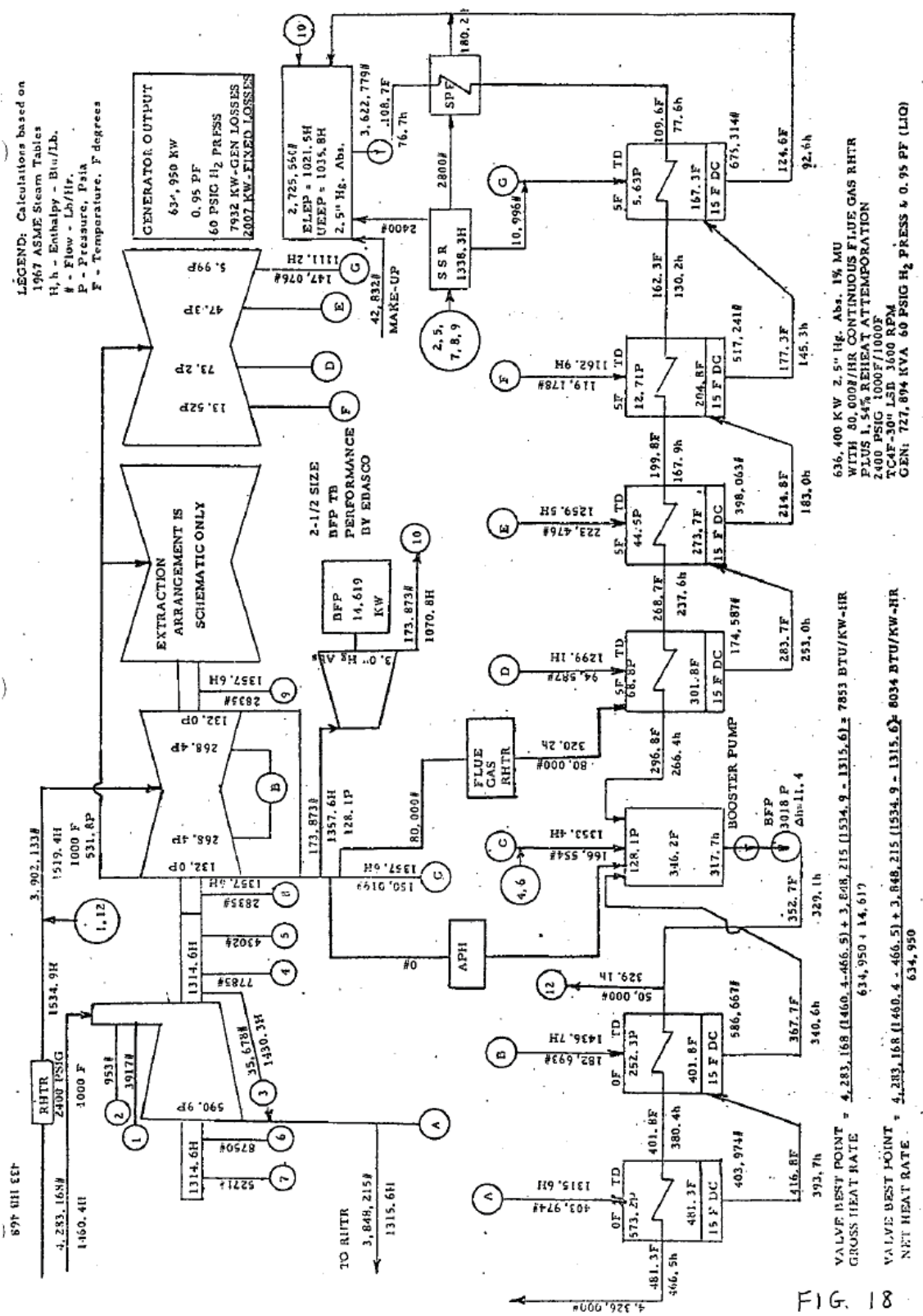


Figure 2-3. Heat Balance Diagram of Steam Turbine Cycle: Somerset Unit 1.

Section 3

**TECHNICAL APPROACH FOR CYCLE MODELING**

Modeling of the turbine cycle and integration of the turbine cycle with the boiler and the CO<sub>2</sub> compression train was performed using PEPSE Version 72 provided by Scientech. PEPSE is a commercial modeling tool based on a mass and energy balance that allows modeling of power cycles, including Rankine, Brayton, and combined cycles. A spreadsheet-based first principles analysis based on conservation of mass and energy including combustion (stoichiometric) calculations, fan and mill power calculations, APH performance calculations, and determination of performance parameters such as boiler efficiency and net unit heat rate, developed by the Energy Research Center (ERC) was also used to determine the flow rate of the flue gas and unit performance. Inputs included coal composition and higher heating value (HHV), and turbine cycle heat rate, determined by PEPSE. This approach has been used by the ERC in many other projects.

The PEPSE model of the Somerset steam turbine cycle is presented in Figure 3-1. Comparison of the predicted and design turbine cycle performance is presented in Table 3-1. The results show that PEPSE predictions are virtually identical to the design data.

**Table 3-1. Comparison of Predicted and Design Turbine Cycle Performance: Somerset Unit 1.**

Parameter	Units	PEPSE Prediction	Design Value	Units	PEPSE Prediction	Design Value
Gross Power Output	MW	634.12	634.95	MW	634.12	634.95
Net Turbine Cycle Heat Rate	kJ/kWh	8,488	8,476	BTU/kWh	8,045	8,034
Gross Turbine Cycle Heat Rate	kJ/kWh	8,297	8,285	BTU/kWh	7,864	7,853
Main Steam Flow Rate	kg/s	539.0	538.9	klb/hr	4,283	4,283
Reheat Steam Flow Rate	kg/s	484.4	484.2	klb/hr	3,849	3,848
IP Turbine Exhaust Flow	kg/s	418.3	416.5	klb/hr	3,325	3,310
LP Turbine Exhaust Flow	kg/s	342.6	343.0	klb/hr	2,723	2,726
Steam Extraction for FWH A	kg/s	50.7	50.8	lb/hr	402,957	403,974
Steam Extraction for FWH B	kg/s	21.5	23.0	lb/hr	171,195	182,693
Steam Extraction for Deaerator	kg/s	18.6	18.9	lb/hr	147,916	150,019
Steam Extraction for BFP	kg/s	21.9	21.9	lb/hr	173,873	173,873
Steam Extraction for FWH D	kg/s	15.3	11.9	lb/hr	121,321	94,587
Steam Extraction for FWH E	kg/s	28.0	28.1	lb/hr	222,281	223,476
Steam Extraction for FWH F	kg/s	14.8	15.0	lb/hr	117,352	119,178
Steam Extraction for FWH G	kg/s	17.7	18.5	lb/hr	140,748	147,076
FW Temperature Leaving FWH A	°C	249.6	249.6	°F	481.3	481.3
FW Temperature Leaving FWH B	°C	205.6	205.4	°F	402.0	401.8
FW Temperature Leaving Deaerator	°C	176.5	178.2	°F	349.7	352.7
FW Temperature Leaving FWH D	°C	149.9	147.1	°F	301.8	296.8
FW Temperature Leaving FWH E	°C	130.0	131.5	°F	266.0	268.7
FW Temperature Leaving FWH F	°C	91.8	93.2	°F	197.2	199.8
FW Temperature Leaving FWH G	°C	71.2	72.4	°F	160.2	162.3
FW Temperature Entering FWH G	°C	43.1	43.1	°F	109.6	109.6



A detail of the spreadsheet model, presented in Figure 3-2, shows flow rates of the primary and secondary air and flue gas around the boiler and the APHs. These flows were determined by performing stoichiometric calculations for the given coal composition and excess oxygen level (excess O<sub>2</sub>) at the economizer exit provided by the AES, and iterating for coal flow rate until the desired gross power output (640 MW) is achieved. APH performance was determined by using the ε-NTU theory of heat exchangers.

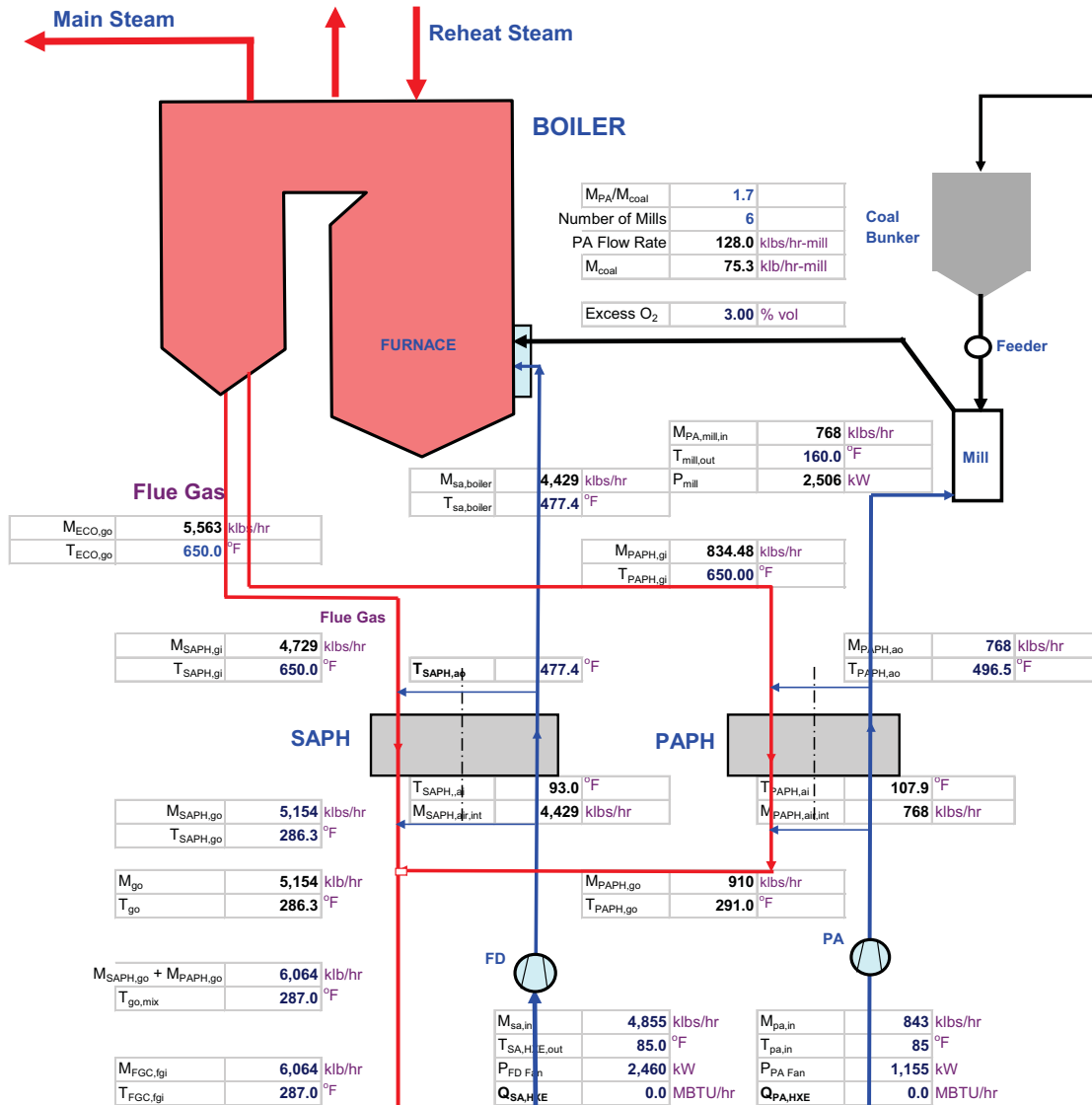


**Figure 3-2. Spreadsheet-Based Mass and Energy Balance Model of Somerset Unit 1: Detail.**

The flow rate of the flue gas, predicted by the mass and energy balance model for Somerset Unit 1 is 763.0 kg/s (6,064 klb/hr), is very close to the design value of 767.6 kg/s (6,100 klb/hr). The predicted value of net unit heat rate (HR<sub>net</sub>) is 0.85% higher compared to the design value, while the predicted value of boiler

efficiency ( $\eta_B$ ) is by 3.3%-point lower compared to the design value. This difference in boiler efficiency is due to differences in coal composition and higher heating value ,HHV (actual vs. design), lower temperature of the flue gas leaving the APHs (142.7 vs. 148.9°C or 288.8 vs. 300°F), and different definitions of boiler efficiency. Boiler efficiency can be defined as:

$$\eta_B = Q_T / (\text{HHV } M_{\text{coal}}) \quad \text{or} \quad \text{Equation 3-1}$$

$$\eta_{B,\text{ASME}} = Q_T / ((\text{HHV} + B) M_{\text{coal}}) \quad \text{Equation 3-2}$$

The net unit heat rate is defined as:

$$\text{HR}_{\text{net}} = \text{HHV } M_{\text{coal}} / (P_G - P_{\text{ss}}) \quad \text{Equation 3-3}$$

The turbine cycle heat rate is defined as:

$$\text{HR}_{\text{cycle,net}} = Q_T / P_G \quad \text{Equation 3-4}$$

$$\text{HR}_{\text{cycle,gross}} = Q_T / (P_G + P_{\text{BFP}}) \quad \text{Equation 3-5}$$

Where  $Q_T$  is the thermal energy transferred to the steam in the boiler,  $M_{\text{coal}}$  is the flow rate of coal burned,  $P_G$  is the gross electrical power output of the generator,  $P_{\text{ss}}$  is station service power, B represents credits to the boiler as defined by the ASME PTC 4.1 (such as heat in entering air, heat in atomizing steam, sensible heat in fuel, pulverizer or crusher power, boiler circulating pump power, primary and secondary air fan power, recirculating gas fan power, heat supplied by moisture in entering air, and heat in cooling water), and  $P_{\text{BFP}}$  is the boiler feed pump power. Station service power or station use is power used to run the power plant and is subtracted from the gross power output to get the plant net power output.

The ASME definition of boiler efficiency is typically accepted as the industry standard. Boiler efficiency defined by Equation 3-1 is used in this study.

Modeling of the CO<sub>2</sub> absorption/scrubbing process by aqueous mono-ethanolamine (MEA) was performed using the software ASPEN Plus version 2006.5 [Aspen Technology, 2006]. The modeling approach is described in Section 5, while details are provided in Appendix A.

A spreadsheet-based model of the CO<sub>2</sub> compression was used to determine CO<sub>2</sub> temperature at the compressor exhaust as a function of the pressure (compression) ratio, and determine amount of compression heat that could be recovered and beneficially used. The approach is described in Appendix B.



## Section 4

### POST-COMBUSTION CO<sub>2</sub> CAPTURE

Chemical absorption is perhaps the most widely used process for separation of CO<sub>2</sub> from flue gas. This process operates on the basic principle of mass transfer with reaction. Separation is achieved through a reversible acid-base reaction between CO<sub>2</sub> and an alkaline agent. The most common CO<sub>2</sub> capture process for post-combustion capture consists of three stages (see Figure 4-1). In the first stage, CO<sub>2</sub> is removed from the flue gas by absorption in a scrubber or absorber column (packed bed or gas/liquid contactor). The rich solvent containing CO<sub>2</sub> is then heated in a reboiler and associated stripper column to release the CO<sub>2</sub>, which is compressed in an additional step for transport to a geological storage site. Heat is supplied to the reboiler using low-pressure (LP) steam extracted from the power plant steam turbine cycle. Steam leaving the stripper is recovered in the condenser at the top of the stripper column and fed back to the desorber. The regenerated lean solvent is recycled back to the absorber via a rich/lean heat exchanger.

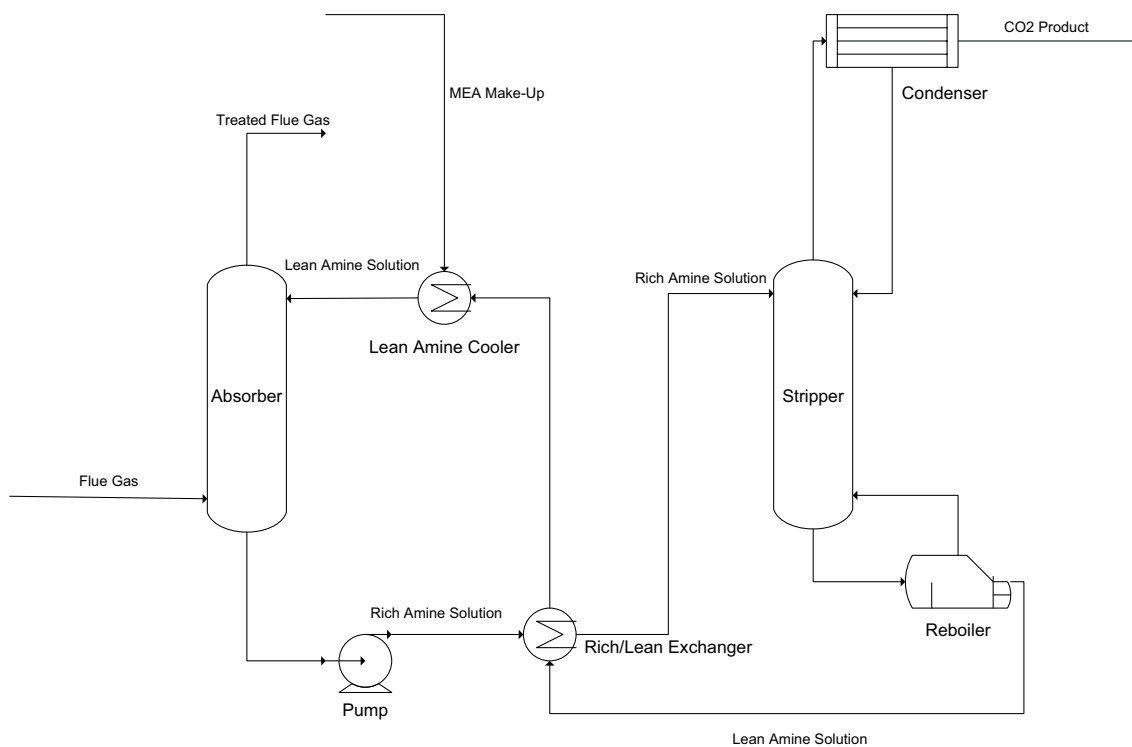


**Figure 4-1. Schematic Diagram of a Typical Post-Combustion Capture System.**

The most energy-intensive aspects of amine-based post-combustion CO<sub>2</sub> capture processes are the supply of heat needed for solvent regeneration and, to a lesser extent with current solvents, shaft power for CO<sub>2</sub> compression. It is generally accepted that the most efficient way to reheat rich solvent in the reboiler is by

steam extracted from the steam turbine cycle [Gibbins, 2007]. Extracted steam for the CO<sub>2</sub> capture process is not available for electrical power production, and the gross power output of the steam turbine is reduced, resulting in an increase in turbine cycle heat rate (turbine cycle efficiency) and net unit heat rate (net unit efficiency). Most post-combustion CO<sub>2</sub> capture processes discussed in the literature and considered being closest for commercial deployment at pulverized coal-fired power plants use amine-based solvents for chemical the absorption processes. Other chemical-based options for absorption, however, are under consideration, including advanced amine solvents, amine-enriched sorbents, aqueous ammonia (NH<sub>3</sub>) solutions and non-amine reagents, such as potassium carbonate and calcium oxide.

## **MEA-BASED CO<sub>2</sub> CAPTURE SYSTEM**

Alkanolamines are considered as the best candidates for post-combustion decarbonization of flue gas. They have been proven well as decarbonization solvents in the gas processing and chemical and petroleum industries. The term amine refers to a group of organic compounds that can be derived from NH<sub>3</sub> by replacing one or more hydrogen atoms by organic radicals. Amines are classified according to the number of hydrogen atoms replaced. Primary amines (RNH<sub>2</sub>) include the monoethanol amine or MEA, which has been the solvent of choice for CO<sub>2</sub> absorption and acid gas removal in general. The MEA-based technology is available for removal of CO<sub>2</sub> at low concentrations. It is commercially available and can be retrofitted to existing power plants. It is also a low cost method because of its high CO<sub>2</sub> reactivity and high absorption capacity, but it has high energy requirements, since it generates the most reaction heat, 1.9 MJ/kg, and, hence, requires the largest amount of heat to liberate the CO<sub>2</sub> from the solvent.

A theoretical parametric study [Abu-Zahra, 2007] indicated that solvent flow rates required for a MEA system for CO<sub>2</sub> capture are of the order of 20 m<sup>3</sup>/metric ton of CO<sub>2</sub> (CO<sub>2</sub> loading in the range of 0.05 kg/kg of solution), with a thermal heat required in the range of 4 GJ/metric ton of CO<sub>2</sub> removed. The presence of water (~70% wt) in the MEA-based solvent is the major cause of energy usage above that required for desorption of the CO<sub>2</sub> and heating the amine solution to saturation temperature. Unfortunately, the use of more concentrated MEA solution leads to severe equipment-corrosion problems. Due to its lowest molecular weight, MEA has the highest theoretical absorption capacity and the lowest boiling point of primary amines, which may promote solvent carryover in the CO<sub>2</sub> removal and regeneration steps. Other drawbacks of MEA are that the flue gas must contain very low levels of NO<sub>x</sub> and SO<sub>x</sub> before it is scrubbed with MEA (because these species react with the amine to form stable, non-regenerable salts, causing a steady loss of the amine), and its high reactivity with carbon oxysulfide (COS) and carbon disulfide (CS<sub>2</sub>), which degrades the solvent.

In the CO<sub>2</sub> stripping process with MEA/water solutions, the flue gas needs to be treated at low pressures and cooled down to temperatures of 40-50°C (104-122°F) because lower temperatures are favored by the

exothermic absorption process and to minimize solvent loss, with regeneration at treatment temperatures of 90-130°C (194-266°F). It is estimated that the energy requirement for the MEA solution process would cause a decrease in power plant efficiency of up to 16% [Cifre, 2008]. The compression of the captured CO<sub>2</sub> for pipeline transport to a storage site would cause an additional decrease in power plant efficiency of 3 to 4%-points. For MEA system implementation, a high-efficiency desulphurization unit will be required to meet stringent SO<sub>x</sub> levels limits for the amine scrubber (10 to 30 mg/Nm<sup>3</sup>), which are lower than limits typically imposed by current environmental regulations. Additionally, to prevent corrosion, it is recommended that the flue gas be treated for NO<sub>2</sub> concentration to be below 20 ppm<sub>v</sub> (dry) [Fluor Daniel, 1991]. Corrosion control is very important in the MEA process, requiring corrosion inhibitors, low concentrations of the MEA solution and appropriate construction materials. The MEA-based process can achieve CO<sub>2</sub> recoveries in excess or 85%, with CO<sub>2</sub> purity levels over 99% by volume.

## **CONVENTIONAL THERMAL INTEGRATION OF POST-COMBUSTION CO<sub>2</sub> CAPTURE PROCESS**

A schematic representation of the conventional thermal integration of the post-combustion CO<sub>2</sub> capture process with the steam turbine cycle is presented in Figure 4-2. The steam required to supply heat to the reboiler is extracted from a crossover between the intermediate pressure (IP) and low pressure (LP) turbine sections.

Since the steam temperature at the extraction point for CO<sub>2</sub> capture process is too high (348.2°C or 658.7°F, for Somerset) to be used in the reboiler, the extracted steam is first expanded through a Let-Down Steam Turbine Generator (LSTG) to a pressure of 324 kPa (47 psia). This pressure was selected based on a reboiler pressure optimization reported in [Ciferno, 2006]. The steam leaving the LSTG is desuperheated to 134.7°C (274.4°F) using condensate from the reboiler. Desuperheating is used to ensure temperature of the steam entering the reboiler would not exceed the value that would promote MEA carryover into the CO<sub>2</sub> stream or cause MEA decomposition (thermal degradation). Desuperheated steam is condensing in the reboiler, transferring its latent heat to the solvent, and leaves the reboiler as a saturated liquid (condensate) at 310 kPa and 134.7°C (45 psia and 274.4°F). A condensate pump is used to increase its pressure to 883 kPa (128 psia), the same as the deaerator pressure. Part of the condensate is recycled to the desuperheater to maintain constant steam temperature at the reboiler inlet as unit load and other operating conditions change. The rest enters the deaerator, supplying additional heat. The conventional thermal integration scheme and compression train employing multi-stage inline CO<sub>2</sub> compressors were used as the benchmark for the calculations in this study. This scheme is referred to as conventional MEA integration (Conventional MEA) or Case 1 in this study.

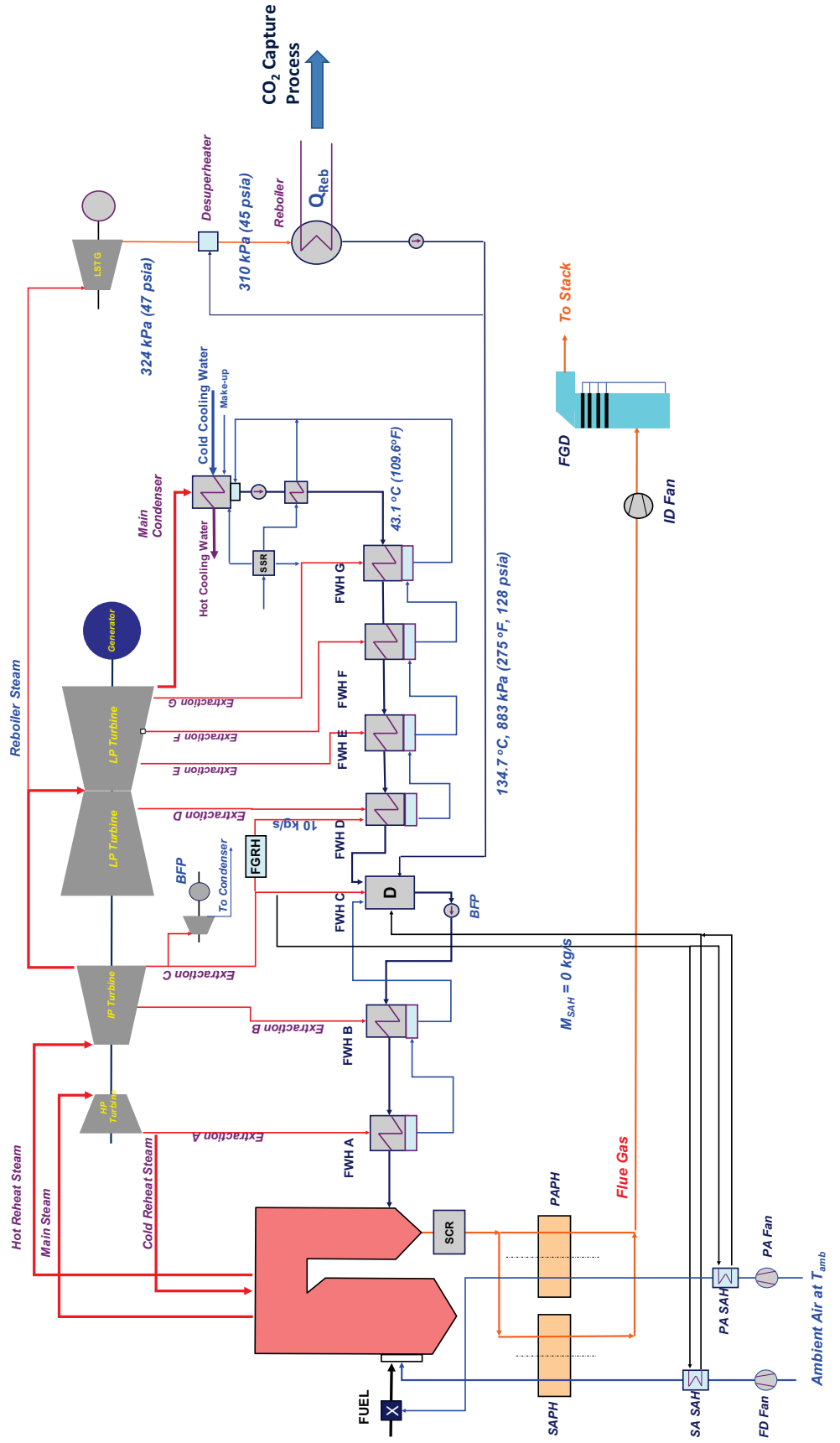


Figure 4-2. Conventional Thermal Integration of the Post-Combustion CO<sub>2</sub> Capture Process.

Calculations were performed over a range of boiler thermal duties, presented in Table 4-1, covering previous generation of amines, state-of-the art-amines, advanced amines, and results obtained by modeling of the MEA-based post-combustion CO<sub>2</sub> capture process (see Section 5 of this study). All values of reboiler thermal duty in Table 4-1 are benchmarked to 90% CO<sub>2</sub> capture efficiency.

**Table 4-1. Values of Reboiler Thermal Duty Used in the Analysis.**

Reboiler Thermal Duty		
BTU/lb CO <sub>2</sub>	GJ/tCO <sub>2</sub>	Comment
2,350	5.47	Previous Generation
2,000	4.65	ASPEN Simulation
1,800	4.19	
1,700	3.95	
1,550	3.60	State-of-the Art
1,400	3.26	Advanced Amines
1,200	2.79	

The results are presented in Figures 4-3 to 4-6. The reduction in total gross power output (main steam turbine generator + LSTG) determined for the host unit, presented in Figure 4-3 as a function of the reboiler thermal duty ( $q_{Reb}$ ), represents reduction in turbine gross power output due to steam extraction for the reboiler. As the results presented in Figure 4-3 show,  $q_{Reb}$  has a major effect on the gross power output because steam extraction for the reboiler decreases linearly as  $q_{Reb}$  is decreased, Figure 4-4 (LP turbine exhaust flow decreases). For the state-of-the-art amines, gross power output is reduced by 14.7% compared to the baseline case (no CO<sub>2</sub> capture). For the  $q_{Reb}$  value determined for MEA in this study, the reduction in gross power output is approximately 19.6%.

The results are also shown for the case where CO<sub>2</sub> compression power was subtracted from the gross power output to illustrate combined effect of CO<sub>2</sub> compression and steam extraction on power output. For the state-of-the-art amines, power output (gross power output – CO<sub>2</sub> compression power) is reduced by 24.1% compared to the baseline case (no CO<sub>2</sub> capture). For the  $q_{Reb}$  value determined for MEA in this study, the reduction in power output is 29%.

Unless noted otherwise, the results on total gross power output will be presented in this report.

The increase in turbine cycle heat rate relative to the baseline (no CO<sub>2</sub> capture) is presented in Figure 4-5 as a function of the reboiler thermal duty. As  $q_{Reb}$  decreases, penalty to the turbine cycle performance decreases because the steam extraction for the reboiler decreases (see Figure 4-4). For the state-of-the art amines, turbine cycle heat rate is 17.2%-points higher, relative to the baseline case. For the  $q_{Reb}$  value determined for the MEA in this study, the increase in turbine cycle heat rate is approximately 24.3% higher compared to the baseline (7.1%-point difference).

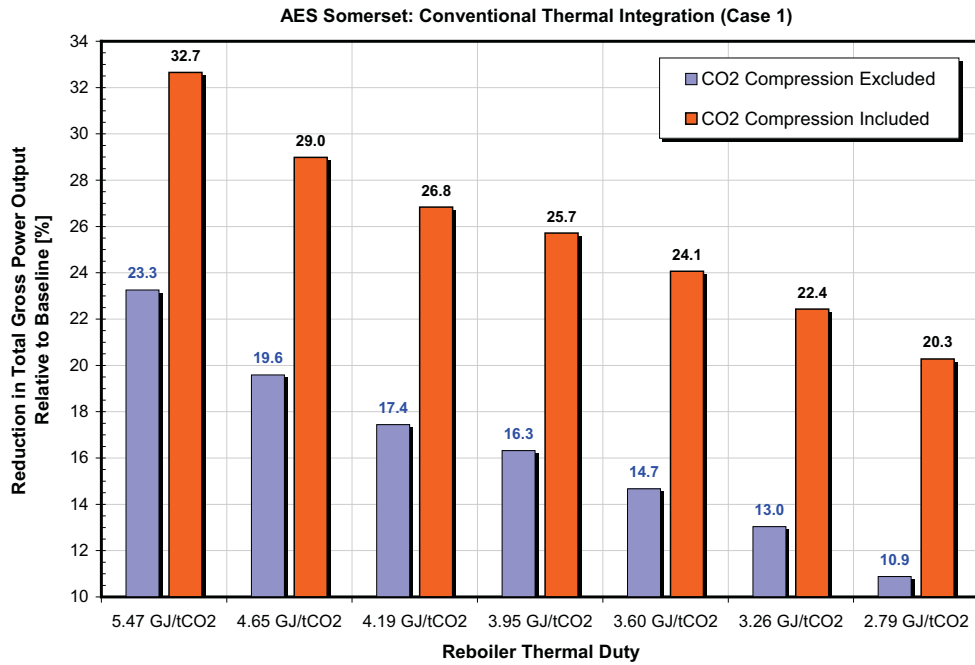


**Figure 4-3. Reduction in Total Gross Power Output due to Conventional CO<sub>2</sub> Capture Relative to Baseline.**

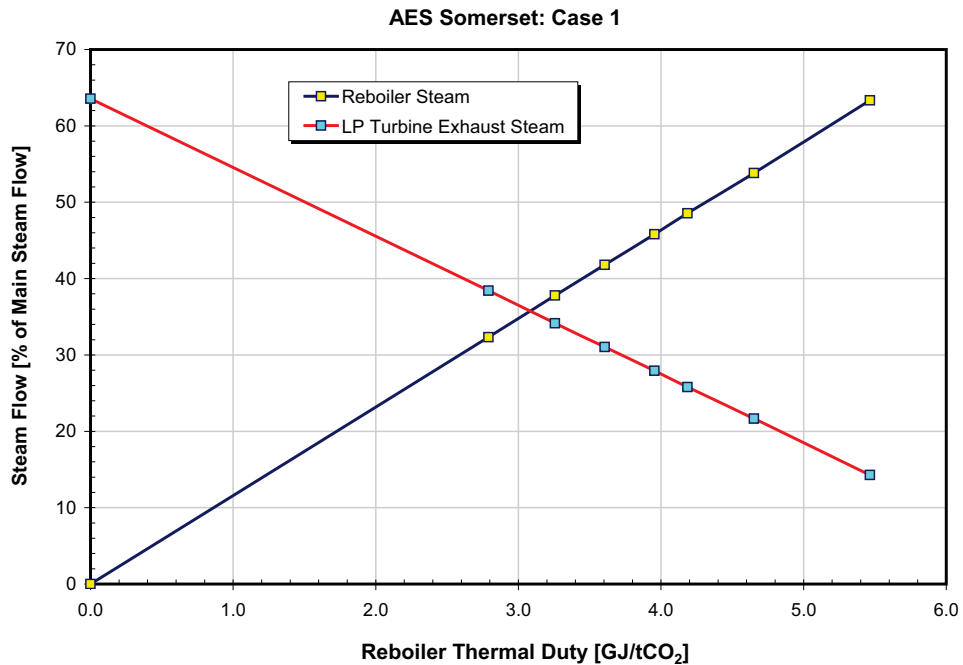


**Figure 4-4. Steam Extraction for the Reboiler and LP Turbine Exhaust Flow as Functions of Reboiler Thermal Duty.**

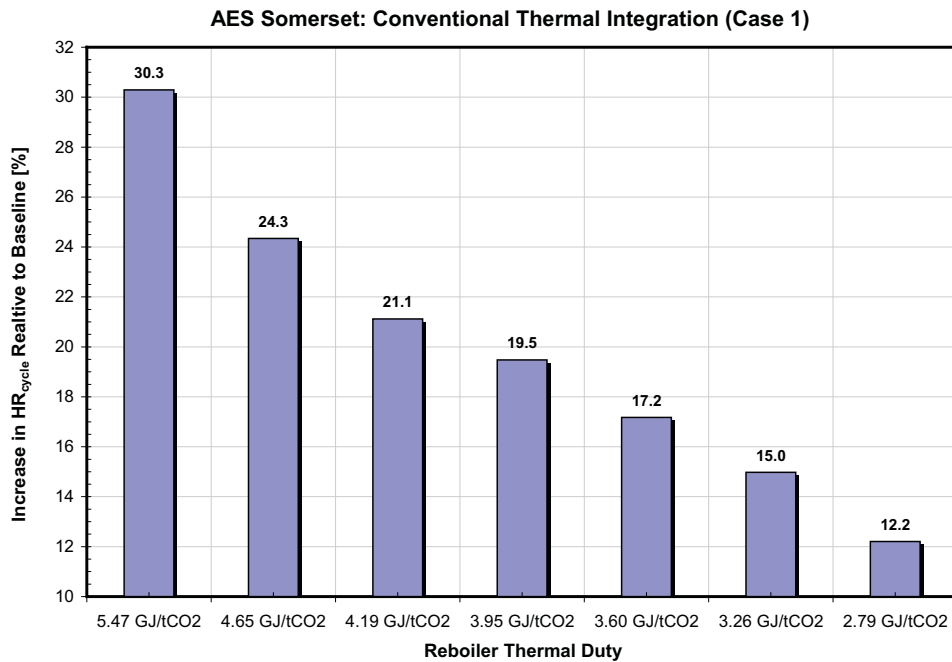


**Figure 4-5. Increase in Turbine Cycle Heat Rate due to Conventional CO<sub>2</sub> Capture Relative to Baseline.**

The decrease in turbine cycle efficiency relative to the baseline (no CO<sub>2</sub> capture) is presented in Figure 4-6 as a function of the reboiler thermal duty. As  $q_{Reb}$  decreases, penalty to the turbine cycle performance due to reboiler steam extraction decreases. For the state-of-the art amines, turbine cycle efficiency is 6.2%-points lower relative to the baseline case. For the  $q_{Reb}$  value determined for the MEA in this study, the decrease in turbine cycle efficiency is approximately 8.3%-points compared to the baseline (no CO<sub>2</sub> capture). Hence, there is a 2.1%-point difference between the state of the art amine and amine used in this study.

Efficiency,  $\eta$ , is defined as:

$$\eta = 3,600/HR \times 100\% \quad \text{Equation 4-1}$$

Where the quantity HR is heat rate expressed in kJ/kWh, and 3,600 is a energy conversion constant in kJ/kWh.

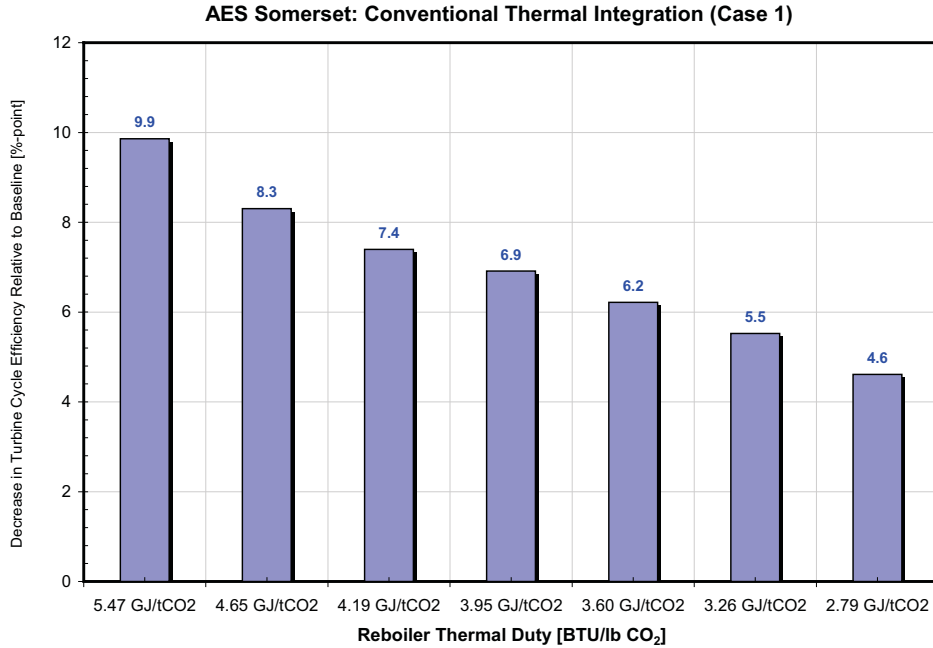


**Figure 4-6. Decrease in Turbine Cycle Efficiency due to Conventional CO<sub>2</sub> Capture Relative to Baseline.**

The increase in net unit heat rate relative to the baseline (no CO<sub>2</sub> capture) is presented in Figure 4-7 as a function of the reboiler thermal duty. As  $q_{\text{Reb}}$  decreases, penalty to unit performance due to the reboiler steam extraction decreases. For the state-of-the art amines, net unit heat rate is 34% higher relative to the baseline case.

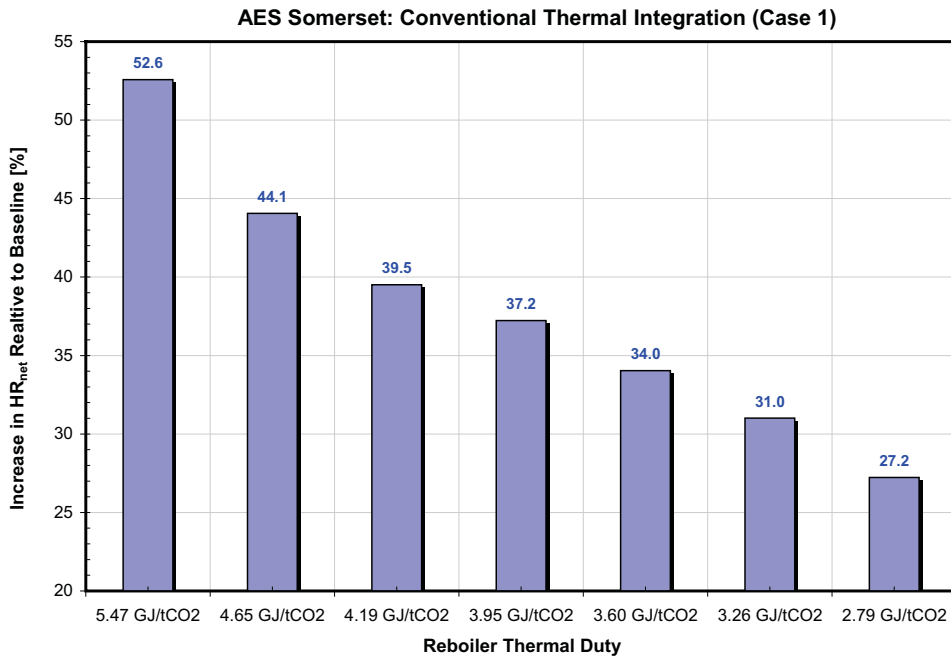


**Figure 4-7. Increase in Net Unit Heat Rate due to Conventional CO<sub>2</sub> Capture Relative to Baseline.**

For the  $q_{Reb}$  value determined for the MEA in this study, the increase in net unit heat rate is approximately 44.1% compared to baseline (10.1%-point difference between the state of the art and amine used in this study). The CO<sub>2</sub> compressor power was included in the net unit heat rate and net unit efficiency calculations.

The decrease in net unit efficiency relative to the baseline (no CO<sub>2</sub> capture) is presented in Figure 4-8 as a function of the reboiler thermal duty. As  $q_{Reb}$  decreases, penalty to unit performance due to the reboiler steam extraction decreases. For the state-of-the art amines, net unit efficiency is 8.8%-points lower relative to the baseline case. This value compares favorably to the 10.6% reduction in net unit efficiency reported in [Ciferno, 2006] for a 430 MW unit. For the  $q_{Reb}$  value determined for the MEA in this study, the decrease in net unit efficiency is approximately 10.6%-point higher compared to baseline (1.8%-point difference between the state of the art and amine used in this study).

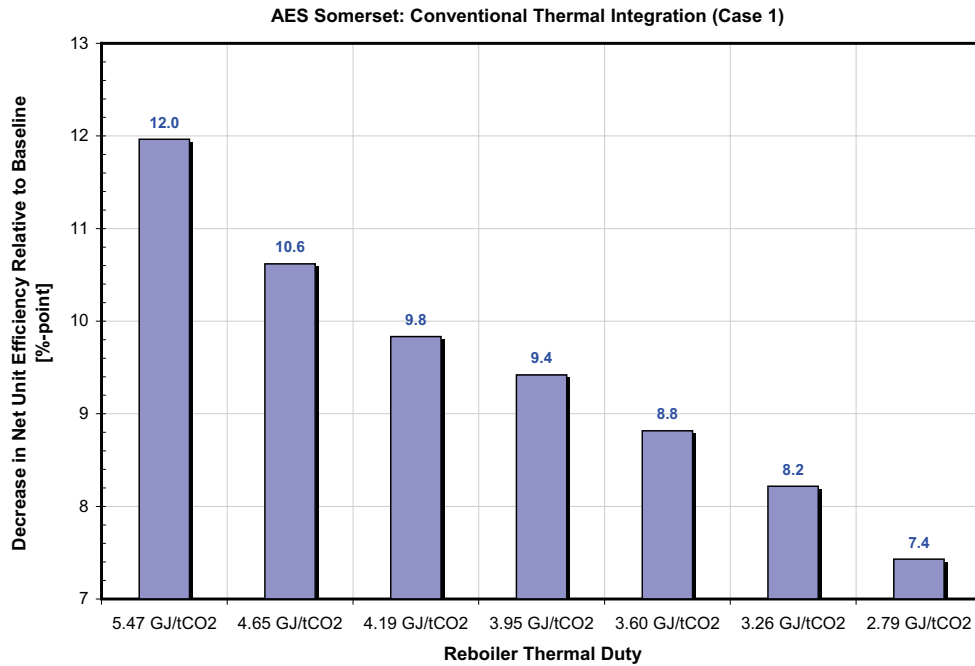


**Figure 4-8. Decrease in Net Unit Efficiency due to Conventional CO<sub>2</sub> Capture Relative to Baseline.**

## ADVANCED THERMAL INTEGRATION OF POST-COMBUSTION CO<sub>2</sub> CAPTURE PROCESS

A schematic representation of advanced thermal integration of the post-combustion CO<sub>2</sub> capture process with the steam turbine cycle is presented in Figure 4-9. The advanced integration process is similar to the conventional integration, except that condensed steam leaving the reboiler flows through a heat exchanger located between the LSTG and reboiler to desuperheat the steam entering the reboiler (see Figure 4-9).

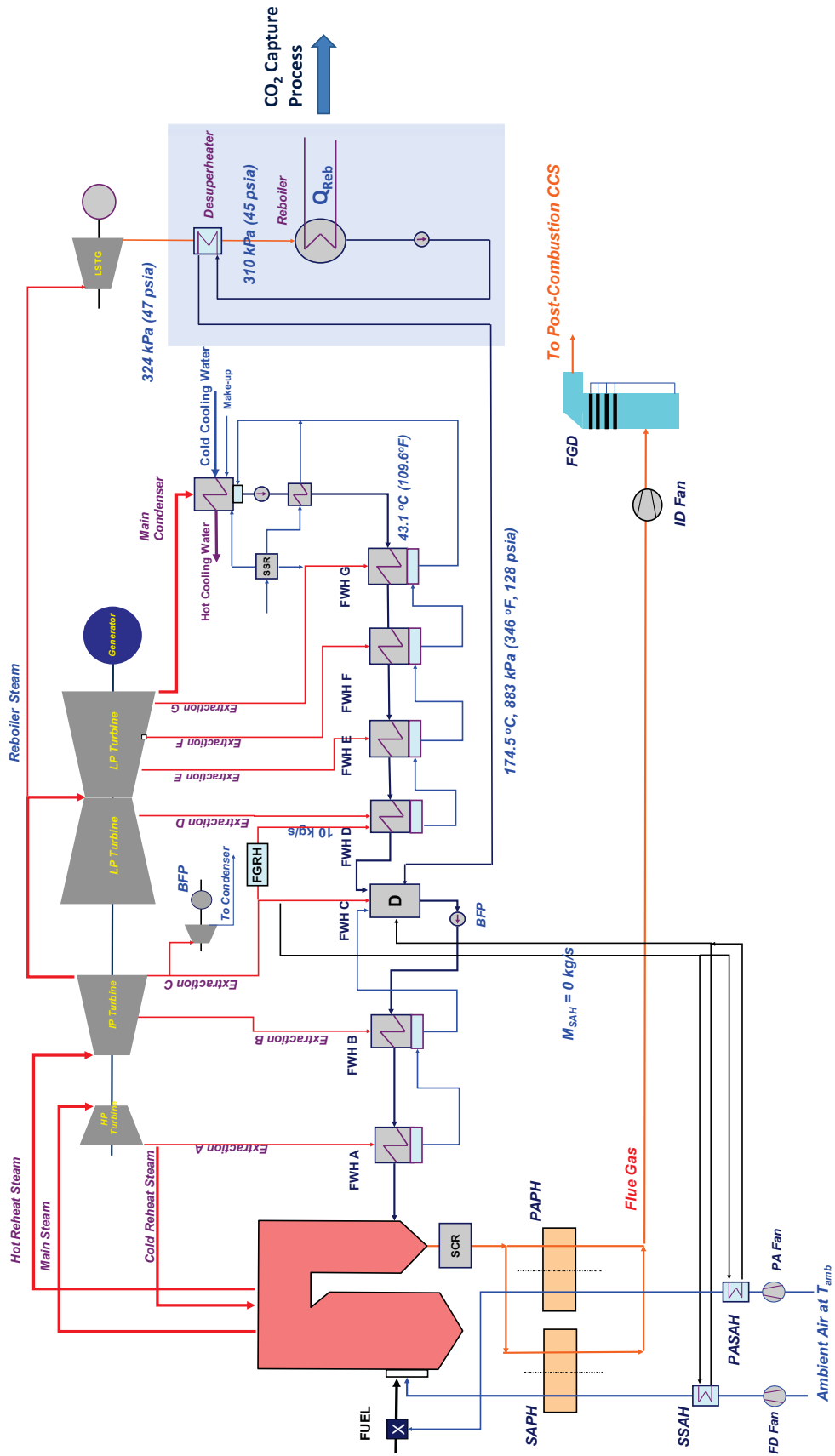
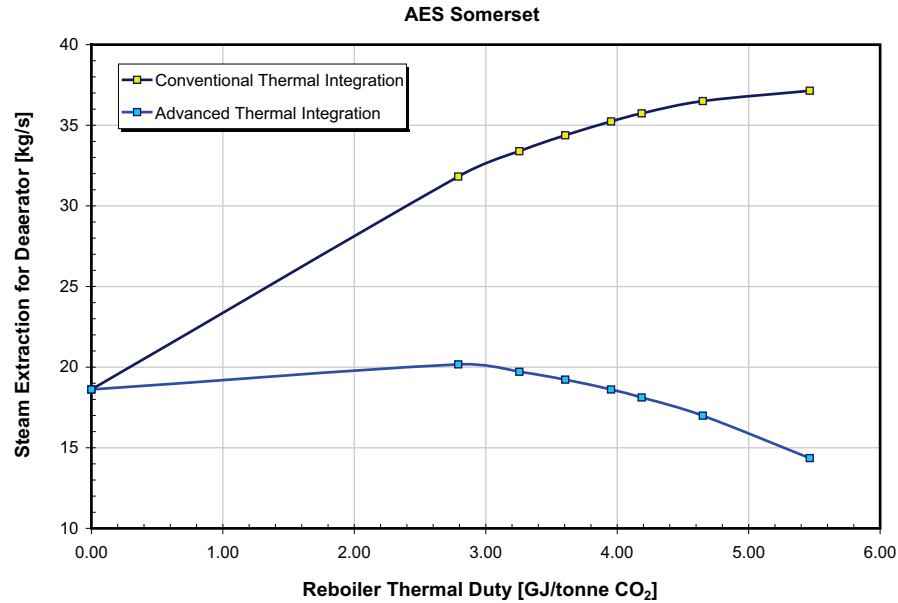


Figure 4-9. Advanced Thermal Integration of Post-Combustion CO<sub>2</sub> Capture Process.

In this configuration the desuperheat heat is used to increase the temperature of the condensate leaving the reboiler from 134.7 to 174.5°C (274.4 to 346°F). The heated condensate enters the deaerator supplying additional heat, which results in lower steam extraction from the main steam turbine for the deaerator (see Figure 4-10), higher turbine power output and better turbine cycle heat rate. The advanced thermal integration is also referred to as Advanced MEA integration or Case 2 in this study. The same thermal integration of the post-combustion CO<sub>2</sub> capture system with the steam turbine cycle was proposed by the University of Stuttgart [Cifre, 2009].



**Figure 4-10. Steam Extraction for the Deaerator: Conventional and Advanced Thermal Integration.**

The results of analysis performed for conventional and advanced thermal integration (Cases 1 and 2) are compared in Figures 4-11 to 4-15. The reduction in total gross power output relative to the baseline (no CO<sub>2</sub> capture) and the absolute difference between the advanced and conventional thermal integrations are presented in Figure 4-11 as functions of the reboiler thermal duty. The results show that in case of the advanced thermal integration, the gross steam turbine power output is higher by 0.33 to 0.72%-points compared to the conventional thermal integration, with smaller improvements corresponding to lower  $q_{Reb}$  values and larger improvements to higher  $q_{Reb}$  values. For the state-of-the-art amines, improvement in the gross power output is 0.41%-points compared to the conventional thermal integration. For the  $q_{Reb}$  value determined for the MEA in this study, improvement associated with use of advanced thermal integration in the gross power output is approximately 0.53%-points.

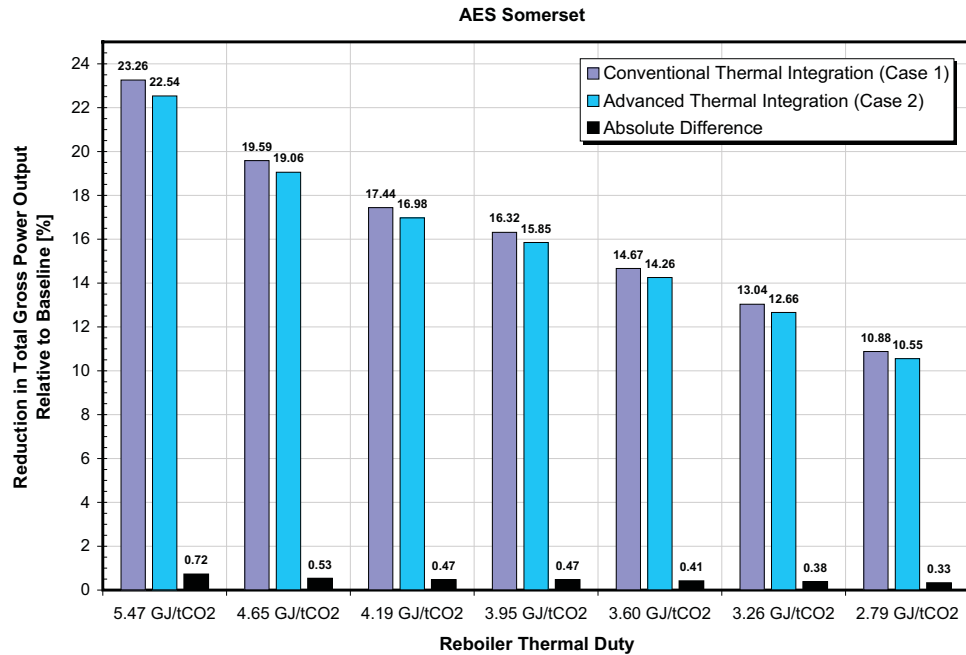


**Figure 4-11. Increase in Total Gross Power Output Relative to Baseline.**

The increase in turbine cycle heat rate and decrease in turbine cycle efficiency relative to the baseline (no CO<sub>2</sub> capture) are presented in Figures 4-12 and 4-13 as functions of reboiler thermal duty. The difference between the advanced and conventional thermal integration is also shown. For the advanced thermal integration and state-of-the-art amines, the increase in turbine cycle heat rate, relative to the baseline is 0.56%-points and the decrease in turbine cycle efficiency is 0.17%-points. For the  $q_{Reb}$  value determined for the MEA in this study, the increase in turbine cycle heat rate is 0.81%-points and the decrease in turbine cycle efficiency is 0.22%-points.

Figures 4-14 and 4-15 show the increase in net unit heat rate and decrease in net unit efficiency relative to the baseline (no CO<sub>2</sub> capture) as functions of the reboiler thermal duty. The difference between the advanced and conventional thermal integration is also presented. For the advanced thermal integration, the increase in net unit heat rate relative to the baseline is 0.77%-points and the decrease in net unit efficiency is 0.43%-points. For the  $q_{Reb}$  value, determined for the MEA in this study, the increase in net unit heat rate is 1.15%-points and the decrease in net unit efficiency is 0.56%-points. These results are in a good agreement with results reported in [Cifre, 2009], where improvement in net unit efficiency of 0.3 to 0.4%-points was predicted for advanced amines.

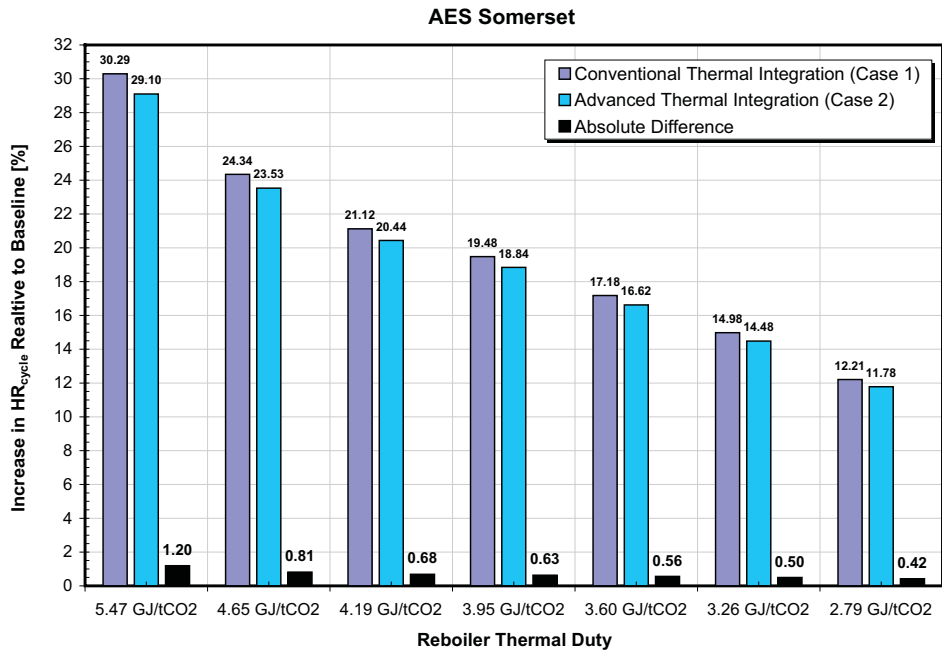


**Figure 4-12. Increase in Turbine Cycle Heat Rate Relative to Baseline.**

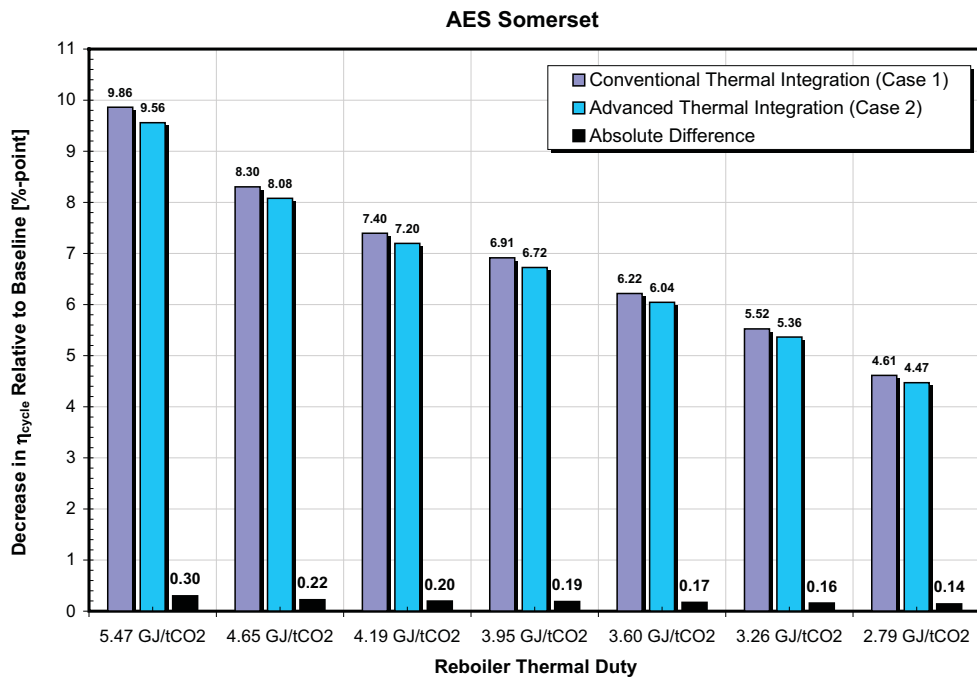


**Figure 4-13. Improvement in Turbine Cycle Efficiency Relative to Baseline.**

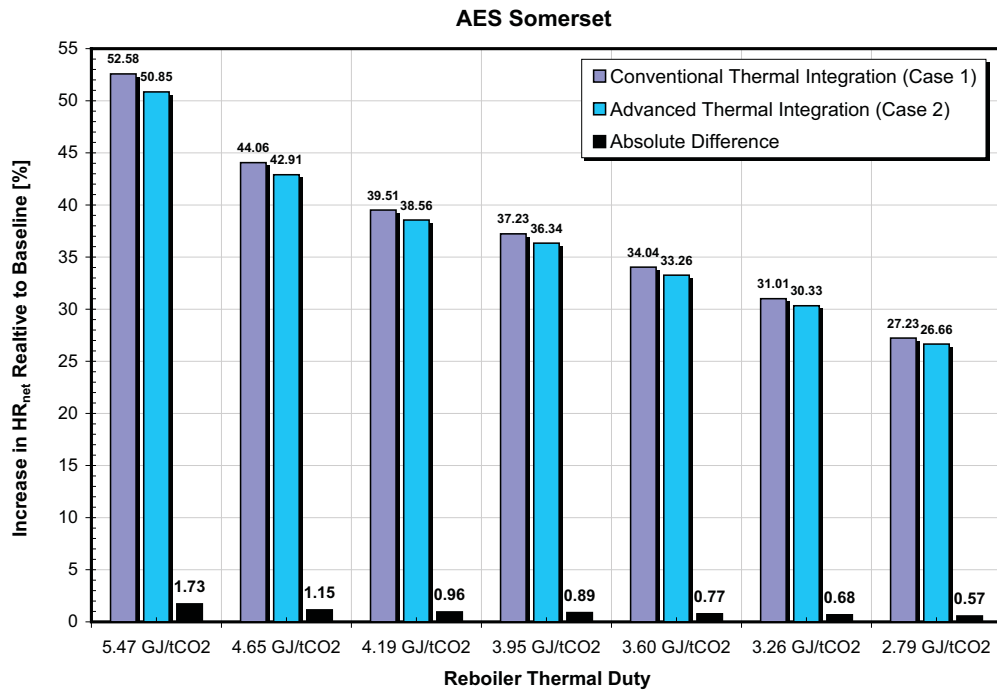


**Figure 4-14. Increase in Net Unit Heat Rate Relative to Baseline.**

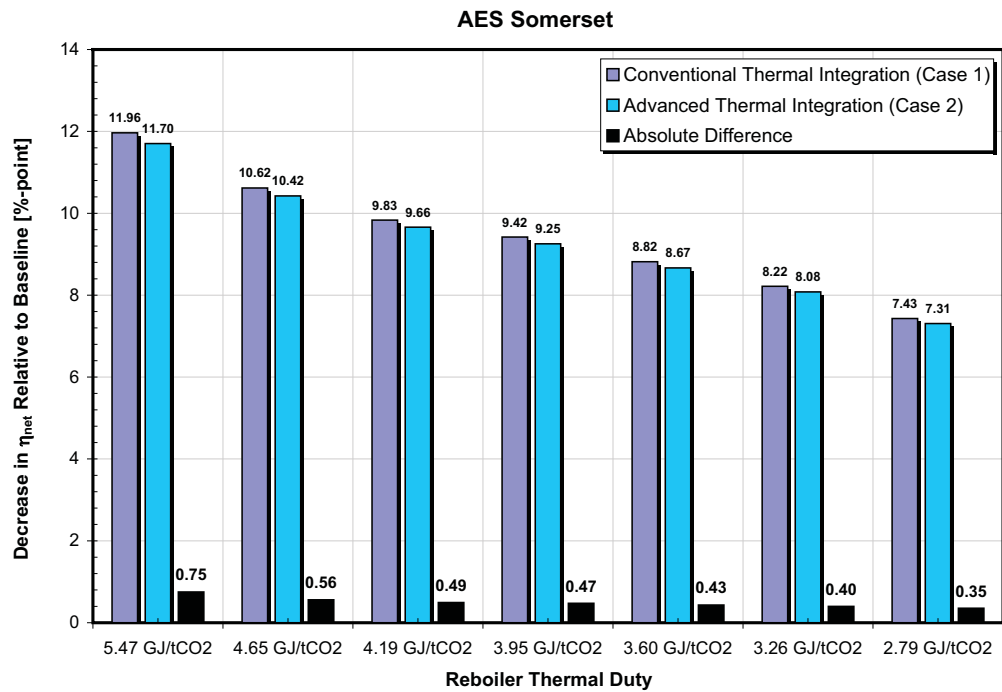


**Figure 4-15. Decrease in Net Unit Efficiency Relative to Baseline.**

The results presented in Figures 4-11 to 4-15 illustrate the effect of improved thermal integration of a post-combustion CO<sub>2</sub> capture system with the steam turbine cycle on plant performance. Furthermore, the results show the importance of developing advanced solvents having lower regeneration energy requirements.

Considering the fact that theoretical minimum energy required for solvent regeneration, based on free energy of mixing calculation (14% CO<sub>2</sub>, 300 K, 1 atm), is about 0.116 GJ/tCO<sub>2</sub> (50 Btu/lb CO<sub>2</sub>) [Stanford University, 2005] and keeping in mind that parameters such as mass transfer coefficient, gas-to-liquid contact area, driving forces, CO<sub>2</sub> carrying capacity of the solvent, reaction rate, sensible heat needed to heat the solvent and evaporate the water add to the theoretical energy requirement, there is room for considerable improvement.



**POST-COMBUSTION CO<sub>2</sub> CAPTURE AND PROCESS MODELING****STATUS OF DEVELOPMENT**

The current development status of the MEA absorption process is that all major components of the CO<sub>2</sub> absorption/desorption process are commercially available but at a smaller scale, and they need to be integrated and optimized for full-scale applications in power plants. The largest industrial application of the MEA process captures about 1,000 tons of CO<sub>2</sub> per day (tCO<sub>2</sub>/d). For comparison, a 500 MW<sub>e</sub> coal-fired unit would require a capacity of roughly 9,000-10,000 tCO<sub>2</sub>/d, assuming 90% CO<sub>2</sub> capture. The most widely used chemical absorption process with MEA is the Fluor Daniel Econamine FG process, with 21 plants built (capacities of plants range from 6 to 1,200 t CO<sub>2</sub>/day). Fluor Daniel markets these CO<sub>2</sub> capture technology's as Econamine FG™ and Econamine FG Plus™ processes. The Fluor Econamine process uses an inhibited 30% by weight MEA solution (for corrosion mitigation) and operates at 55°C and 1 atm. This process can recover between 85-90% CO<sub>2</sub> in a typical flue gas, while producing a product of >95% pure CO<sub>2</sub>. The Electric Power Research Institute (EPRI) and Fluor Daniel studied [Fluor, 1991] MEA retrofits for 20, 50 and 90% CO<sub>2</sub> removal on an existing and new 500 MW<sub>e</sub> PC-fired plant. In the 90% CO<sub>2</sub> removal retrofit case 110 MW<sub>e</sub> (22 MW<sub>e</sub> of power for scrubbing, 51 MW<sub>e</sub> for CO<sub>2</sub> compression and 38 MW<sub>e</sub> for auxiliaries) was the estimated power requirement with a reduction in unit efficiency from 35 to 23%, and an increase in the cost of electricity (COE) in excess of 100% (4.2 to 9.3 cents/kWh).

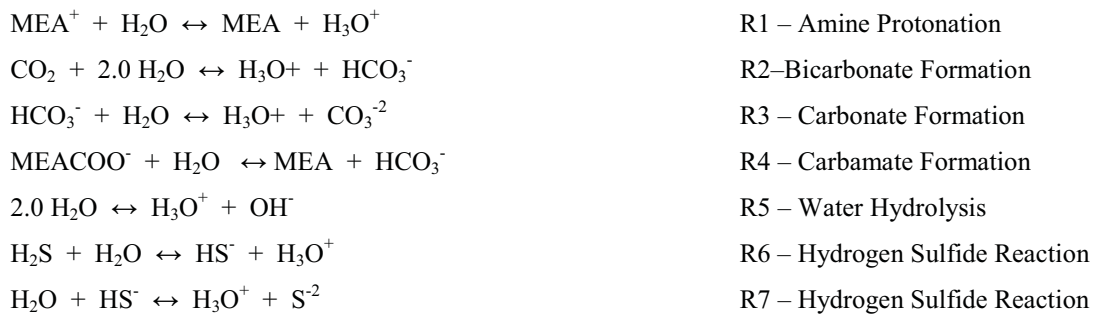
Another MEA-based commercial system that has been studied for full-scale applications is the Kerr-McGee/ABB Lummus amine process. This process uses a 15-20% by weight MEA solution with no inhibitors. The lack of inhibitors requires the use of stainless steel equipment. This process can recover >96% of CO<sub>2</sub> from typical flue gas, with a product stream of 95-98% pure CO<sub>2</sub>. The Kerr-McGee/ABB Lummus technology has been installed at 3 plants with capacities ranging from 200 to 800 tCO<sub>2</sub>/d. Operating temperatures for this process are 40-60°C for the absorbing column and 100-140°C for the regeneration stage.

Alstom Power Inc. teamed up with American Electric Power (AEP), ABB Lummus Global, Inc, the DOE and the Ohio Coal Development Office (OCDO) to conduct a study to evaluate the feasibility of this technology applied to an existing PC-fired plant. The analysis for this case showed a decrease in overall plant thermal efficiency of 60% (35% to 21%), with net MW<sub>e</sub> reduction of 132 MW<sub>e</sub> (or 28% from the baseline case). CO<sub>2</sub> recovery was found at 96% with a liquid CO<sub>2</sub> product stream with 99.95% purity [Nsakala, 2006].

## MEA PROCESS MODELING

Several researchers have modeled the MEA absorption process, with most of the conclusions focusing on reducing the thermal energy requirement of the system [Rao, 2002], [Chapel, 1999], [Alie, 2005], [Singh, 2003], [Mohammad, 2007] and [Cifre 2009]. Chapel, 1999 reported results of modeling of the Econamine FG™ process. The required regeneration energy from this study was 4.2 GJ/tCO<sub>2</sub>. Alie, 2005 proposed a flow sheet decomposition method for MEA system simulation, finding a lowest energy requirement of 4.0 GJ/tCO<sub>2</sub>. An effort was made in these simulations to keep a water balance in the system. Singh, 2003 modeled the MEA process for a 400 MW<sub>e</sub> coal-fired plant, finding a baseline specific thermal energy requirement equal to 3.8 GJ/tCO<sub>2</sub>. Mohammad, 2007 performed an analytical MEA system optimization for a 600 MW<sub>e</sub> coal-fired power plant aimed at reducing the energy requirement for solvent regeneration. It was found that by optimizing the lean solvent loading, the amine solvent concentration and the stripper operating pressure, a minimal energy requirement of 3.0 GJ/tCO<sub>2</sub> was obtained, lower than the base case of 3.9 GJ/tCO<sub>2</sub>. Optimal solvent process conditions, however, might not be realizable for the MEA solution, due to constraints imposed by corrosion and solvent degradation. Cifre, 2009 included results of simulations performed for a 600 and 1,000 MW<sub>e</sub> plants. This study targeted improvements in overall power plant performance. Optimization results were included that show optimized energy demand for regeneration for both plants at approximately 4.1 GJ/tCO<sub>2</sub>. These results included improvements in plant cycle efficiency by the use of modified CO<sub>2</sub> compression and extraction steam attemperation.

In this study, modeling of a MEA-based CO<sub>2</sub> capture system for a coal-fired unit was performed using the software ASPEN Plus version 2006.5 [Aspen Technology, 2006]. ASPEN is used for the design, simulation and optimization of chemical and coal power processes. The MEA-CO<sub>2</sub> capture system was modeled as a steady-state flow system, operating under equilibrium conditions. The RADFRAC subroutine of ASPEN was used for solution of the equilibrium chemistry. The thermodynamics and transport properties were modeled using the named “MEA Property Insert” feature in ASPEN, which describes the MEA-H<sub>2</sub>O-CO<sub>2</sub> thermodynamic system, included the electrolytes. The equilibrium reactions included in this model are:



The unit modeled in this project was Somerset Unit 1. Somerset Unit 1 is a 655 MW<sub>e</sub> pulverized coal-fired boiler located in town of Somerset in Niagara County, New York on the shore of Lake Ontario. This unit reported annual CO<sub>2</sub> emissions of approximately 5.07 million tCO<sub>2</sub> (2006), or 655 kg/MWh<sub>e</sub> (assuming a 0.85 capacity factor). The unit fires the Pittsburgh No. 8 bituminous coal, with an average wet CO<sub>2</sub> concentration in the flue gas of approximately 13% by volume. The flue gas conditions and composition entering the MEA system model are included in Table 5-1.

**Table 5-1. Flue Gas Conditions and Composition.**

<b>Flue Gas Conditions</b>		
Mass Flow Rate	kg/s	<b>770.2</b>
Pressure	kPa	<b>101</b>
Temperature	°C	<b>128.3</b>
<b>Composition</b>		
CO <sub>2</sub>	% vol	<b>13.17</b>
H <sub>2</sub> O	% vol	<b>6.42</b>
O <sub>2</sub>	% vol	<b>4.51</b>
SO <sub>2</sub>	% vol	<b>0.21</b>
N <sub>2</sub>	% vol	<b>75.69</b>

A detailed ASPEN diagram of the MEA-CO<sub>2</sub> absorption system model is presented in Figure 5-1. The flue gas from the power plant flows into a contact cooler (COOLER1), then the flue gas passes a separator (SEP) and are transported with a gas blower to overcome the pressure drop caused by the MEA absorber. Another heat exchanger (COOLER2) is used to set the temperature of the flue gas at the inlet of the absorber in the range from 30 to 60°C. A packed bed absorber is used for the aqueous MEA solution to react chemically with the CO<sub>2</sub> in the flue gas. The absorber was simulated using 12 equilibrium stages at 180 kPa, and a temperature at the top stage of 65°C (as determined by the exothermic reaction in the absorber tower). The treated flue gas (TREATGAS) is released from the top stage of the absorber. A water wash scrubber has been used in some simulations in the literature to recover water and MEA vapor to decrease solvent losses. This option was not used in these simulations. Instead, the CO<sub>2</sub> concentration in the clean exhaust flue gas stream was set at 1.0% by volume.

The rich solvent containing chemically bound CO<sub>2</sub> is pumped to the stripper via a rich/lean crossflow heat exchanger (setup using the COOLER3/COOLER4 arrangement), which heats the rich solvent to a temperature (90°C) close to the stripper operating temperature. This arrangement contributes at reducing the thermal duty of the stripper reboiler unit. The chemical solvent is regenerated in the stripper. The stripper was simulated with an operating pressure in the range from 100 to 200 kPa. The temperature of the stripper is set by its operating pressure. Four equilibrium stages were found adequate in achieving equilibrium conditions in the stripper, with the rich amine solution entering at the 1<sup>st</sup> stage. An integrated stripper/reboiler design was used from the ASPEN library of components. Heat is supplied to the reboiler

using low-pressure steam. It is recommended that the reboiler temperature should not exceed 122°C to prevent MEA degradation and avoid corrosion from becoming significant [Cifre, 2009]. The heat provided by the reboiler is used to heat the solvent, produce steam that acts as stripping gas and to provide the required desorption heat for the removal of the chemically-bound CO<sub>2</sub>. A condenser (COOLER5) and flash tank at the outlet of the stripper are used to recover CO<sub>2</sub> and MEA, with the concentrated CO<sub>2</sub> stream (COLDCO2) leaving at an outlet temperature of 25°C. The purity of the CO<sub>2</sub> product stream was set at >98%. Finally, the lean solvent flows back to the absorber through a mixer, where make-up MEA solution is added, and via the rich/lean cross heat exchanger arrangement and an additional cooler (COOLER6). This cooler brings the temperature of the lean amine solution further down to the absorber level.

Initial conditions for the CO<sub>2</sub> scrubbing process using MEA were set as follows:

- CO<sub>2</sub> removal, 90% by weight
- Aqueous solution preparation, 30% by weight MEA
- Concentrated CO<sub>2</sub> stream purity, >98%
- CO<sub>2</sub> concentration in clean flue gas, <1.0%
- Absorber operating pressure, at 180 kPa
- Stripper operating pressure, 100 kPa
- Absorber flue gas inlet temperature, 40°C

These conditions provided the basis for a reference baseline case, as well as information on baseline values of parameters of interest. Simulation using the baseline conditions specified above resulted in a CO<sub>2</sub> mass recovery of 534 t/h; solvent mass flow rate of 10,793 ton solvent per hour; amine rich and lean loadings (mol CO<sub>2</sub>/mol MEA) of 0.48 and 0.24, respectively; stripper MEA-reboiler and condenser temperatures of 103.0 and 96.3°C, respectively; and a reboiler heat duty of 855.5 MW<sub>th</sub> or 5.76 GJ/tCO<sub>2</sub>. The solvent mass flow rate was mainly determined by the design specification that requires a CO<sub>2</sub> concentration in clean flue gas of less than 1.0%. The energy demand for CO<sub>2</sub> regeneration represents 43.1% of the thermal power of the unit (assuming 33% unit efficiency). The energy requirement for the baseline case of 5.76 GJ/tCO<sub>2</sub> is higher than results obtained by simulations reported by [Alie, 2005], [Chapel, 1999], [Cifre, 2009], [Mohammad, 2007], [Singh, 2003], and [Rao, 2002] which are in the range from 3.8 to 4.2 GJ/tCO<sub>2</sub>. Still, it should be mentioned that this baseline result does not correspond to an optimized design, and the model does not present a system with zero overall water balance. Heating and evaporation of added water for the MEA solution contributes to increase in the energy requirement for the CO<sub>2</sub>-MEA system.

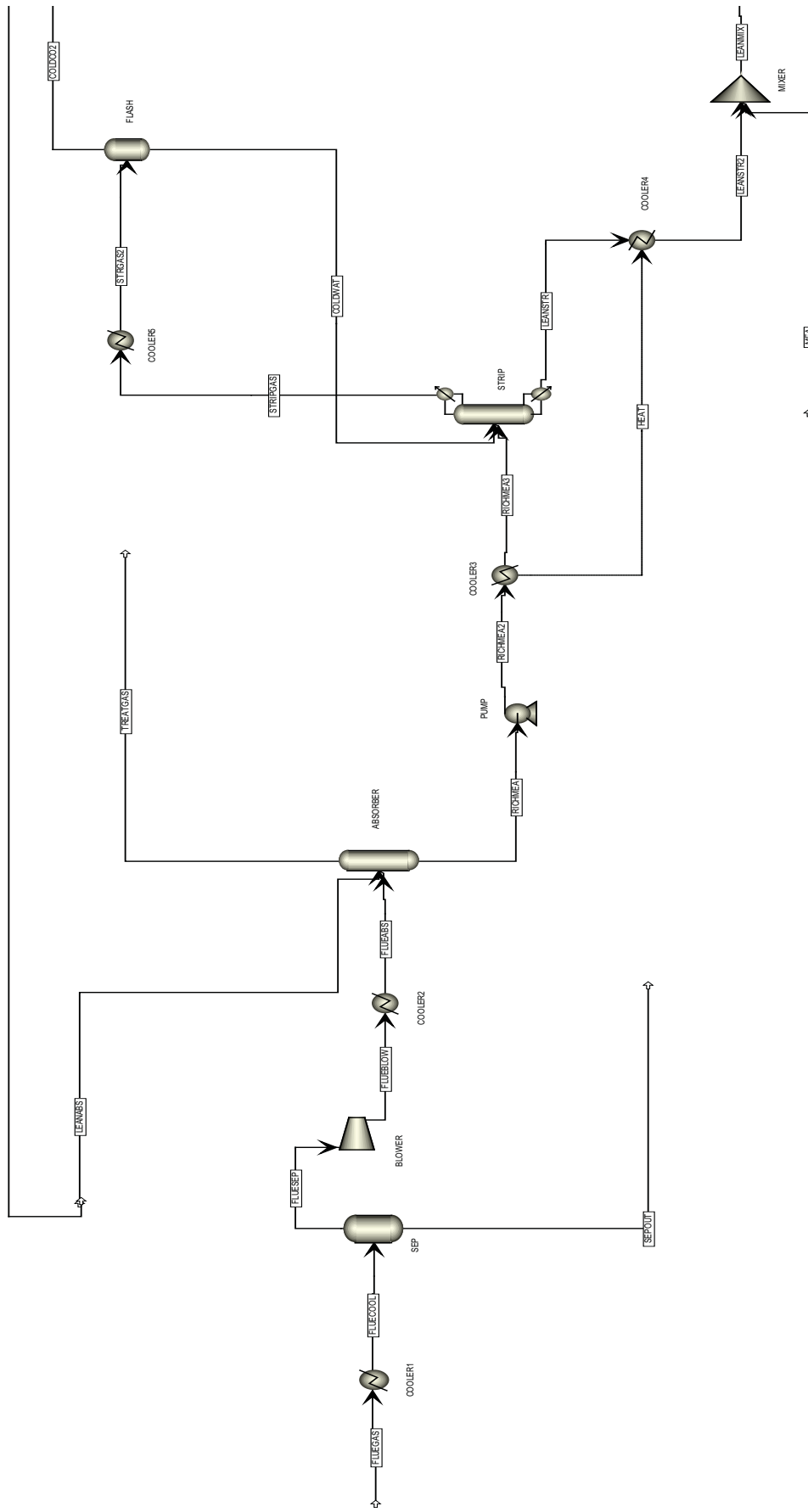


Figure 5-1. ASPEN Model Diagram of the MEA-CO<sub>2</sub> Capture System.

## PARAMETRIC STUDY – DESIGN OPTIMIZATION

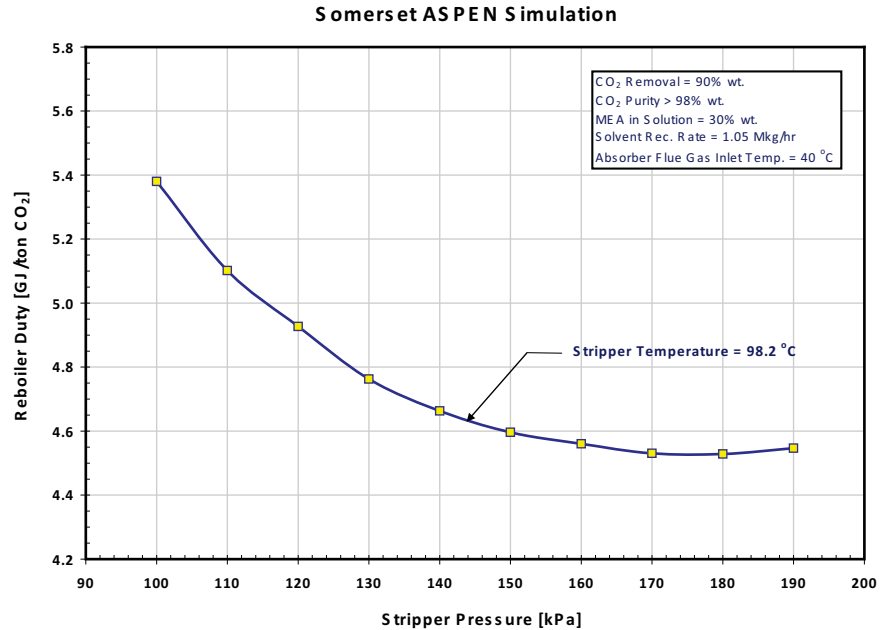
A sensitivity analysis was performed, where parameters that are known to affect the performance of the CO<sub>2</sub> capture process were varied from their baseline level to obtain improvements in the MEA system performance. The following process parameters were varied:

- The stripper operating pressure.
- The solvent circulation rate/the CO<sub>2</sub> lean solvent loading (mol CO<sub>2</sub>/mol MEA).
- The MEA weight percentage in the absorption solvent.
- The CO<sub>2</sub> removal percentage.
- The flue gas/lean solvent temperature.

The indicator used to evaluate the performance of the CO<sub>2</sub> absorption/desorption process was the thermal energy required in the stripper (GJ energy/ton CO<sub>2</sub> removed). This indicator was chosen because it presents information of both the operating and capital costs. The thermal energy is expected to be the major contributor to the MEA-based system production costs. The thermal energy also impacts the amount of solvent required to produce a required CO<sub>2</sub> removal and flue gas purity affect the size of the equipment, and the capital cost of the system.

The effect of the stripper pressure was investigated in a series of simulations that varied the desorber operating conditions from 100 to 200 kPa, while other operating parameters were maintained at baseline conditions. Changes in a stripper pressure are accompanied by changes in absorber temperature. It is expected that at higher operating pressures (and temperature) the CO<sub>2</sub> release from the solvent and amine regeneration is favored. Figure 5-2 shows the reboiler duty in GJ/tCO<sub>2</sub> is reduced with increased stripper pressure. The reboiler duty drops by approximately 0.9 GJ/tCO<sub>2</sub> (a 15.8% reduction) from operating at 100 kPa to operation at 180 kPa. Thus, an optimal stripper operating pressure was chosen at 190 kPa.

Although, higher stripper pressure values would reduce the amount of compression work needed for the CO<sub>2</sub> product stream, higher stripper pressures and temperatures will increase the rich solvent boiling point, requiring steam from the plant thermal cycle with a better quality. Additionally, larger stripper pressures will have an impact on the rich amine pump selection and the design and construction cost of the stripper vessel. It should be mentioned that the maximum stripper temperature obtained at the optimal stripper pressure of 190 kPa was 98.2°C is below the 122°C limit recommended to prevent solvent degradation and corrosion problems.



Results of the sensitivity of the MEA-reboiler duty to solvent flow rate are shown in Figure 5-3. The solvent circulation flow rate was varied by approximately 55 % from 7,115 to 16,115 t/h. The conditions of the other parameters that impact MEA system performance are included in the figure. This sensitivity was achieved by varying the degree of solvent regeneration in the stripper to achieve the same CO<sub>2</sub> removal capacity. The solvent flow rate directly affects the CO<sub>2</sub>/amine lean solvent loading. The results in Figure 5-3 show there is an optimal solvent loading, which was found at 11,539 t/h or 0.24 mol CO<sub>2</sub>/mol MEA. At solvent loadings below the optimal value, the thermal energy required with the stripping steam to regenerate the solvent is high, to be able to achieve a given amount of CO<sub>2</sub> removal. At solvent loadings larger than the optimal value, the energy required to heat up the solution to the saturation temperature dominates the required thermal energy amount. The reboiler duty at the optimum lean solvent loading is 4.55 GJ/tCO<sub>2</sub>. The 0.24 mol CO<sub>2</sub>/mol MEA value was used as the baseline solvent loading and is also the optimal lean solvent loading. Nevertheless, the results of Figure 5-3 show that improvements as large as 56.6% could be achieved by operating the CO<sub>2</sub>-MEA system at optimal levels of solvent recirculation flow rate. It should be pointed out that the lower the solvent recirculation rate, the pumping work, pressure drop in system components, and system design will be greatly reduced.

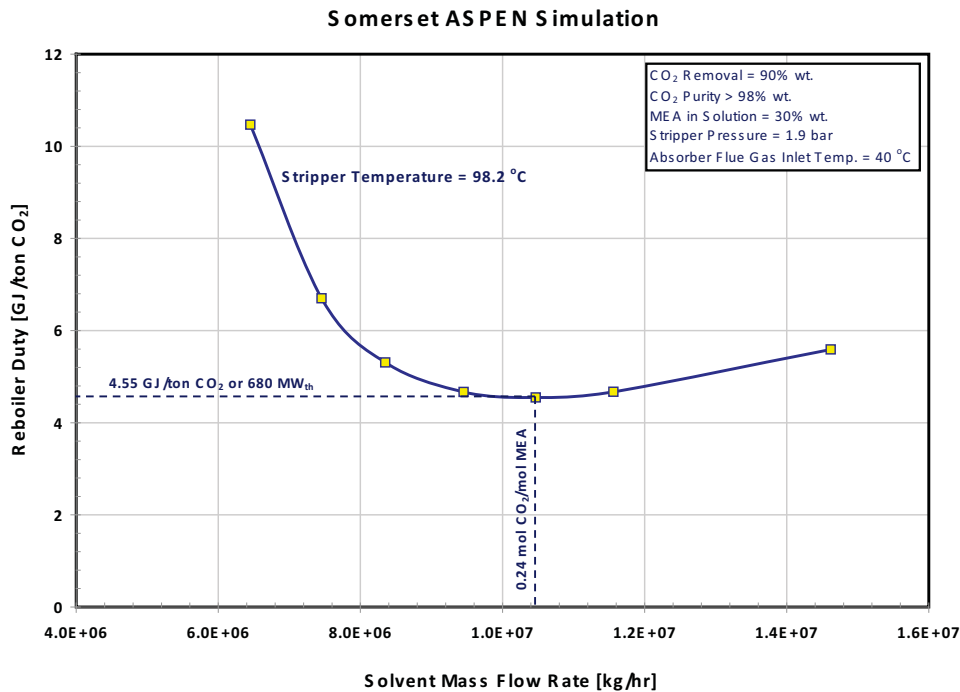


**Figure 5-3. Effect of Solvent Mass Flow on Reboiler Duty.**

The effect of MEA concentration on the reboiler thermal energy requirement was investigated in the range from 16 to 40% by weight. Typical values of this concentration used in studies reported in the literature are 30% by weight. Higher levels of MEA concentration are believed to have a detrimental effect on system component corrosion and would require the use of corrosion inhibitors. Figure 5-4 shows the reboiler energy requirement decreases as the MEA concentration in the absorption solvent increases. The gain in reboiler duty at MEA concentrations in excess of 30%, however, is not that significant. The reduction in reboiler duty by increasing the MEA concentration in solution from 16 to 30% is 2.3 GJ/tCO<sub>2</sub> or 33.6%. Additionally, MEA concentration in the solvent larger than 30% appears to promote higher MEA content in the clean flue gas stream, which would require an additional washing component in the CO<sub>2</sub>-MEA system. The typical MEA concentration value of 30% resulted in a MEA concentration in the flue gas of approximately 12 ppm<sub>v</sub>. The value of 30% by weight MEA in the solvent was considered the optimal MEA concentration.

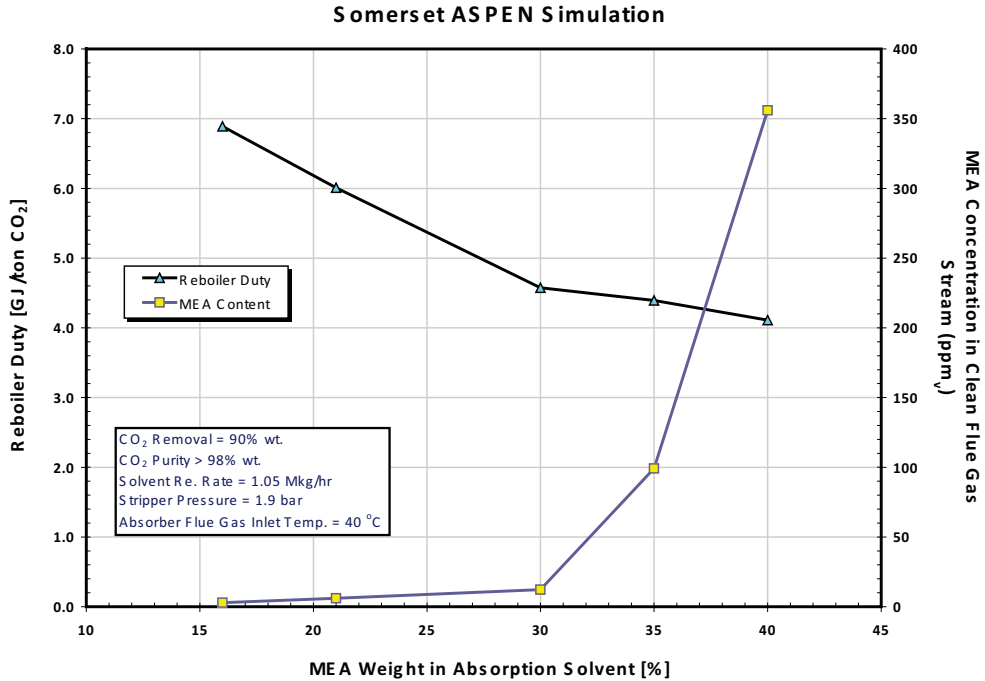


**Figure 5-4. Effect of MEA Concentration in Solvent on Reboiler Duty.**

The impact of the amount of CO<sub>2</sub> removed from the flue gas on the reboiler duty was also investigated in a series of calculations that involved variations of the percentage of CO<sub>2</sub> removed in the range from 24.8 to 95.2%. This range was determined by achieving convergence of the ASPEN model. The results, shown in Figure 5-5 indicate that increasing the percent CO<sub>2</sub> removed from approximately 25 to 85% results in reductions in reboiler duty from 5.8 to 4.5 GJ/tCO<sub>2</sub>, or 33.6%. The reason for this level of improvement is associated with the higher solvent loadings, which increases the driving force in the absorber. Working at 90% CO<sub>2</sub> removal, which was selected as the baseline CO<sub>2</sub> removal condition, does not represent a significant change in the reboiler thermal input. The 90% level of CO<sub>2</sub> removal is considered optimal for the CO<sub>2</sub>-MEA system.

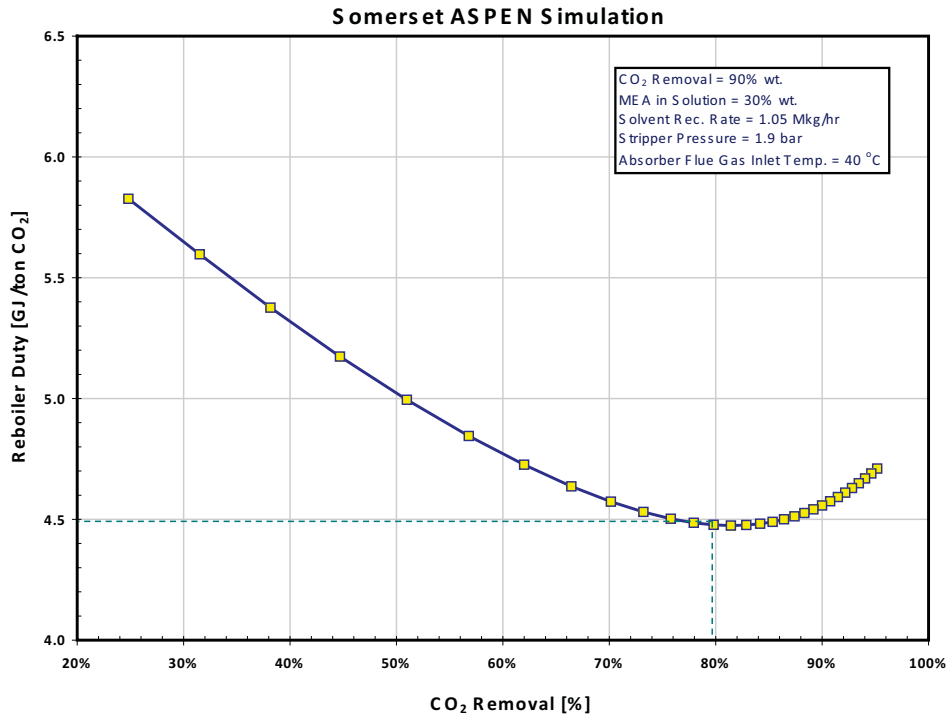


**Figure 5-5. Effect of CO<sub>2</sub> Removal on Reboiler Duty.**

Another set of parameters that were investigated for their impact on the thermal energy required by the stripper reboiler were the flue gas temperature and the lean solvent temperature. The flue gas temperature entering the absorber vessel and the lean solvent temperature was varied from 30 to 60°C. Higher temperatures of both of those streams will result in a higher operating temperature of the absorber and more MEA evaporation from the top of the absorber. The baseline case conditions with regard to the flue gas and solvent temperature were 40°C for both. Figure 5-6 shows that decreasing the flue gas temperature at the inlet of the absorber has a positive impact on the reboiler duty; however, the effect is of second order. The possible cause for this effect is that the rich solvent loading is higher at lower material flow temperature into the absorber vessel. The overall impact for the range of temperatures varied in the simulations amounts to only about 0.7% reduction in the thermal energy requirement. Similar results were achieved for the lean solvent temperature. Thus, the optimal temperature for the lean solvent and flue gas at the absorber was set at 40°C.

Two additional parameters that were studied, but were not part of the sensitivity analysis to achieve optimal design/operation of the amine system that minimize the energy penalty due to the thermal energy required by the reboiler, were the CO<sub>2</sub> concentration in the flue gas entering the CO<sub>2</sub> capture system and the unit load. Figures 5-7 and 5-8 show the results of the simulations performed for both parameters, respectively. Variations in the level of CO<sub>2</sub> concentration in the flue gas could be a consequence of variations in the coal feedstock quality, by natural variability in the fuel, promoted by fuel switching or removal of moisture

from the flue gas. Fuel switching is a common practice in the coal-fired industry to take advantage of reduced emissions of nitrogen oxide (NO<sub>x</sub>) and sulfur dioxide (SO<sub>2</sub>). Variations in unit load are common for units that cycle load due to dispatch requirements. In these cases, the flue gas flow rate or loading to the CO<sub>2</sub>-MEA system would be reduced according to the reduction in fuel and air to the unit. Another aspect that is covered by the simulations that involves partial loading of flue gas, or proportionally CO<sub>2</sub> mass flow rate, is the use of MEA modules for partial (less than 90%) CO<sub>2</sub> capture. A modular CO<sub>2</sub> control approach has the benefit of deferring full CO<sub>2</sub> emissions compliance, based on a phased CO<sub>2</sub> reduction regulation.

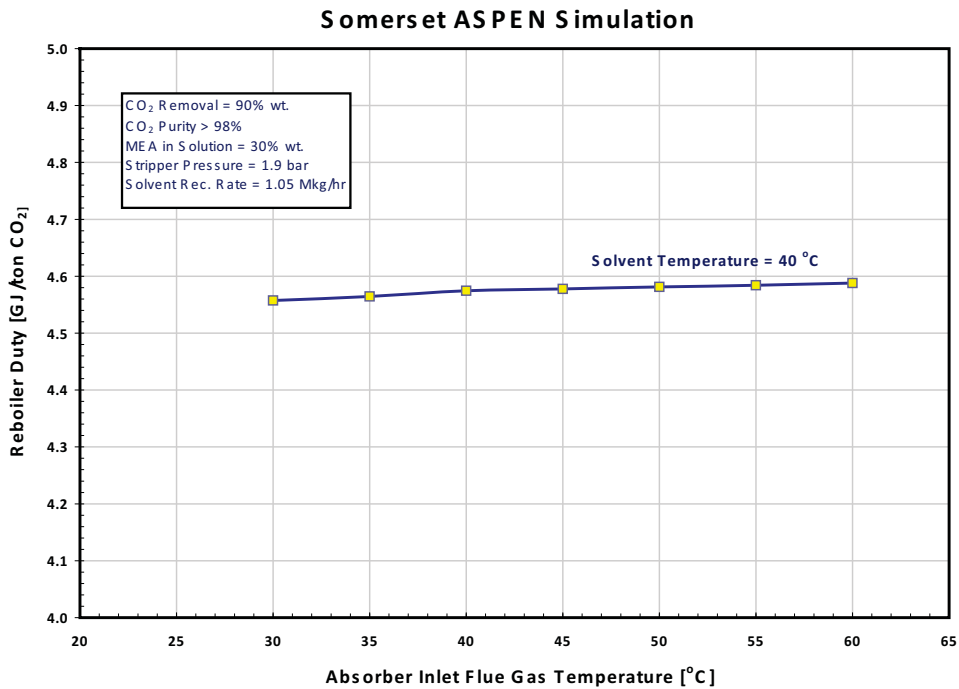


**Figure 5-6. Effect of Absorber Inlet Flue Gas Temperature on Reboiler Duty.**

Figure 5-7 shows the effect of changing CO<sub>2</sub> concentration in the flue gas on the required thermal energy in the reboiler. As expected, a more concentrated CO<sub>2</sub> stream, which could be achieved by removing moisture from the flue gas, would result in an increase in the required thermal energy to the reboiler. It would, however, result in a reduction in reboiler thermal duty. For the range of CO<sub>2</sub> concentrations used in simulation of partial CO<sub>2</sub> capture (8 to 24% CO<sub>2</sub>), the reboiler duty decreased by 21.2%. Figure 5-8 shows that the effect of flue gas flow rate on thermal energy required by the stripper (expressed in MW<sub>th</sub>) is linear, i.e., reboiler duty remains constant (4.55 GJ/t CO<sub>2</sub> in this case).

### Somerset ASPEN Simulation

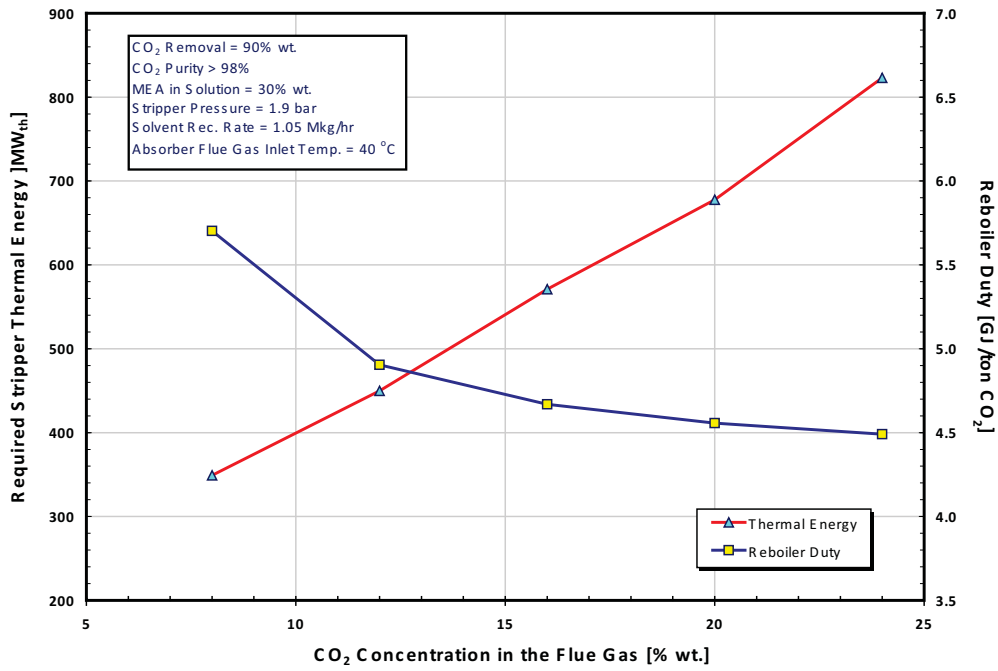


Figure 5-7. Effect of CO<sub>2</sub> Concentration in the Flue Gas on Reboiler Duty and Thermal Energy.

### Somerset ASPEN Simulation

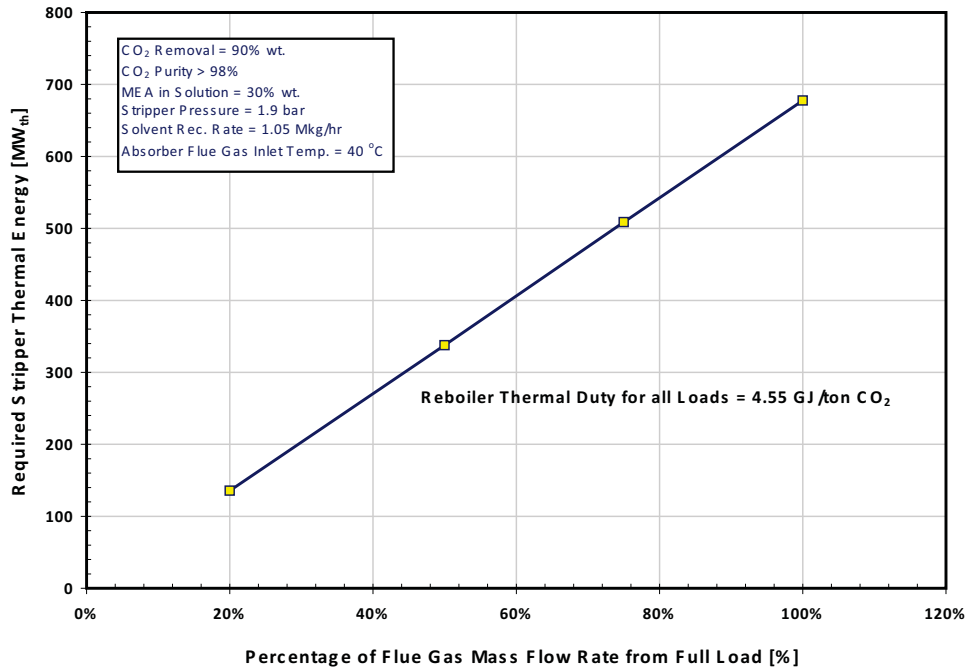


Figure 5-8. Effect of Flue Gas Flow Rate on Reboiler Duty.

Based on results of parametric analysis, optimal operating conditions for the amine system that minimize the MEA-reboiler duty, and consequently, the energy penalty in the power plant steam cycle were selected. The optimal parameters, summarized in Table 5-2, are: stripper pressure at 190 kPa, solvent mass flow rate of 10,827 ton solvent per hour (an equivalent amine lean loading of 0.24 mol CO<sub>2</sub>/mol MEA), MEA concentration in the absorption liquid at 30% by weight, CO<sub>2</sub> removal at 90%, and lean solvent and flue gas inlet temperature at 40°C. Simulation using the optimal conditions specified above resulted in a CO<sub>2</sub> mass recovery of 535 t/h, amine rich loadings of 0.48 mol CO<sub>2</sub>/mol MEA, stripper-reboiler and condenser temperatures of 121.10 and 100.3°C, respectively; and a reboiler thermal duty of 667.6 MW<sub>th</sub> or 4.56 GJ/tCO<sub>2</sub>. The reboiler thermal duty for CO<sub>2</sub> regeneration represents 20.8% reduction from the level achieved by a design/operation of the CO<sub>2</sub>-MEA systems at less than optimal conditions, and 26% reduction with respect to the worst case (see Table 5-2).

**Table 5-2. Optimal and Worst MEA System Operating Points.**

MEA System Operating Point		Optimal	Worst
Flue Gas Mass Flow Rate	t/h	3,050	3,050
Solvent Mass Flow Rate	t/h	10,827	10,793
MEA Concentration in Absorption Liquid	% wt	30.0	30.0
Amine Rich Loading	mol CO <sub>2</sub> /mol MEA	0.480	0.480
Amine Lean Loading	mol CO <sub>2</sub> /mol MEA	0.240	0.240
Stripper Reboiler Temperature	°C	121.1	103.0
Stripper Condenser Temperature	°C	100.3	96.3
Stripper pressure	kPa	190	100.0
Bottom to Feed Molar Ratio		0.975	0.905
Reboiler Heat Required	MW <sub>th</sub>	677.6	855.5
Reboiler Duty	GJ/hr	2,439	2,794
<b>Reboiler Duty</b>	<b>GJ/t CO<sub>2</sub></b>	<b>4.56</b>	<b>5.76</b>
CO <sub>2</sub> Removal	% wt	90.00	90.00
CO <sub>2</sub> Purity	% wt	98.36	98.36
Mass Flow Rate of CO <sub>2</sub> Captured	t/h	535.3	534.4
MEA Concentration in Clean Flue Gas	ppm	122.0	330.1
CO <sub>2</sub> Concentration in Clean Flue Gas	ppm	1.01	1.01



## Section 6

### BOILER-TURBINE CYCLE INTEGRATION

The temperature of the flue gas leaving the boiler is commonly reduced in an air preheater (APH), where sensible heat in the flue gas leaving the economizer is used to preheat combustion air. Preheating of combustion air has a significant positive effect on boiler efficiency. Common practice is to recover sensible heat from the flue gas until the temperature of the flue gas drops to approximately 150°C (300°F). The primary impediment to recovering heat by additional cooling is the risk of condensing sulfuric acid on the APH heat transfer surfaces and downstream ductwork [Sarunac, 2009].

To protect the APH heat transfer surfaces at the cold end of the APH from deposition of sulfuric acid and subsequent corrosion and fouling, the temperature of the inlet air to the APH is commonly increased in a Primary Air Steam Air Heater (PSAH) and Secondary (Combustion) Air Steam Air Heater (SSAH) located upstream of the APH. As presented in Figure 6-1 heat to the PSAH and SSAH is supplied by the steam extracted from the steam turbine cycle (typically from the deaerator extraction). The flow rate of extracted steam depends on the temperature of air entering the PSAH and SSAH (ambient temperature) and on the temperature of air entering the APH required to maintain a Cold End Average Temperature (CEAT). The CEAT is defined as:

$$\text{CEAT} = (T_{\text{APH,ai}} + T_{\text{APH,go}})/2 \quad \text{Eqn. 6-1}$$

Where:

$T_{\text{APH,ai}}$  Temperature of air entering the APH

$T_{\text{APH,go}}$  Temperature of flue gas leaving the APH

CEAT is usually determined empirically and represents a tradeoff between “acceptable” acid deposition rate in the cold end (CE) layer of the APH and net unit heat rate (net unit efficiency). For the Somerset unit, the empirically determined value of CEAT for the secondary APH (SAPH) is 104°C (220°F). The value of CEAT for the primary APH (PAPH) is lower, 87.8°C (190°F). These CEAT values were used in this study. The analysis was performed over a range of ambient temperatures from approximately -15 to 30°C, which corresponds to seasonal changes in ambient temperature at the host site.

As presented in Figure 6-1, preheating of the APH inlet air can also be accomplished by using sensible heat recovered from the flue gas. The sensible heat for air preheating could be recovered from the flue gas by the flue gas cooler ( $\text{FGC}_{\text{APH}}$ ) located downstream of the APH. This method of air preheating is referred to as advanced air preheating.

Because FGC operates below the acid dewpoint, its heat transfer surfaces have to be manufactured of corrosion-resistant plastic or corrosion-resistant alloys and the casing has to be protected against corrosion. Following design specifications of a FGC manufacturer (The Swiss company, Flucorex), a minimum temperature of the flue gas ( $T_{fg,min}$ ) to the FGD reactor of 71.1°C (160°F) was selected in this study.

The results of the process analysis show the temperature of the flue gas exiting the  $FGC_{APH}$  is higher than  $T_{fg,min}$ . A second FGC ( $FGC_{FWH}$ ), located downstream of the  $FGC_{APH}$  could then be used to recover remaining sensible heat from the flue gas. The recovered heat would be used to heat the condensate, as presented in Figure 6-1. This is accomplished by bypassing a certain percentage of the condensate flow around the LP FWHs D, E, F and G and heating it in a bypass heat exchanger. The condensate bypass is a function of the heat recovered in the  $FGC_{FWH}$  which, for the given value of CEAT, also depends on the ambient temperature.

The optimal use of heat recovered from the flue gas for air preheating and condensate heating was determined by considering the tradeoffs between the two heating approaches and CEAT constraints, and determining the effect on the turbine cycle and net unit heat rate. As shown in Section 7 of the report, the best use of heat recovered from the flue gas is in the MEA-reboiler. The analysis was performed by using a spreadsheet-based mass and energy balance model of the plant described in Section 3 of the report. The case where combustion air is preheated by the SAH (PSAH and SSAH) was analyzed to provide reference for other cases. Details are presented in Appendix B.

### **OPTIMAL USE OF HEAT RECOVERED FROM THE FLUE GAS**

The results for all three analyzed cases (air preheating by SAH, advanced air preheating, and advanced air preheating in combination with the feedwater heating) are compared in Figures 6-2 to 6-5. The comparison of turbine cycle heat rate for all three cases, presented in Figure 6-2, shows that the best turbine cycle performance is achieved when the advanced air preheating is combined with the feedwater heating at the air temperature to the APH being equal to the design value of the ambient temperature of 29.4°C (85°F).

The turbine cycle performance is the worst for the case where combustion air is preheated in the SAH using steam extracted from the steam turbine cycle at the lowest value of the ambient temperature and the highest value of air temperature into the APH, which result in the highest steam extraction flow and, therefore, highest penalty to the turbine cycle performance.

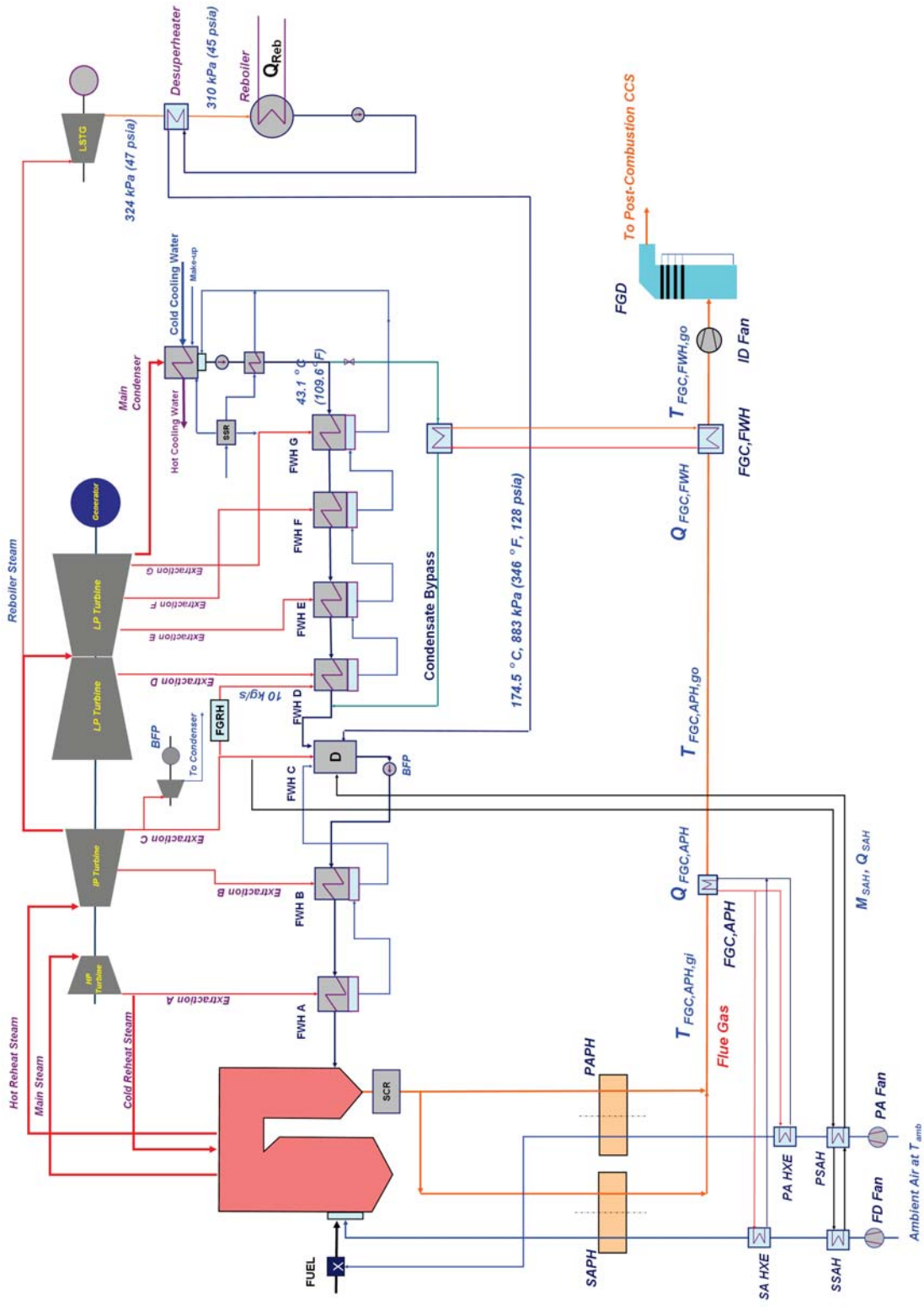
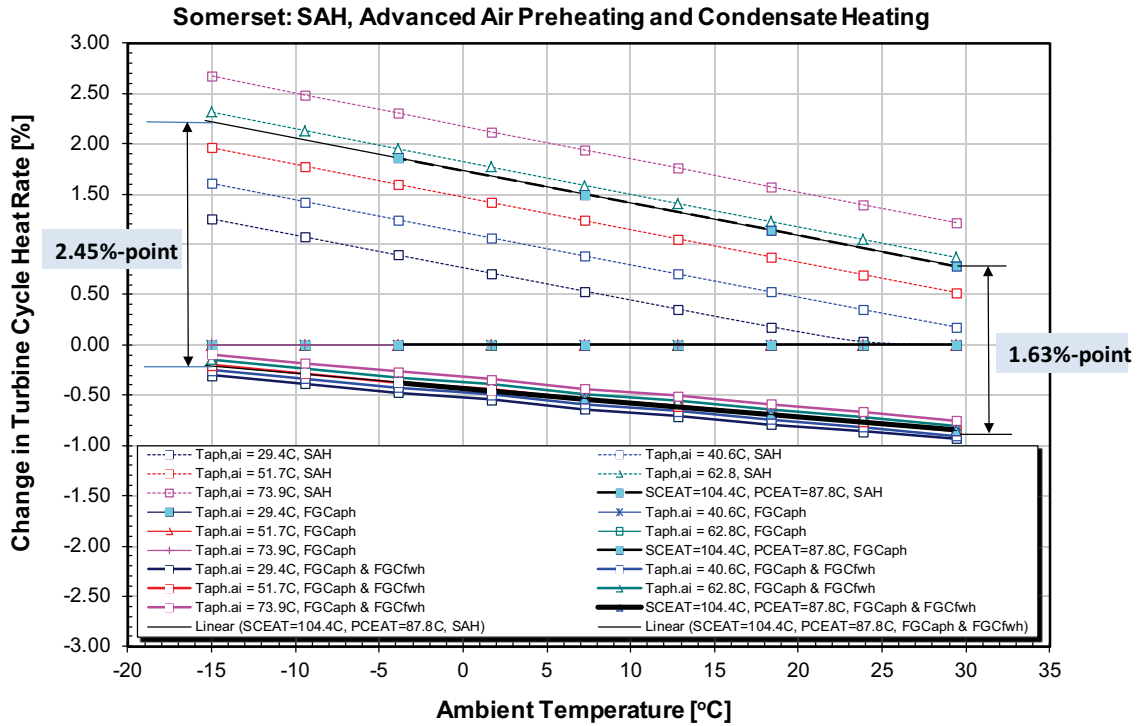


Figure 6-1. Schematic Representation of Air Preheating and Condensate Heating.



**Figure 6-2. Change in Turbine Cycle Heat Rate: SAH Air Preheating, Advanced Air Preheating, and Advanced Air Preheating Combined with the Condensate Heating.**

At the design value of the ambient temperature and operating conditions satisfying the SCEAT and PCEAT set points, turbine cycle heat rate for the case where the advanced air preheating is combined with the condensate heating is approximately 1.63%-points lower compared to the SAH air preheating<sup>3</sup>. This difference increases as ambient temperature decreases. At the ambient temperature of -15°C the difference is approximately 2.45%-points. In addition, while in case of SAH air preheating, temperature of combustion air to the APH has a large effect on the turbine cycle heat rate (approximately 1.4%-points max); in case of the advanced air preheating combined with the condensate heating, temperature of the combustion air to the APH has a very small effect on the turbine cycle performance (approximately 0.2%-points max).

The comparison of net unit heat rate for all three cases, presented in Figure 6-3, shows that the best unit performance is achieved when the advanced air preheating is combined with the condensate heating at the highest value of air temperature to the APH (lowest value of the flue gas temperature leaving the unit), and design value of the ambient temperature of 29.4°C (85°F).

<sup>3</sup> 1% heat rate improvement for the Somerset unit corresponds to annual savings of \$1,500,000.

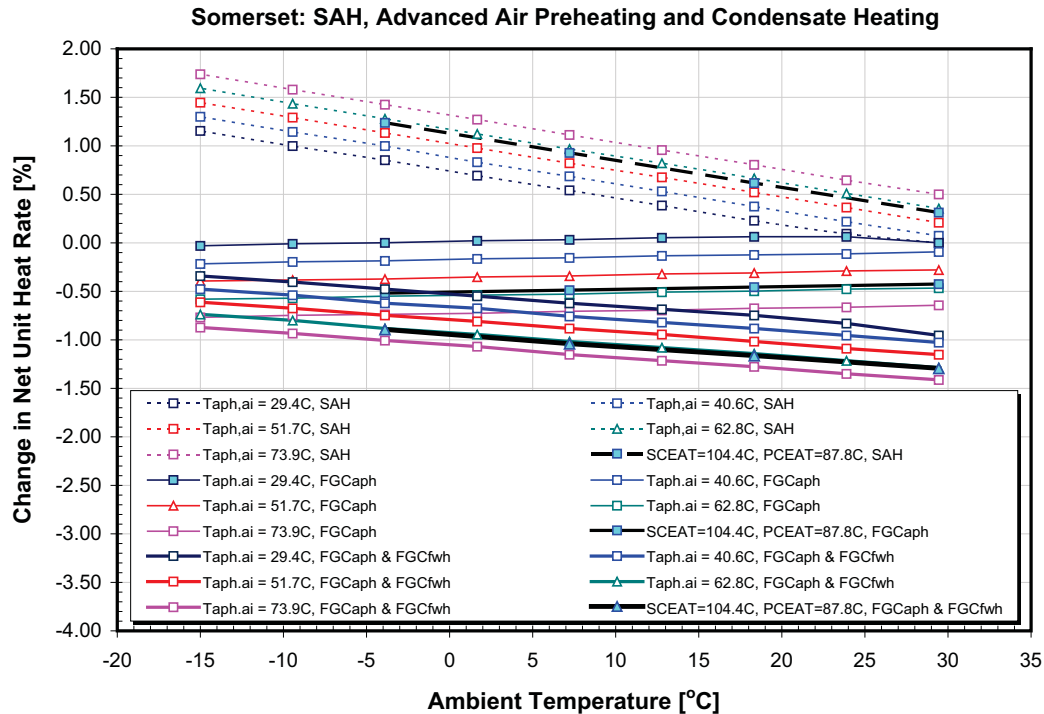


**Figure 6-3. Change in Net Unit Heat Rate: SAH Air Preheating, Advanced Air Preheating, and Advanced Air Preheating Combined with the Condensate Heating.**

Similar to the turbine cycle performance, the net unit performance is the worst for the case where combustion air is preheated in the SAH using steam extracted from the steam turbine cycle at the lowest ambient temperature and the highest air temperature into the APH (highest steam extraction flow, highest penalty to the turbine cycle performance, highest temperature of the flue gas leaving the plant, and highest flue gas sensible heat loss).

At the design value of the ambient temperature and operating conditions satisfying the SCEAT and PCEAT set points, the net unit heat rate for the case where the advanced air preheating is combined with the condensate heating is by approximately 1.6%-point lower compared to the SAH air preheating. This difference increases as the ambient temperature decreases. At the ambient temperature of -15°C the difference is approximately 2.4%-points.

The optimal use of heat recovered from the flue gas is presented in Figure 6-4 where heat input to the condensate flow is shown as a percentage of the maximum amount of heat that can be recovered from the flue gas ( $Q_{FGC,MAX}$ ). The results are presented as functions of the ambient temperature and temperature of combustion air at the APH inlet.

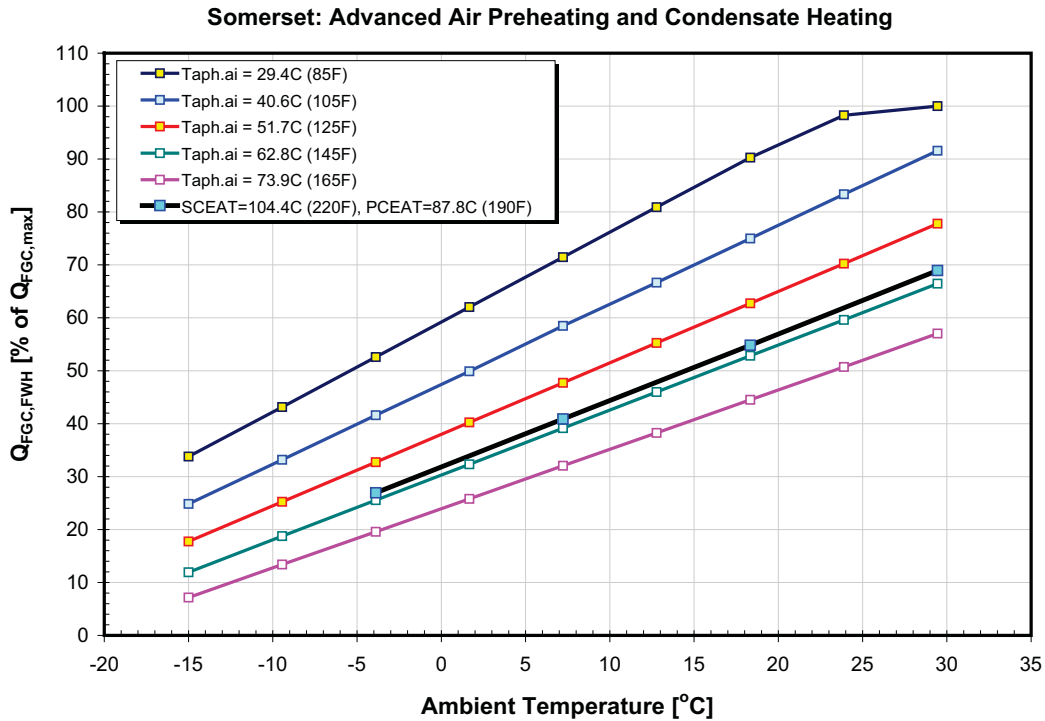


**Figure 6-4. Optimal Use of Heat Recovered From the Flue Gas.**

At the design value of ambient temperature and operating conditions satisfying the SCEAT and PCEAT set points, the best net unit heat rate is achieved by using approximately 69% of the maximum available heat from the flue gas for the condensate flow heating. At the ambient temperature of -15°C the best unit performance is achieved by using approximately 12% of the maximum available heat for the condensate flow heating. A kink in the line representing design value of the air temperature at the APH inlet of 29.4°C (85°F) at ambient temperature of 29.4°C (85°F) is due to the fact that no preheating of combustion air is needed at this operating condition.

## Section 7

### **THERMAL INTEGRATION OF THE TURBINE CYCLE AND CO<sub>2</sub> STRIPPER WITH PLANT HEAT SOURCES**

As presented in Section 4, post-combustion CO<sub>2</sub> capture has a significant negative effect on plant performance (efficiency) and capacity (gross power output). This effect can be offset, in part, by:

- Thermal integration of the steam turbine cycle with the power plant heat sources (flue gas leaving the APH and CO<sub>2</sub> compression train) to improve the steam turbine cycle and unit performance.
- Thermal integration of the CO<sub>2</sub> stripper and steam turbine cycle with the plant heat sources and CO<sub>2</sub> compression train to reduce steam extraction for the MEA-reboiler and improve the steam turbine cycle and unit performance.

The results for both approaches and a number of integration scenarios, based on the advanced thermal integration concept described in Section 4, are presented and discussed in this section. The analyses were performed over a range of boiler thermal duties presented in Table 4-1 assuming constant ambient temperature of 29.4°C (85°F).

### **THERMAL INTEGRATION OF THE TURBINE CYCLE WITH PLANT HEAT SOURCES AND CO<sub>2</sub> COMPRESSION HEAT**

Five thermal integration schemes, referred to as A, B, B-R, C, and C-R, based on the advanced thermal integration of the post-combustion CO<sub>2</sub> capture with the steam turbine cycle, were developed and analyzed.

#### **Modification A**

A schematic representation of Modification A of the advanced thermal integration of the post-combustion CO<sub>2</sub> capture with the steam turbine cycle and the boiler is presented in Figure 7-1. The modification makes use of sensible heat recovered from the flue gas for the condensate flow heating. CO<sub>2</sub> compression is accomplished by conventional multi-stage inline compressors.

The results of the analysis show that sensible heat that could be recovered from the flue gas by the FGC<sub>FWH</sub> is sufficient to heat 100% of the feedwater flow, allowing two to four LP FWHs to be bypassed, thus eliminating two to four steam extractions for the LP FWHs and increasing power output of the LP steam turbine. The number of bypassed LP FWHs depends on the reboiler thermal duty  $q_{\text{Reb}}$ .

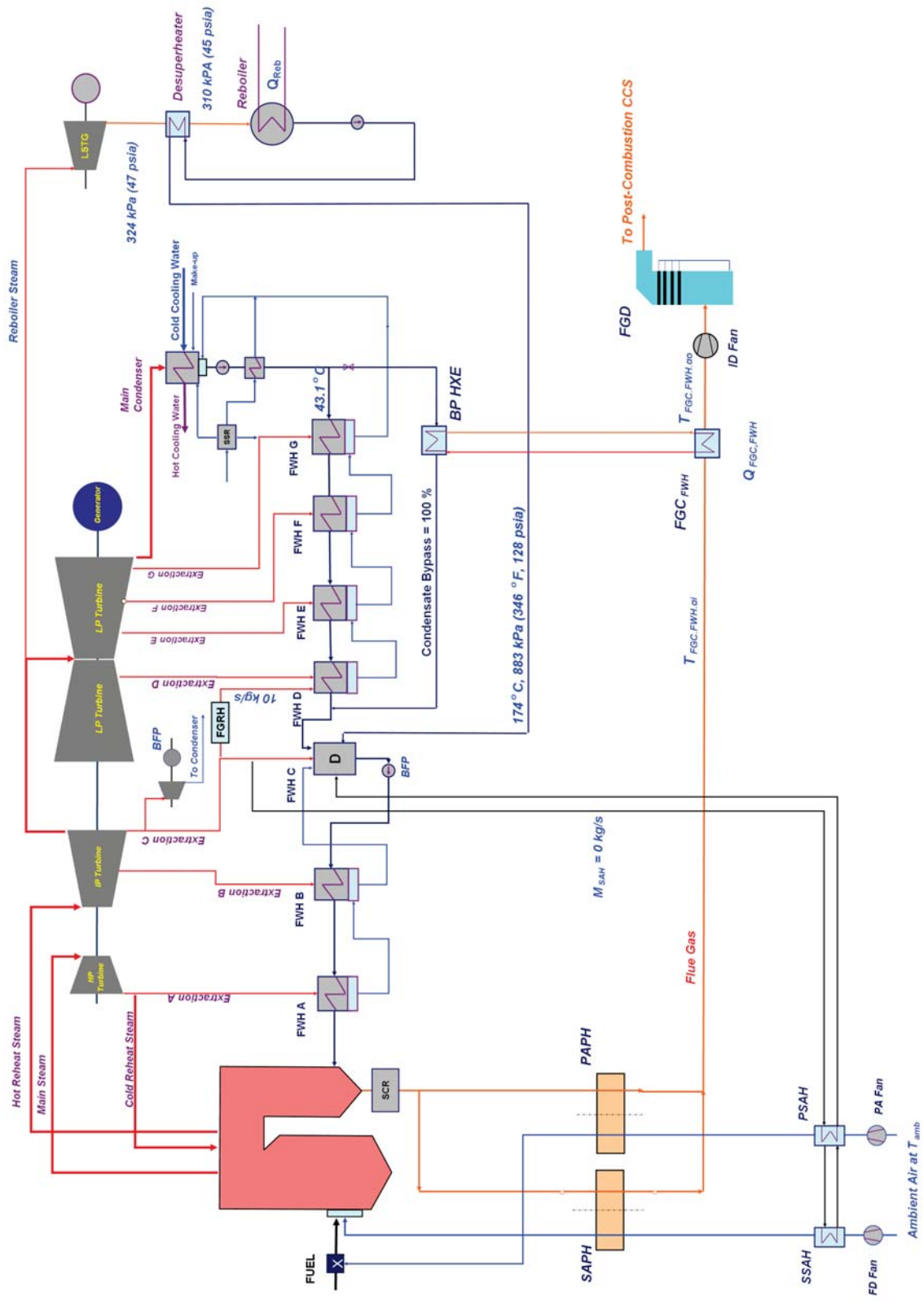


Figure 7-1. Advanced Thermal Integration of Post-Combustion CO<sub>2</sub> Capture: Modification A.

As presented in Figure 4-4, the LP turbine exhaust flow decreases linearly with the increase in  $q_{Reb}$  as more steam needs to be extracted for the reboiler. Therefore, for small values of  $q_{Reb}$ , corresponding to the advanced amines, the condensate flow leaving the main stream condenser is large and sensible heat recovered from the flue gas is insufficient to replace all four LP FWHs. Please note that minimum flue gas temperature at the FGD inlet of 71.1°C (160°F), recommended by the FGC manufacturer Floccorrex, was used in the analysis. The condensate flow to the LP FWH, sensible heat recovered from the flue gas, temperature of the condensate flow leaving the bypass heat exchanger (BP HXE) and bypassed LP FWHs are summarized in Table 7-1 as functions of  $q_{Reb}$ . The results presented in the last row correspond to the baseline (no CO<sub>2</sub> capture) conditions. The quantity  $M_{MST}$  represents the main steam flow rate. These results were obtained for the host unit.

**Table 7-1. Condensate Flow to LP FWH, Sensible Heat Recovered from Flue Gas, Condensate Temperature Leaving BP HXE, and Bypassed LP FWHs as Functions of Reboiler Thermal Duty: Modification A.**

Reboiler Heat Duty		Condensate Flow Entering LP FWH		$Q_{FGC,FWH}$		Bypass Temperature Leaving BP HXE		Bypassed LP Feedwater Heater			
GJ/t CO <sub>2</sub>	CO <sub>2</sub>	kg/s	klb/hr	MW <sub>th</sub>	MBTU/hr	°C	°F	D	E	F	G
5.47	2,350	117	953	75.9	259	104.7	221	x	x	x	x
4.65	2,000	161	1,316	67.8	231	104.7	221	x	x	x	x
4.19	1,800	186	1,517	62.2	212	104.7	221	x	x	x	x
3.95	1,700	199	1,622	59.1	202	104.7	221	x	x	x	x
3.60	1,550	216	1,763	49.8	170	99.8	212		x	x	x
3.26	1,400	232	1,896	41.2	141	95.0	203			x	x
2.79	1,200	255	2,081	31.6	108	89.6	193			x	x
0.00	0	370	3,025	0.0	0	NA	NA				

### Modifications B and B-R

A conceptual schematic representation of Modification B of the advanced thermal integration of the post-combustion CO<sub>2</sub> capture with the steam turbine cycle and the CO<sub>2</sub> compression train is presented in Figure 7-2. The sensible heat recovered from the CO<sub>2</sub> compression process is used for the condensate flow heating. Two types of the CO<sub>2</sub> compressors were investigated in this study: a conventional multi-stage inline compressor, and advanced two-stage shock-wave Ramgen Power Systems compressor. The CO<sub>2</sub> compression and determination of the compression heat are discussed in the Appendix C. Thermal integration with the conventional multi-stage inline compressor is referred as Modification B, while thermal integration with the Ramgen Power Systems compressor is referred as Modification B-R.

The condensate flow entering the LP FWH, the condensate temperature leaving the BP HXE, and bypassed LP FWHs are presented in Table 7-2 as functions of  $q_{Reb}$ . Corresponding results for the Ramgen CO<sub>2</sub> compression train are presented in Table 7-3.

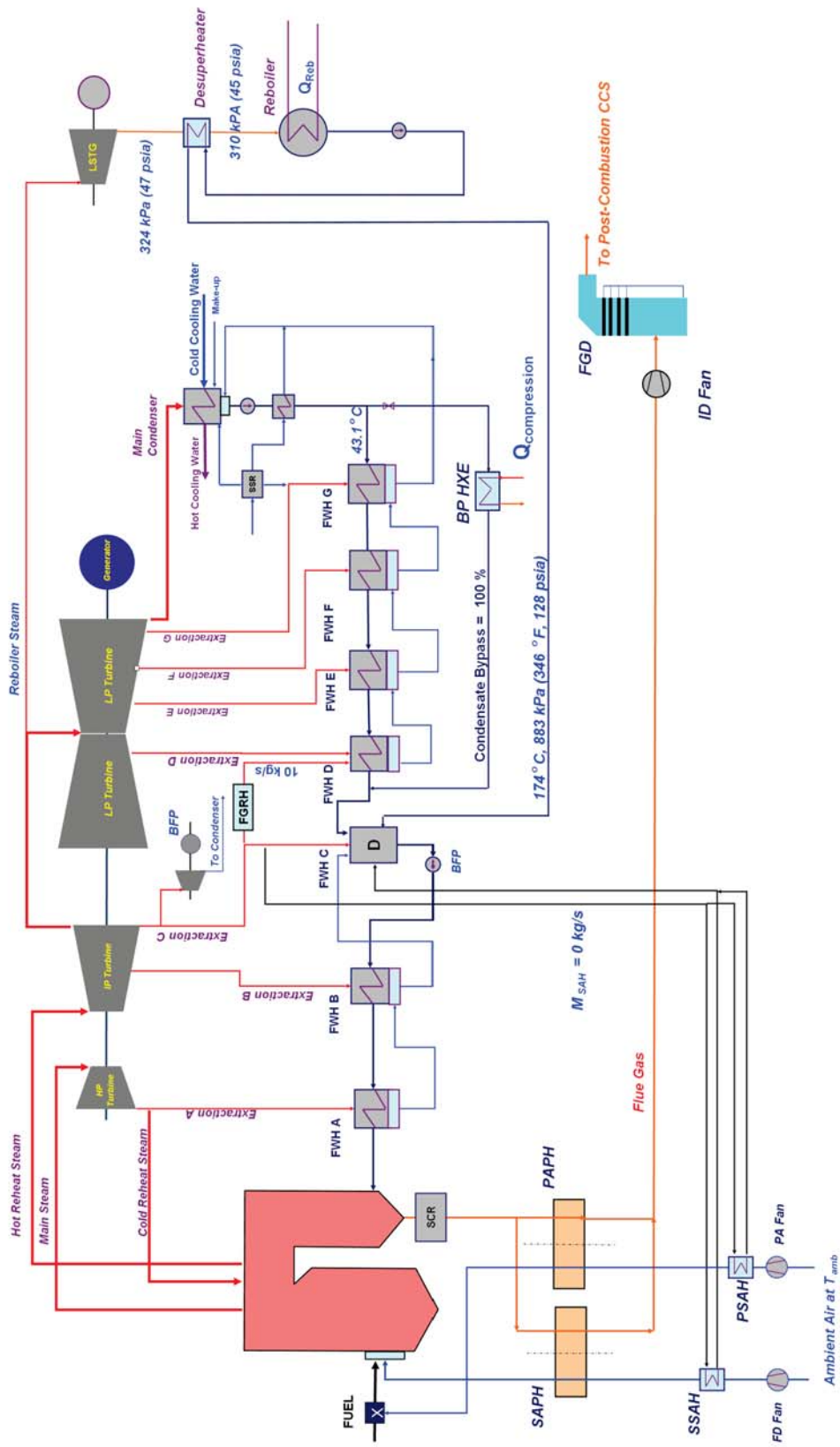


Figure 7-2. Advanced Thermal Integration of Post-Combustion CO<sub>2</sub> Capture: Modification B.

**Table 7-2. Condensate Flow Entering LP FWH, Condensate Temperature Leaving BP HXE, and Bypassed LP FWHs as Functions of Reboiler Thermal Duty: Modification B – Inline CO<sub>2</sub> Compressor.**

Reboiler Heat Duty		Condensate Flow Entering LP FWH		Condensate Bypass Temperature Leaving BP HXE		Bypassed LP Feedwater Heater (FWH)			
GJ/t CO <sub>2</sub>	BTU/lb CO <sub>2</sub>	kg/s	klb/hr	°C	°F	D	E	F	G
5.47	2,350								
4.65	2,000	166	1,322	108	227	x	x	x	x
4.19	1,800	189	1,505	100	212	x	x	x	x
3.95	1,700	201	1,599	97	206		x	x	x
3.60	1,550	218	1,733	92	198			x	x
3.26	1,400	235	1,867	89	192			x	x
2.79	1,200	258	2,052	85	184			x	x
0.00	0	381	3,025	NA	NA				

**Table 7-3. Condensate Flow Entering LP FWH, Condensate Temperature Leaving BP HXE, and Bypassed LP FWHs as Functions of Reboiler Thermal Duty: Modification B-R – Ramgen CO<sub>2</sub> Compressor.**

Reboiler Heat Duty		Condensate Flow Entering LP FWH		Condensate Bypass Temperature Leaving BP HXE		Bypassed LP Feedwater Heater (FWH)			
GJ/t CO <sub>2</sub>	BTU/lb CO <sub>2</sub>	kg/s	klb/hr	°C	°F	D	E	F	G
5.47	2,350								
4.65	2,000	178	1,411	150	302	x	x	x	x
4.19	1,800	201	1,595	137	279	x	x	x	x
3.95	1,700	213	1,690	132	269	x	x	x	x
3.60	1,550	230	1,830	125	257	x	x	x	x
3.26	1,400	248	1,970	119	246	x	x	x	x
2.79	1,200	271	2,156	112	234		x	x	x
0.00	0	381	3,025	NA	NA				

### Modifications C and C-R

Modification C of the advanced thermal integration of the post-combustion CO<sub>2</sub> capture including integration with the steam turbine cycle, the boiler and CO<sub>2</sub> compression train is presented in Figure 7-3. This modification makes use of the sensible heat recovered from the flue gas and the CO<sub>2</sub> compression process for the condensate heating. The condensate bypass flow is heated in the BP HXE 1 by the heat recovered from the flue gas and in the BP HXE 2 by the heat recovered from the CO<sub>2</sub> compression.

Similar to Modification B, the conventional multi-stage inline CO<sub>2</sub> compressor, and the advanced two-stage shock-wave Ramgen Power Systems CO<sub>2</sub> compressor were investigated. Thermal integration including the inline compressor is referred to as Modification C, while integration including the Ramgen compressor is referred to as Modification C-R. Determination of the CO<sub>2</sub> compression heat is presented in the Appendix C.

The condensate flow entering the LP feedwater heater (FWH), the condensate temperature leaving the BP HXE 1 (heated by the heat recovered from the flue gas) and BP HXE 2 (heated by the heat recovered from the inline multi-stage CO<sub>2</sub> compression train), and bypassed LP FWHs are presented in Table 7-4 as



functions of  $q_{Reb}$ . Corresponding results for the two-stage Ramgen CO<sub>2</sub> compressor are presented in Table 7-5.

The results presented in Tables 7-1 to 7-5 show that the number of bypassed LP FWHs increases as more heat is provided to the steam turbine cycle from the flue gas and CO<sub>2</sub> compression. Modifications C and C-R allow all LP FWHs to be bypassed. The condensate bypass temperature leaving the BP HXE2 is higher for Modification C-R, compared to Modification C because the amount of heat available for the condensate heating is higher.

**Table 7-4. Condensate Flow Entering LP FWH, Condensate Temperature Leaving BP HXE 1 and 2, and Bypassed LP FWHs as Functions of Reboiler Thermal Duty: Modification C – Inline CO<sub>2</sub> Compressor.**

Reboiler Heat Duty		Condensate Flow Entering LP FWH		Condensate Bypass Temp. Leaving BP HXE 1		Condensate Bypass Temp. Leaving BP HXE 2		Bypassed LP Feedwater Heater (FWH)			
GJ/t CO <sub>2</sub>	BTU/lb CO <sub>2</sub>	kg/s	klb/hr	°C	°F	°C	°F	D	E	F	G
5.47	2,350	130	1,034	105	221	156	312	x	x	x	x
4.65	2,000	176	1,399	105	221	143	289	x	x	x	x
4.19	1,800	201	1,600	105	221	138	280	x	x	x	x
3.95	1,700	214	1,703	104	219	135	276	x	x	x	x
3.60	1,550	232	1,847	99	210	130	266	x	x	x	x
3.26	1,400	251	1,991	95	203	125	257	x	x	x	x
2.79	1,200	275	2,188	90	194	119	247	x	x	x	x
0.00	0	381	3,025	NA	NA	NA	NA				

**Table 7-5. Condensate Flow Entering LP FWH, Condensate Temperature Leaving BP HXE 1 and 2, and Bypassed LP FWHs as Functions of Reboiler Thermal Duty: Modification C-R – Ramgen CO<sub>2</sub> Compressor.**

Reboiler Heat Duty		Condensate Flow Entering LP FWH		Condensate Bypass Temp. Leaving BP HXE 1		Condensate Bypass Temp. Leaving BP HXE 2		Bypassed LP Feedwater Heater (FWH)			
GJ/t CO <sub>2</sub>	BTU/lb CO <sub>2</sub>	kg/s	klb/hr	°C	°F	°C	°F	D	E	F	G
5.47	2,350										
4.65	2,000	192	1,522	105	221	174	345	x	x	x	x
4.19	1,800	213	1,692	105	221	169	336	x	x	x	x
3.95	1,700	224	1,783	102	215	163	325	x	x	x	x
3.60	1,550	242	1,923	97	207	154	309	x	x	x	x
3.26	1,400	260	2,064	94	200	147	296	x	x	x	x
2.79	1,200	284	2,256	89	193	138	281	x	x	x	x
0.00	0	381	3,025	NA	NA	NA	NA				

## THERMAL INTEGRATION OF THE CO<sub>2</sub> STRIPPER AND TURBINE CYCLE WITH PLANT HEAT SOURCES AND COMPRESSION HEAT

Three schemes, referred to as Modifications D, E, and F, for thermal integration of the CO<sub>2</sub> stripper and steam turbine cycle with the boiler and CO<sub>2</sub> compression train were developed and analyzed. All integration schemes are based on the advanced thermal integration of the post-combustion CO<sub>2</sub> capture with the steam turbine cycle and CO<sub>2</sub> compression train.

## Modification D

A schematic representation of Modification D of the advanced thermal integration of the post-combustion CO<sub>2</sub> capture process with the steam turbine cycle, the boiler and the multi-stage inline CO<sub>2</sub> compression train is presented in Figure 7-4. The high-grade sensible heat recovered from the flue gas is used in the reboiler, while the mid-grade CO<sub>2</sub> compression heat is used for the condensate heating.

As presented in Figure 7-4, a portion of the flue gas flow leaving the boiler is bypassed around the PAPH and SAPH to provide heat to a Bypass Evaporator. The flue gas bypass would decrease the temperature of the flue gas leaving the APHs, which would result in higher acid deposition rates, accelerated corrosion and fouling. To prevent this, the temperature of the primary and combustion air has to be increased. In the proposed configuration, the primary and combustion air is preheated in the PAPH and SAPH to maintain the PCEAT and SCEAT set-points by using heat recovered from the flue gas by the flue gas cooler (FGC<sub>APH</sub>).

The Bypass Evaporator provides a low pressure saturated steam at 137°C and 331 kPA (278°F and 48 psia) to the reboiler. The steam condenses in the reboiler releasing approximately 53 MW<sub>th</sub> of heat (7.5 to 14.5% of the reboiler thermal duty, depending on the q<sub>Reb</sub> value), thus resulting in lower steam extraction from the steam turbine cycle for the reboiler. The condensate flows through the heat exchanger HXE to be sub-cooled, transferring 3.3 MW<sub>th</sub> of heat to the condensate, and through a pump to increase its pressure to 331 kPA (48 psia) before re-entering the Bypass Evaporator. Sub-cooling is needed to maintain a reasonable approach to the Bypass Evaporator and reduce its size.

The condensate flow entering the LP FWH, feedwater temperature leaving the BP HXE (heated by the heat recovered from the inline CO<sub>2</sub> compression train), and bypassed LP FWHs are summarized in Table 7-6 as functions of q<sub>Reb</sub>.

**Table 7-6. Condensate Flow Entering LP FWH, Condensate Temperature Leaving the BP HXE and Bypassed LP FWHs as Functions of Reboiler Thermal Duty: Modification D – Inline CO<sub>2</sub> Compressor.**

Reboiler Heat Duty		Condensate Flow Entering LP FWH		Condensate Bypass Temperature Leaving BP HXE		Bypassed LP Feedwater Heater (FWH)			
GJ/t CO <sub>2</sub>	BTU/lb CO <sub>2</sub>	kg/s	klb/hr	°C	°F	D	E	F	G
5.47	2,350	146	1,163	115	240	x	x	x	x
4.65	2,000	188	1,491	99	211	x	x	x	x
4.19	1,800	211	1,676	93	200			x	x
3.95	1,700	222	1,766	91	195			x	x
3.60	1,550	239	1,901	87	189			x	x
3.26	1,400	256	2,037	84	184			x	x
2.79	1,200	279	2,219	81	178			x	x
0.00	0	381	3,025	NA	NA				

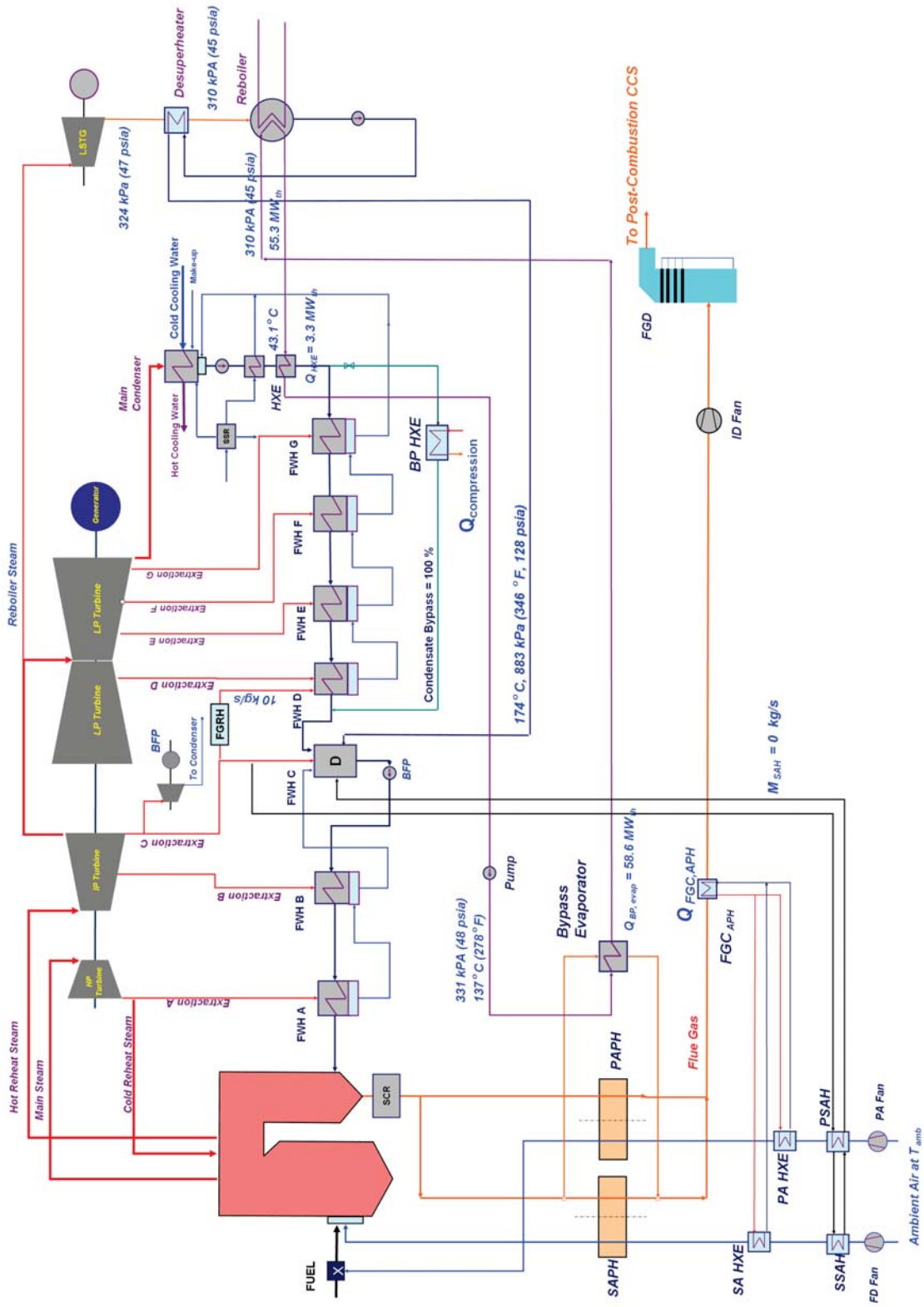


Figure 7-4. Advanced Thermal Integration of Post-Combustion CO<sub>2</sub> Capture: Modification D.

### Modification E

A conceptual schematic representation of Modification E of the advanced thermal integration of the post-combustion CO<sub>2</sub> capture process with the steam turbine cycle and a two-stage shock-wave Ramgen Power Systems CO<sub>2</sub> compression train is presented in Figure 7-5. The high-grade CO<sub>2</sub> compression heat is supplied to the reboiler, while the mid-grade CO<sub>2</sub> compression heat is used for the condensate heating. The high-grade CO<sub>2</sub> compression heat is used in a Ramgen Evaporator to provide a low pressure saturated steam at 137°C and 331 kPa (278°F and 48 psia) to the reboiler. This steam condenses in the reboiler releasing 49.5 MW<sub>th</sub> of heat (6.7 to 13.1% of the reboiler thermal duty, depending on the q<sub>Reb</sub> value), thus resulting in a lower steam extraction from the steam turbine cycle for the reboiler. The condensate flows through a pump, which increases its pressure to 331 kPa (48 psia) before re-entering the Ramgen Evaporator. The mid-grade CO<sub>2</sub> compression heat is used to heat the condensate bypass flow, which is split in two equal streams to utilize heat from the first and second Ramgen compression stages.

The condensate flow entering the LP FWH, feedwater temperature leaving the BP HXE (heated by the mid-grade heat recovered from the Ramgen CO<sub>2</sub> compression train), and bypassed LP FWHs are summarized in Table 7-7 as functions of of q<sub>Reb</sub>.

### Modification F

A conceptual schematic representation of Modification F of the advanced thermal integration of the post-combustion CO<sub>2</sub> capture process with the steam turbine cycle, the boiler, and a two-stage Ramgen Power Systems CO<sub>2</sub> compression train, presented in Figure 7-6, represents a combination of Modifications D and E. The high-grade sensible heat recovered from the flue gas and the high-grade CO<sub>2</sub> compression heat is used in the reboiler. The mid-grade CO<sub>2</sub> compression heat is used to heat the condensate bypass flow, which is split in two equal streams to utilize heat from the first and second Ramgen compression stages. The LP steam provided by the Bypass and Ramgen Evaporators condenses in the reboiler releasing approximately 105 MW<sub>th</sub> of heat (14 to 27.7% of the reboiler thermal duty, depending on the q<sub>Reb</sub> value), thus resulting in a lower steam extraction from the steam turbine cycle for the reboiler.

**Table 7-7. Condensate Flow Entering LP FWH, Condensate Temperature Leaving the BP HXE, and Bypassed LP FWHs as Functions of Reboiler Thermal Duty: Modification E – Ramgen CO<sub>2</sub> Compressor.**

Reboiler Heat Duty		Condensate Flow Entering LP FWH		Condensate Bypass Temperature Leaving BP HXE		Bypassed LP Feedwater Heater (FWH)			
GJ/t CO <sub>2</sub>	BTU/lb CO <sub>2</sub>	kg/s	klb/hr	°C	°F	D	E	F	G
5.47	2,350	140	1,113	104	219	x	x	x	x
4.65	2,000	182	1,443	88	191			x	x
4.19	1,800	204	1,619	83	181			x	x
3.95	1,700	215	1,711	80	176			x	x
3.60	1,550	232	1,847	77	171			x	x
3.26	1,400	249	1,981	74	166			x	x
2.79	1,200	273	2,168	71	160			x	x
0.00	0	381	3,025	NA	NA				

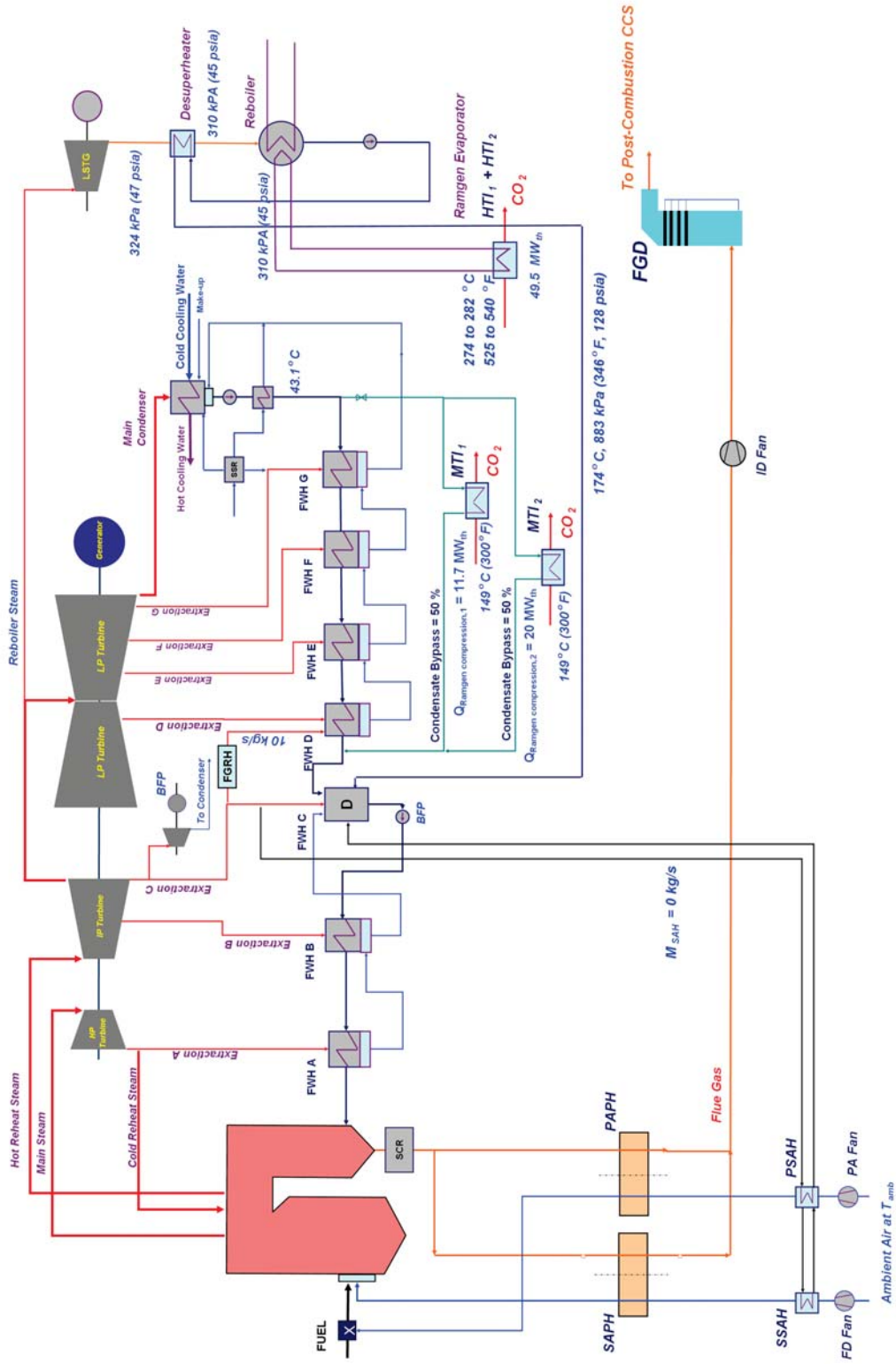


Figure 7-5. Advanced Thermal Integration of Post-Combustion CO<sub>2</sub> Capture: Modification E.



The condensate flow entering the LP FWH, condensate temperature leaving the BP HXE (heated by the heat recovered from a two-stage Ramgen CO<sub>2</sub> compression train), and bypassed LP FWHs are presented in Table 7-8 as functions of  $q_{Reb}$ .

**Table 7-8. Condensate Flow Entering LP FWH, Condensate Temperature Leaving BP HXE and Bypassed LP FWHs as Functions of Reboiler Thermal Duty: Modification F – Ramgen CO<sub>2</sub> Compressor.**

Reboiler Heat Duty		Condensate Flow Entering LP FWH		Condensate Bypass Temp. Entering LP FWH		Condensate Bypass Temp. Leaving BP HXE		Bypassed LP Feedwater Heater (FWH)			
GJ/t CO <sub>2</sub>	BTU/lb CO <sub>2</sub>	kg/s	klb/hr	°C	°F	°C	°F	D	E	F	G
5.47	2,350	162	1,286	54	130	100	213	x	x	x	x
4.65	2,000	203	1,611	52	125	87	188			x	x
4.19	1,800	225	1,787	51	123	82	179			x	x
3.95	1,700	237	1,880	50	122	80	175			x	x
3.60	1,550	254	2,015	49	121	77	170			x	x
3.26	1,400	271	2,150	49	120	74	166			x	x
2.79	1,200	293	2,331	48	119	71	161				x
0.00	0	381	3,025	43	110	NA	NA				

## RESULTS

The effects of thermal integration on gross power output and net unit efficiency for Modifications A to F presented in Figures 7-7 to 7-10 show that thermal integration has a significant effect on cycle and unit performance, with Modification F resulting in best performance. The results for all parameters of interest are presented in graphical and tabular forms in Appendix C.

Figure 7-7 compares the effect of thermal integration on the gross power output relative to the baseline (no CO<sub>2</sub> capture). The comparison relative to the baseline is a measure of the penalty that would be incurred by retrofit or implementation of the post-combustion CO<sub>2</sub> capture process. As discussed in Section 4,  $q_{Reb}$  has a major effect on plant performance; as  $q_{Reb}$  decreases performance penalties associated with the post-combustion CO<sub>2</sub> capture decrease. For the state-of-the-art amines, thermal integration reduces penalty in the gross power output by 4.29%-points (from 14.67 to 10.38%). For the  $q_{Reb}$  value, determined for the MEA in this study, thermal integration reduces penalty in gross power output by 4.72%-points (from 19.59 to 14.87 %).

The improvement in gross power output for modifications A to F relative to the conventional thermal integration is presented in Figure 7-8. The comparison relative to the conventional MEA integration represents improvement to be achieved by thermal integration. The improvement in gross power output relative to the conventional thermal integration is highest for Modifications F and C-R. For the state-of-the-art amines Modification F improves gross power output relative to the conventional thermal integration by 5.03%. For the  $q_{Reb}$  value, determined for the MEA in this study and Modification F, improvement in gross power output relative to the conventional thermal integration is 5.87%.

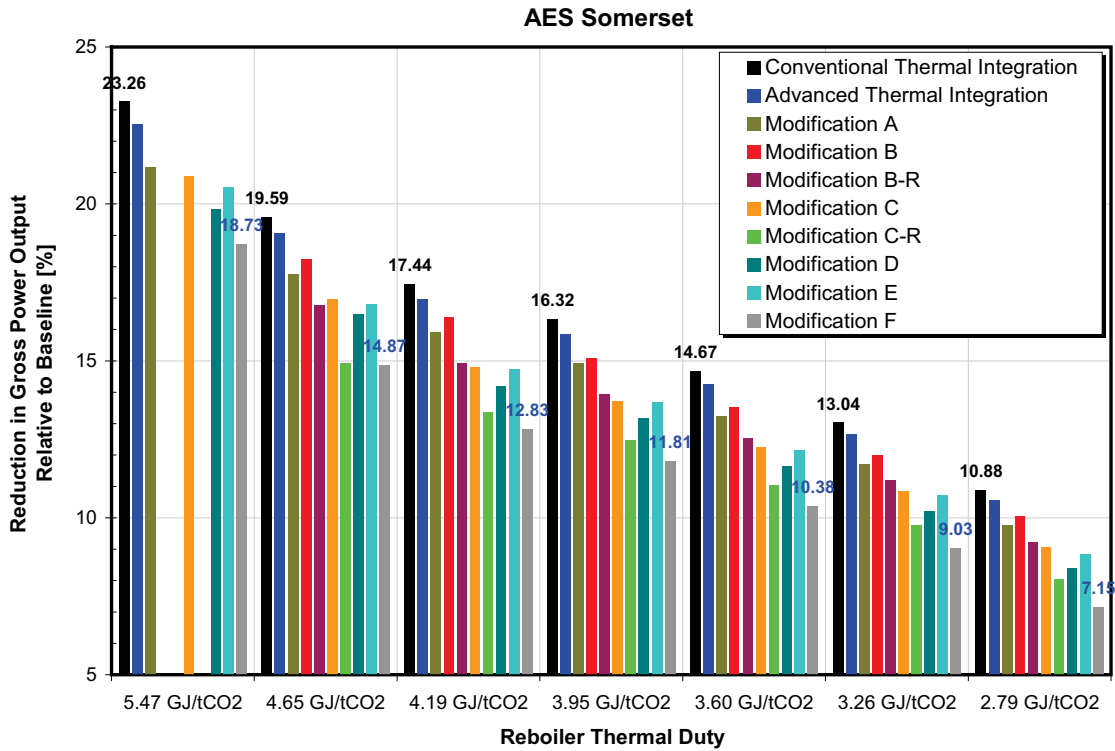


Figure 7-7. Reduction in Gross Power Output Relative to Baseline (no CO<sub>2</sub> capture) vs.  $q_{Reb}$ .

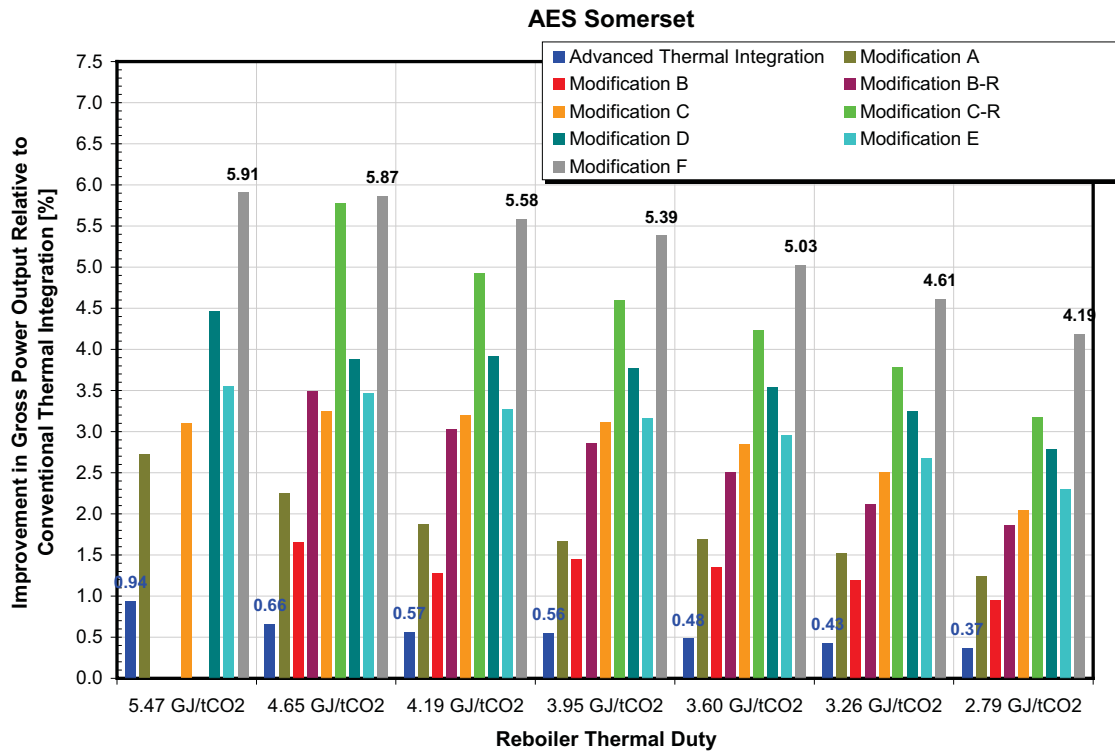
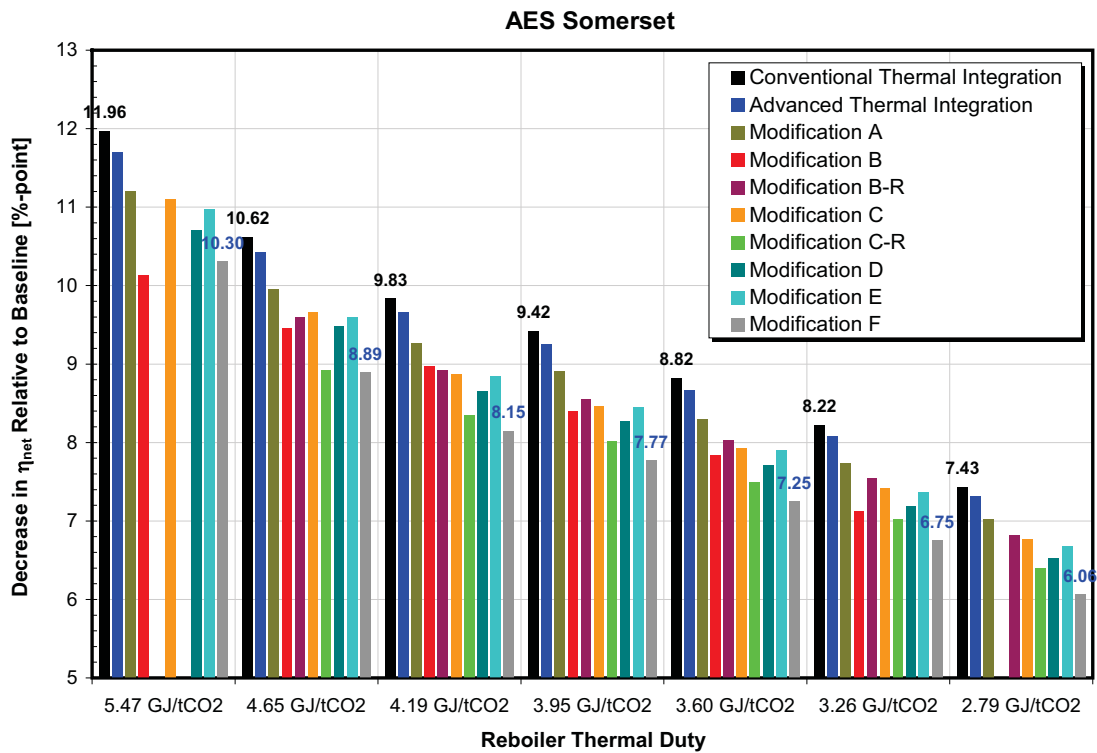


Figure 7-8. Improvement in Gross Power Output Relative to Conventional Thermal Integration vs.  $q_{Reb}$ .

The effect of thermal integration on the net unit efficiency relative to the baseline (no CO<sub>2</sub> capture) is presented in Figure 7-9. The quantity  $q_{Reb}$  has a major effect on net unit efficiency; the penalty in  $\eta_{net}$  decreases as  $q_{Reb}$  is reduced. For the state-of-the-art amines Modification F reduces penalty in net unit efficiency relative to the baseline by 1.57%-points (from 8.82 to 7.25%-points). For the  $q_{Reb}$  value, determined for the MEA in this study, Modification F reduces penalty in net unit heat rate by 1.73%-points (from 10.62 to 8.89%-points) relative to the baseline.

The improvement in net unit efficiency relative to the conventional thermal integration is presented in Figure 7-10. Similar to the power output, the improvement in  $\eta_{net}$  relative to the conventional thermal integration is highest for Modifications F and C-R. For the state-of-the-art amines Modification F improves net unit efficiency relative to the conventional thermal integration by 1.57%-points. For the  $q_{Reb}$  value, determined for the MEA in this study and Modification F, the improvement in net unit efficiency relative to the conventional thermal integration is 1.73%-points.



**Figure 7-9. Decrease in Net Unit Efficiency Relative to Baseline vs.  $q_{Reb}$ .**

Thermal integration of the CO<sub>2</sub> stripper, CO<sub>2</sub> compression train, and steam turbine cycle reduces steam extraction from the steam turbine cycle for the reboiler which also improves performance of the steam turbine cycle and plant performance, offsetting part of performance and capacity penalties associated with the retrofit or implementation of the post-combustion CO<sub>2</sub> capture process. A number of thermal

integration options were developed and analyzed, including advanced thermal integration, referred to as Advanced MEA, and Modifications A to F to the Advanced MEA. Basic features of these thermal integration options are summarized in Table 7-9. Thermal integration of two types of the CO<sub>2</sub> compressors was investigated: a conventional multi-stage inline compressor, and the advanced two-stage shock-wave Ramgen Power Systems compressor.

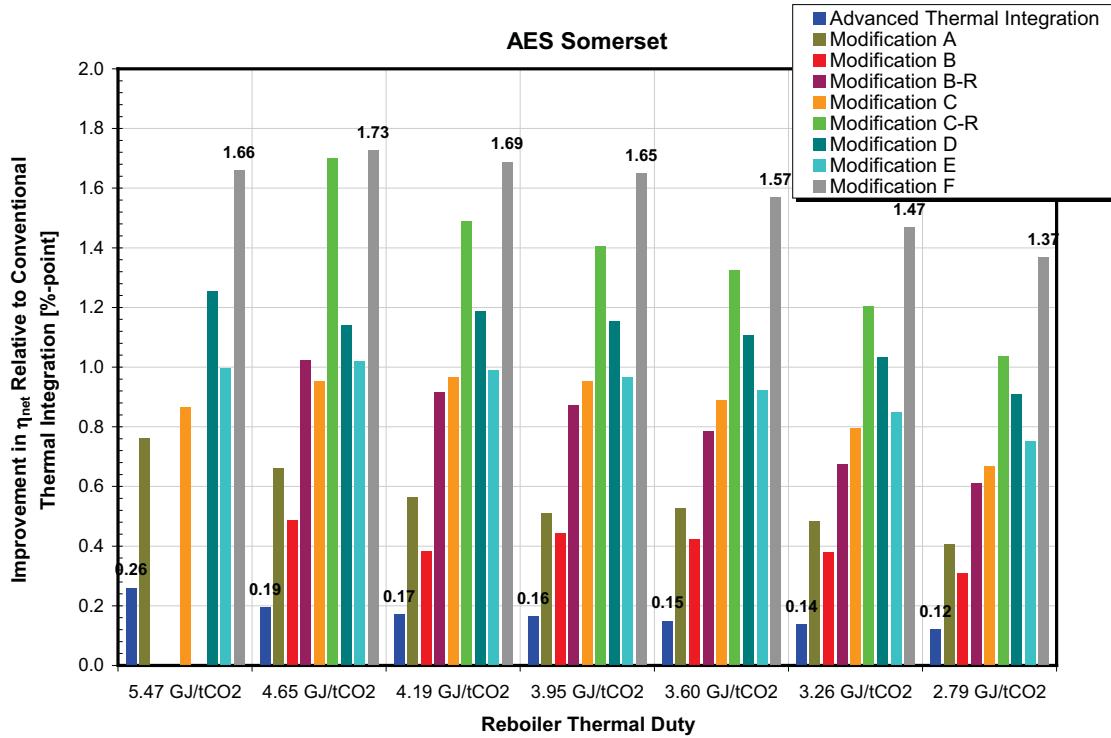


Figure 7-10. Improvement in Net Unit Efficiency Relative to Conventional Thermal Integration vs.  $q_{Reb}$ .

Table 7-9. Basic Features of Analyzed Thermal Integrations Options.

MEA Integration	Control of Steam Temperature into Reboiler	Temperature of Reboiler Condensate Entering Deaerator [°C]	Sources of Heat for Condensate (LP Fedwater Heating)		CO <sub>2</sub> Compressor Type	Sources of Heat for Reboiler			Reboiler Heat Provided by Steam [%]
			Flue Gas	CO <sub>2</sub> Compression Heat		LP Steam	Flue Gas	CO <sub>2</sub> Compression	
Conventional MEA	Desuperheat by reboiler condensate	134.7			Inline	x			100.0
Advanced MEA	Cooling by reboiler condensate	174.5	x			x			
Modification A						x			
Modification B				x					
Modification B-R				x					
Modification C				x	x	Inline	x		
Modification C-R				x	x	Ramgen	x		
Modification D						Inline	x	x	
Modification E				Ramgen	x		x	89.9	
Modification F				Ramgen	x	x	x	78.6	

The effect of investigated thermal integration options on gross power output and net unit efficiency is summarized in Table 7-10 for the state-of-the-art amines. The results are compared to the baseline case (no CO<sub>2</sub> capture) and to the conventional thermal integration. As discussed earlier, the comparison relative to

the baseline is a measure of the penalty that would be incurred by retrofit or implementation of the post-combustion CO<sub>2</sub> capture process, while the comparison relative to the conventional MEA integration represents improvement that could be achieved by thermal integration. The reduction in unit performance and capacity relative to the baseline is the lowest and improvement relative to Conventional MEA is the highest for Modifications F and C-R.

**Table 7-10. Effect of Thermal Integration on Unit Performance: State-of-the-Art Amines.**

Rankine Cycle				
State-of-the-Art Amines	Change in P <sub>G</sub> Relative to Baseline	Change in η <sub>net</sub> Relative to Baseline	Improvement in P <sub>G</sub> Relative to Conventional MEA	Improvement in η <sub>net</sub> Relative to Conventional MEA
	%	%-point	%	%-point
Conventional MEA	-14.67	-8.82		
Advanced MEA	-14.26	-8.67	0.48	0.15
Modification A	-13.23	-8.29	1.69	0.53
Modification B	-13.51	-8.39	1.36	0.42
Modification B-R	-12.52	-8.03	2.51	0.78
Modification C	-12.24	-7.93	2.85	0.89
Modification C-R	-11.05	-7.49	4.24	1.32
Modification D	-11.65	-7.71	3.54	1.11
Modification E	-12.15	-7.89	2.95	0.92
Modification F	-10.38	-7.25	5.03	1.57
<b>Baseline = No CO<sub>2</sub> Capture</b>				

In summary, thermal integration of the CO<sub>2</sub> stripper, CO<sub>2</sub> compression train, and steam turbine cycle reduces steam extraction from the steam turbine for the reboiler improves the cycle and plant performance. Thermal integration should be applied to existing and newly built plants to be equipped with the post-combustion CO<sub>2</sub> capture process. The best analyzed integration option (Modification F) improves the gross power output by 5% and net unit efficiency by 1.57%-points relative to the conventional thermal integration (referred to as the Conventional MEA).

Also, different thermal integration options are evaluated, the cost of heat exchange and associated equipment has to be considered. For example, the cost of the FGC is approximately 10 times higher compared to the finned tube heat exchanger.



## Section 8

### **PARTIAL CO<sub>2</sub> CAPTURE**

In previous sections of the report the analysis of a number of thermal integration options (conventional and advanced thermal integration, and modifications A to F to the advanced thermal integration) was performed assuming 100% of the flue gas is treated by the post-combustion CO<sub>2</sub> capture system; resulting in 90% CO<sub>2</sub> capture.

Partial CO<sub>2</sub> capture and its effect on plant gross power output and performance was investigated in this section. Partial CO<sub>2</sub> capture involves treatment of less than 100% of the flue gas leaving the plant and modular design of the CO<sub>2</sub> scrubbing system. Partial CO<sub>2</sub> capture could be the first step toward reducing CO<sub>2</sub> emissions from existing power plants, which is expected to speed up deployment of the post-combustion CO<sub>2</sub> capture because initial capital investment and associated risk will be smaller. Other reasons for considering partial CO<sub>2</sub> capture include gathering operational experience on a smaller and easier-to-operate system and implementing design changes and improvements on subsequent CO<sub>2</sub> capture modules. Also, partial CO<sub>2</sub> capture could be implemented on smaller and older power plants to reduce CO<sub>2</sub> emissions with moderate loss of performance and capacity.

Partial CO<sub>2</sub> capture was investigated for the conventional thermal integration (Figure 4-2), advanced thermal integration (Figure 4-9) and Modifications A, B, C and D to the advanced thermal integration (Figures 7-1, 7-2 and 7-3) for  $q_{\text{Reb}}$  values of 3.95 and 4.65 GJ/tonne CO<sub>2</sub> (1,700 and 2,000 Btu/lb CO<sub>2</sub>). The results are presented in Figures 8-1 to 8-8.

As percentage of CO<sub>2</sub> capture decreases, the amount of heat that needs to be supplied to the reboiler and steam flow to the reboiler decrease because less flue gas needs to be treated. The effect of CO<sub>2</sub> capture on the reboiler steam flow is presented in Figure 8-1. The results show that reboiler steam flow is a linear function of the percentage of CO<sub>2</sub> capture. The steam flow to the reboiler for Modification D is lower compared to other analyzed cases because a portion of the heat to the reboiler is provided by the flue gas (see Figure 7-4).

Reduced steam flow to the reboiler increases steam flow through the LP turbine (Figure 8-2). The steam flow through the LP turbine is higher for Modification D, compared to other analyzed modifications because a portion of heat to the reboiler is provided by the flue gas. Higher steam flow through the LP turbine increases gross turbine power output and improves performance of the steam turbine cycle and the unit. The improvement in gross power output for the conventional thermal integration relative to the 90% CO<sub>2</sub> capture is presented in Figure 8-3 as a function of percentage of CO<sub>2</sub> capture and  $q_{\text{Reb}}$ . The

improvement in gross power output varies linearly with the percentage of CO<sub>2</sub> capture and increases as CO<sub>2</sub> capture decreases. Also, the improvement in gross power output is higher for higher values of q<sub>Reb</sub>.

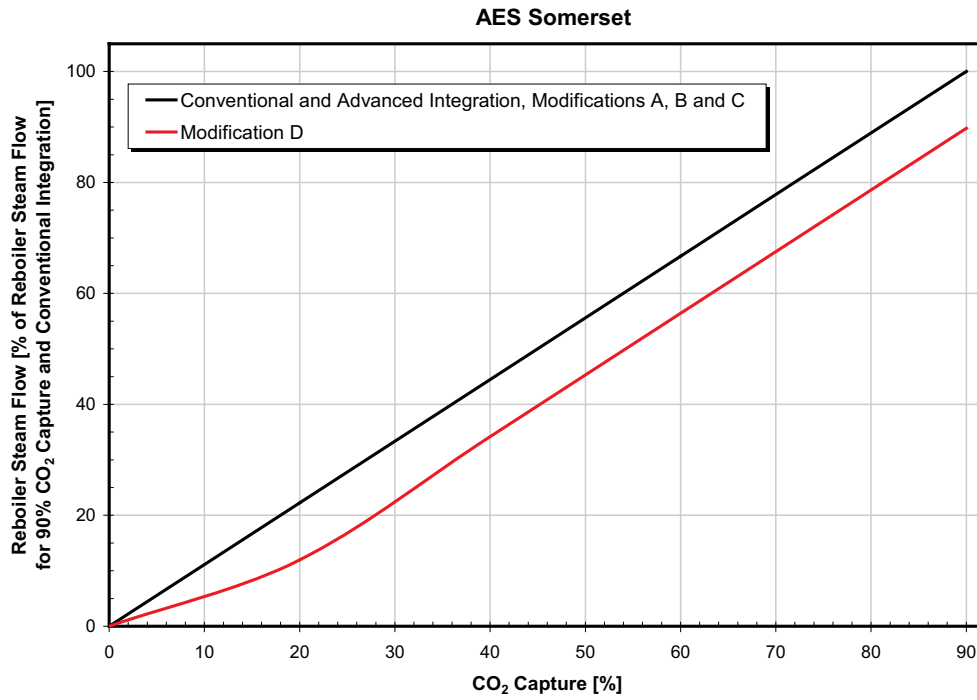


Figure 8-1. Reboiler Steam Flow as a Function of Percentage of CO<sub>2</sub> Capture.

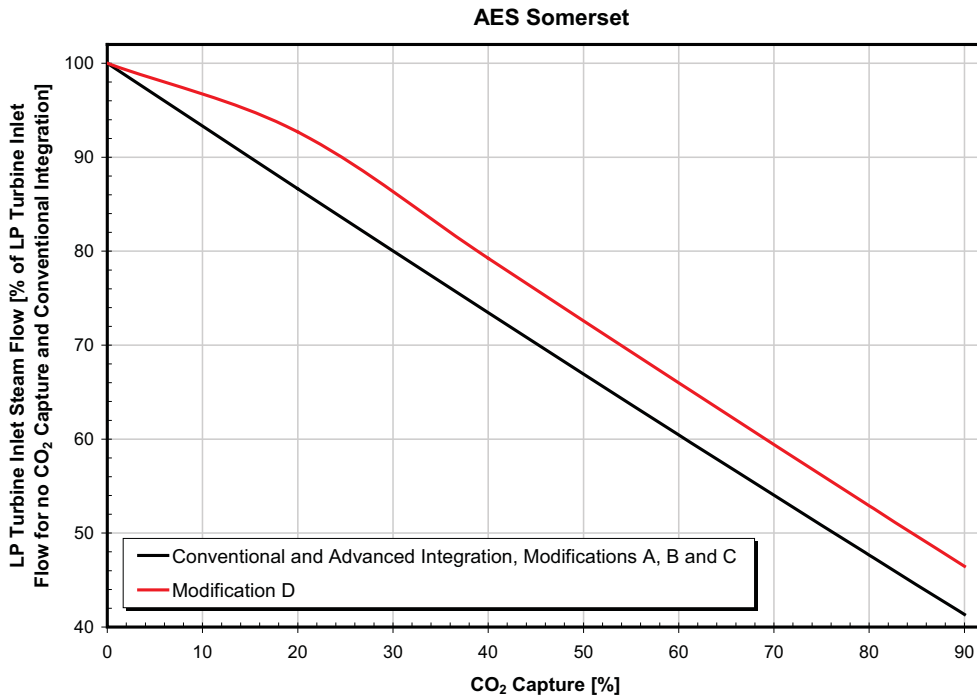
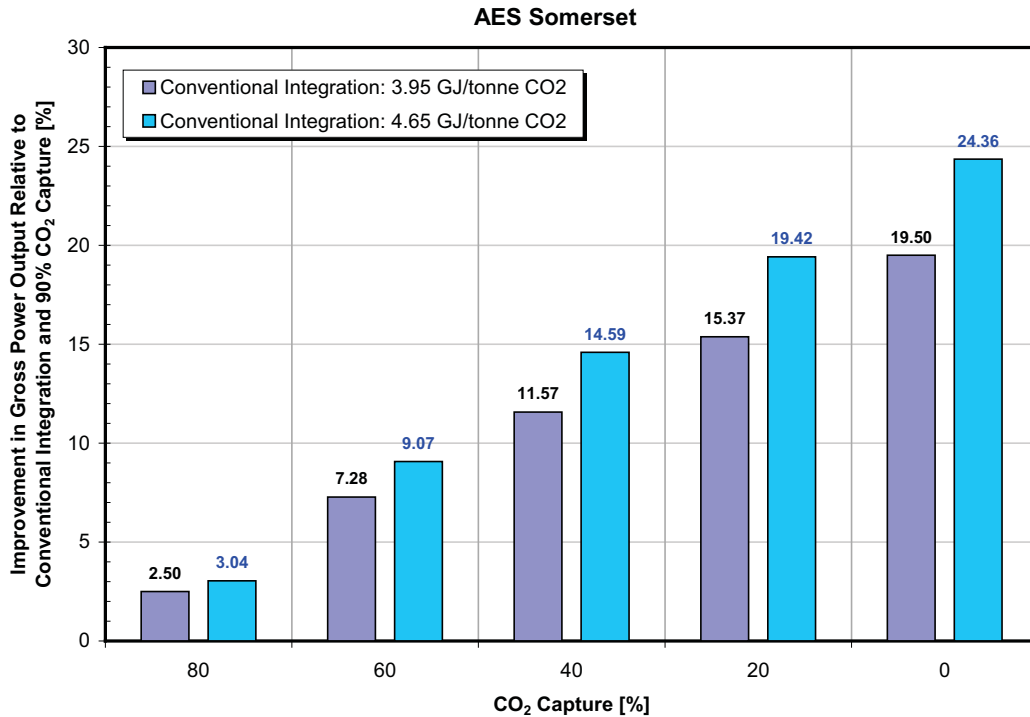


Figure 8-2. LP Turbine Inlet Steam Flow as a Function of Percentage of CO<sub>2</sub> Capture.



**Figure 8-3. Improvement in Gross Power Output as a Function of Percentage of CO<sub>2</sub> Capture and  $q_{Reb}$ .**

The effect of partial CO<sub>2</sub> capture on turbine cycle and unit performance relative to the conventional thermal integration and 90% CO<sub>2</sub> capture for the conventional and advanced thermal integrations and modifications A, B, C and D to the conventional thermal integration and  $q_{Reb}$  value of 3.95 GJ/tonne CO<sub>2</sub> (1,700 BTU/lb CO<sub>2</sub>) is shown in Figures 8-4 to 8-8.

As presented in Figure 8-4, improvement in the gross power output varies linearly with the percentage of CO<sub>2</sub> capture and is highest for Modification D. Improvements in turbine cycle heat rate and turbine cycle efficiency relative to the conventional thermal integration and 90% CO<sub>2</sub> capture are presented in Figures 8-5 and 8-6. Both quantities improve as percentage of CO<sub>2</sub> capture is decreased because of the lower flue gas flow rate that needs to be treated. For example, operating with 40% CO<sub>2</sub> capture would increase gross power output by 11.6 to 14%, relative to the conventional thermal integration and 90% CO<sub>2</sub> capture. This increase in power output would improve turbine cycle heat rate by 10.4 to 12.2% and turbine cycle efficiency by 4.1 to 5%-points, relative to the conventional thermal integration and 90% CO<sub>2</sub> capture. In other words, in case of the conventional thermal integration operation with 40% CO<sub>2</sub> capture would reduce penalty in turbine cycle efficiency to approximately 40% of the penalty that would be incurred with 90% CO<sub>2</sub> capture.

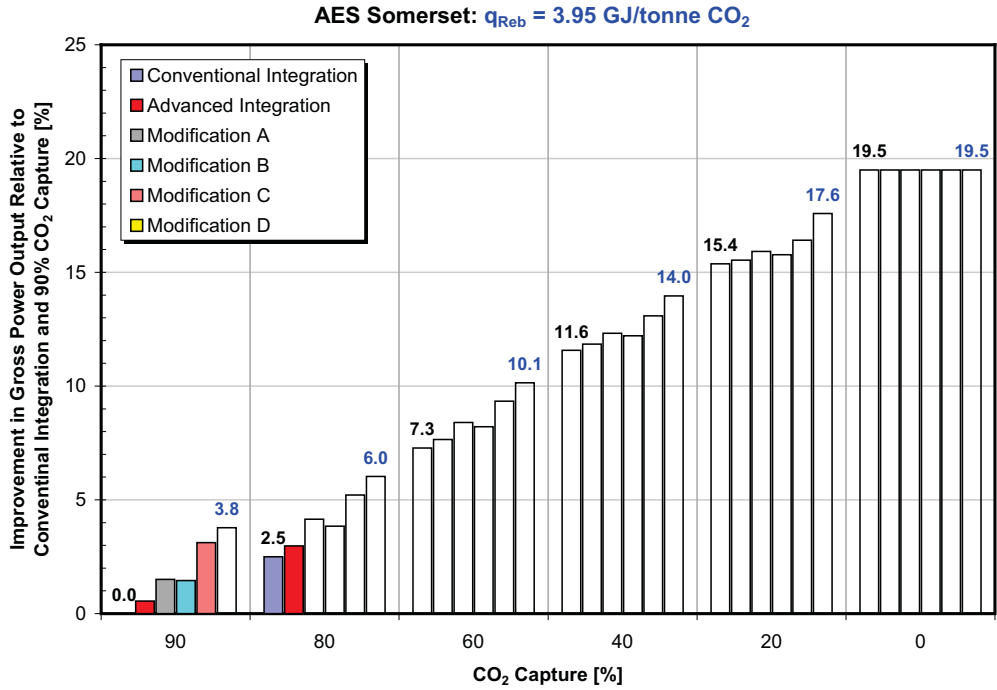


**Figure 8-4. Improvement in Gross Power Output as a Function of Percentage of CO<sub>2</sub> Capture.**

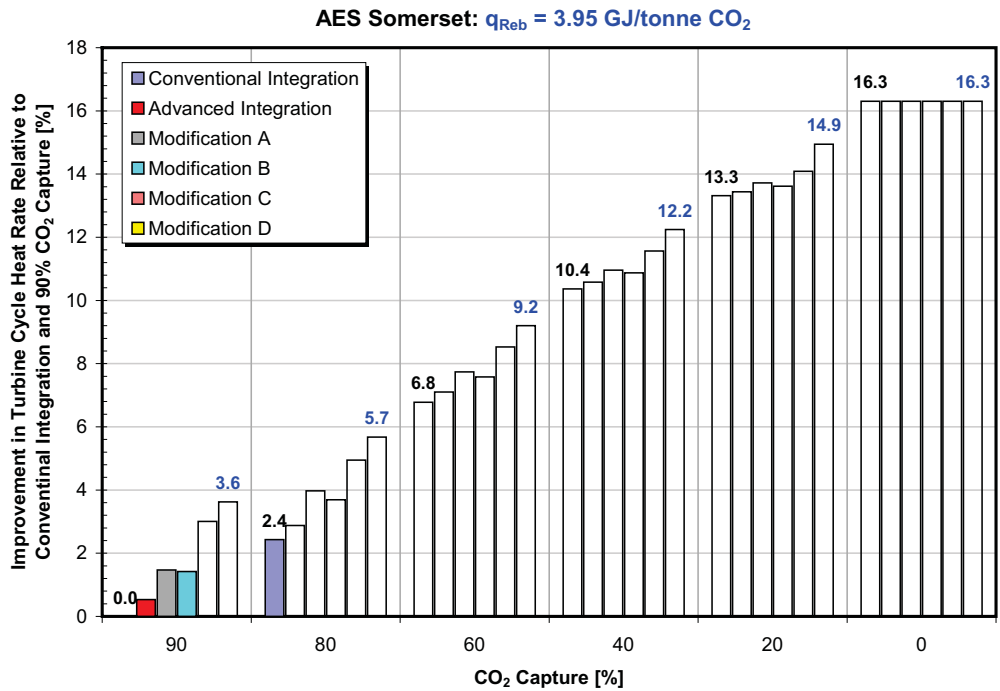


**Figure 8-5. Improvement in Turbine Cycle Heat Rate as a Function of Percentage of CO<sub>2</sub> Capture.**

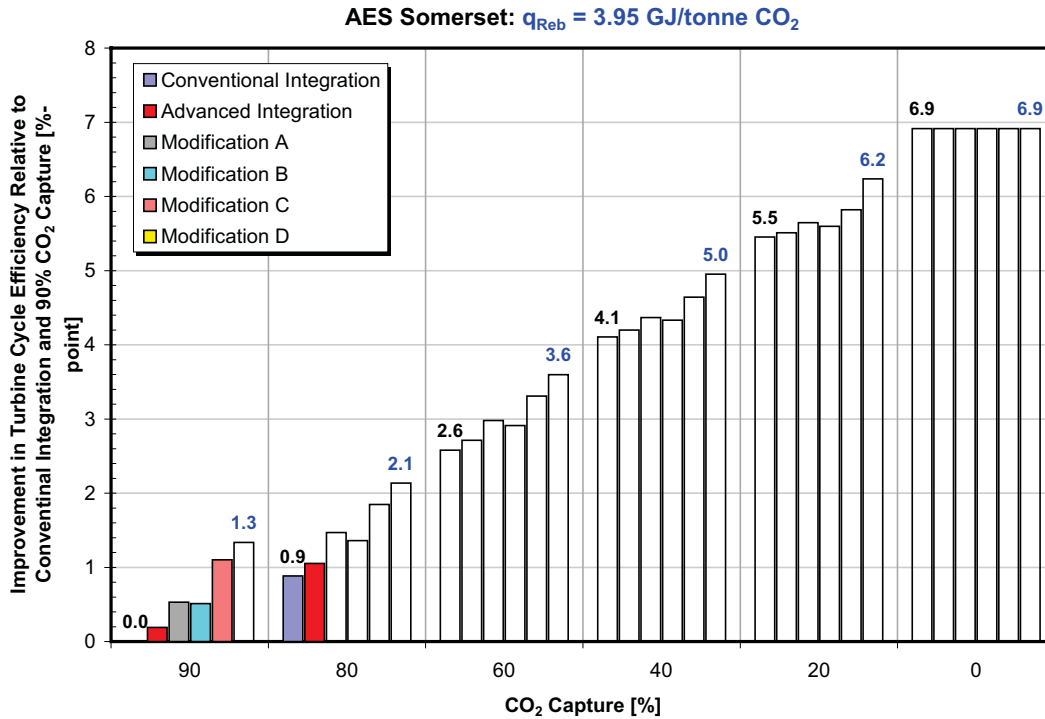


**Figure 8-6. Improvement in Turbine Cycle Efficiency as a Function of Percentage of CO<sub>2</sub> Capture.**

Improvements in net unit heat rate and net unit efficiency, relative to the conventional thermal integration and 90% CO<sub>2</sub> capture are presented in Figures 8-7 and 8-8 as function of percentage of CO<sub>2</sub> capture. Similar to the turbine cycle performance, net unit performance improves as percentage of CO<sub>2</sub> removal is lowered. For example, operation with 40% CO<sub>2</sub> capture would improve net unit heat rate by 17.8 to 19.7% and net unit efficiency by 5.5 to 6.2%-points relative to the 90% CO<sub>2</sub> capture and conventional thermal integration. The improvement in net unit performance is larger compared to the improvement in turbine cycle performance because of the CO<sub>2</sub> compression work, which is also reduced by the partial CO<sub>2</sub> capture.

As discussed earlier, partial CO<sub>2</sub> capture should be considered as a staged approach to full (90%) CO<sub>2</sub> capture or it could be implemented at older and less efficient power plants to reduce their carbon footprint with moderate performance penalty and significantly lower initial capital investment.

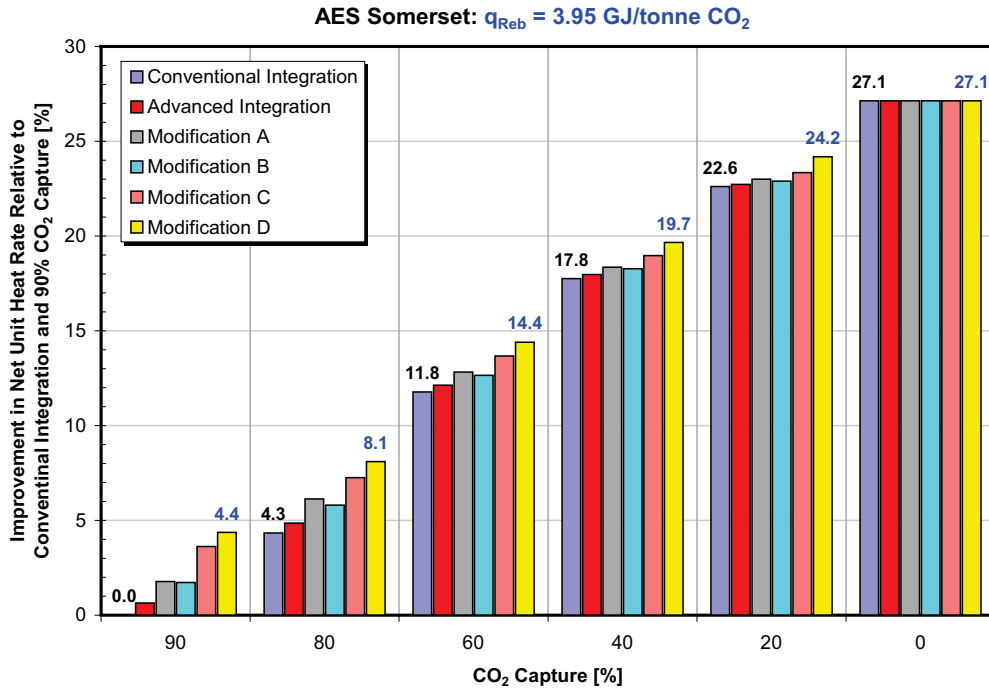


**Figure 8-7. Improvement in Net Unit Heat Rate as a Function of Percentage of CO<sub>2</sub> Capture.**

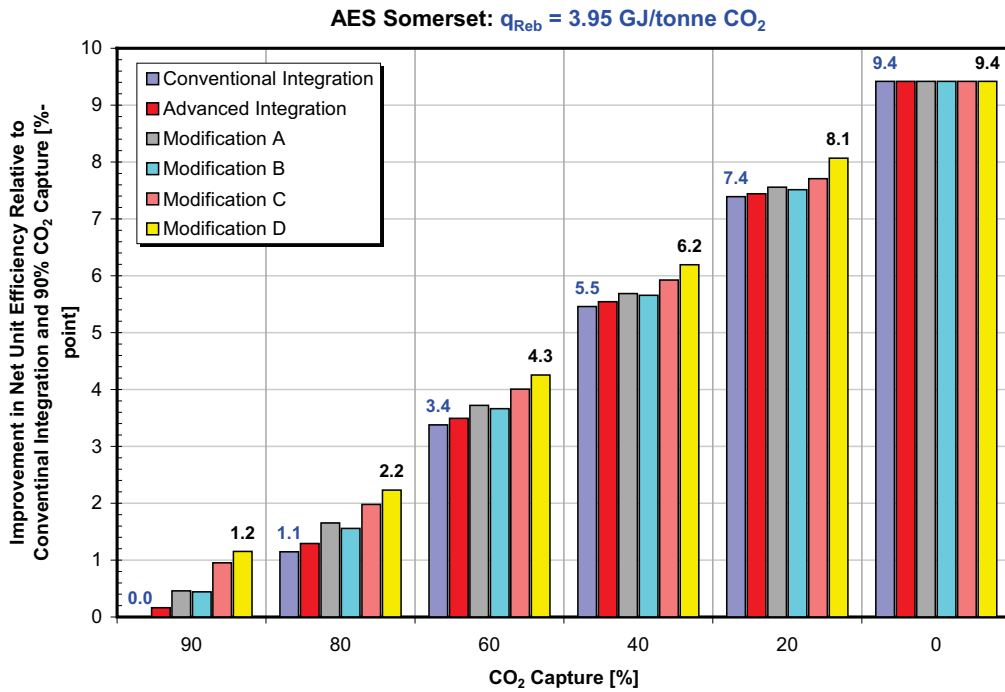


**Figure 8-8. Improvement in Net Unit Efficiency as a Function of Percentage of CO<sub>2</sub> Capture.**

## Section 9

### **RANKINE-BRAYTON CYCLE INTEGRATION**

Integration of Rankine and Brayton cycles was analyzed to determine efficiency (heat rate) improvements that can be achieved at existing power plants by using heat recovered from the Brayton cycle hot effluent to increase steam flow through the steam turbine and offset power loss to be incurred due to reboiler steam extraction. The ultimate goal of the cycle integration is efficiency improvement of the Rankine cycle and reduction of the capacity penalty to be incurred by implementation of the post-combustion CO<sub>2</sub> capture. This approach can be applied to existing larger coal-fired power plants to be retrofitted with post-combustion CO<sub>2</sub> capture, enabling them to continue operation in a carbon-constrained world.

The fueling options considered for the Brayton cycle include: hydrogen- and biogas-fired turbine. In the later case, biogas is produced by gasification of biomass in a fluidized bed gasifier, while the leftover char is burned in the boiler. In these analyses, both fueling options result in zero CO<sub>2</sub> emissions from the Brayton cycle when transportation and storage energy for biomass or hydrogen is excluded as these energy requirements are site specific. In addition, hydrogen is assumed to be produced by renewable or nuclear sources off-peak. Based on these assumptions, the power output and heat provided to the Rankine cycle through thermal integration do not contribute to the plant CO<sub>2</sub> emissions.

As a first step, the analysis was performed to determine optimal integration of the Rankine and Brayton cycles. Thermal integration, considered in the analysis and presented in Figure 9-1, involves use of the hot combustion turbine exhaust to generate steam in a heat recovery steam generator (HRSG). A turbine exhaust temperature of 670°C (1,238°F) and HRSG exhaust of 188°C (370°F) were used in the analysis.

This value of turbine exhaust temperature corresponds to a pressure ratio (PR) of 17, turbine inlet temperature (TIT) of 1,343°C (2,450°F) and turbine efficiency of 86%. The steam generated in the HRSG can be used either for feedwater heating in a HP FWH, in a reboiler, or it could be split in certain proportion to provide heat to both the feedwater and the reboiler. The exhaust leaving the HRSG is used for condensate heating in a LP FWH. To determine optimal heat use, the feedwater bypass through the HP FWH was parametrically varied from 100 to 0 %, resulting in a corresponding split in the HRSG thermal output between the HP FWH and the reboiler. The results for the analyzed cases (advanced thermal integration of the post combustion CO<sub>2</sub> capture system and Modifications C and D) show the best turbine cycle and combined cycle performance (Figure 9-2) is achieved when 100% of the HRSG thermal duty is used for HP the feedwater heating. This is because the steam extracted from the steam turbine cycle for the HP feedwater heating is of higher quality than a reboiler steam extracted from the IP turbine exhaust. Also, as steam extractions for the HP feedwater heating are decreased and eliminated, the steam flow through the steam turbine increases, resulting in higher power output of the steam turbine cycle. Therefore, subsequent

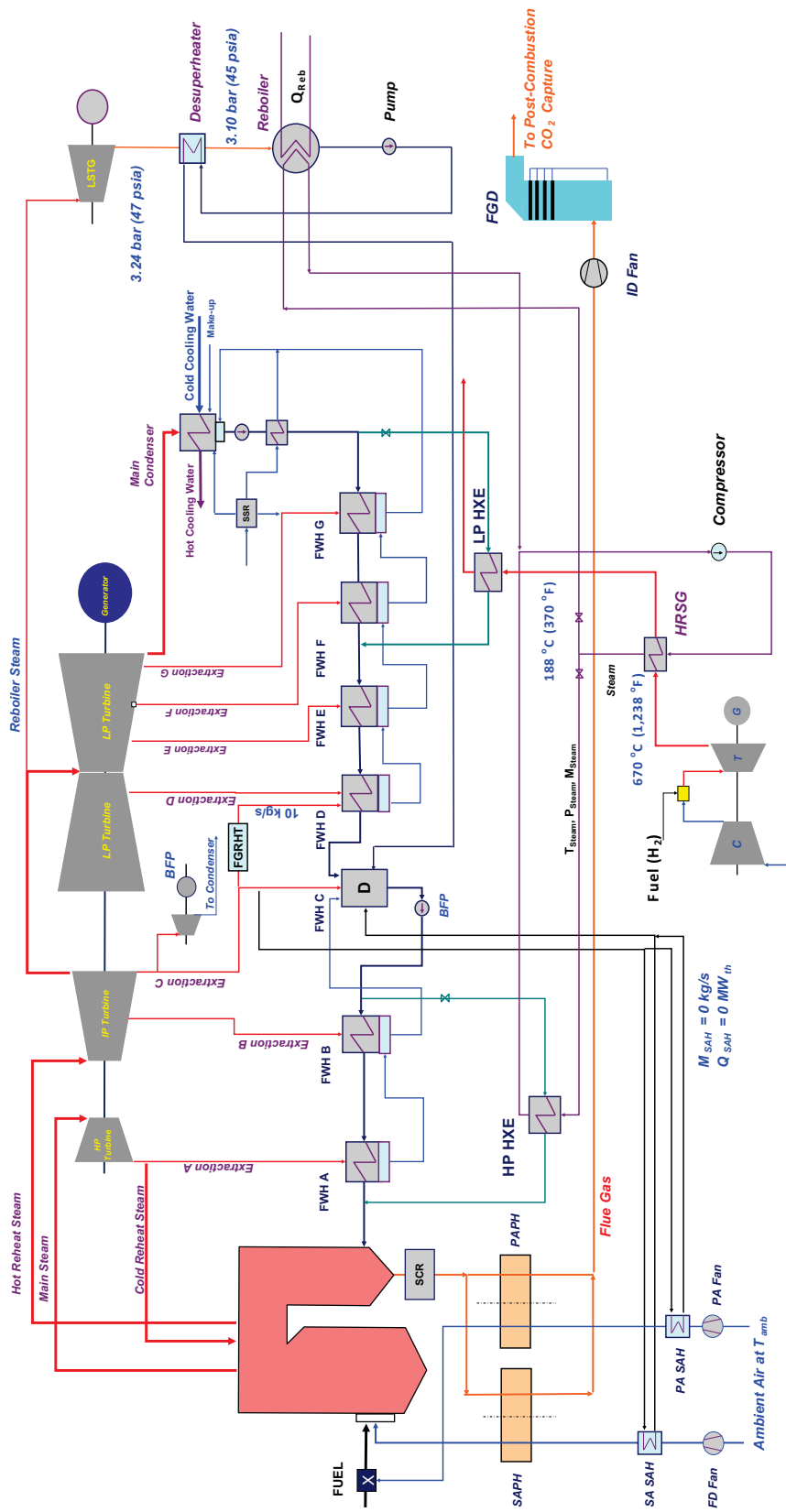
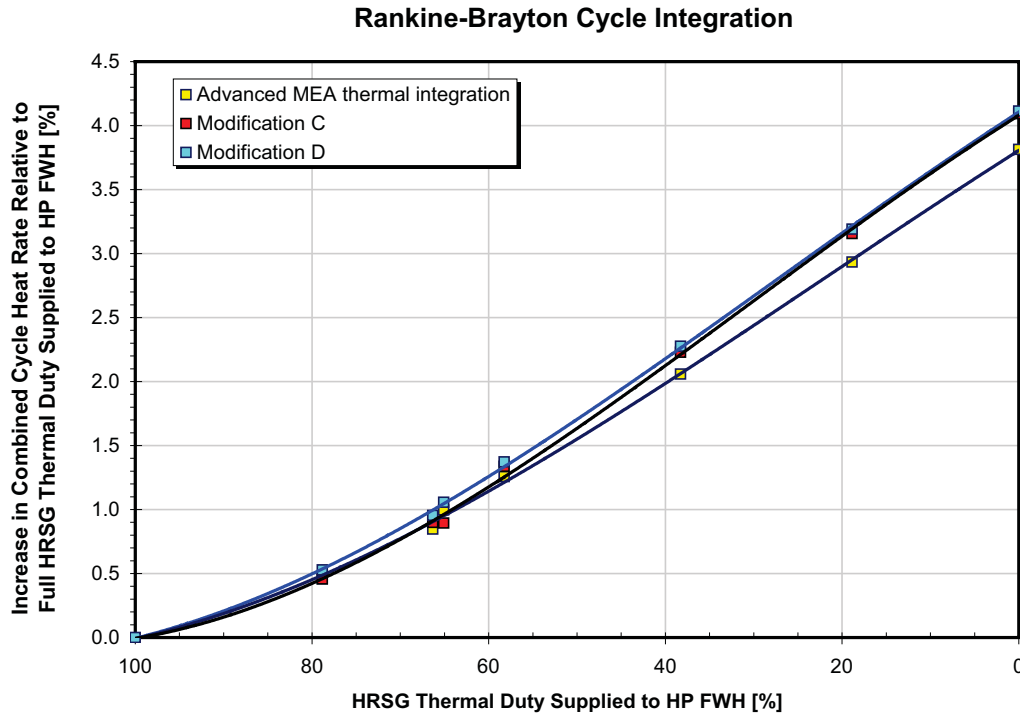


Figure 9-1. Thermal Integration of Rankine and Brayton Cycles.

analyses of the cycle integration were performed for the case where 100% of the HRSG thermal duty is used for the HP feedwater heating.



**Figure 9-2. Increase in Combined Cycle Heat Rate Relative to the Case Where Full HRSG Thermal Duty is Supplied to the HP FWH.**

## HYDROGEN-FUELED BRAYTON CYCLE

Hydrogen can be produced from diverse domestic feedstocks using a variety of process technologies. Hydrogen-containing compounds such as fossil fuels, biomass or even water can be a source of hydrogen. Thermochemical processes can be used to produce hydrogen from biomass and from fossil fuels such as coal, natural gas and petroleum. Power generated from sunlight, wind and nuclear sources can be used to produce hydrogen electrolytically. Sunlight alone can also drive photolytic production of hydrogen from water, using advanced photoelectrochemical and photobiological processes.

The DOE Hydrogen Program activity is focused on advancing cost-effective, efficient production of hydrogen from renewable, fossil and nuclear energy resources.

**Hydrogen from Natural Gas.** The Offices of Energy Efficiency and Renewable Energy (EERE) and Fossil Energy (FE) are working to reduce the cost of producing hydrogen via steam methane reforming. EERE is focused on distributed hydrogen production from natural gas and bio-derived liquid feedstocks and FE is focused on sub-centralized and centralized hydrogen production. Although hydrogen from

natural gas is certainly a viable near-term option, it is not viewed by DOE as a long-term solution because it does not help solve the greenhouse gas (GHG) or energy security issues.

**Hydrogen from Coal.** Research sponsored by the Office of Fossil Energy is focused on advancing the technologies needed to produce hydrogen from coal-derived synthesis gas and to build and operate a zero emissions, high-efficiency co-production power plant that will produce hydrogen from coal along with electricity. The FE is also investigating carbon sequestration technologies, in associated programs, as an option for managing and stabilizing greenhouse gas emissions from coal-fired plants.

**Hydrogen from Nuclear Power.** Research sponsored by the Office of Nuclear Energy (NE) is focused on developing the commercial-scale production of hydrogen using heat from a nuclear energy system. Key research areas include high-temperature thermochemical cycles, high-temperature electrolysis, and reactor/process interface issues.

**Hydrogen from Renewable Resources.** Research sponsored by the EERE is focused on developing advanced technologies for producing hydrogen from domestic renewable energy resources that minimize environmental impacts. Key research areas include electrolysis, thermochemical conversion of biomass, photolytic and fermentative micro-organism systems, photoelectrochemical systems, and high-temperature chemical cycle water splitting.

**Hydrogen Turbines.** DOE runs the Advanced Turbine System (ATS) program with a goal to develop ultra high-efficiency utility-scale natural gas-fueled turbines, hydrogen-fired (hydrogen from coal, Integrated Gasification Combined-Cycle (IGCC)-Based Near-Zero Emissions Concept), and oxygen-fired turbines enabling near-zero emission coal-based power plants. Development of hydrogen-fueled turbines with comparable performance to natural gas-fueled turbines, however, represents a significant challenge in combustion technology. On the positive side, the significant progress and accomplishments already made, and ongoing work in adapting turbines to syngas are applicable to hydrogen conversion because technical challenges are similar in many respects, [NETL, 2005]. This technology is expected to be commercially available by 2020.

Assuming hydrogen will be available from one of the above-mentioned sources, the analysis was performed for the conventional (Figure 4-2) and advanced (Figure 4-9) thermal integration of the post-combustion MEA CO<sub>2</sub> removal process (Conventional and Advanced MEA) and Modifications A, B, C and D (Figures 7-1 to 7-4) for  $q_{\text{Reb}}$  values in the 2.79 to 5.47 GJ/tonne CO<sub>2</sub> (1,200 and 2,350 Btu/lb CO<sub>2</sub>) range. The results are compared to the baseline (no CO<sub>2</sub> capture) and conventional MEA integration for Rankine cycle (no cycle integration). The Brayton cycle was sized to provide sufficient amount of heat to

replace steam extractions for the HP FWHs A and B, resulting in power output of the hydrogen-fueled turbine of 140.5 MW<sub>el</sub>. Calculations were performed by using a Brayton cycle efficiency of 32.91%.

### **Rankine Cycle**

The effect of Rankine-Brayton cycle integration on performance of the Rankine cycle is large, as presented in Figures 9-3 to 9-6, with Modification D resulting in best performance. The results concerning reduction in gross power output of the Rankine cycle, incurred by the CO<sub>2</sub> capture, relative to the baseline (no CO<sub>2</sub> capture, no cycle integration) are presented in Figure 9-3. For the state-of-the-art amines and Conventional MEA, reduction in power output is decreased from 14.67 to 3% by cycle integration; while for Modification D reduction in power output is decreased from 11.65 to 0.70%. For the q<sub>Reb</sub> value, determined for the MEA in this study and Conventional MEA integration, cycle integration decreases reduction in power output incurred by the CO<sub>2</sub> capture from 19.59 to 7.62%; while for Modification D power reduction is decreased from 16.47 to 4.75%.

The results concerning improvement in gross power output of the Rankine cycle relative to the Conventional MEA and no cycle integration are presented in Figure 9-4. For the state-of-the-art amines and Advanced MEA, improvement in power output is increased from 0.48 to 14.45% by cycle integration; while for Modification D improvement in power output is increased from 3.54 to 16.37%. For the q<sub>Reb</sub> value determined for the MEA in this study and advanced MEA integration, cycle integration improves power output from 0.66 to 15.68%; while for Modification D power improvement, relative to the Conventional MEA is increased from 3.88 to 18.46%.

A decrease in net efficiency ( $\eta_{\text{net}}$ ) of the Rankine cycle-based plant relative to the baseline (no CO<sub>2</sub> capture) is presented in Figure 9-5. For the state-of-the-art amines and Conventional MEA, reduction in  $\eta_{\text{net}}$  is decreased by 3.69%-points (from 8.82 to 5.13%-point) by cycle integration; while for Modification D, the reduction in  $\eta_{\text{net}}$  is decreased by 3.46%-points (from 7.71 to 4.25%-points). For the q<sub>Reb</sub> value, determined for the MEA in this study and the conventional MEA integration, cycle integration reduces the decrease in  $\eta_{\text{net}}$  by 3.83%-points (from 10.62 to 6.79%-point); while for Modification D decrease in  $\eta_{\text{net}}$  is reduced by 3.78%-points (from 9.48 to 5.70%-points).

Improvement in  $\eta_{\text{net}}$  of the Rankine cycle-based plant relative to the Conventional MEA and no cycle integration is presented in Figure 9-6. For state-of-the-art amines and advanced MEA, cycle integration increases improvement in  $\eta_{\text{net}}$  from 0.15 to 3.82%-points; while for Modification D, the improvement in  $\eta_{\text{net}}$  is increased from 1.11 to 4.57%-points. For the q<sub>Reb</sub> value, determined for the MEA in this study and advanced MEA integration, cycle integration improves  $\eta_{\text{net}}$  from 0.19 to 4.00%-points; while for

Modification D, the improvement in  $\eta_{\text{net}}$  relative to the Conventional MEA increases from 1.14 to 4.92% points.

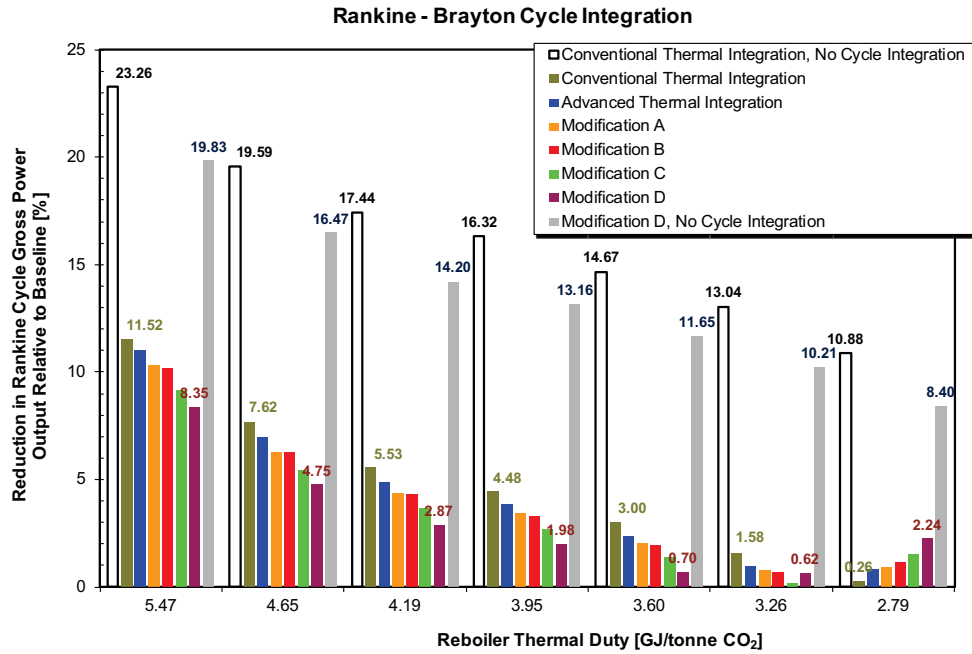


Figure 9-3. Reduction in Power Output of the Rankine Cycle Relative to the Baseline (no CO<sub>2</sub> capture) as Function of  $q_{\text{Reb}}$ , Cycle Integration, and Thermal Integration of the Post-Combustion MEA CO<sub>2</sub> Capture.

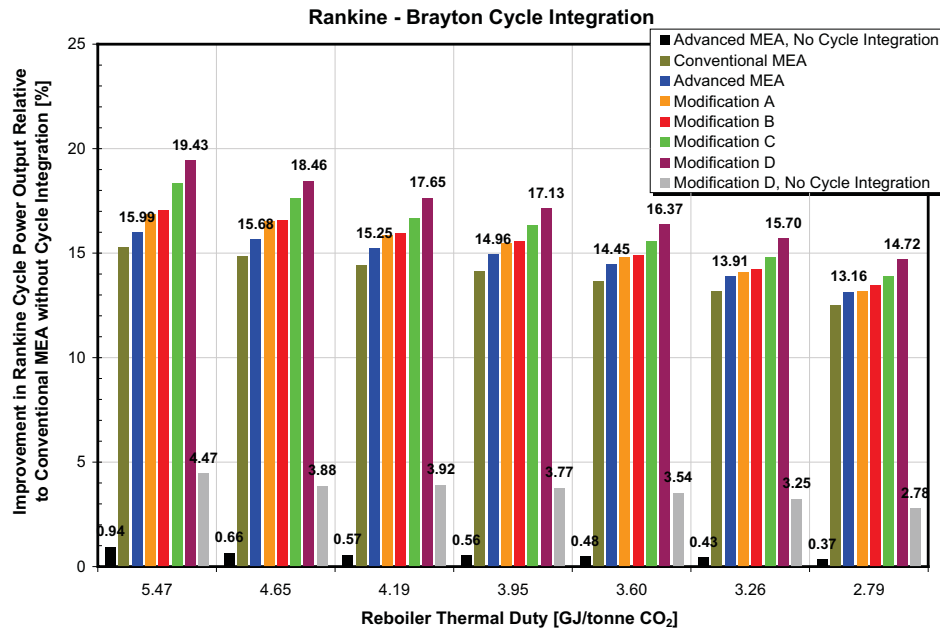


Figure 9-4. Improvement in Power Output of the Rankine Cycle Relative to the Conventional MEA as Function of  $q_{\text{Reb}}$ , Cycle Integration, and Thermal Integration of the Post-Combustion MEA CO<sub>2</sub> Capture.

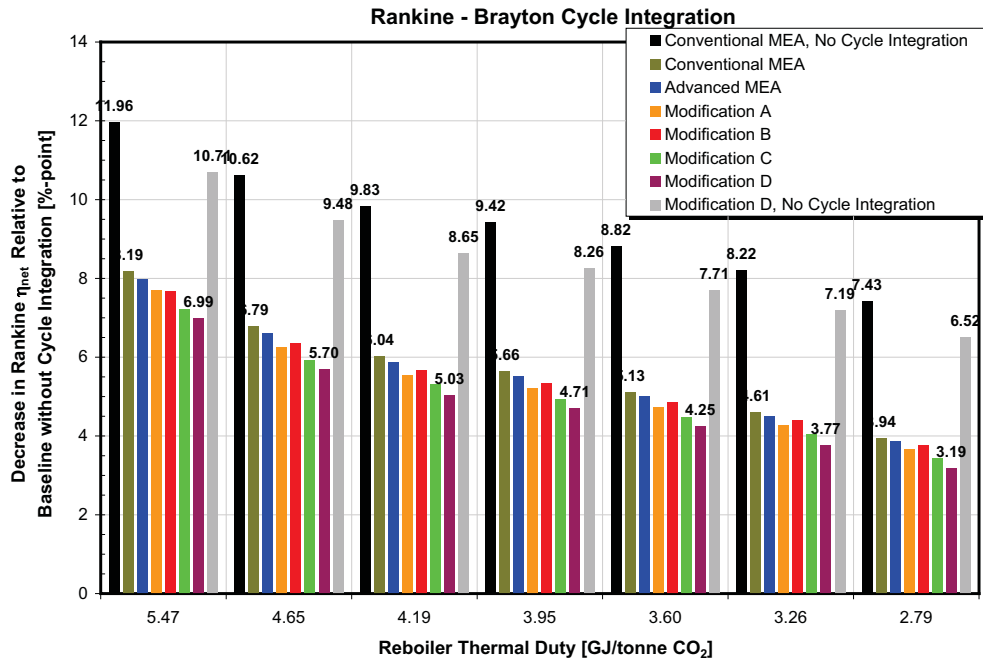


Figure 9-5. Decrease in Net Efficiency of the Rankine Cycle Relative to the Baseline (no CO<sub>2</sub> capture) as Function of  $q_{Reb}$ , Cycle Integration, and Thermal Integration of the Post-Combustion MEA CO<sub>2</sub> Capture.

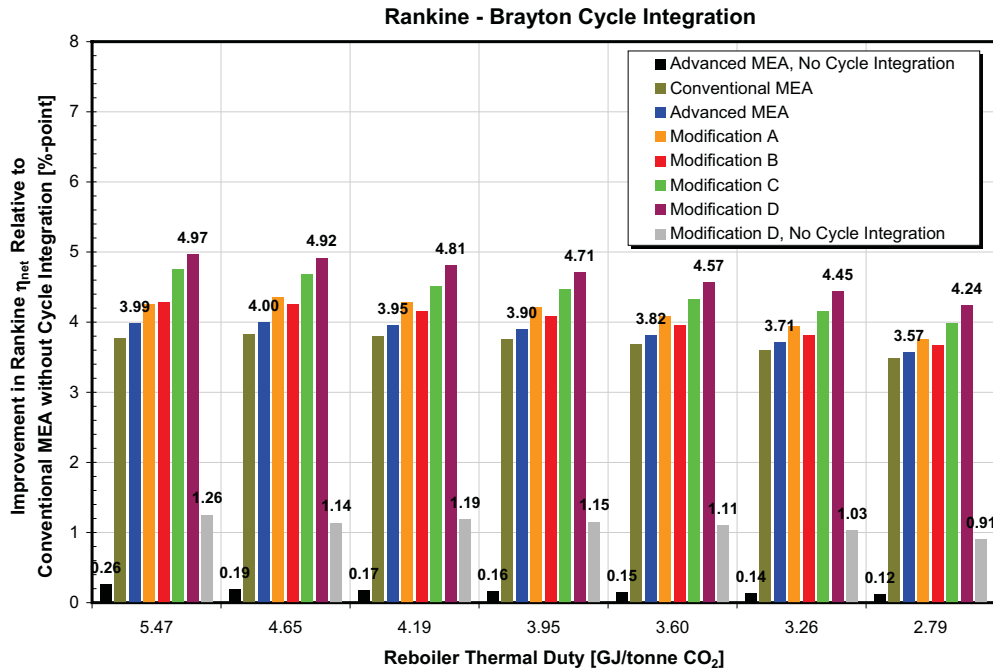
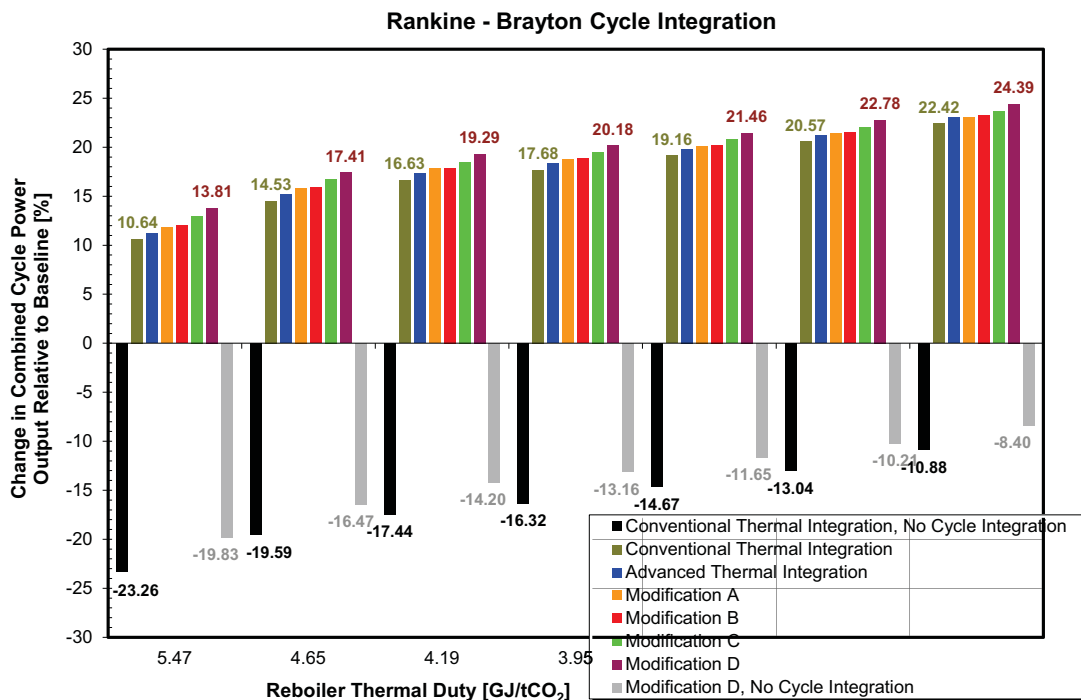


Figure 9-6. Improvement in Net Efficiency of the Rankine Cycle Relative to the Conventional MEA as Function of  $q_{Reb}$ , Cycle Integration, and Thermal Integration of the Post-Combustion MEA CO<sub>2</sub> Capture.

## Combined Cycle

The effect of the Rankine-Brayton cycle integration on the combined cycle performance is large, as presented in Figures 9-7 to 9-10, with Modification D resulting in best performance. The results concerning reduction in the gross power output of the combined cycle incurred by the CO<sub>2</sub> capture, relative to the baseline (no CO<sub>2</sub> capture, no cycle integration), are presented in Figure 9-7. The power output of the combined cycle is greatly increased by the cycle integration. For state-of-the-art amines and Conventional MEA, the power output of the combined cycle is higher by 19.16%, relative to the baseline, while without cycle integration power output is lower by 23.26%. For Modification D, power output of the combined cycle 21.46% is higher compared to the baseline, while without cycle integration it is 11.65% lower. For the  $q_{Reb}$  value, determined for the MEA in this study and the conventional MEA integration, cycle integration increases the power output of the combined cycle by 14.53%, compared to 19.59% decrease without cycle integration. For Modification D, cycle integration increases the power output of the combined cycle by 17.41%, compared to a 17.44% decrease without cycle integration.



**Figure 9-7. Change in Power Output of the Combined Cycle Relative to the Baseline (no CO<sub>2</sub> capture) Without Cycle Integration as Function of  $q_{Reb}$ , Cycle Integration, and Thermal Integration of the Post-Combustion MEA CO<sub>2</sub> Capture.**

The results concerning improvement in gross power output of the combined cycle, relative to the Conventional MEA with no cycle integration, presented in Figure 9-8, show power output of the combined cycle is greatly increased by cycle integration. For the state-of-the-art amines and Advanced MEA, cycle

integration increases power output from 0.48 to 40.42%, relative to the Conventional MEA; while for Modification D power output is increased from 3.54 to 42.34%. For the  $q_{Reb}$  value, determined for the MEA in this study and advanced MEA integration, cycle integration improves power output from 0.66 to 43.23%, relative to the Conventional MEA; while for Modification D, the power output is increased from 3.88 to 18.46%.

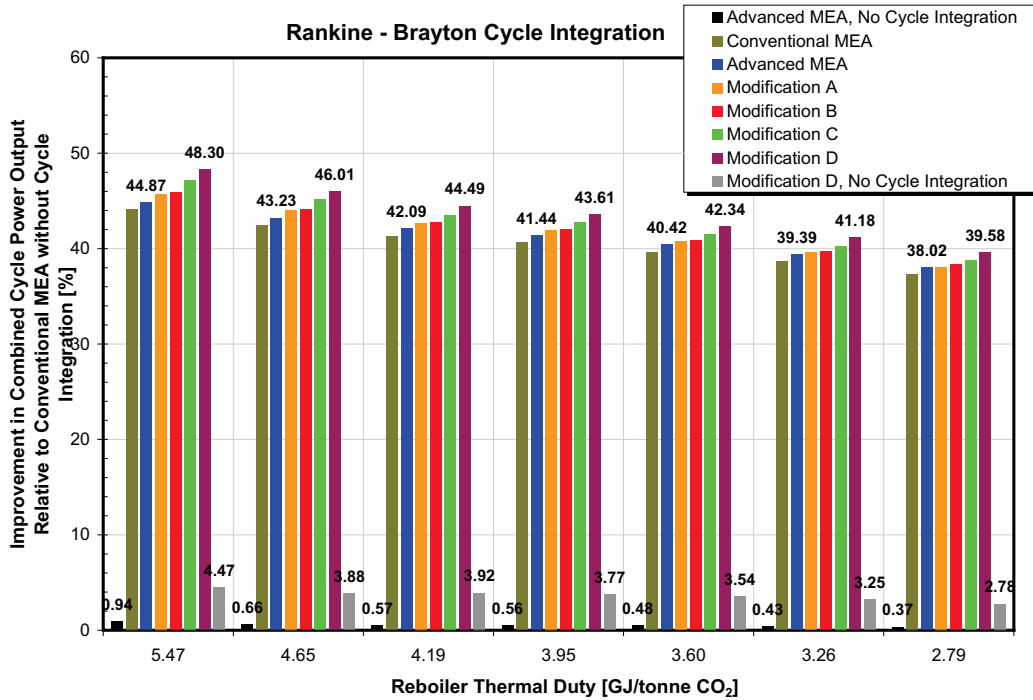


**Figure 9-8. Improvement in Power Output of the Combined Cycle Relative to the Conventional MEA Without Cycle Integration as Function of  $q_{Reb}$ , Cycle Integration, and Thermal Integration of the Post-Combustion MEA CO<sub>2</sub> Capture.**

The results concerning the decrease in net unit efficiency of the combined cycle, to be incurred by the CO<sub>2</sub> capture, relative to the baseline (no CO<sub>2</sub> capture, no cycle integration) are presented in Figure 9-9. The results show that the decrease net unit efficiency of the combined cycle is reduced by about 50% compared to the Rankine cycle-based unit. For the state-of-the-art amines and Conventional MEA, the decrease in net unit efficiency of the combined cycle is 4.48%-points, while without cycle integration the decrease in net unit efficiency that would be incurred by the CO<sub>2</sub> capture is 8.82%-point. For Modification D, the decrease in net unit efficiency of the combined cycle is 3.77%-points compared to the baseline. Without cycle integration the decrease in net unit efficiency is 7.71%-points.

For the  $q_{Reb}$  value determined for MEA in this study and conventional MEA integration, cycle integration reduces the decrease in unit efficiency of the combined cycle by 5.82%-points, compared to 10.62%-points

without cycle integration. For Modification D, cycle integration reduces the decrease in net unit efficiency of the combined cycle by 4.94%-points, compared to the 10.62%-points decrease with no cycle integration.

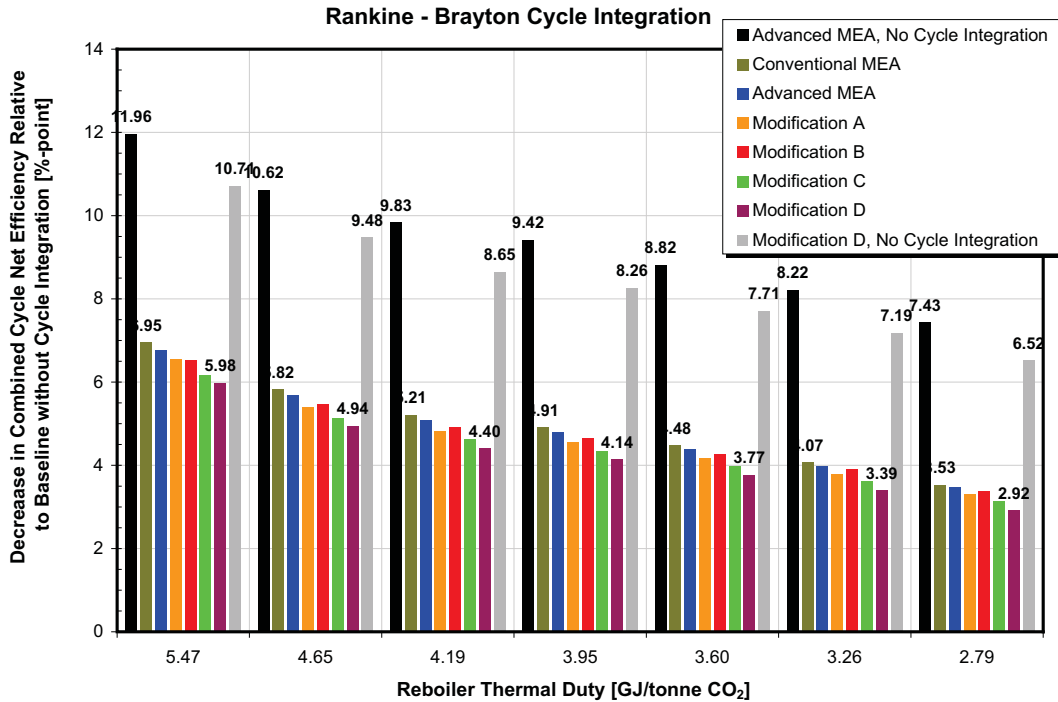


**Figure 9-9. Decrease in Net Unit Efficiency of the Combined Cycle Relative to the Baseline (no CO<sub>2</sub> capture) Without Cycle Integration as Function of  $q_{Reb}$ , Cycle Integration, and Thermal Integration of the Post-Combustion MEA CO<sub>2</sub> Capture.**

In summary, cycle integration has a large positive effect on performance of the combined cycle. Some of the results are presented in Table 9-1. In addition to increasing plant gross power output, reduction in net plant efficiency relative to the baseline (Rankine cycle, no CO<sub>2</sub> capture) that would be incurred by the retrofit or implementation of post-combustion CO<sub>2</sub> capture is decreased by the factor of two. Cycle integration also reduces penalties in turbine cycle heat rate, turbine cycle efficiency, and net unit heat rate that would be incurred by implementation of the post-combustion CO<sub>2</sub> capture process.

**Table 9-1. Rankine-Brayton Cycle Integration: Hydrogen-Fired Turbine, FWHs A and B.**

Hydrogen-Fired Turbine, HP FWHs A and B				
State-of-the-Art Amines	Integrated Rankine-Brayton Cycle		Rankine Cycle	
	Change in P <sub>G</sub> Relative to Baseline	Change in $\eta_{net}$ Relative to Baseline	Change in P <sub>G</sub> Relative to Baseline	Change in $\eta_{net}$ Relative to Baseline
MEA Integration	%	%-point	%	%-point
Advanced MEA	19.82	-4.38	-14.26	-8.67
Modification D	21.46	-3.77	-11.65	-7.71
<b>Baseline = Rankine Cycle, No CO<sub>2</sub> Capture</b>				

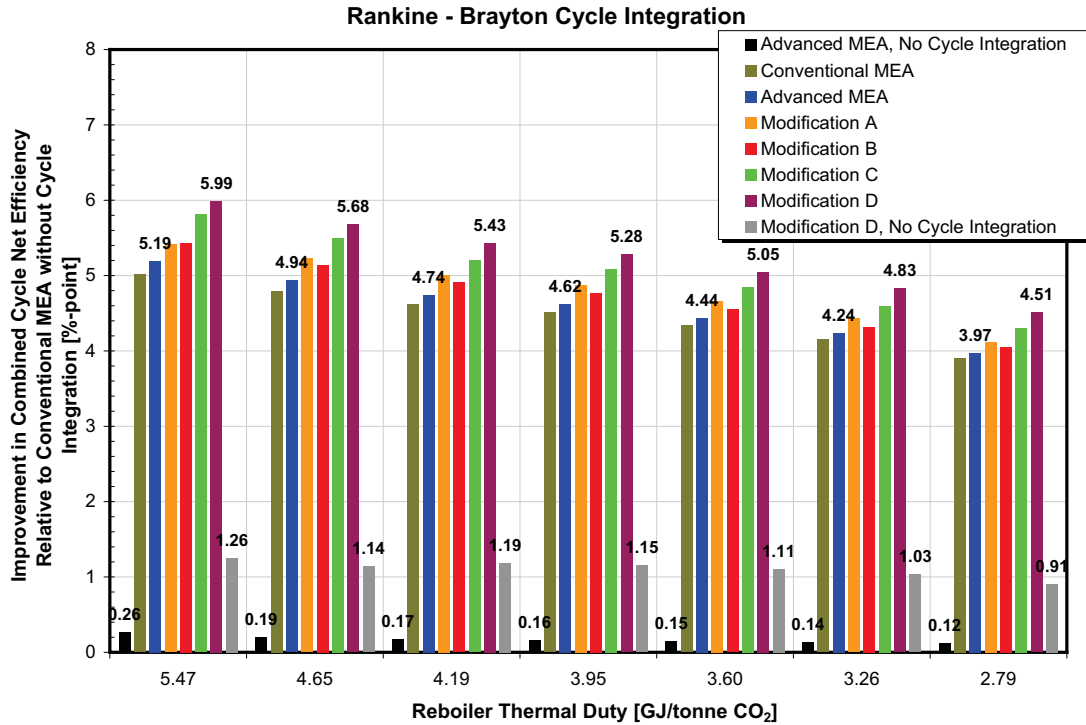


**Figure 9-10. Improvement in Net Unit Efficiency of the Combined Cycle Relative to the Conventional MEA Without Cycle Integration as Function of  $q_{Reb}$ , Cycle Integration, and Thermal Integration of the Post-Combustion MEA CO<sub>2</sub> Capture.**

The analysis was extended to the case where the Brayton cycle was sized to provide heat to replace steam extraction only for the HP FWH A. This decreased power output of the hydrogen-fired turbine to approximately 95 MW<sub>el</sub>. Due to the lower power output, calculations were performed by using a Brayton cycle efficiency of 32.71%. Some of the results are summarized in Table 9-2. For this case and the state-of-the-art amines, performance improvement, although being smaller compared to the case where steam extractions for both HP FWHs are eliminated, is still significant.

**Table 9-2. Rankine-Brayton Cycle Integration: Hydrogen-Fired Turbine, FWH A.**

Hydrogen-Fired Turbine, HP FWH A				
State-of-the-Art Amines	Integrated Rankine-Brayton Cycle		Rankine Cycle	
	Change in P <sub>G</sub> Relative to Baseline	Change in $\eta_{net}$ Relative to Baseline	Change in P <sub>G</sub> Relative to Baseline	Change in $\eta_{net}$ Relative to Baseline
MEA Integration	%	%-point	%	%-point
Advanced MEA	8.35	-4.84	-14.26	-8.67
Modification D	10.61	-5.56	-11.65	-7.71
<b>Baseline = Rankine Cycle, No CO<sub>2</sub> Capture</b>				

## BIOMASS GASIFICATION SYNGAS-FUELED BRAYTON CYCLE

The Energy Information Administration's estimation of biomass resources shows there are 590 million wet tons of biomass available in the United States on an annual basis; 20 million wet tons (enough to supply about 3 Gigawatts of capacity) are available today at prices of \$1.25 per million Btu or less. The average price of coal to electric utilities in 2001 was \$1.23/MBtu [Zia, 2002] (significantly higher today).

Biomass gasification is the conversion of an organically derived, carbonaceous feedstock by partial oxidation into a gaseous product, synthesis gas "syngas" or biogas consisting primarily of hydrogen (H<sub>2</sub>) and carbon monoxide (CO), with lesser amounts of carbon dioxide (CO<sub>2</sub>), water (H<sub>2</sub>O), methane (CH<sub>4</sub>), higher hydrocarbons (C<sub>2</sub>+), and nitrogen (N<sub>2</sub>). The reactions are carried out at elevated temperatures, 500-1400°C, and atmospheric or elevated pressures up to 33 bar (480 psia). The oxidant used can be air, pure oxygen, steam or a mixture of these gases. Air-blown gasifiers typically produce a product gas containing a relatively high concentration of nitrogen with a low heating value.

The chemistry of biomass gasification is complex. Biomass gasification proceeds primarily via a two-step process, pyrolysis followed by gasification. Pyrolysis is the decomposition of the biomass feedstock by heat. This step, also known as devolatilization, is endothermic and produces 75 to 90% volatile materials in the form of gaseous and liquid hydrocarbons. The remaining nonvolatile material, containing high carbon content, is referred to as char [Ciferno and Marano, 2002].

Both dedicated biomass and biomass co-firing are used in the electricity generation sector. New dedicated biomass capacity is represented in the National Energy Modeling System (NEMS) as biomass integrated gasification combined-cycle (BIGCC) technology. The syngas leaving the gasifier has to be cleaned to remove particulates and tar by employing either a low-temperature or high-temperature gas cleaning. In low-temperature cleaning, the gas is cooled with water, and particulates are removed in a series of cyclone vessels. Hot gas cleanup technology is relatively new, and DOE and many industrial partners are conducting tests to demonstrate the technology. There are advantages and disadvantages associated with both processes.

The cold gas cleaning was selected in this study. The heat recovered from the syngas leaving the biomass gasifier would be used in the turbine cycle, see Figure 9-11. The syngas is cooled in the high temperature (HTHR) and low temperature (LTHR1 and LTHR2) heat exchangers from 900°C (1,650°F) to 90 to 120°C (194 to 248°F). Particulates are removed in cyclones. The rest of the syngas cleanup equipment is not shown here. Recovered heat is used for heating of the HP feedwater in the HP HXE A1 and HP HXE B1, and for heating of the LP condensate in the LP HXE 1. The heat from the hot flue gas leaving the syngas-

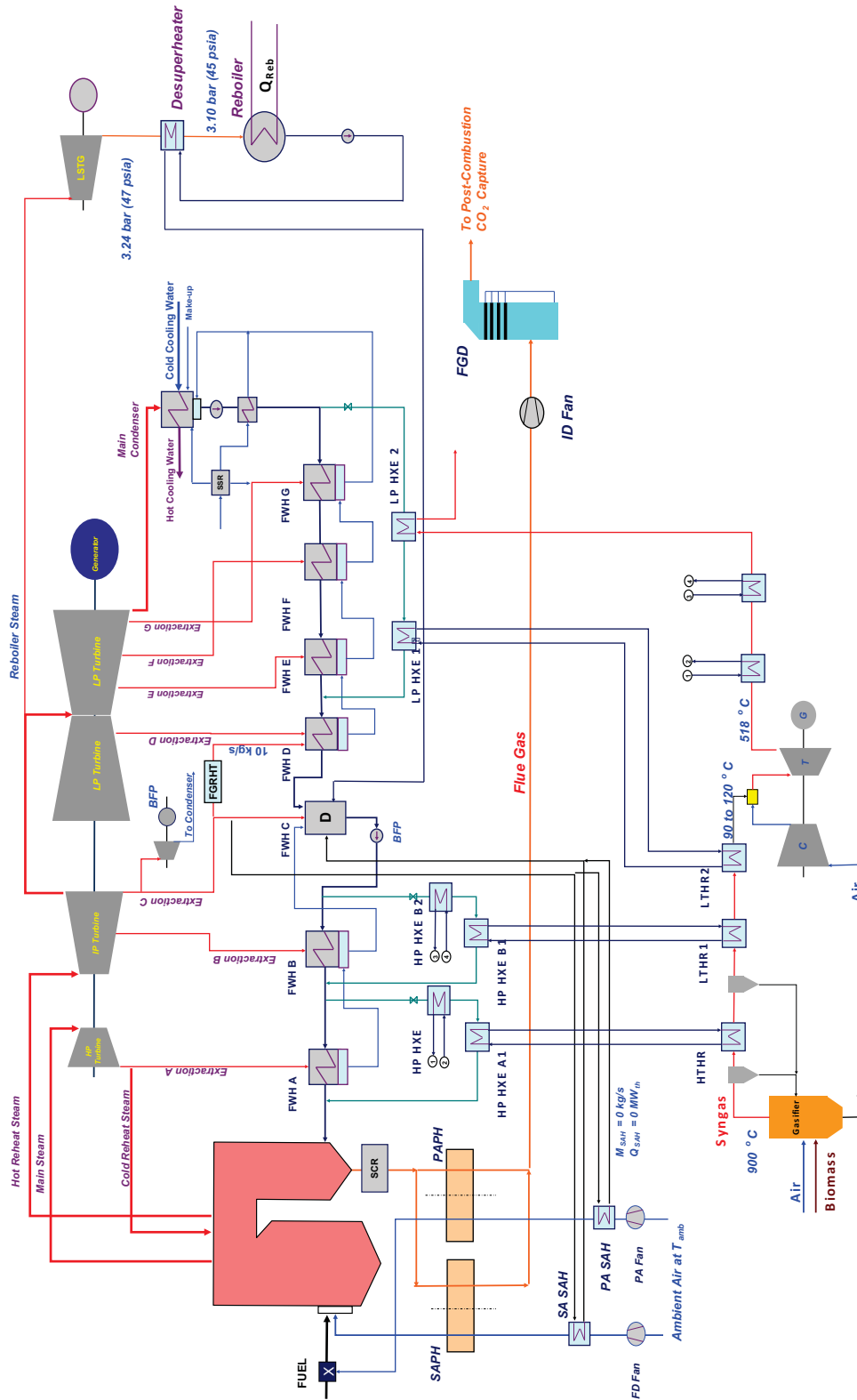


Figure 9-11. Schematic of Rankine and Biomass-Fueled Brayton Cycles: Advanced MEA Integration.

fired turbine at 518°C (965°F) is recovered and used for heating of the HP feedwater in the HP HXE A2 and HP HXE B2, and for heating of the LP condensate in the LP HXE 2.

The turbine exhaust (outlet) temperature (TOT) of 518°C (965°F), used in the analysis, corresponds to the pressure ratio of 12, turbine inlet temperature (TIT) of 890°C (1,636°F) and turbine efficiency of 70%. To keep the amount of biomass needed manageable, economically harvestable and sustainable, the Brayton cycle was sized to provide sufficient amount of heat to replace the steam extraction for the HP FWH A and partially for HP FWH B, resulting in a power output of the syngas-fueled turbine of approximately 33 MW<sub>el</sub>. Due to the small turbine size, and low TIT and PR, calculations were performed by using a value of Brayton cycle efficiency of 16.83%.

Analysis of the effect of cycle integration on performance of the Rankine and combined cycle was performed for the advanced (Figure 4-9) thermal integration of the post-combustion MEA CO<sub>2</sub> removal process (Advanced MEA) and Modifications C and D (Figures 7-3 and 7-4) to the Advanced MEA for values of q<sub>Reb</sub> in the 2.79 to 5.47 GJ/tonne CO<sub>2</sub> (1,200 to 2,350 Btu/lb CO<sub>2</sub>) range. A schematic representation of the integrated Rankine-Brayton cycle and Advanced MEA is presented in Figure 9-11.

### **Rankine Cycle**

The effect of integration of the Rankine and biomass-fueled Brayton cycle on the performance of the Rankine cycle is significant, as presented in Figures 9-12 to 9-15 with Modification D resulting in best performance. The reduction in the gross power output of the Rankine cycle incurred by the CO<sub>2</sub> capture relative to the baseline (no CO<sub>2</sub> capture, no cycle integration) is presented in Figure 9-12. The results show cycle integration has a large positive effect on the power output; for the state-of-the-art amines and Modification D to the Conventional MEA, the reduction in power output is decreased from 11.65 to 3.11%. For the q<sub>Reb</sub> value determined for the MEA in this study and Modification D, the power reduction is decreased from 16.47 to 7.32%.

The results concerning improvement in the gross power output of the Rankine cycle relative to the Conventional MEA and no cycle integration are presented in Figure 9-13. For the state-of-the-art amines and Modification D, improvement in power output is increased from 3.54 to 13.55%. For the q<sub>Reb</sub> value, determined for the MEA in this study and Modification D, cycle integration improves the power output from 3.88 to 15.25%.

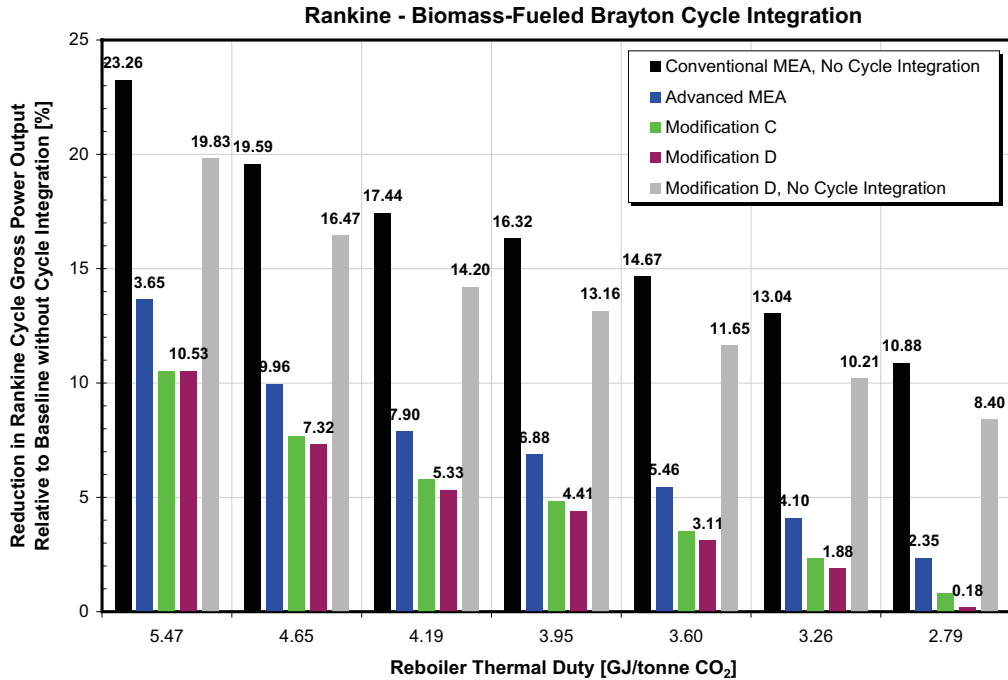


**Figure 9-12. Reduction in Power Output of the Rankine Cycle Relative to the Baseline (No CO<sub>2</sub> Capture, No Cycle Integration) as Function of  $Q_{reb}$ , Cycle Integration, and Thermal Integration of the Post-Combustion MEA CO<sub>2</sub> Capture.**

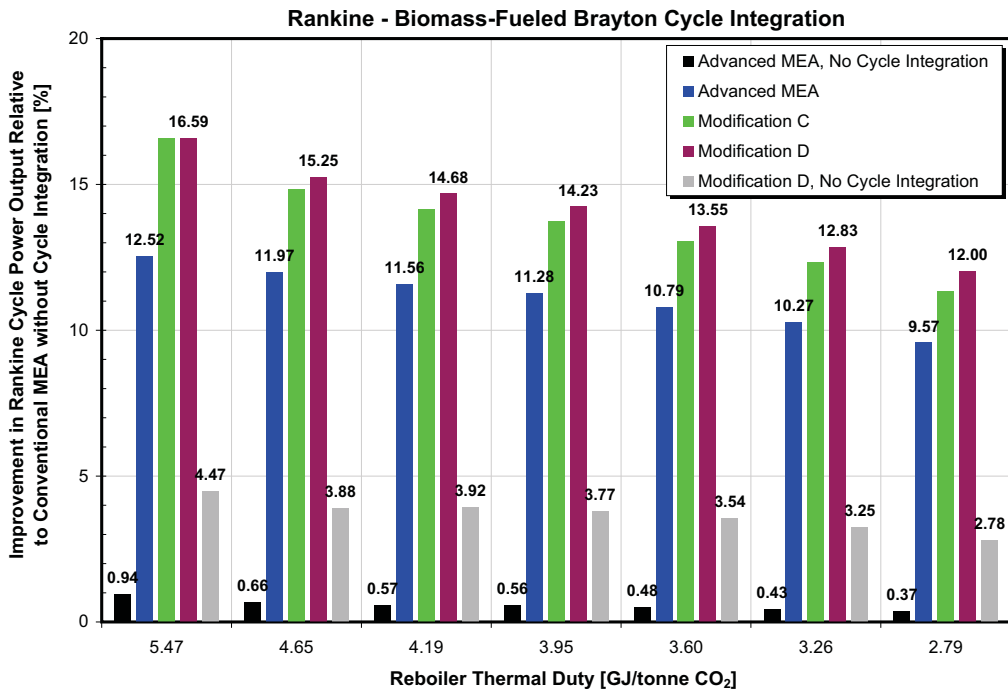


**Figure 9-13. Improvement in Power Output of the Rankine Cycle Relative to the Conventional MEA as Function of  $q_{reb}$ , Cycle Integration, and Integration of the Post Combustion MEA CO<sub>2</sub> Capture.**

Decrease in net efficiency ( $\eta_{\text{net}}$ ) of the Rankine cycle-based plant relative to the baseline (no CO<sub>2</sub> capture, no cycle integration) is presented in Figure 9-14. For the state-of-the-art amines and Modification D to the Conventional MEA, cycle integration reduces decrease in  $\eta_{\text{net}}$  by 2.86%-points (from 7.71 to 4.85%-point) For the  $q_{\text{Reb}}$  value, determined for the MEA in this study and Modification D, decrease in  $\eta_{\text{net}}$  is reduced by 3.10%-points (from 9.48 to 6.38%-point) by cycle integration.

Improvement in  $\eta_{\text{net}}$  of the Rankine cycle-based plant relative to the Conventional MEA and no cycle integration is presented in Figure 9-15. For state-of-the-art amines and Modification D to the Advanced MEA, cycle integration increases improvement in  $\eta_{\text{net}}$  from 1.11 to 3.97%-points. For the  $q_{\text{Reb}}$  value determined for the MEA in this study and Modification D, the improvement in  $\eta_{\text{net}}$  relative to the conventional MEA increases from 1.14 to 4.24%-points.

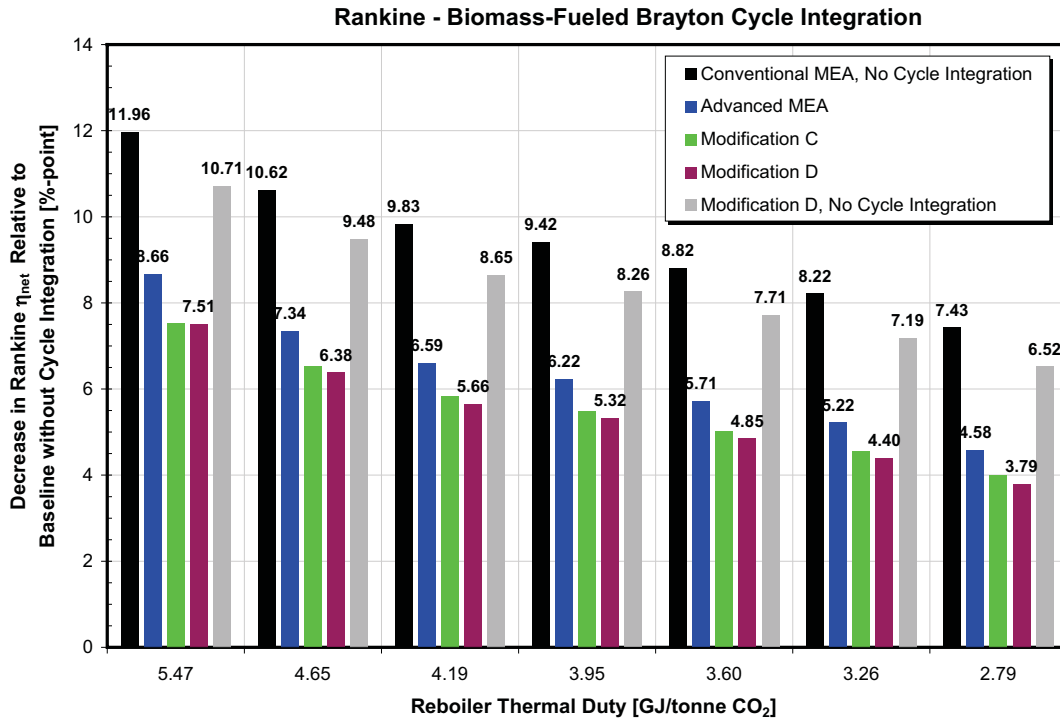


**Figure 9-14. Decrease in Net Efficiency of the Rankine Cycle Relative to the Baseline (no CO<sub>2</sub> capture) as Function of  $q_{\text{Reb}}$ , Cycle Integration, and Thermal Integration of the Post-Combustion MEA CO<sub>2</sub> Capture.**

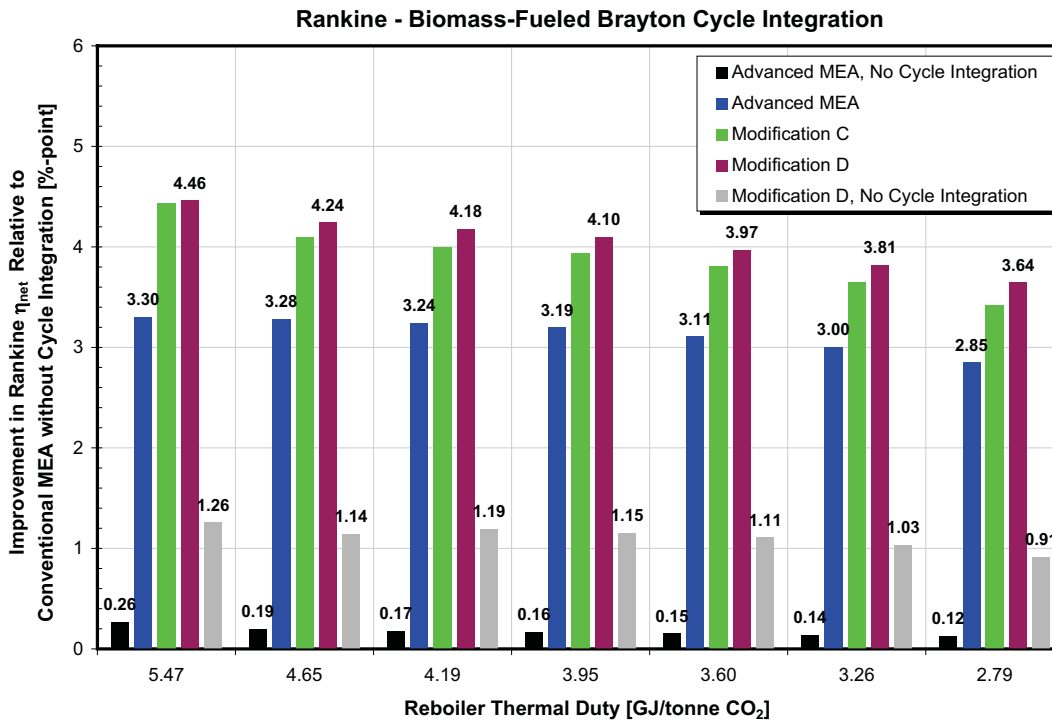


**Figure 9-15: Improvement in Net Efficiency of the Rankine Cycle Relative to the Conventional MEA as Function of  $q_{\text{Reb}}$ , Cycle Integration, and Thermal Integration of the Post-Combustion MEA CO<sub>2</sub> Capture.**

### Combined Cycle

The effect of cycle integration on the combined cycle performance is large, as presented in Figures 9-16 to 9-19 with Modification D resulting in best performance. The change in the gross power output of the combined cycle incurred by CO<sub>2</sub> capture, relative to the baseline (no CO<sub>2</sub> capture, no cycle integration) is presented in Figure 9-16. For the state-of-the-art amines and Modification D to the Conventional MEA, cycle integration increases power output by 2.10%, compared to 11.65% decrease with no cycle integration. For the  $q_{\text{Reb}}$  value, determined for the MEA in this study and Modification D, cycle integration increases power output by 2.12%, compared to 16.47% decrease without cycle integration.

The results concerning improvement in gross power output of the combined cycle relative to the Conventional MEA with no cycle integration are presented in Figure 9-17. For the state-of-the-art amines and Modification D, improvement in power output is increased from 3.54 to 19.65%. For the  $q_{\text{Reb}}$  value, determined for the MEA in this study and Modification D, cycle integration improves power output from 3.88 to 21.72%.

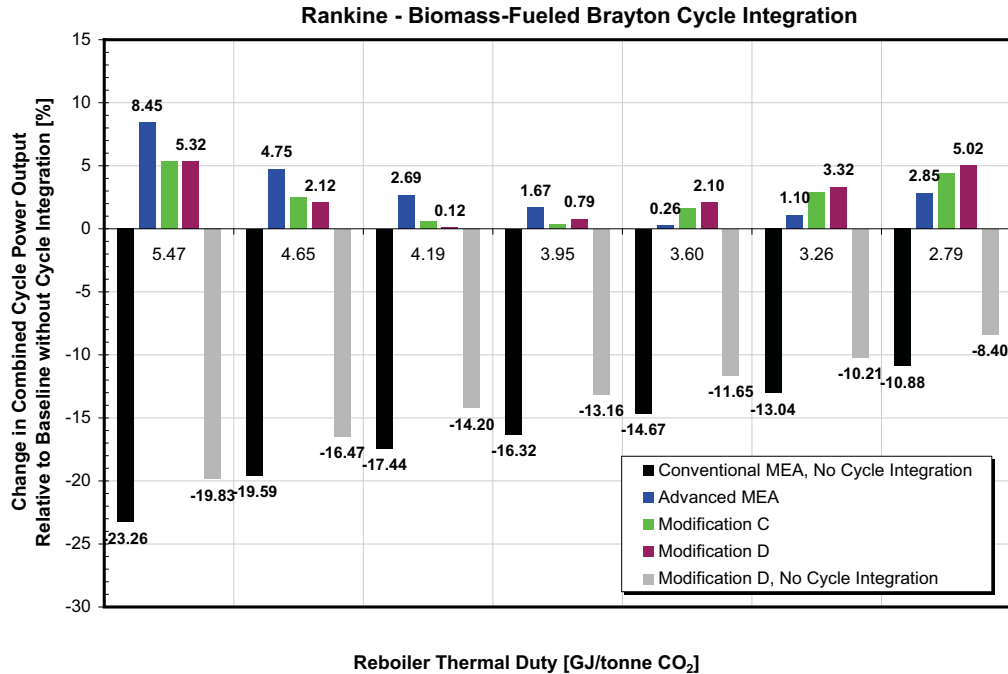


Figure 9-16. Change in Power Output of the Combined Cycle Relative to the Baseline (no CO<sub>2</sub> capture, no cycle integration) as Function of  $q_{Reb}$ , Cycle Integration, and Thermal Integration of the Post-Combustion MEA CO<sub>2</sub> Capture.

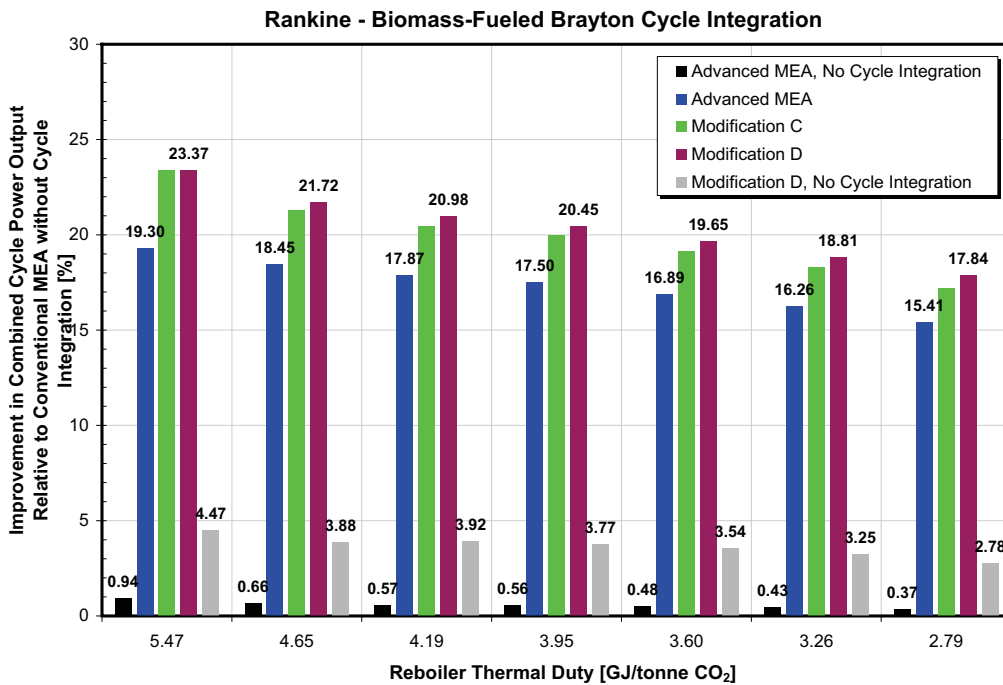
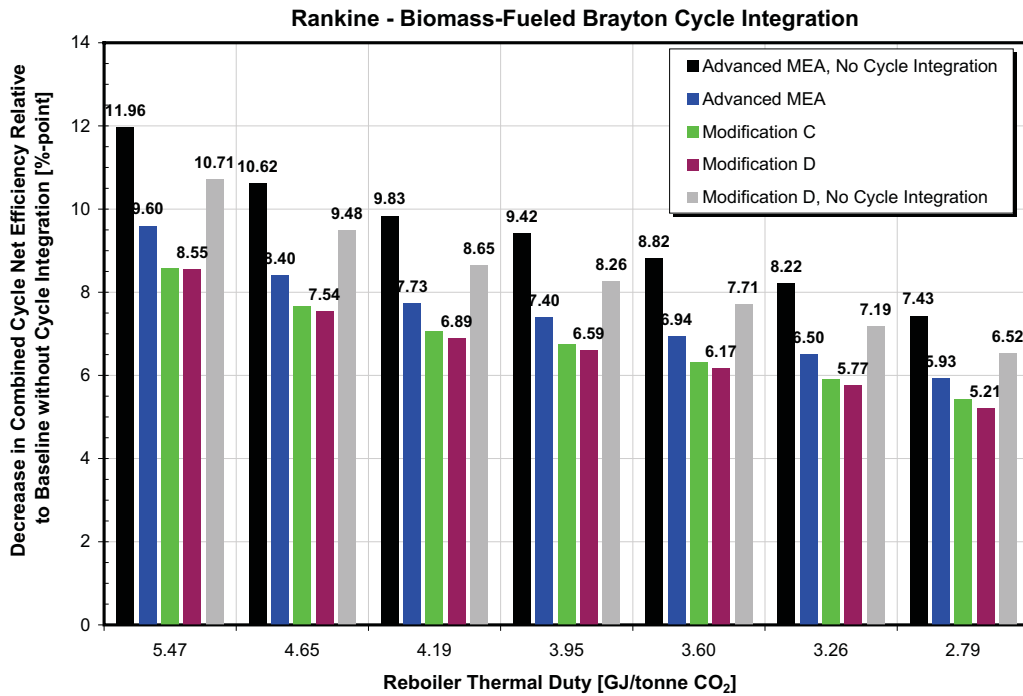


Figure 9-17. Improvement in Power Output of the Combined Cycle Relative to the Conventional MEA Without Cycle Integration as Function of  $q_{Reb}$ , Cycle Integration, and Thermal Integration of the Post-Combustion MEA CO<sub>2</sub> Capture.

The decrease in net efficiency ( $\eta_{net}$ ) of the combined cycle, relative to the baseline (no CO<sub>2</sub> capture, no cycle integration) is presented in Figure 9-18. For the state-of-the-art amines and Modification D to the Conventional MEA, cycle integration reduces decrease in  $\eta_{net}$  by 1.54%-points (from 7.71 to 6.17%-point) For the  $q_{Reb}$  value, determined for the MEA in this study and Modification D, the decrease in  $\eta_{net}$  is reduced by 1.94%-points (from 9.48 to 7.54%-point) by cycle integration.

Improvement in  $\eta_{net}$  relative to the Conventional MEA and no cycle integration is presented in Figure 9-19. For state-of-the-art amines and Modification D to the Advanced MEA, cycle integration increases improvement in  $\eta_{net}$  from 1.11 to 2.65%-points. For the  $q_{Reb}$  value determined for the MEA in this study and Modification D, improvement in  $\eta_{net}$  relative to the conventional MEA increases from 1.14 to 3.08%-points.



**Figure 9-18: Decrease in Net Unit Efficiency of the Combined Cycle Relative to the Baseline (no CO<sub>2</sub> capture, no cycle integration) as Function of  $q_{Reb}$ , Cycle Integration, and Thermal Integration of the Post-Combustion MEA CO<sub>2</sub> Capture.**

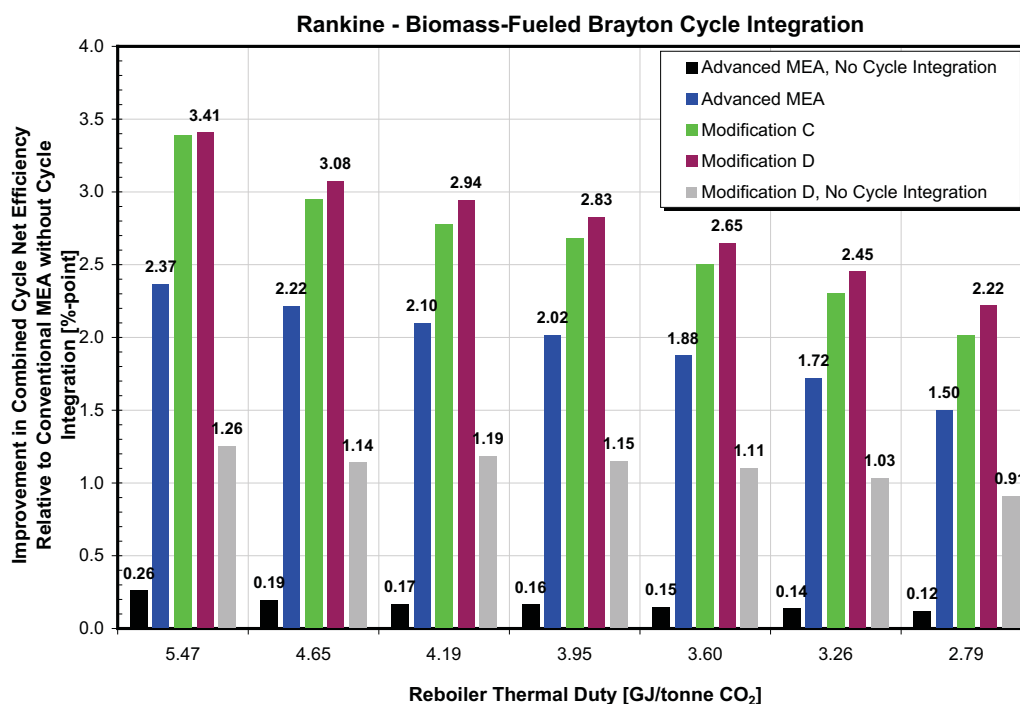


**Figure 9-19. Improvement in Net Unit Efficiency of the Combined Cycle Relative to the Conventional MEA Without Cycle Integration as Function of  $q_{Reb}$ , Cycle Integration, and Thermal Integration of the Post-Combustion MEA CO<sub>2</sub> Capture.**

In summary, integration of the Rankine and biogas-fired Brayton cycles has a significant positive effect on performance of the combined cycle. Some of the results are presented in Table 9-3. Performance improvement is lower compared to the hydrogen-fired option mainly because of the low calorific value of biogas which adversely affects efficiency of the Brayton cycle due to low TIT. Increasing size of the Brayton cycle to provide heat for both HP FWHs would help improve performance of the combined cycle provided sufficient amount of biomass is available and a sustainable harvest is possible.

**Table 9-3. Rankine-Brayton Cycle Integration: Biogas-Fired Turbine.**

Biogas-Fired Turbine, HP FWH A				
State-of-the-Art Amines	Integrated Rankine-Brayton Cycle		Rankine Cycle	
	Change in P <sub>G</sub> Relative to Baseline	Change in $\eta_{net}$ Relative to Baseline	Change in P <sub>G</sub> Relative to Baseline	Change in $\eta_{net}$ Relative to Baseline
MEA Integration	%	%-point	%	%-point
Advanced MEA	0.26	-6.94	-14.26	-8.67
Modification D	2.10	-6.17	-11.65	-7.71
<b>Baseline = Rankine Cycle, No CO<sub>2</sub> Capture</b>				

## CONCLUSIONS AND RECOMMENDATIONS

### GENERAL

Atmospheric levels of CO<sub>2</sub> have increased over the last 150 years from around 280 to 360 ppm. CO<sub>2</sub> is a greenhouse gas that is considered as a most likely cause of a global temperature increase. Concerns about the effect of anthropogenic emissions of CO<sub>2</sub> on global climate will undoubtedly result in regulations restricting CO<sub>2</sub> emissions from existing and newly built emitting sources. Early reduction in anthropogenic CO<sub>2</sub> emissions is of utmost importance; the sooner CO<sub>2</sub> emissions are curtailed, the smaller the future reduction and lower the cost to stabilize CO<sub>2</sub> concentration in the atmosphere at desired level.

While oxy-fuel, IGCC, and post-combustion carbon capture and sequestration (CCS) technologies are viable options for the newly built power plants, it is very likely that a significant percentage of existing power plants will be retrofitted with post-combustion CO<sub>2</sub> capture technology. The major barriers to implementation of this technology are high cost, significant reduction in power plant output, and high performance penalty.

Considering time required for commercialization and significant market penetration of advanced or alternative power generation and CCS technologies, the most effective and commercially available approach for reducing CO<sub>2</sub> emissions from existing coal-fired plants is efficiency improvement. Higher efficiency will lower fuel use, which will reduce emissions and offset part of the efficiency and capacity losses which would be incurred by retrofit of the post-combustion CO<sub>2</sub> capture and other CCS technologies to existing units [Sarunac, 2009].

Project goals included optimization of the MEA-based post-combustion CO<sub>2</sub> capture to reduce energy requirements for CO<sub>2</sub> capture, determination of efficiency improvements that could be achieved at existing power plants by thermal integration of the steam turbine cycle, boiler, CO<sub>2</sub> compression train and post-combustion CO<sub>2</sub> capture process, and integration of Rankine and Brayton cycles to offset efficiency and capacity losses that would be incurred by retrofit or implementation of post-combustion CO<sub>2</sub> capture. Partial CO<sub>2</sub> capture, involving treatment of 20 to 100% of the flue gas leaving the plant and modular design of the CO<sub>2</sub> scrubbing system, was also investigated.

## BOILER-TURBINE CYCLE INTEGRATION

Thermal integration of the boiler and turbine cycle, analyzed in this study, involves recovery of heat from the flue gas in a flue gas cooler (FGC) and its use for air preheating (advanced air preheating) and condensate heating. The optimal use of recovered heat was determined by considering effects of air preheating and associated cold end average temperature (CEAT) constraints and condensate heating on the turbine cycle and net unit heat rate. Air preheating in a steam air heater (SAH) was used as a benchmark.

The optimal use of heat recovered from the flue gas is presented in Figure 10-1 where heat input to the condensate ( $Q_{FGC,FWH}$ ) is shown as a percentage of the maximum amount of heat that can be recovered from the flue gas ( $Q_{FGC,MAX}$ ). The results are presented as functions of the ambient temperature and temperature of combustion air at the air preheater (APH) inlet. For a given CEAT, the optimal split of heat used for air preheating and condensate heating depends on the ambient temperature. For Somerset and design values of ambient temperature and CEAT, best performance is achieved when approximately 70% of heat recovered from the flue gas is used for condensate heating. For lower ambient temperature more heat is required for air preheating; for ambient temperature of  $-15\text{ }^{\circ}\text{C}$  best performance is achieved when 12% of recovered heat is used for condensate heating and 88% for air preheating.

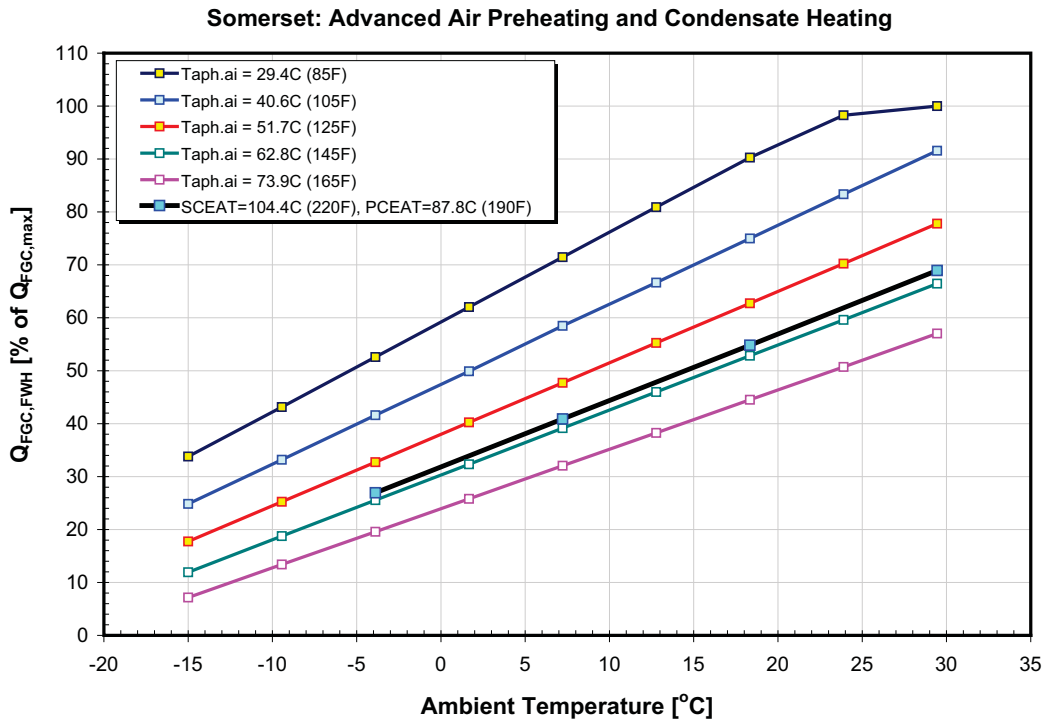


**Figure 10-1: Optimal Use of Heat Recovered From the Flue Gas.**

At design value of the ambient temperature and operating conditions satisfying the secondary CEAT (SCEAT) and primary (PCEAT) set points, use of heat recovered from the flue gas results in approximately 1.6%-points<sup>4</sup> lower turbine cycle and net unit heat rate compared to the SAH air preheating. This difference increases as ambient temperature decreases. At the ambient temperature of -15°C turbine cycle net unit heat rate is approximately 2.45%-points lower compared to the SAH air preheating (see Figures 6-2 and 6-3).

### **OPTIMIZATION OF MEA-BASED POST-COMBUSTION CO<sub>2</sub> CAPTURE PROCESS**

Modeling of the CO<sub>2</sub> absorption/scrubbing process by aqueous MEA for a host power plant configuration was performed using ASPEN Plus version 2006.5 [Aspen Technology, 2006]. The process model was used to determine optimal combination of key operating parameters (stripper operating pressure, solvent circulation rate/theCO<sub>2</sub> lean solvent loading (mol CO<sub>2</sub>/mol MEA), MEA weight percentage in the absorption solvent, CO<sub>2</sub> removal percentage, and flue gas/lean solvent temperature) resulting in lowest energy requirements for CO<sub>2</sub> capture. The set of optimal operating parameters, presented in Table 10-1, results in 20.8% reduction in reboiler thermal duty from design conditions, and 26% from the non-optimal case.

**Table 10-1. Optimal and Worst MEA System Operating Points.**

<b>MEA System Operating Point</b>	<b>Optimal</b>	<b>Worst</b>	
Flue Gas Mass Flow Rate	t/h	3,050	3,050
Solvent Mass Flow Rate	t/h	10,827	10,793
MEA Concentration in Absorption Liquid	% wt	30.0	30.0
Amine Rich Loading	mol CO <sub>2</sub> /mol MEA	0.480	0.480
Amine Lean Loading	mol CO <sub>2</sub> /mol MEA	0.240	0.240
Stripper Reboiler Temperature	°C	121.1	103.0
Stripper Condenser Temperature	°C	100.3	96.3
Stripper pressure	kPa	190	100.0
Bottom to Feed Molar Ratio		0.975	0.905
Reboiler Heat Required	MW <sub>th</sub>	677.6	855.5
Reboiler Duty	GJ/hr	2,439	2,794
<b>Reboiler Duty</b>	<b>GJ/t CO<sub>2</sub></b>	<b>4.56</b>	<b>5.76</b>
CO <sub>2</sub> Removal	% wt	90.00	90.00
CO <sub>2</sub> Purity	% wt	98.36	98.36
Mass Flow Rate of CO <sub>2</sub> Captured	t/h	535.3	534.4
MEA Concentration in Clean Flue Gas	ppm	122.0	330.1
CO <sub>2</sub> Concentration in Clean Flue Gas	ppm	1.01	1.01

<sup>4</sup> For a host unit, 1% improvement in net unit heat rate results in annual savings of \$1,500,000.

**THERMAL INTEGRATION OF THE TURBINE CYCLE AND CO<sub>2</sub> STRIPPER WITH PLANT HEAT SOURCES**

Owing to steam extraction from intermediate pressure (IP) turbine exhaust for a reboiler, post-combustion CO<sub>2</sub> capture has a significant negative effect on plant performance (efficiency) and capacity (power output). Thermal integration of the steam turbine cycle with boiler and CO<sub>2</sub> compression train reduces steam extractions from the turbine for condensate and feedwater heating, increases turbine power output, improves cycle and plant performance and offsets, in part, negative effects of post-combustion CO<sub>2</sub> capture.

A number of thermal integration options was developed and analyzed in the study, including Advanced MEA and Modifications A to F to the Advanced MEA. Basic features of these thermal integration options are summarized in Table 10-2. Thermal integration of two types of the CO<sub>2</sub> compressors was investigated: a conventional multi-stage inline compressor, and the advanced two-stage shock-wave Ramgen Power Systems compressor.

**Table 10-2. Basic Features of Analyzed Thermal Integrations Options.**

MEA Integration	Control of Steam Temperature into Reboiler	Temperature of Reboiler Condensate Entering Deaerator [°C]	Sources of Heat for Condensate (LP Fedwater Heating)		CO <sub>2</sub> Compressor Type	Sources of Heat for Reboiler			Reboiler Heat Provided by Steam [%]	
			Flue Gas	CO <sub>2</sub> Compression Heat		LP Steam	Flue Gas	CO <sub>2</sub> Compression		
Conventional MEA	Desuperheat by reboiler condensate	134.7			Inline	x			100.0	
Advanced MEA	Cooling by reboiler condensate	174.5				x				
Modification A			x			x				
Modification B				x		x				
Modification B-R				x		Ramgen	x			
Modification C				x	x	Inline	x			
Modification C-R				x	x	Ramgen	x			
Modification D				Inline	x	x		88.7		
Modification E				Ramgen	x		x	89.9		
Modification F				Ramgen	x	x	x	78.6		

The effect of investigated thermal integration options on gross power output and net unit efficiency for the state-of-the-art amines is summarized in Table 10-3. The results are compared to the baseline case (no CO<sub>2</sub> capture) and to the conventional thermal integration. The comparison relative to the baseline is a measure of the penalty that would be incurred by retrofit or implementation of the post-combustion CO<sub>2</sub> capture process, while comparison relative to the conventional MEA integration represents improvement achievable by thermal integration. The reduction in unit performance and capacity relative to the baseline is lowest and the improvement relative to Conventional MEA is highest for Modifications F and C-R.

Thermal integration should be considered for the existing and newly built plants. The best analyzed thermal integration option (Modification F) improves gross power output by 5% and net unit efficiency by 1.57%-points, relative to the Conventional MEA.

Also, when evaluating different thermal integration options, the cost of heat exchange and associated equipment has to be considered in addition to the performance improvement. For example, the cost of a FGC operating below acid dewpoint is approximately 10 times higher compared to the finned tube heat exchanger operating above the acid dewpoint.

**Table 10-3. Effect of Thermal Integration on Unit Performance: State-of-the-art amines.**

Rankine Cycle				
State-of-the-Art Amines	Change in $P_G$	Change in $\eta_{net}$	Improvement in $P_G$	Improvement in $\eta_{net}$
	Relative to Baseline	Relative to Baseline	Relative to Conventional MEA	Relative to Conventional MEA
MEA Integration	%	%-point	%	%-point
Conventional MEA	-14.67	-8.82		
Advanced MEA	-14.26	-8.67	0.48	0.15
Modification A	-13.23	-8.29	1.69	0.53
Modification B	-13.51	-8.39	1.36	0.42
Modification B-R	-12.52	-8.03	2.51	0.78
Modification C	-12.24	-7.93	2.85	0.89
Modification C-R	-11.05	-7.49	4.24	1.32
Modification D	-11.65	-7.71	3.54	1.11
Modification E	-12.15	-7.89	2.95	0.92
Modification F	-10.38	-7.25	5.03	1.57
<b>Baseline = No CO<sub>2</sub> Capture</b>				

### PARTIAL CO<sub>2</sub> CAPTURE

Partial CO<sub>2</sub> capture involves treatment of 20 to 100% of the flue gas leaving the plant, and involves modular design of the CO<sub>2</sub> scrubbing system. Partial CO<sub>2</sub> capture could be the first step toward reducing CO<sub>2</sub> emissions from the existing power plants, which is expected to speed up deployment of the post-combustion CO<sub>2</sub> capture because of the lower initial capital investment and associated risk.

Other reasons for considering partial CO<sub>2</sub> capture include: gathering operating experience on a smaller and easier-to-operate and maintain system and implementing design changes and improvements on subsequent CO<sub>2</sub> capture modules. Also, partial CO<sub>2</sub> capture could be implemented on smaller and older power plants to reduce CO<sub>2</sub> emissions with moderate performance penalty and significantly lower initial capital investment.

The effect of partial CO<sub>2</sub> capture on plant performance was investigated for the conventional and advanced MEA integrations, and Modifications A, B, C and D to the advanced MEA integration, for  $q_{reb}$  values of 3.95 and 4.65 GJ/tonne CO<sub>2</sub> (1,700 and 2,000 Btu/lb CO<sub>2</sub>).

As the percentage of CO<sub>2</sub> capture decreases, the amount of heat that needs to be supplied to the reboiler and steam flow to the reboiler decrease because the flue gas flow rate that needs to be treated is lower resulting in a lower amount of CO<sub>2</sub> that needs to be captured. The reduced steam extraction to the reboiler increases steam flow through the low pressure (LP) turbine, which increases turbine power output. The improvement in cycle and plant performance varies linearly with the percentage of CO<sub>2</sub> capture and increases as percentage of CO<sub>2</sub> capture decreases and  $q_{\text{Reb}}$  increases.

For example, operating with 40% CO<sub>2</sub> capture increases gross power output by 11.6 to 14% (depending on the thermal integration option), relative to the conventional MEA integration and 90% CO<sub>2</sub> capture. This increase in power output improves turbine cycle heat rate by 10.4 to 12.2%, turbine cycle efficiency by 4.1 to 5%-points, net unit heat rate by 17.8 to 19.7%, and net unit efficiency by 5.5 to 6.2%-points, relative to the conventional thermal integration and 90% CO<sub>2</sub> capture. The improvement in net unit performance is larger compared to the improvement in turbine cycle performance because of the CO<sub>2</sub> compression work, which is also reduced by partial CO<sub>2</sub> capture.

### **RANKINE-BRAYTON CYCLE INTEGRATION**

Integration of the Rankine and Brayton cycles was analyzed to determine efficiency (heat rate) improvements that could be achieved at existing power plants by using heat recovered from the Brayton's cycle hot effluent to increase steam flow through the steam turbine and offset power loss due to reboiler steam extraction. The ultimate goal of the Rankine-Brayton cycle integration is efficiency improvement of the Rankine cycle and reduction of the capacity penalty that would be incurred by implementation of the post-combustion CO<sub>2</sub> capture technology. Cycle integration can be applied to existing larger coal-fired power plants that would be retrofitted by the post-combustion CO<sub>2</sub> capture, enabling them to continue operation in a carbon-constrained world.

The fueling options considered for the Brayton cycle included hydrogen- and biogas-fired turbine. In the latter case, biogas (syngas) is produced by gasification of biomass in a fluidized bed gasifier, while the leftover char is burned in the boiler.

Optimal integration of the Rankine and Brayton cycles was determined by parametrically varying heat provided by the Brayton cycle for the high pressure (HP) feedwater heating and for reboiler. The best Rankine and combined cycle performance is achieved when 100% of the heat is used for the HP feedwater heating. This is because the steam extracted from the steam turbine cycle for the HP feedwater heating is of higher quality compared to the reboiler steam extracted from the IP turbine exhaust. Also, as steam extractions for the HP feedwater heating are decreased and eliminated, the steam flow through the turbine increases, resulting in higher power output of the steam turbine cycle.

For the hydrogen-fired turbine option, the Brayton cycle was sized to provide sufficient amount of heat to replace steam extractions for the HP FWHs A and B (top two high pressure FWHs). This resulted in the power output of the hydrogen-fired turbine of 140.5 MW<sub>el</sub>. Calculations were performed by using a Brayton cycle efficiency of 32.91%. As shown in Table 10-4, cycle integration has a large positive effect on performance of the combined cycle. In addition to increasing the plant gross power output by approximately 20%, reduction in net plant efficiency relative to the baseline (Rankine cycle, no CO<sub>2</sub> capture) is decreased by approximately factor of two, i.e. from 8.67 and 7.71% to 4.38 to 3.77%.

**Table 10-4. Rankine-Brayton Cycle Integration: Hydrogen-Fired Turbine, FWHs A and B.**

<b>Hydrogen-Fired Turbine, HP FWHs A and B</b>				
<b>State-of-the-Art Amines</b>	<b>Integrated Rankine-Brayton Cycle</b>		<b>Rankine Cycle</b>	
	Change in P <sub>G</sub> Relative to Baseline	Change in η <sub>net</sub> Relative to Baseline	Change in P <sub>G</sub> Relative to Baseline	Change in η <sub>net</sub> Relative to Baseline
MEA Integration	%	%-point	%	%-point
Advanced MEA	<b>19.82</b>	<b>-4.38</b>	<b>-14.26</b>	<b>-8.67</b>
Modification D	<b>21.46</b>	<b>-3.77</b>	<b>-11.65</b>	<b>-7.71</b>
<b>Baseline = Rankine Cycle, No CO<sub>2</sub> Capture</b>				

The analysis was extended to the case where the Brayton cycle was sized to provide sufficient amount of heat to replace steam extraction for the HP FWH A only. This decreased power output of the hydrogen-fired turbine to approximately 95 MW<sub>el</sub>. Due to the lower power output, calculations were performed by using a Brayton cycle efficiency of 32.71%. The results presented in Table 10-5, show that performance improvement, although being smaller compared to the case where steam extractions for both HP FWHs are eliminated, is still significant; approximately 9.5% increase in gross power output, and 60% decrease in net unit efficiency relative to the baseline.

**Table 10-5. Rankine-Brayton Cycle Integration: Hydrogen-Fired Turbine, FWH A.**

<b>Hydrogen-Fired Turbine, HP FWH A</b>				
<b>State-of-the-Art Amines</b>	<b>Integrated Rankine-Brayton Cycle</b>		<b>Rankine Cycle</b>	
	Change in P <sub>G</sub> Relative to Baseline	Change in η <sub>net</sub> Relative to Baseline	Change in P <sub>G</sub> Relative to Baseline	Change in η <sub>net</sub> Relative to Baseline
MEA Integration	%	%-point	%	%-point
Advanced MEA	<b>8.35</b>	<b>-4.84</b>	<b>-14.26</b>	<b>-8.67</b>
Modification D	<b>10.61</b>	<b>-5.56</b>	<b>-11.65</b>	<b>-7.71</b>
<b>Baseline = Rankine Cycle, No CO<sub>2</sub> Capture</b>				

For the biogas-fired turbine option, in order to keep the amount of biomass needed manageable, economically harvestable and sustainable, Brayton cycle was sized to provide sufficient amount of heat to replace steam extraction for the HP FWH A and partially for the HP FWH B. This resulted in a power

output of the biogas-fired turbine of approximately 33 MW<sub>el</sub>. Due to low turbine inlet temperature (TIT) and compressor pressure ratio (PR), calculations were performed by using a Brayton cycle efficiency of 16.83%. Some of the results are summarized in Table 10-6. Performance improvement, compared to the baseline, is lower compared to the hydrogen-fired option mainly because of the low calorific value of biogas which adversely affects efficiency of the Brayton cycle due to low TIT. Increasing the size of the Brayton cycle to provide heat for both HP FWHs would help improve performance of the combined cycle provided sufficient amount of biomass is available and a sustainable harvest is possible.

**Table 10-6. Rankine-Brayton Cycle Integration: Biogas-Fired Turbine.**

<b>Biogas-Fired Turbine, HP FWH A</b>				
<b>State-of-the-Art Amines</b>	<b>Integrated Rankine-Brayton Cycle</b>		<b>Rankine Cycle</b>	
	Change in P <sub>G</sub> Relative to Baseline	Change in η <sub>net</sub> Relative to Baseline	Change in P <sub>G</sub> Relative to Baseline	Change in η <sub>net</sub> Relative to Baseline
MEA Integration	%	%-point	%	%-point
Advanced MEA	<b>0.26</b>	<b>-6.94</b>	<b>-14.26</b>	<b>-8.67</b>
Modification D	<b>2.10</b>	<b>-6.17</b>	<b>-11.65</b>	<b>-7.71</b>
<b>Baseline = Rankine Cycle, No CO<sub>2</sub> Capture</b>				

Cycle integration has a significant positive effect on performance and capacity. Capacity losses could be eliminated and performance losses halved. The cost of this option is significantly higher compared to the thermal integration, but significantly lower compared to a Greenfield (newly built) combined cycle.

In summary, results of the study show that thermal integration and use of heat recovered from the flue gas and CO<sub>2</sub> compression can improve efficiency and increase power output of power plants that would be equipped with the post-combustion CO<sub>2</sub> capture technology, and offset, in part, performance penalty associated with the retrofit or implementation of the technology. The best thermal integration option analyzed in this study would improve gross power output by 5% and net unit efficiency by 1.57%-points, relative to the conventional MEA. It is highly recommended thermal integration be applied at existing power plants to allow their operation in a carbon-constrained world. Additionally, thermal integration needs to be incorporated into design of the newly built power plants to improve efficiency.

Project results will provide advanced use of innovative strategies for superior plant performance and CO<sub>2</sub> emissions reduction, and support implementation of CO<sub>2</sub> reduction technologies at coal-fired power plants. It is expected project results will help improve ambient air quality and foster business and technology development in New York State.

Section 11

**REFERENCES**

Abu-Zahra, M., et al., CO<sub>2</sub> Capture from Power Plants Part I. A Parametric Study of the Technical Performance Based on Monoethanolamine. International Journal of Greenhouse Gas Control I (3007) 37-46.

Alie, C., et al., Simulation of CO<sub>2</sub> Capture Using MEA Scrubbing: A Flowsheet Decomposition Method. Energy Conversion Management (2005), 46, p. 475-487.

ASPEN Plus, 2006 Aspen Plus Version 2006.5. Aspen Technology, Inc., Cambridge, Massachusetts.

“Carbon Sequestration Technology Roadmap and Program Plan 2007.” NETL.

Chapel, D., et al., Recovery of CO<sub>2</sub> from Flue Gases: Commercial Trends. Canadian Society of Chemical Engineers (1999).

Ciferno, J., CO<sub>2</sub> Capture form Existing Coal-Fired Power Plants, NETL, December 2006.

Cifre, P., et al., Integration of a Chemical Process Model in a Power Plant Modeling Tool for the Simulation of an Amine Based CO<sub>2</sub> Scrubber. Fuel (2009) 88, p.2481-2488.

Elwell, L. and Grant, W., Overview of Carbon Dioxide Capture Technologies for Coal-Fired Power Plants. MPR Associates, Inc., January 14, 2005, [http://www.mpr.com/news-and-publications/white-papers/C02\\_Sequestration.pdf](http://www.mpr.com/news-and-publications/white-papers/C02_Sequestration.pdf).

Engineering and Economic Evaluation of CO<sub>2</sub> Removal from Fossil-Fuel-Fired Power Plants. IE-7365, Fluor Daniel, Irvine, California, 1991.

Galindo Cifre, P., et al., Integration of a Chemical Process Model in a Power Plant Modeling Tool for the Simulation of an Amine Based CO<sub>2</sub> Scrubber. Presented at 33<sup>rd</sup> International Technical Conference on Coal Utilization and Fuel Systems, June 1 - 5, 2008, Clearwater, Florida, USA.

Gibbins, J. and Chalmers, H., Initial Evaluation of the Impact of Post-Combustion Capture of Carbon Dioxide on Supercritical Pulverized Coal Power Plant Part Load Performance. Fuel article in press, 2007.

Global Climate & Energy project, An Assessment of Carbon Capture Technology and Research Opportunities, GCEP Energy Assessment Analysis, Technical Assessment Report, Stanford University, Spring 2005, [http://gcep.stanford.edu/pdfs/assessments/carbon\\_capture\\_assessment.pdf](http://gcep.stanford.edu/pdfs/assessments/carbon_capture_assessment.pdf)

Jared P. Ciferno and John J. Marano, Benchmarking Biomass Gasification Technologies for Fuels, Chemicals and Hydrogen Production. Prepared for DOE, June 2002

Mohammad, R., et al., CO<sub>2</sub> Capture from Power Plants Part I. A Parametric Study of the Technical Performance Based on Monoethanolamine. International Journal of Greenhouse Gas Control I (2007) p.37-46.

Narula, R., et al., Incremental Cost of CO<sub>2</sub> Reduction in Power Plants. Proceedings of IGTI, ASME Turbo Expo 2002, June 2002, Amsterdam, the Netherlands.

NETL Turbine Program, Enabling Near Zero Emission Coal-Based Power Generation. June 2005, <http://www.netl.doe.gov/technologies/coalpower/turbines/refshelf/brochures/Brochure%209-19-05.pdf>.

Nsakala, N., et al., Engineering Feasibility of CO<sub>2</sub> Capture on an Existing US Coal-Fired Power Plant. Presented at 1<sup>st</sup> National Conference on Carbon Sequestration, May 2001, Washington, DC.

Rao, A. and Rubin, E., A., Technical, Economic and Environmental Assessment of Amine-Based CO<sub>2</sub> Capture Technology for Power Plant Greenhouse Gas Control. Environmental Sci. Tech. (2002), 36, p. 4467-4475.

Sarunac, Nenad, Increasing Efficiency and Reducing Emissions of Existing Pulverized Coal-Fired Units. Final Technical Report, October 1, 2007 through March 31, 2009, Prepared for Illinois Clean Coal Institute, ICCI Project Number: 07-1/5.1A-1, ERC Report Number 09-400-16-16, October 6, 2009.

Singh, D., et al., Techno-Economic Study of CO<sub>2</sub> Capture form an Existing Coal-Fired Power Plant: MEA Scrubbing vs. O<sub>2</sub>/CO<sub>2</sub> Recycle Combustion. Energy Conversion Management (2003), 44, p. 3073-3091.

Wark, Kenneth, Thermodynamics, 4<sup>th</sup> Edition. P. 830, Table A-4, McGraw Hill, New York, 1983.

Zia, Haq, Biomass for Electricity Generation. Energy Information Administration / Biomass for Electricity Generation, July 2002, <http://www.eia.doe.gov/oiaf/analysispaper/biomass/pdf/biomass.pdf>

**APPENDIX A**  
**OPTIMAL USE OF HEAT RECOVERED FROM THE FLUE GAS**

The temperature of the flue gas leaving the boiler is commonly reduced in an air preheater (APH), where sensible heat in the flue gas leaving the economizer is used to preheat combustion air. Preheating of combustion air has a significant positive effect on boiler efficiency. Common practice is to recover sensible heat from flue gas until temperature of the flue gas drops to approximately 150°C (300°F). The primary impediment to recovering heat by additional cooling is the risk of condensing sulfuric acid on the APH heat transfer surfaces and downstream ductwork [Sarunac, 2009].

To protect the APH heat transfer surfaces at the cold end of the APH from deposition of sulfuric acid and subsequent corrosion and fouling, temperature of the inlet air is commonly increased in a Steam Air Heater (SAH) located upstream of the APH. At the host unit Primary Air SAH (PSAH) and Secondary (combustion) Air SAH (SSAH) are used to increase the temperature of the primary and secondary air at the APH inlet. As presented in Figure A-1 heat to the PSAH and SSAH is supplied by the steam extracted from the steam turbine cycle (typically from the deaerator steam extraction). The flow rate of the extracted steam depends on the temperature of air entering the SAH (ambient temperature) and on the temperature of air entering the APH required to maintain a Cold End Average Temperature (CEAT). The CEAT is defined as:

$$\text{CEAT} = (T_{\text{APH,ai}} + T_{\text{APH,go}})/2 \quad \text{Eqn. A-1}$$

Where:

$T_{\text{APH,ai}}$  Temperature of air entering the APH

$T_{\text{APH,go}}$  Temperature of flue gas leaving the APH

The value of CEAT is usually determined empirically and represents a tradeoff between “acceptable” acid deposition rate in the cold end (CE) layer of the APH and net unit heat rate (net unit efficiency). For the host unit, the empirically determined value of CEAT for the secondary APH (SAPH) is 104°C (220°F). The value of CEAT for the primary APH (PAPH) is lower, 87.8°C (190°F). These CEAT values were used in this study. The analysis was performed over a range of ambient temperatures from approximately -15 to 30°C, which corresponds to seasonal changes at the host site.

As presented in Figure A-1, preheating of the APH inlet air can also be accomplished by using sensible heat recovered from the flue gas. The sensible heat for the air preheating could be recovered from the flue

gas by a flue gas cooler ( $FGC_{APH}$ ) located downstream of the APH. This method of air preheating is referred to as advanced air preheating.

Because the FGC operates below the acid dewpoint its heat transfer surfaces have to be manufactured of corrosion-resistant plastic or corrosion-resistant alloys, and the casing protected from corrosion. Following design specifications of a FGC manufacturer (The Swiss company, Flucorex), a minimum temperature of the flue gas ( $T_{fg,min}$ ) to the FGD reactor of  $71.1^{\circ}C$  ( $160^{\circ}F$ ) was selected in this study.

The results of the analysis presented in Figure A-7 show temperature of the flue gas exiting the  $FGC_{APH}$  is higher than  $T_{fg,min}$ . A second FGC ( $FGC_{FWH}$ ), located downstream of the  $FGC_{APH}$  could then be used to recover remaining sensible heat from the flue gas. The recovered heat would be used to heat the condensate flow, as presented in Figure 6-1. This is accomplished by bypassing certain percentage of the condensate flow around the LP FWHs D, E, F and G and heating it in a bypass heat exchanger. The condensate bypass flow is a function of the heat recovered in the  $FGC_{FWH}$  which, for the given value of CEAT, also depends on the ambient temperature.

The optimal use of heat recovered from the flue gas for air preheating and condensate heating was determined by considering tradeoffs between the two heating approaches and CEAT constraints, and determining the effect on turbine cycle and net unit heat rate. As shown in Section 7, the best use of heat recovered from the flue gas is in the reboiler.

The analysis was performed by using a spreadsheet-based mass and energy balance model of the plant described in Section 3. The case where combustion air is preheated in the SAH was used as a benchmark for other cases.

### **STEAM AIR PREHEATING (SAH)**

The flow rate of the extracted steam for the SAH depends on the ambient air temperature and the temperature of the air entering the APH (exiting SAH) needed to maintain the secondary APH CEAT (SCEAT) and primary APH CEAT (PCEAT) set points. The total heat ( $Q_{SAH}$ ) supplied by the extraction steam to the SSAH and PSAH is presented in Figure A-2 as a function of the ambient temperature and temperature of air leaving the SAH. The total SAH heat input required to maintain PCEAT and SCEAT set points at the host init is also shown.

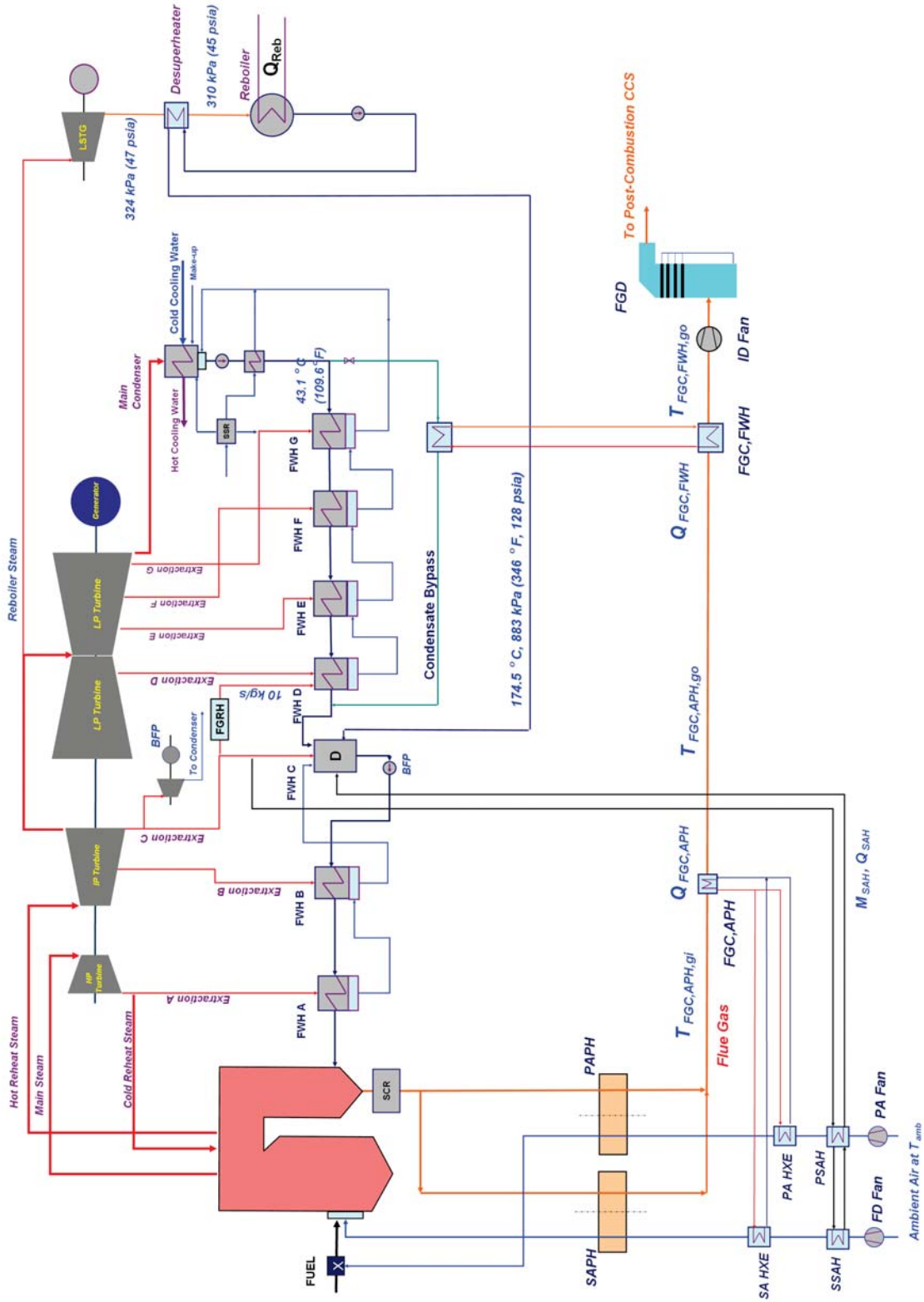
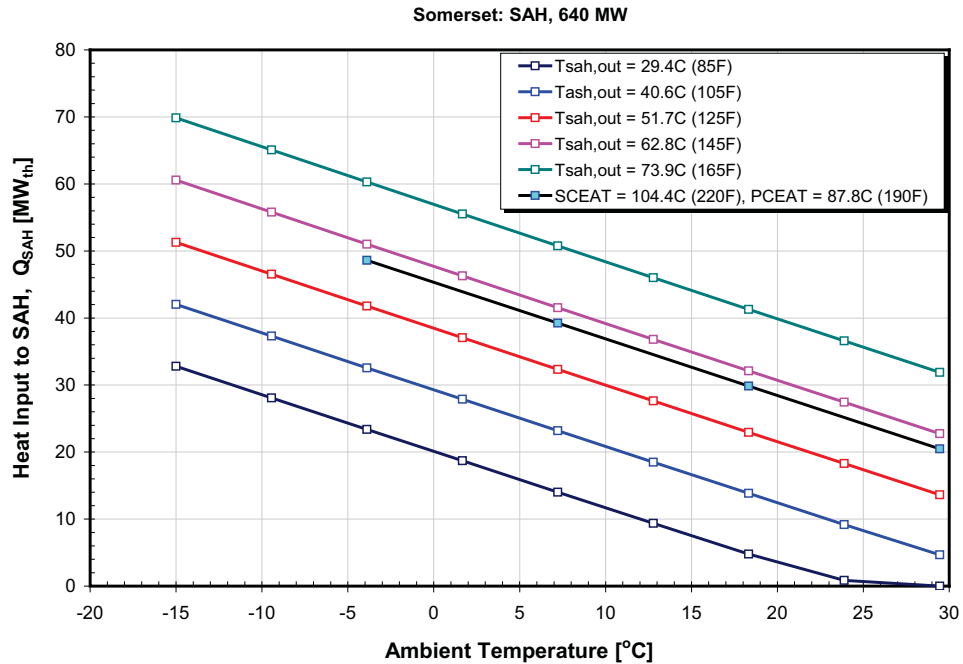


Figure A-1: Schematic Representation of Air Preheating and Condensate Heating.



**Figure A-2. Total Heat Input to the SAH.**

Steam extraction from the steam turbine cycle has a negative effect on the turbine cycle and net unit heat rate. The effect of steam extraction for the SAH on turbine cycle heat rate is presented in Figure A-3 as a function of the ambient temperature and temperature of the air leaving the SAH (entering the APH). Depending on the ambient temperature, and operating with steam extraction flow needed to maintain SCEAT and PCEAT set points, the turbine cycle heat rate is by 0.8 to 2.2% higher compared to the zero extraction (baseline). The effect of steam extraction for the SAH on the net unit heat rate, presented in Figure A-4, is similar to the turbine cycle heat rate.

A kink in the line representing design value of the air temperature at the APH inlet of 29.4°C (85°F) at ambient temperature of 29.4°C (85°F) is due to the fact that no preheating of combustion air and, therefore, no steam extraction is needed at this operating condition.

Boiler efficiency is presented in Figure A-5 as a function of the ambient air temperature and temperature of air leaving the SAH. The results show that boiler efficiency improves as air temperature at the APH inlet increases due to higher heat input to the boiler.

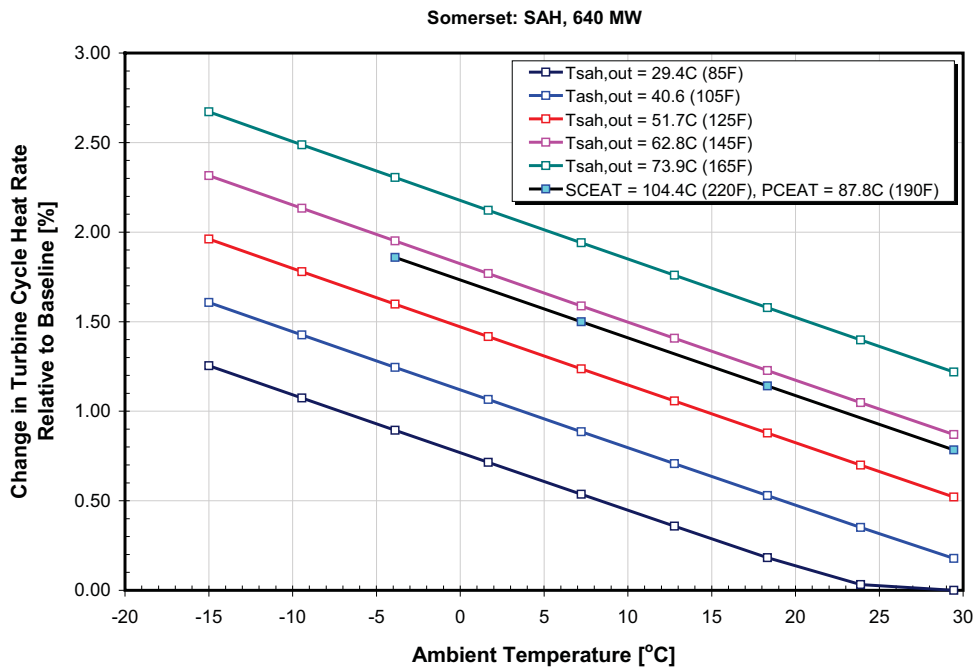


**Figure A-3. Change in Turbine Cycle Heat Rate Due to Steam Extraction for SAH.**

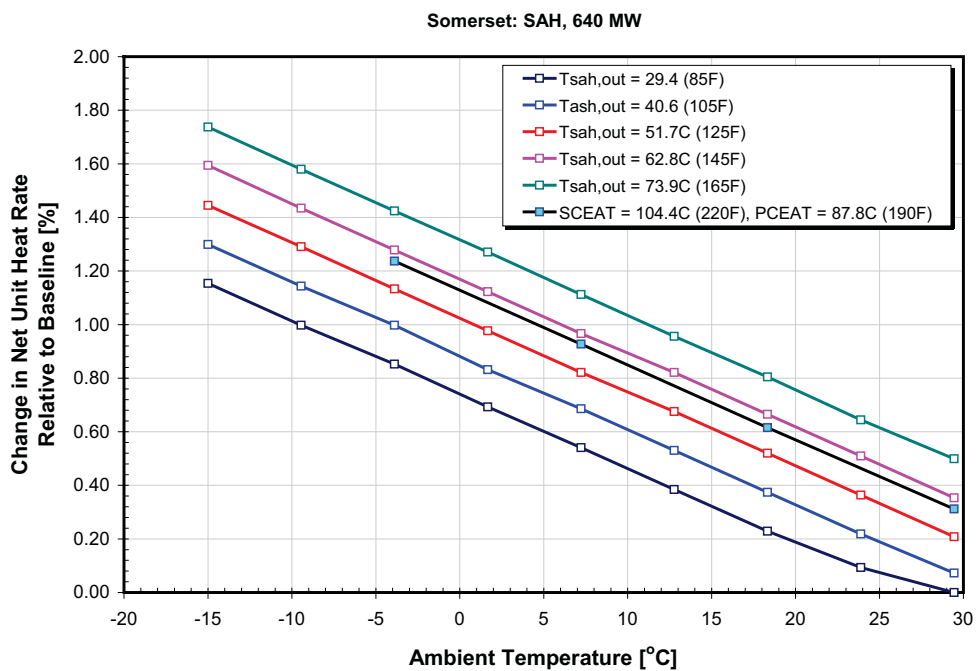


**Figure A-4. Change in Net Unit Heat Rate Due to Steam Extraction for SAH.**

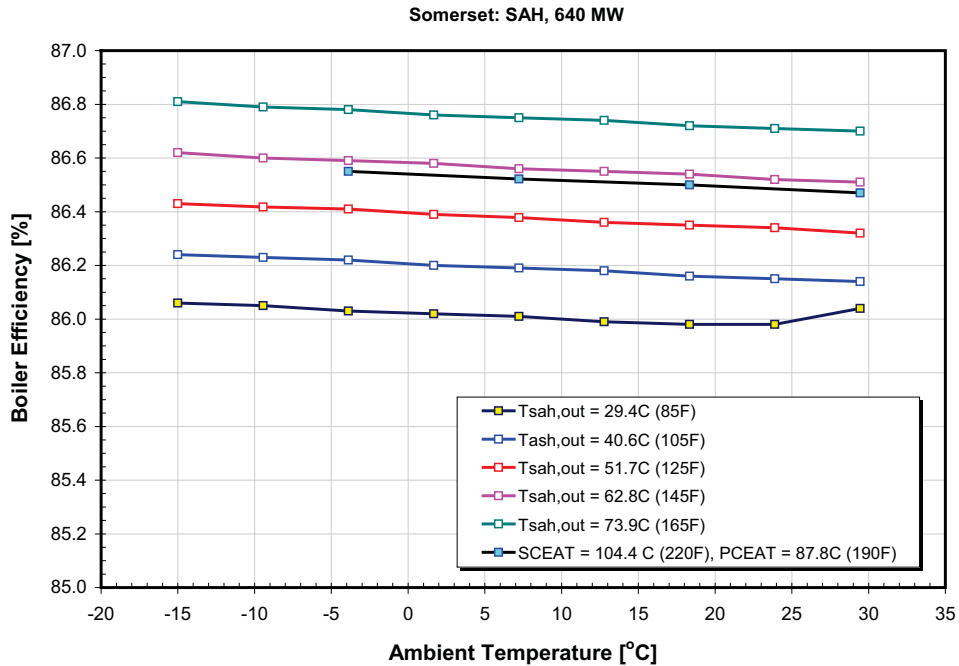


**Figure A-5. Change in Boiler Efficiency due to Air Preheating by SAH.**

#### ADVANCED AIR PREHEATING

As presented in Figure A-1, air preheating can be accomplished by using sensible heat recovered from the flue gas by the flue gas cooler ( $FGC_{APH}$ ) located downstream of the APH. This method of air preheating is referred to as advanced air preheating. Advanced air preheating has a positive effect on turbine cycle performance because steam extraction from the steam cycle for the SAH is not needed. It also improves net unit heat rate and boiler efficiency because of the lower flue gas temperature leaving the FGC compared to the APH outlet [Sarunac, 2009]. Nevertheless, additional heat exchangers are needed.

The total heat recovered by the  $FGC_{APH}$  and transferred to the primary and secondary air is presented in Figure A-6 as a function of the ambient temperature and temperature of the air leaving the SAH. The total heat input to the primary and secondary air required to maintain the PCEAT and SCEAT set points at the host unit is also shown. Compared to the heat input to combustion air required in case of the air preheating by SAH, the heat input to combustion air required in case of the advanced air preheating is slightly lower. This is due to slightly lower air flows resulting from better unit performance. A kink in the line representing the design value of air temperature at the APH inlet of 29.4°C (85°F) at ambient temperature of 29.4°C (85°F) is due to the fact that no preheating of combustion air is needed at this operating condition.

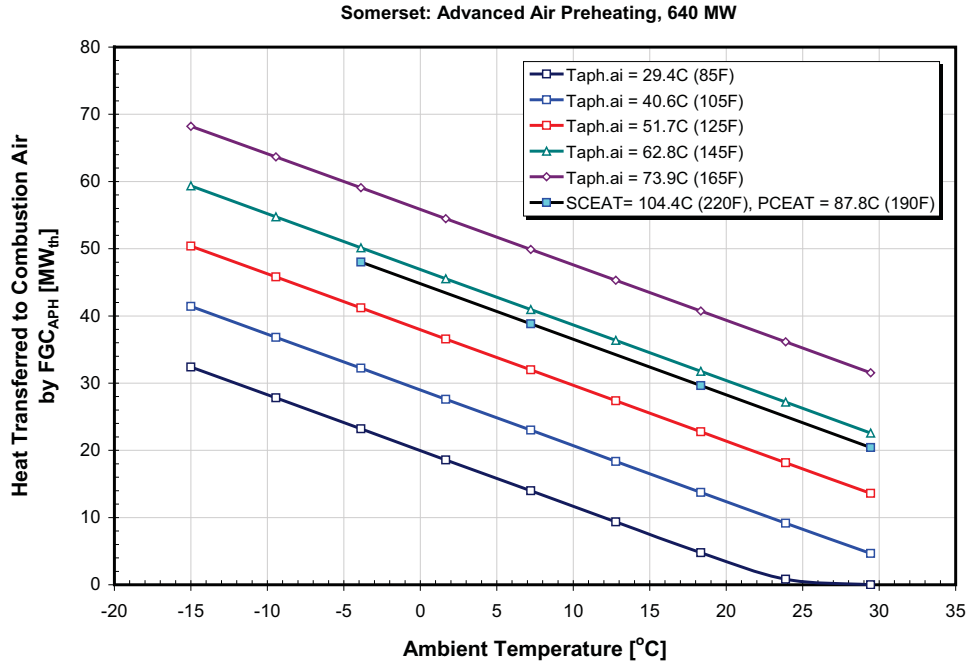
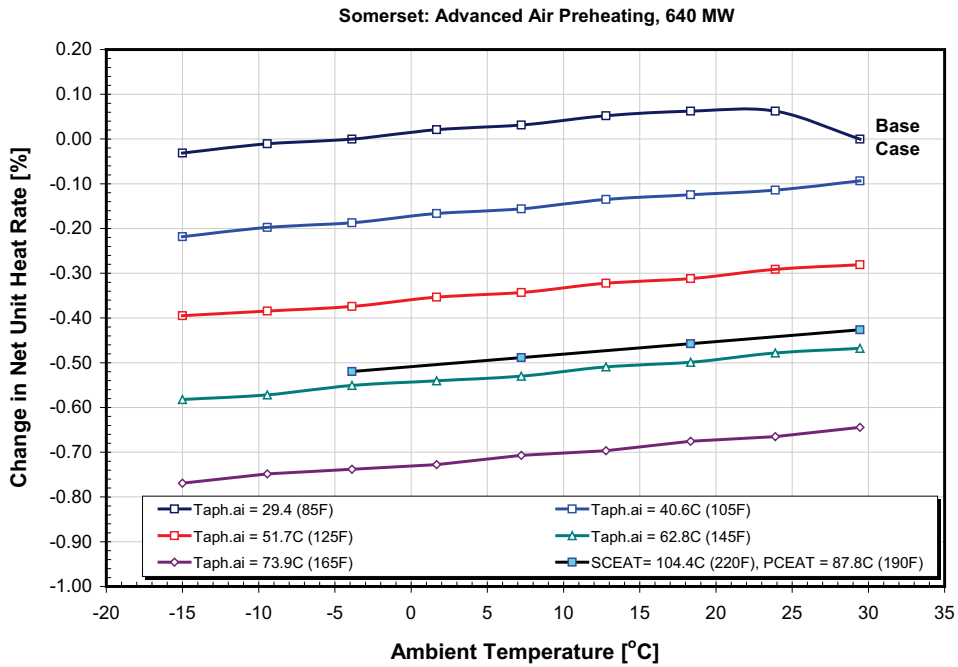
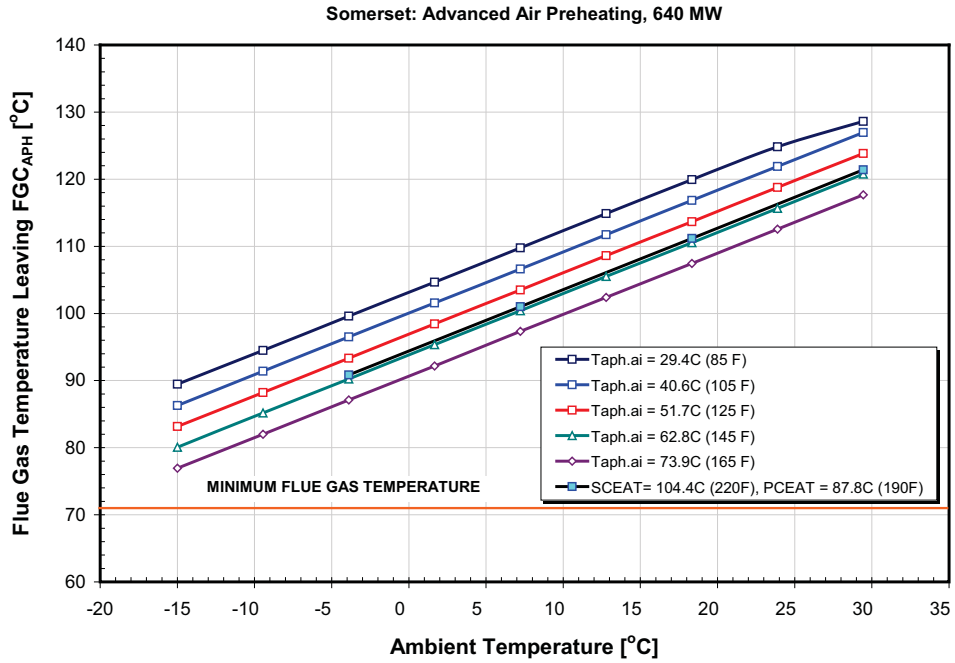


**Figure A-6. Heat Transferred to Combustion Air by the FGC<sub>APH</sub>.**

The temperature of the flue gas leaving the FGC<sub>APH</sub> is presented in Figure A-7. The value of this parameter decreases as the ambient temperature decreases and the air temperature entering the APH increases, but remains above the minimum flue gas temperature specified by the FGC manufacturer.

Since no steam extraction from the steam turbine cycle is needed, the turbine cycle heat rate remains unaffected. The effect of the advanced air preheating on the net unit heat rate is presented in Figure A-8. The results show that the net unit heat rate improves as temperature of air to the APH is increased, resulting in a lower temperature of the flue gas leaving the FGC<sub>APH</sub> (Figure A-7) and lower sensible flue gas loss.



Depending on the ambient temperature the net unit heat rate with heat recovery from the flue gas set to maintain the SCEAT and PCEAT set points at the host unit, is by approximately 0.4 to 0.5% lower compared to the baseline case<sup>5</sup>.

Boiler efficiency is presented in Figure A-9 as a function of the ambient air temperature and temperature of the air entering the APH. The results show that boiler efficiency improves as the air temperature at the APH inlet increases due to higher heat input to the boiler.

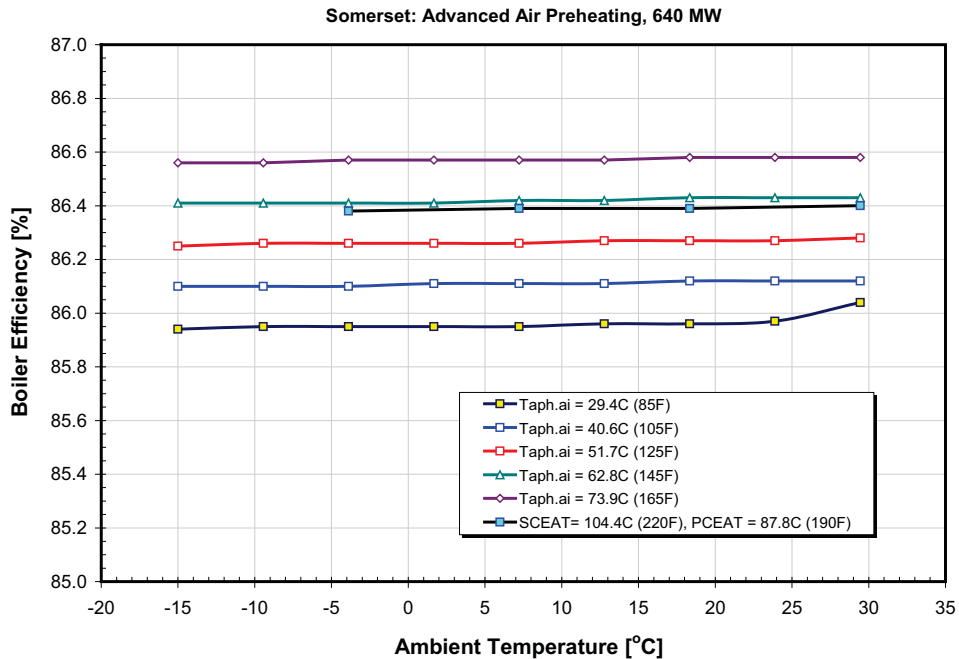


Figure A-9. Change in Boiler Efficiency Due to Advanced Air Preheating.

### ADVANCED AIR PREHEATING AND FEEDWATER HEATING

As shown in Figure A-7, temperature of the flue gas exiting the  $FGC_{APH}$  is higher than the minimum value ( $T_{fg,min}$ ) specified by the FGC manufacturer, allowing additional sensible heat to be recovered from the flue gas by the  $FGC_{FWH}$ , located downstream of the  $FGC_{APH}$  (see Figure A-1)<sup>6</sup>. The heat recovered by the  $FGC_{FWH}$  is used to heat the main condensate by bypassing a certain percentage of the condensate flow around the LP FWHs D, E, F and G and heating it in a bypass heat exchanger.

The effect of bypassing the LP FWHs heaters on turbine cycle heat rate is presented in Figure A-10, where improvement in turbine cycle heat rate is shown as a function of the external heat input (sensible heat recovered from the flue gas) to the condensate (feedwater) flow for several FWH bypassing scenarios. The

<sup>5</sup> 1% improvement in net unit heat rate for the host unit corresponds to annual savings of \$1,500,000.

<sup>6</sup> In practice  $FGC_{APH}$  and  $FGC_{FWH}$  will be integrated into one flue gas cooler heating two streams.

results show that the largest improvement in turbine cycle performance is achieved when all four LP FWHs heaters (D, E, F and G) are bypassed. The magnitude of the achievable improvement depends on the amount of available heat.

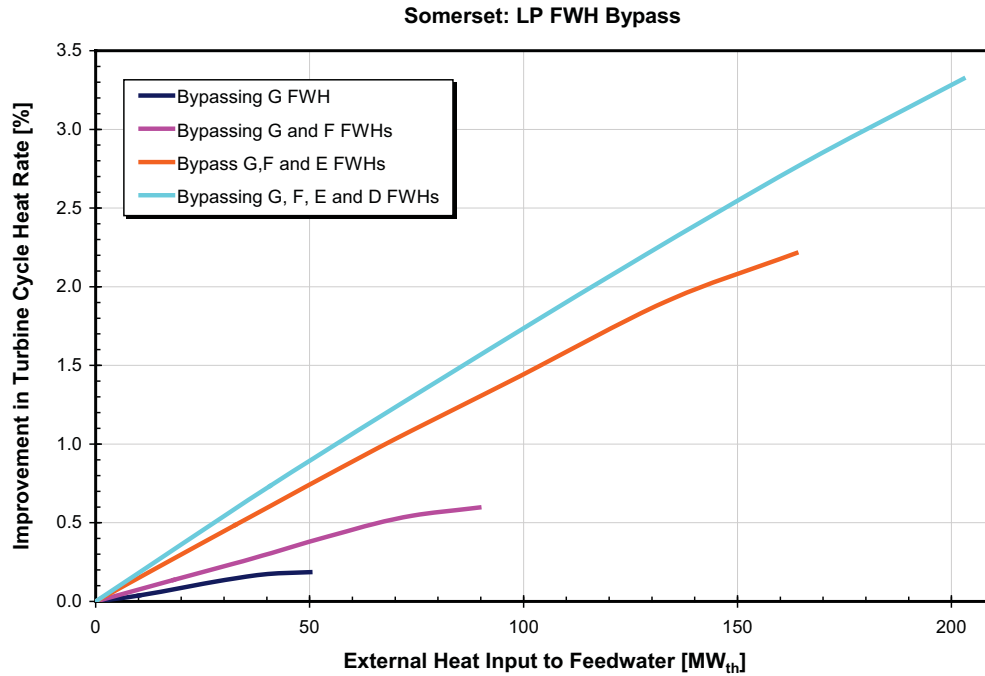


**Figure A-10. Effect of External Heat Input to the LP Feedwater Heaters on Turbine Cycle Heat Rate.**

The heat recovered from the flue gas that can be used for the condensate heating is presented in Figure A-11, while the heat recovered by the  $FGC_{APH}$  for the advanced air preheat is presented in Figure A-6. As shown in Figure A-11, the maximum amount of sensible heat recovered from the flue gas by the  $FGC_{FWH}$  that could be used for the condensate heating for the host unit is approximately 50 MW<sub>th</sub> resulting in approximately 0.9% improvement in turbine cycle heat rate (Figure A-10).

The change in turbine cycle heat rate is presented in Figure A-12 as a function of the ambient temperature and temperature of the air entering the APH. As discussed earlier, in case of the advanced air preheating, turbine cycle heat rate is not affected because no steam extraction for air preheating is needed. In the case where sensible heat recovered from the flue gas is used for advanced air preheating and condensate heating, turbine cycle heat rate improves because the LP FWHs are partially bypassed and steam extractions from the turbine are reduced. The bypass condensate flow is heated by the heat recovered from the flue gas. The improvement in turbine cycle performance increases as the ambient temperature is increased and the air temperature to the APH is decreased because less heat is needed for the air heating; increasing the amount of heat available for the condensate flow heating (Figure A-11).

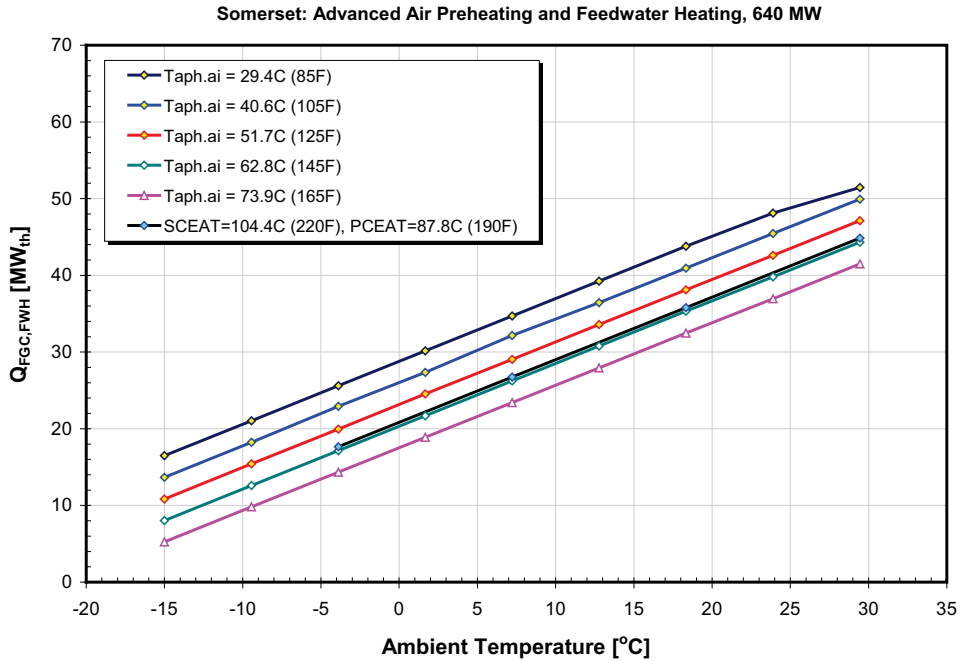


**Figure A-11. Heat Recovered from Flue Gas Available for LP Feedwater Heaters.**

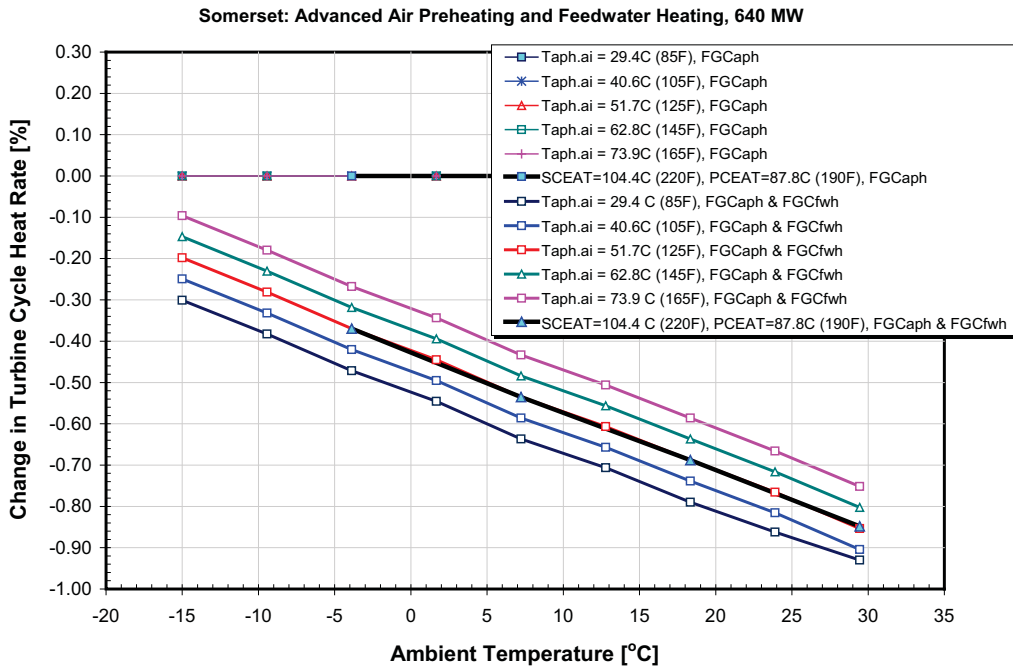


**Figure A-12. Change in Turbine Cycle Heat Rate: Advanced Air Preheating and Condensate Flow Heating.**

Changes in net unit heat rate for the cases of advanced air preheating and advanced air preheating combined with condensate heating are compared in Figure A-13. In both cases the net unit heat rate improves as the air temperature to the APH increases because of the lower temperature of the flue gas

leaving the plant. In the case where advanced air preheating is combined with condensate heating, improvement in net unit heat rate is larger compared to the advanced air preheating because of the additional heat recovered from the flue gas that is supplied to the steam turbine cycle and lower temperature of the flue gas leaving the plant.

Depending on the ambient temperature, the net unit heat rate for the case where advanced air preheating is combined with condensate heating and SCEAT and PCEAT set points are maintained, is by approximately 0.9 to 1.3%-points lower compared to the baseline case.

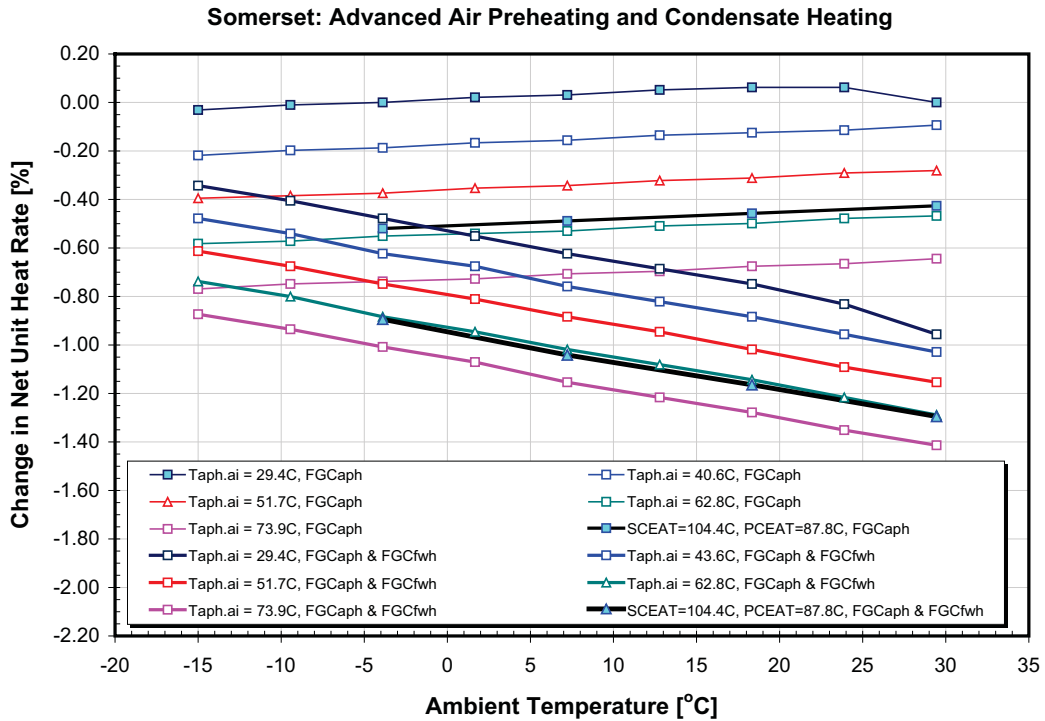


**Figure A-13. Change in Net Unit Heat Rate: Advanced Air Preheating and Condensate Flow Heating.**

Boiler efficiency values for cases of the advanced air preheating and advanced air preheating combined with condensate heating are compared in Figure A-14. In both cases boiler efficiency improves as air temperature to the APH increases because of lower temperature of the flue gas leaving the unit and higher heat input to the boiler with the combustion air. Also, as expected, the values of boiler efficiency for both cases are virtually identical.

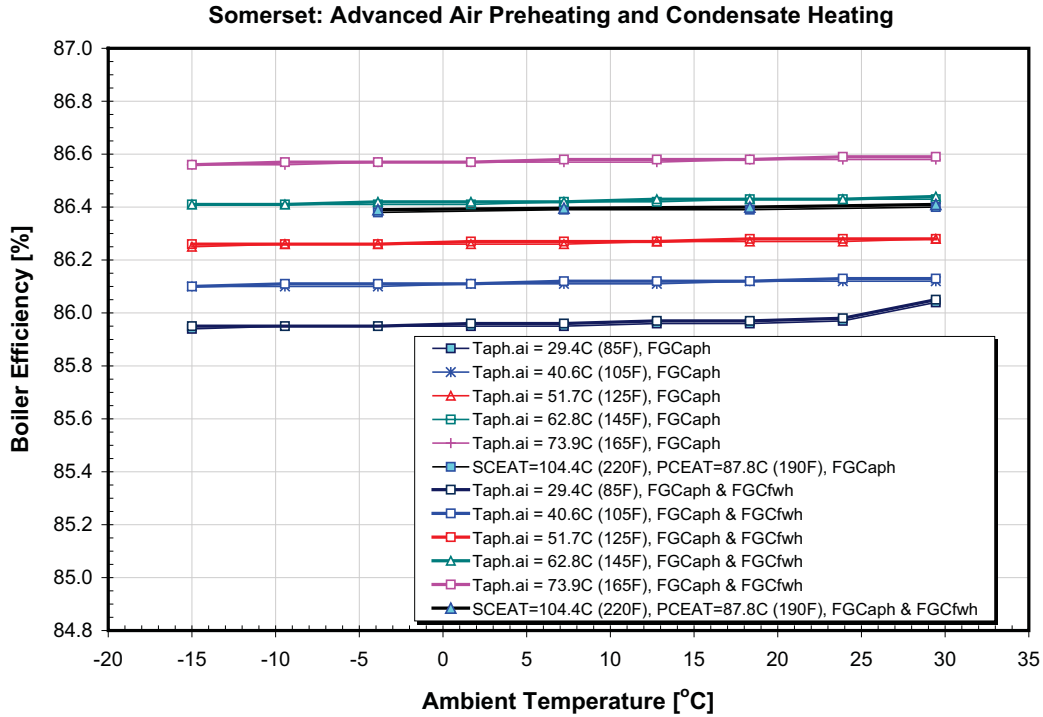


**Figure A-14. Change in Boiler Efficiency: Advanced Air Preheating and Condensate Flow Heating.**

**COMPARISON OF STEAM AIR PREHEATING, AND ADVANCED AIR PREHEATING WITH OR WITHOUT FEEDWATER HEATING**

The results for all three analyzed cases (air preheating by SAH, advanced air preheating, and advanced air preheating in combination with the feedwater heating) are compared in Figures A-15 to A-17. The comparison of turbine cycle heat rate for all three cases, presented in Figure A-15, shows that the best turbine cycle performance is achieved when the advanced air preheating is combined with the condensate heating and air temperature to the APH is equal to the design value of the ambient temperature of 29.4°C (85°F).

The turbine cycle performance is the worst for the case where combustion air is preheated in the SAH using steam extracted from the steam turbine cycle at the lowest value of the ambient temperature and highest value of the air temperature into the APH, which result in highest steam extraction flow and, therefore, highest penalty to the turbine cycle performance.

At the design value of the ambient temperature and operating conditions satisfying the SCEAT and PCEAT set points, turbine cycle heat rate for the case where the advanced air preheating is combined with the condensate heating is by approximately 1.63%-points lower compared to the SAH air preheating. This difference increases as ambient temperature decreases. At the ambient temperature of -15°C the difference

is approximately 2.45%-points. In addition, while in case of the SAH air preheating, temperature of combustion air to the APH has a large effect on turbine cycle heat rate (approximately 1.4%-points max); in case of the advanced air preheating combined with the condensate heating temperature of the combustion air to the APH has a very small effect on turbine cycle performance (approximately 0.2%-points max).

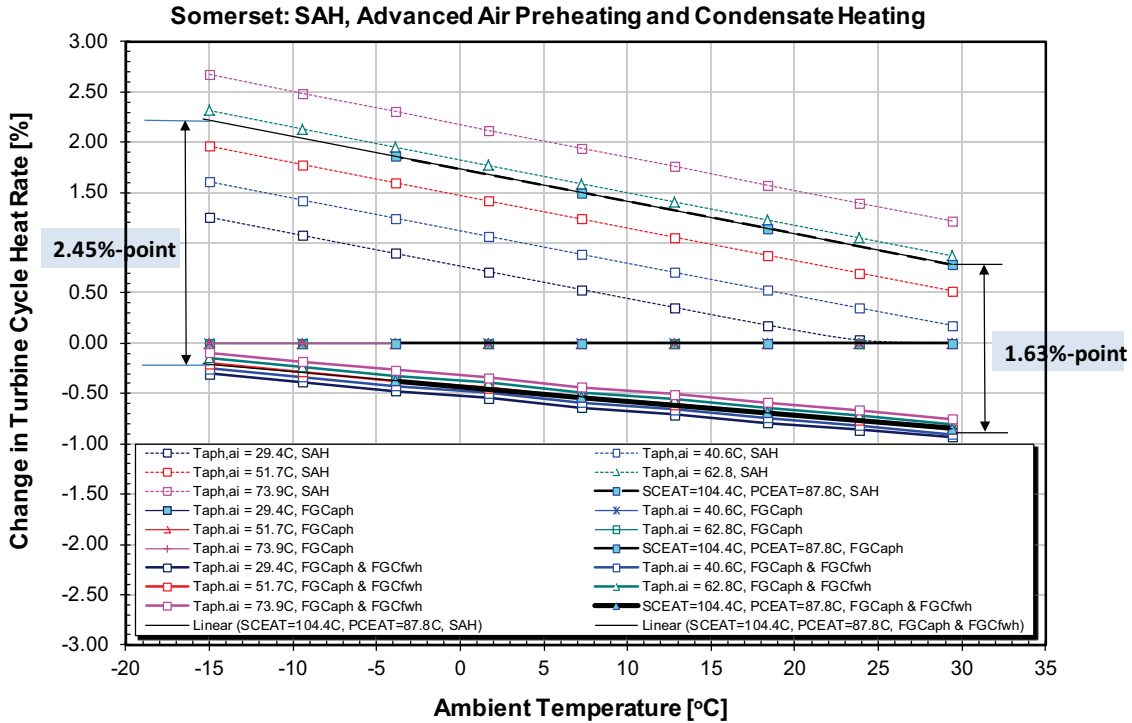


**Figure A-15. Change in Turbine Cycle Heat Rate: SAH, Advanced Air Preheating, and Advanced Air Preheating Combined with Condensate Flow Heating.**

The comparison of net unit heat rate for all three cases, presented in Figure A-16, shows that the best unit performance is achieved in the case where the advanced air preheating is combined with the condensate heating at the highest value of the air temperature to the APH (lowest value of the flue gas temperature leaving the plant), and design value of the ambient temperature of 29.4°C (85°F).

Similar to the turbine cycle performance, the net unit performance is the worst for the case where combustion air is preheated in the SAH using steam extracted from the steam turbine cycle at the lowest value of ambient temperature and highest value of air temperature into the APH (highest steam extraction flow, highest penalty to turbine cycle performance, highest temperature of the flue gas leaving the unit, and highest sensible heat loss).

At the design value of ambient temperature and operating conditions satisfying the SCEAT and PCEAT set points, the net unit heat rate for the case where the advanced air preheating is combined with the feedwater heating is by approximately 1.6%-point lower compared to the SAH air preheating. This difference

increases as the ambient temperature decreases. At the ambient temperature of -15°C the difference is approximately 2.4%-points.

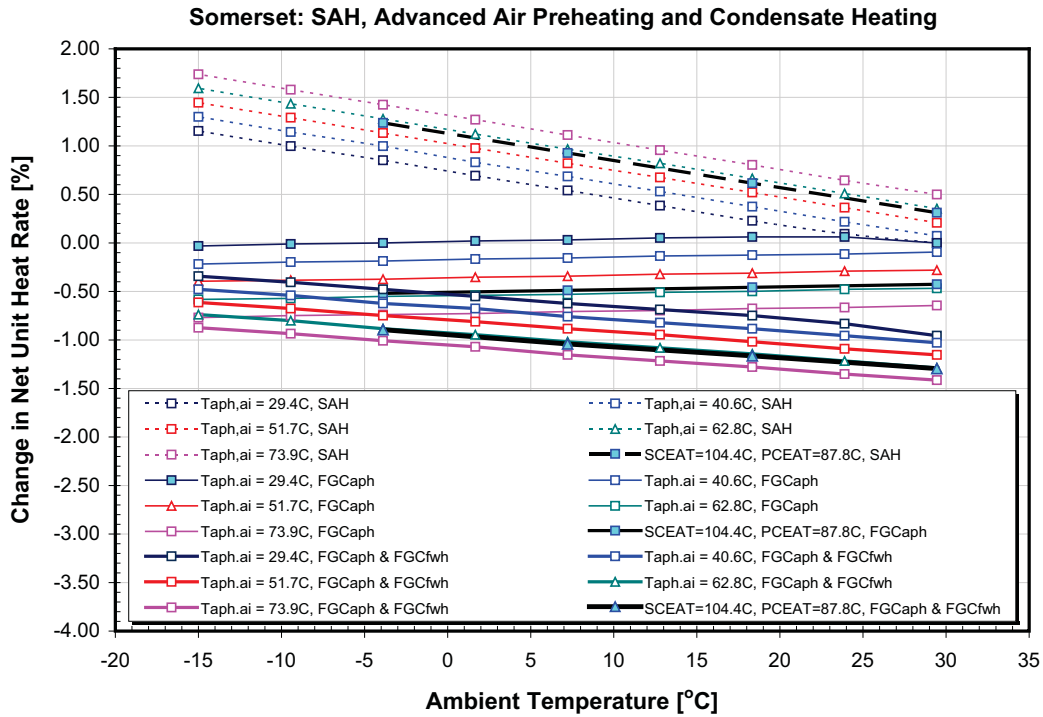


**Figure A-16. Change in Net Unit Heat Rate: SAH Air Preheating, Advanced Air Preheating, and Advanced Air Preheating Combined with Condensate Flow Heating.**

The optimal use of heat recovered from the flue gas is presented in Figure A-17 where heat input to the condensate flow is shown as a percentage of the maximum amount of heat that can be recovered from the flue gas ( $Q_{FGC,MAX}$ ). The results are presented as functions of the ambient temperature and temperature of combustion air at the APH inlet.

At the design value of ambient temperature and operating conditions satisfying the SCEAT and PCEAT set points, the best net unit heat rate is achieved by using approximately 69% of the maximum available heat from the flue gas for the condensate heating. At the ambient temperature of -15°C the best unit performance is achieved by using approximately 12% of the maximum available heat for the condensate heating.

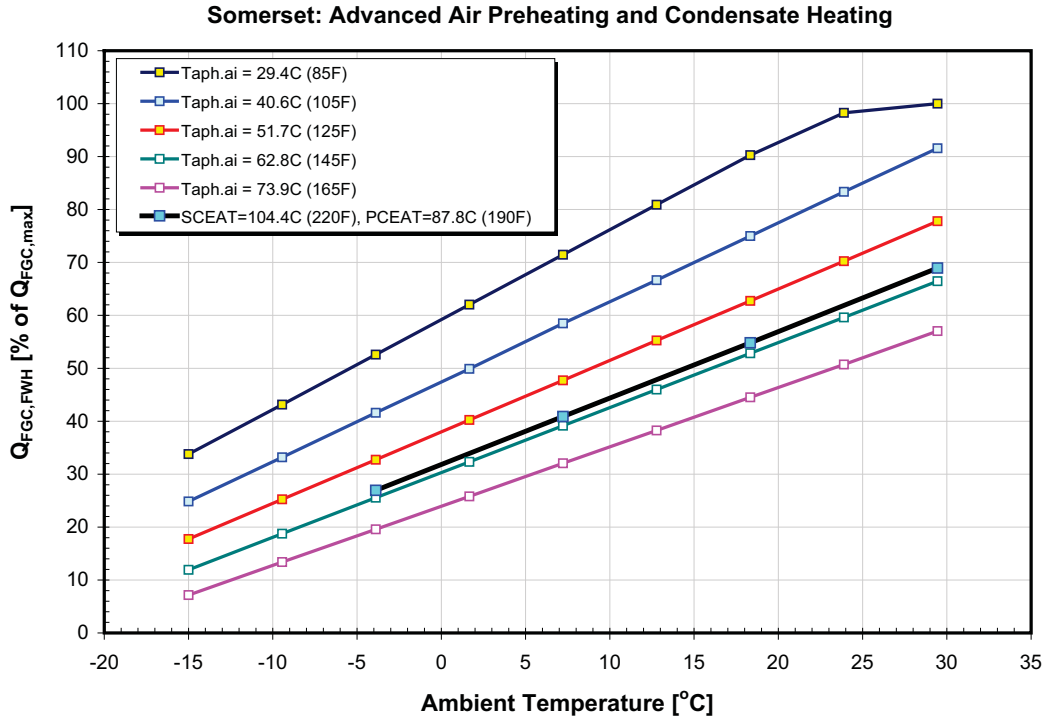


**Figure A-17. Optimal Use of Heat Recovered from the Flue Gas.**

A kink in the line representing design value of the air temperature at the APH inlet of 29.4°C (85°F) at ambient temperature of 29.4°C (85°F) is due to the fact that no preheating of combustion air and, therefore, no steam extraction is needed at this operating condition.

The boiler efficiency values for all three cases are compared in Figure A-18. In all cases boiler efficiency improves as air temperature to the APH increases because of the higher sensible heat input to the boiler with the combustion air. Also, as expected, the values of boiler efficiency for cases of advanced air preheating and advanced air preheating combined with the condensate flow heating are virtually identical.

Somerset: SAH, Advanced Air Preheating and Condensate Heating

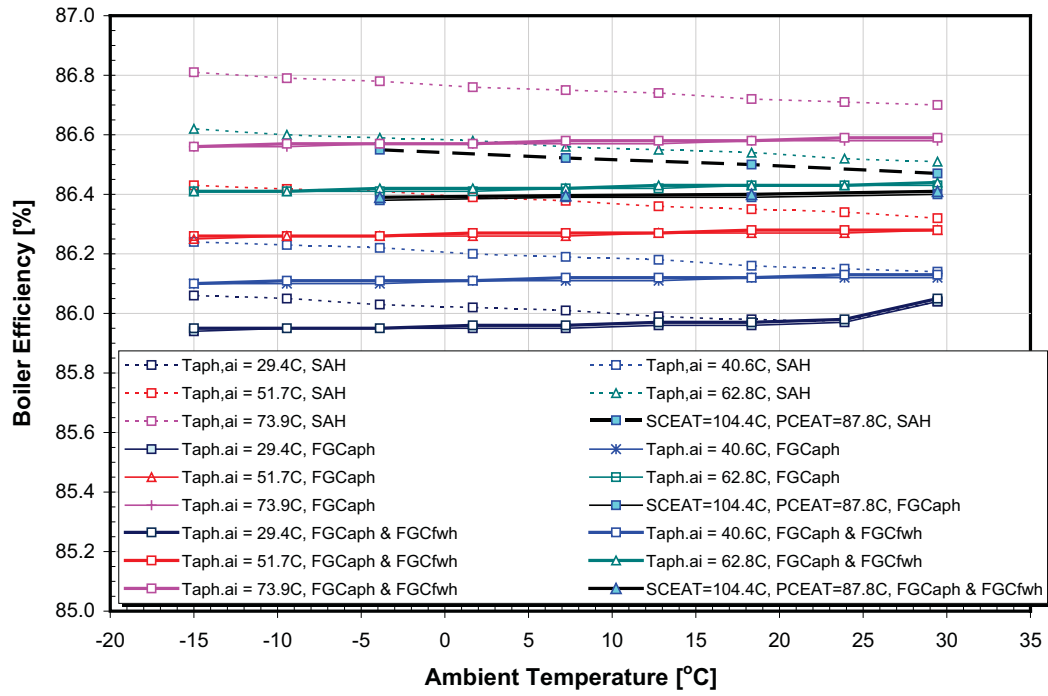


Figure A-18. Change in Boiler Efficiency: SAH Air Preheating, Advanced Air Preheating, and Advanced Air Preheating Combined with Condensate Flow Heating.



## APPENDIX B

### CO<sub>2</sub> COMPRESSION AND COMPRESSION HEAT

As described in Section 7 of the report, thermal integration options, referred to as Modification B, C, and D employ CO<sub>2</sub> compression heat recovered from a conventional multi-stage inline centrifugal compressor to heat the condensate (see Figures 7-2, 7-3, and 7-4). Condensate heating by external heat source reduces or eliminates steam extractions for the LP FWHs and improves performance of the steam turbine cycle. The CO<sub>2</sub> compression heat, recovered from a two-stage shock-wave Ramgen compression train, is utilized in thermal integration options B-R, C-R, E and F (Figures 7-2, 7-3, 7-5 and 7-6) to provide heat for the condensate heating and for the reboiler.

A schematic of the proposed heat recovery from a conventional inline CO<sub>2</sub> compressor is presented in Figure B-1. A three casing arrangement consisting of the LP, IP, and HP compressor casings was analyzed. Four compression stages per housing and stage pressure ratio (PR) of 1.49 were selected to achieve discharge pressure of 15,283 kPa (152.8 bar or 2,217 psia). Due to the Mach number limitations, the stage pressure ratio for the inline centrifugal CO<sub>2</sub> compressor is in the 1.5 to 1.6 range. The isentropic gas temperature rise across a compression stage ( $\Delta T_{is}$ ) was calculated by from the following expression from Gas Dynamics:

$$\Delta T_{is} = (PR^c - 1)T_{in} \quad \text{Eqn. B-1}$$

Where the quantity  $c$  is defined as  $c = \kappa / (\kappa - 1)$ ,  $T_{in}$  is gas temperature at the stage inlet, and  $\kappa$  is the ratio of gas specific heats at constant pressure ( $c_p$ ) and volume ( $c_v$ ). Since both  $c_p$  and  $c_v$  vary with temperature,  $\kappa$  is also a function of the gas temperature. Functional relationship between  $\kappa$  and temperature for the CO<sub>2</sub>, presented in Figure B-2, was used in the calculations. Thermodynamic data for CO<sub>2</sub> are from [Wark, 1983].

The actual gas temperature rise per stage ( $\Delta T_{act}$ ) was calculated from:

$$\Delta T_{act} = \Delta T_{is} / \eta_{is} \quad \text{Eqn. B-2}$$

The quantity  $\eta_{is}$  is a stage isentropic efficiency (or stage efficiency). Typical values of  $\eta_{is}$  for the inline centrifugal compressor were used in the calculations. Calculated actual stage temperature rise is in the 50 to 60°C (90 to 110°F) range, consistent with data provided in the open literature. For the selected discharge pressure of 152.8 bar, the pressure ratio for individual compressor castings is 4.93. The corresponding discharge temperature from individual compressor casings is in the 195°C (380°F) range.

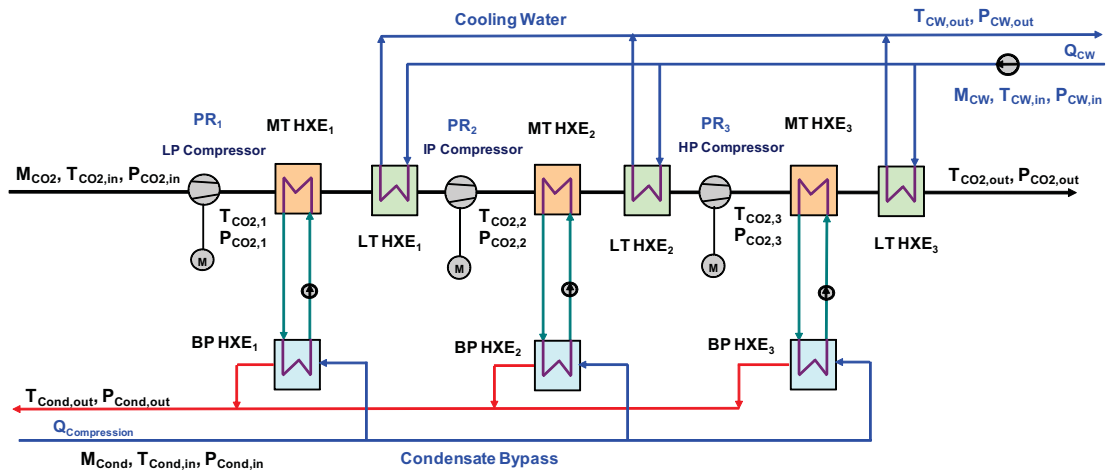


**Figure B-1. Schematic Representation of Heat Recovery from a Three-Stage Inline CO<sub>2</sub> Compressor.**

The proposed thermal integration for recovery of CO<sub>2</sub> compression heat from the inline compressor is presented in Figure B-1. The mid-grade heat of the compression ( $Q_{compression}$ ), recovered by the medium-temperature heat exchangers MT HXE<sub>1</sub> to MT HXE<sub>3</sub>, located downstream of the LP, IP and HP compressor casings, is used for condensate heating in the BP HXE<sub>1</sub> to BP HXE<sub>3</sub>. The amount of compression heat that could be recovered for the condensate heating for the host unit and thermal integration options B and D is approximately 28 MW<sub>th</sub>, the actual amount depending on the final CO<sub>2</sub> pressure (110 or 150 bar). The compressed CO<sub>2</sub> is further cooled from 85°C (185°F) in the LT HXE<sub>1</sub> to LT HXE<sub>3</sub> to 41°C (105°C) prior to entering the next compression casing or being discharged to a CO<sub>2</sub> pipeline. The final cooling temperature was selected to keep CO<sub>2</sub> in the supercritical fluid state and help prevent formation of carbonic acid (H<sub>2</sub>CO<sub>3</sub>). Carbonic acid is corrosive and could cause corrosion of the compressor impellers and heat exchangers. Removal of water from the CO<sub>2</sub> stream (also referred to as the moisture knockout) is outside the scope of work of this project and is not presented in Figure B-1. Some of the available methods for moisture removal during CO<sub>2</sub> compression include TEG, molecular sieves, and desiccant dryers.

The low grade heat of compression, approximately 20 MW<sub>th</sub> for the host unit and selected cooling temperatures, is removed in low-temperature heat exchangers LT HXE<sub>1</sub> to LT HXE<sub>3</sub> by the cooling water. When the ambient air temperature is low, this low grade heat can be used for building heating or in the plant tank farm. The unused portion of the low grade heat would be rejected to the environment.

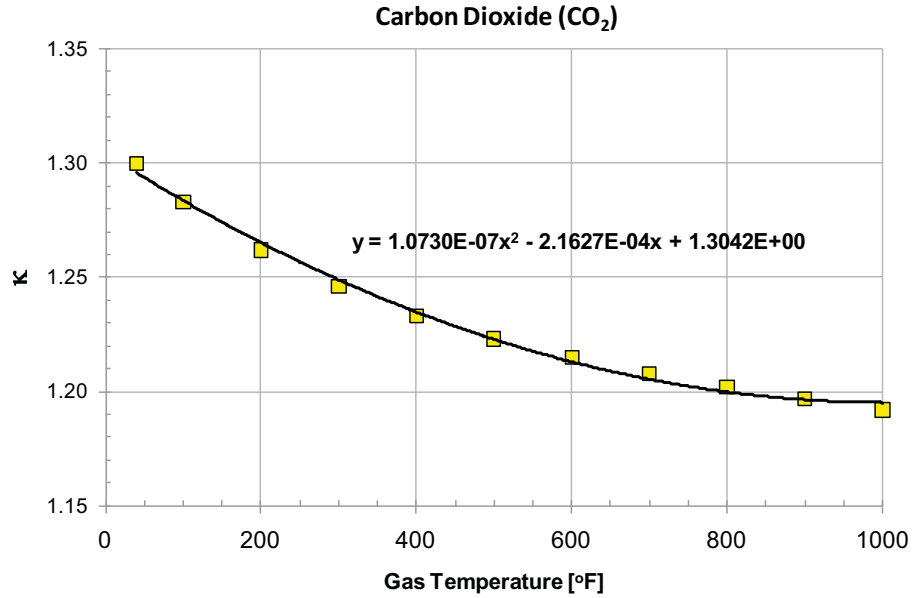


**Figure B-2.  $\kappa$  as a Function of Gas Temperature: Carbon Dioxide.**

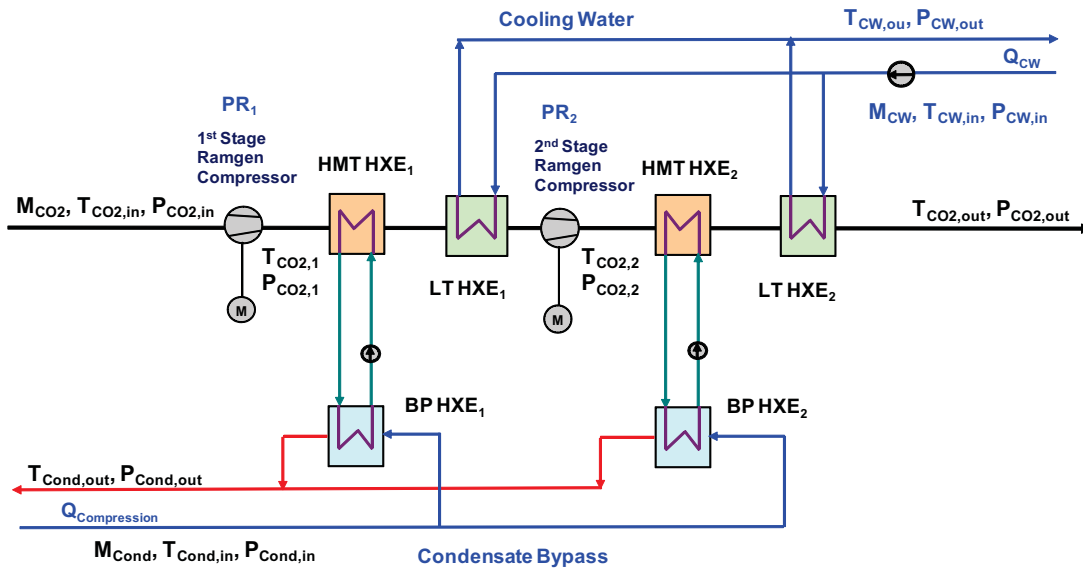


**Figure B-3. Schematic Representation of Heat Recovery for Condensate Heating From a Two-Stage Ramgen CO<sub>2</sub> Compressor.**

A schematic of the proposed heat recovery from a two-stage Ramgen CO<sub>2</sub> compressor for the condensate heating is presented in Figure B-3. Ramgen Power Systems is developing a new compression technology for heavy gases, such as CO<sub>2</sub> (molecular weight 44 kg/mole) based on a supersonic shock wave where fluid velocity is converted into the pressure through a series of planar shocks. The supersonic speed of the fluid (in excess of Mach number 2), relative to the compressor rotor, is achieved through high rotational speed of

the compressor rotor (approximately 30,000 RPM). This approach allows PR in excess of 10 to be achieved in a single compression stage, thus allowing total pressure ratio of 100 to be achieved in two compression stages.

In addition to simplifying the CO<sub>2</sub> compression process, due to the high discharge temperature from the first and second compression stages (270 to 280°C (525 to 540°F) for PR of 11) the Ramgen compression technology offers a possibility of using compression heat more efficiently compared to a conventional inline compressor. Also, the Ramgen CO<sub>2</sub> compression technology has a significant advantage compared to the internally-gear intercooled CO<sub>2</sub> compressor where temperature rise across a compression stage of approximately 50°C (90°F) results in the stage discharge temperature of approximately 90°C (194°F). This temperature is too low to be beneficially used and has to be rejected to the environment.

Thermal integration for recovery of CO<sub>2</sub> compression heat from the two-stage Ramgen compressor is presented schematically in Figure B-3. The high to mid-grade heat of compression ( $Q_{\text{compression}}$ ) is recovered in the high-medium-temperature heat exchangers HMT HXE<sub>1</sub> and HMT HXE<sub>2</sub>, located downstream of the first and second compressor stages, and used for condensate heating in the BP HXE<sub>1</sub> and BP HXE<sub>2</sub>. The amount of compression heat that could be recovered for the condensate heating at the host unit is the 60 to 70 MW<sub>th</sub> range, the actual amount depending on the final CO<sub>2</sub> pressure (110 or 150 bar) and thermal integration option. For example, the amount of compression heat that could be beneficially used for condensate heating is higher for thermal integration option B-R, compared to option C due to the lower condensate temperature entering the BP HXE<sub>1</sub> and BP HXE<sub>2</sub>.

After exiting the HMT HXE<sub>1</sub> and HMT HXE<sub>2</sub> compressed CO<sub>2</sub> is further cooled to 41°C (105°C) in the LT HXE<sub>1</sub> prior to entering the next compression stage and in the LT HXE<sub>2</sub> prior to discharge to a CO<sub>2</sub> pipeline. The final cooling temperature was selected to keep CO<sub>2</sub> in the supercritical fluid state and help prevent formation of carbonic acid (H<sub>2</sub>CO<sub>3</sub>). Removal of water from the CO<sub>2</sub> stream is outside the scope of work of this project and is not presented in Figure B-3.

The low grade heat of compression is removed in the LT HXE<sub>1</sub> and LT HXE<sub>2</sub> by the cooling water. When the ambient air temperature is low, this low-grade heat could be used for building heating or in the plant tank farm. The unused portion of the low grade heat would be rejected to the environment.

Thermal integration for recovery of the CO<sub>2</sub> compression heat from the two-stage Ramgen compressor for the condensate heating and for generating LP steam for the reboiler is presented schematically in Figure B-4. The high-grade heat of compression is recovered in the high-temperature heat exchangers HT HXE<sub>1</sub> and HT HXE<sub>2</sub>, located downstream of the first and second compressor stages and used to provide heat to the Ramgen Evaporator that generates LP steam for the reboiler (thermal integration options E and F). The

amount of high-grade compression heat that could be recovered for the reboiler at the host unit is approximately  $50 \text{ MW}_{\text{th}}$ .

The mid-grade heat of compression is recovered in the medium-temperature heat exchangers  $\text{MT HXE}_1$  and  $\text{MT HXE}_2$  and used for condensate heating in the medium-temperature condensate heaters  $\text{MT}_1$  and  $\text{MT}_2$ . The amount of compression heat that could be recovered for the condensate heating at the host unit is approximately  $30 \text{ MW}_{\text{th}}$ , the actual amount depending on the final  $\text{CO}_2$  pressure (110 or 150 bar) and thermal integration option.

After exiting the  $\text{MT HXE}_1$  and  $\text{MT HXE}_2$  compressed  $\text{CO}_2$  is further cooled to  $41^\circ\text{C}$  ( $105^\circ\text{C}$ ) in the  $\text{LT HXE}_1$  prior to entering the next compression stage and in the  $\text{LT HXE}_2$  prior to discharging it to a  $\text{CO}_2$  pipeline. The low-grade heat of compression, approximately  $10 \text{ MW}_{\text{th}}$  for the host unit, is removed in the  $\text{LT HXE}_1$  and  $\text{LT HXE}_2$  by the cooling water.

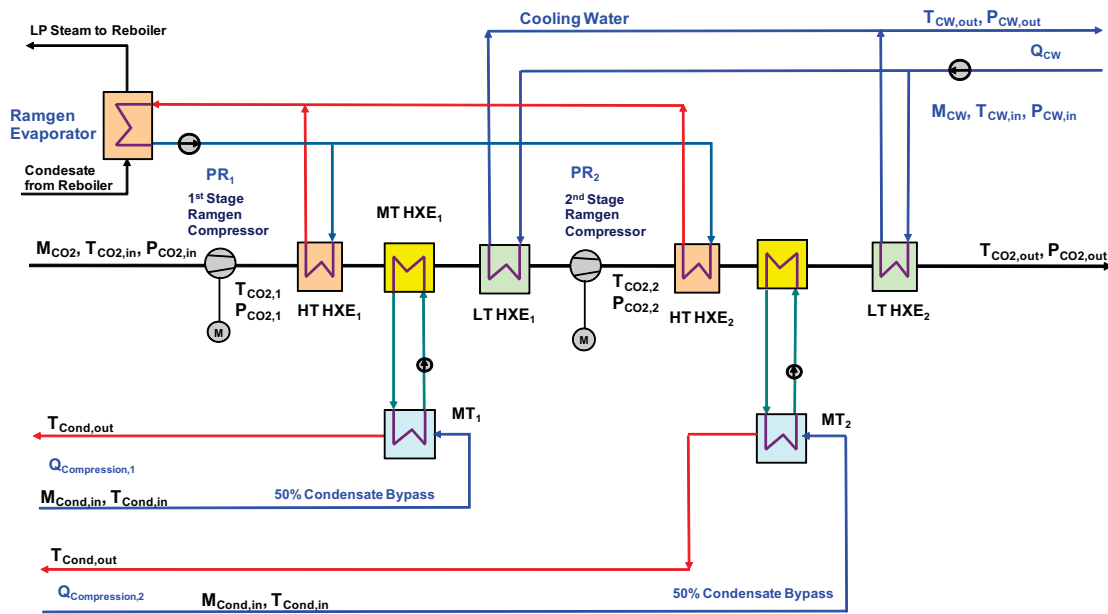


**Figure B-4. Schematic Representation of Heat Recovery for Solvent Regeneration and Condensate Heating from a Two-Stage Ramgen  $\text{CO}_2$  Compressor.**



**APPENDIX C**  
**THERMAL INTEGRATION OF THE TURBINE CYCLE AND CO<sub>2</sub> STRIPPER**  
**WITH PLANT HEAT SOURCES: RESULTS**

The effects of thermal integration on power plant performance for Modifications A to F described in Section 7 are presented in Figures C-1 to C-10 and summarized in Tables C-1 to C-10. The results show that thermal integration has a significant positive effect on cycle and unit performance, with Modification F resulting in best performance. Also, as discussed in Section 4,  $q_{Reb}$  has a major effect on plant performance; as  $q_{Reb}$  decreases, performance penalties associated with the post-combustion CO<sub>2</sub> capture decrease. Figure C-1 and Table C-1 compare effect of thermal integration on the gross power output relative to the baseline (no CO<sub>2</sub> capture). For the state-of-the-art amines, thermal integration reduces penalty in gross power output by 4.29%-points (from 14.67 to 10.38%). For the  $q_{Reb}$  value, determined for the MEA in this study, thermal integration reduces penalty in gross power output by 4.72%-points (from 19.59 to 14.87 %).

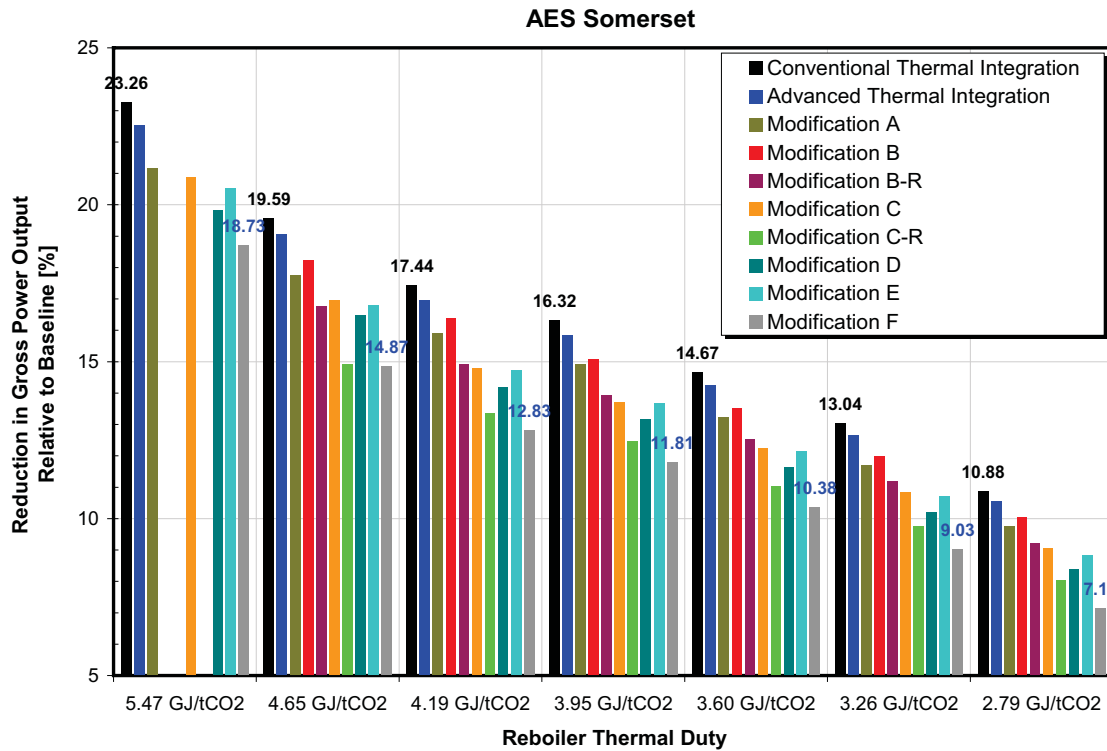


**Figure C-1. Reduction in Gross Power Output Relative to Baseline (no CO<sub>2</sub> capture) VS.  $q_{Reb}$ .**

The improvement in gross power output relative to the conventional thermal integration is summarized in Figure C-2 and Table C-2. The improvement in gross power output relative to the conventional thermal integration is highest for Modifications F and C-R. For the state-of-the-art amines Modification F

improves the gross power output relative to the conventional thermal integration by 5.03%. For the  $q_{Reb}$  value, determined for the MEA in this study and Modification F, improvement in gross power output relative to the conventional thermal integration is 5.87%.

**Table C-1. Reduction in Gross Power Output Relative to Baseline (no CO<sub>2</sub> capture) vs.  $q_{Reb}$**

Reboiler Heat Duty		Conventional Integration	Advanced Integration	Modification B	Modification B	Modification B-R	Modification D	Modification D	Modification A	Modification C	Modification C-R	Modification E	Modification F
		Reduction in Total Gross Power Output Relative to Baseline											
GJ/t CO <sub>2</sub>	BTU/lb CO <sub>2</sub>	%											
5.47	2,350	23.26	22.54				19.83	19.83	21.17	20.88		20.53	18.73
4.65	2,000	19.59	19.06	18.00	18.26	16.78	16.47	16.47	17.77	16.97	14.94	16.80	14.87
4.19	1,800	17.44	16.98	16.13	16.39	14.94	14.20	14.20	15.90	14.80	13.38	14.74	12.83
3.95	1,700	16.32	15.85	14.92	15.10	13.93	13.16	13.16	14.92	13.71	12.47	13.67	11.81
3.60	1,550	14.67	14.26	13.36	13.51	12.52	11.65	11.65	13.23	12.24	11.05	12.15	10.38
3.26	1,400	13.04	12.66	11.85	12.00	11.19	10.21	10.21	11.71	10.86	9.75	10.71	9.03
2.79	1,200	10.88	10.55	9.90	10.04	9.22	8.40	8.40	9.77	9.06	8.05	8.83	7.15
0.00	0	0.00	0.00	0.00	0.00	0.00	0.00	0.00	0.00	0.00	0.00	0.00	0.00

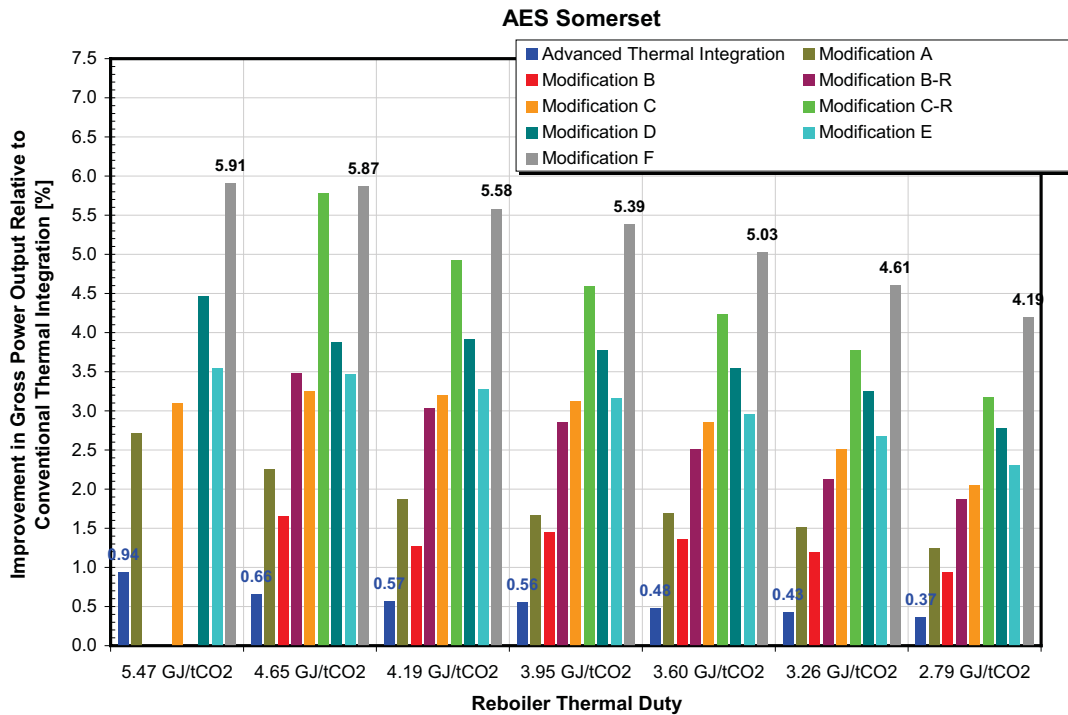


**Figure C-2. Improvement in Gross Power Output Relative to Conventional Thermal Integration vs.  $q_{Reb}$ .**

**Table C-2. Improvement in Gross Power Output Relative to Conventional Thermal Integration vs.  $q_{Reb}$ .**

Reboiler Heat Duty		Advanced Integration	Modification B	Modification B	Modification B-R	Modification D	Modification D	Modification A	Modification C	Modification C-R	Modification E	Modification F	
		Improvement in Total Gross Power Output Relative to Conventional Thermal Integration (Case 1)											
GJ/t CO <sub>2</sub>	BTU/lb CO <sub>2</sub>	%											
5.47	2,350	0.94				4.47	4.47	2.72	3.10		3.55	5.91	
4.65	2,000	0.66	1.98	1.66	3.49	3.88	3.88	2.26	3.25	5.78	3.47	5.87	
4.19	1,800	0.57	1.59	1.27	3.03	3.92	3.92	1.87	3.20	4.92	3.28	5.58	
3.95	1,700	0.56	1.67	1.45	2.86	3.77	3.77	1.67	3.12	4.59	3.17	5.39	
3.60	1,550	0.48	1.54	1.36	2.51	3.54	3.54	1.69	2.85	4.24	2.95	5.03	
3.26	1,400	0.43	1.37	1.20	2.12	3.25	3.25	1.52	2.51	3.78	2.67	4.61	
2.79	1,200	0.37	1.10	0.95	1.87	2.78	2.78	1.25	2.05	3.18	2.30	4.19	
0.00	0	0.00	0.00	0.00	0.00	0.00	0.00	0.00	0.00	0.00	0.00	0.00	

Figure C-3 and Table C-3 compare effect of thermal integration on turbine cycle heat rate ( $HR_{cycle}$ ) relative to the baseline (no  $CO_2$  capture). As  $q_{Reb}$  decreases, increase in  $HR_{cycle}$  associated with the post-combustion  $CO_2$  capture decreases. For the state-of-the-art amines, thermal integration reduces increase in  $HR_{cycle}$  by 5.60%-points (from 17.18 to 11.58%). For the  $q_{Reb}$  value, determined for the MEA in this study, thermal integration reduces increase in  $HR_{cycle}$  associated with the post-combustion  $CO_2$  capture by 6.88%-points (from 24.34 to 17.46 %).

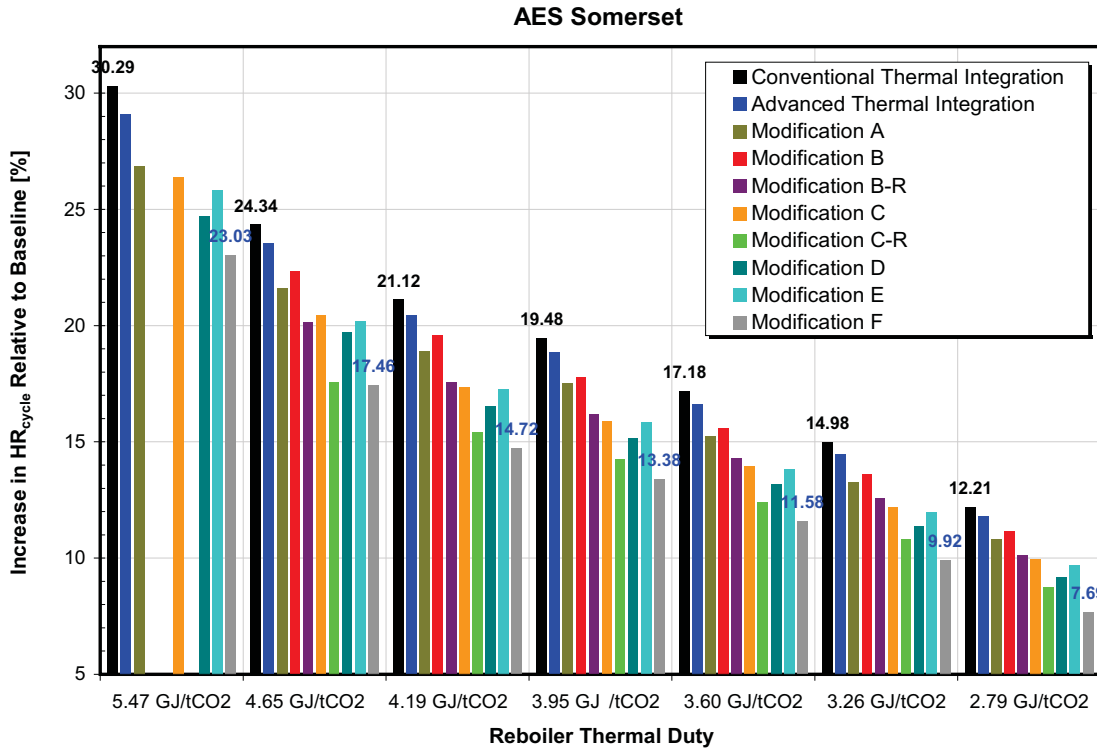


Figure C-3. Increase in Turbine Cycle Heat Rate Relative to Baseline vs.  $q_{Reb}$ .

Table C-3. Reduction in Turbine Cycle Heat Rate Relative to Baseline (no  $CO_2$  capture) vs.  $q_{Reb}$ .

Reboiler Heat Duty		Conventional Integration	Advanced Integration	Modification B	Modification B	Modification B-R	Modification D	Modification D	Modification A	Modification C	Modification C-R	Modification E	Modification F
		Increase in Gross Turbine Cycle Heat Rate Relative to Baseline											
CO <sub>2</sub>	GJ/tCO <sub>2</sub>	%											
2,350	5.47	30.29	29.10				24.73	24.73	26.85	26.40		25.84	23.03
2,000	4.65	24.34	23.53	21.94	22.33	20.17	19.71	19.71	21.61	20.44	17.57	20.18	17.46
1,800	4.19	21.12	20.44	19.23	19.60	17.55	16.55	16.55	18.90	17.37	15.43	17.28	14.72
1,700	3.95	19.48	18.84	17.53	17.78	16.17	15.15	15.15	17.53	15.88	14.24	15.82	13.38
1,550	3.60	17.18	16.62	15.41	15.61	14.31	13.18	13.18	15.24	13.94	12.42	13.82	11.58
1,400	3.26	14.98	14.48	13.43	13.63	12.59	11.37	11.37	13.26	12.17	10.80	11.99	9.92
1,200	2.79	12.21	11.78	10.98	11.15	10.15	9.17	9.17	10.82	9.95	8.75	9.68	7.69
0	0.00	0.00	0.00	0.00	0.00	0.00	0.00	0.00	0.00	0.00	0.00	0.00	0.00

The improvement in  $HR_{cycle}$  relative to the conventional thermal integration is summarized in Figure C-4 and Table C-4. The improvement in  $HR_{cycle}$  relative to the conventional thermal integration is highest for Modifications F and C-R. For the state-of-the-art amines Modification F improves  $HR_{cycle}$  relative to the

conventional thermal integration by 4.78%. For the  $q_{Reb}$  value, determined for the MEA in this study and Modification F, improvement in  $HR_{cycle}$  relative to the conventional thermal integration is 5.54%.

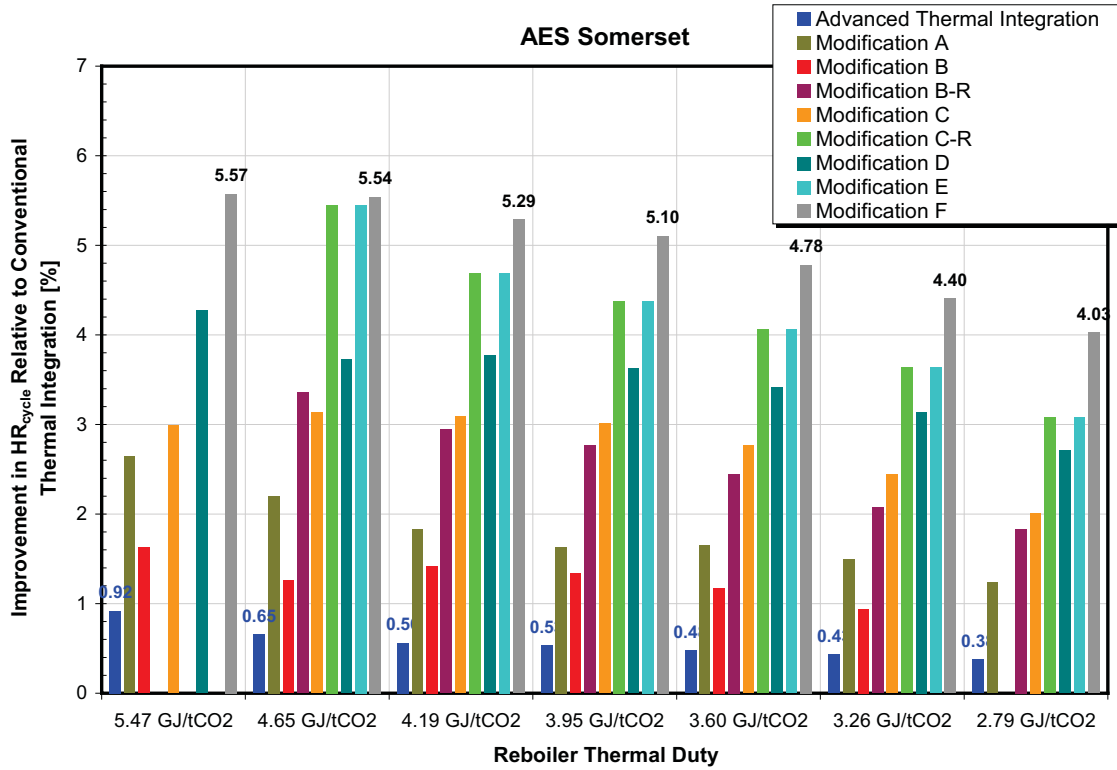


Figure C-4. Improvement in Turbine Cycle Heat Rate Relative to Conventional Thermal Integration vs.  $q_{Reb}$ .

Table C-4. Improvement in Gross Power Output Relative to Conventional Thermal Integration vs.  $q_{Reb}$ .

Reboiler Heat Duty		Advanced Thermal Integration	Modification B	Modification B	Modification B-R	Modification D	Modification D	Modification A	Modification C	Modification C-R	Modification E	Modification F
Improvement in Turbine Cycle Heat Rate Relative to Conventional Thermal Integration (Case 1)												
BTU/lb CO <sub>2</sub>	GJ/t CO <sub>2</sub>	%										
2,350	5.47	0.92				4.27	4.27	2.64	2.99		3.42	5.57
2,000	4.65	0.65	1.93	1.62	3.36	3.73	3.73	2.20	3.14	5.45	3.35	5.54
1,800	4.19	0.56	1.56	1.26	2.94	3.77	3.77	1.83	3.09	4.69	3.17	5.29
1,700	3.95	0.53	1.63	1.42	2.77	3.63	3.63	1.63	3.01	4.38	3.06	5.10
1,550	3.60	0.48	1.51	1.34	2.45	3.41	3.41	1.66	2.76	4.06	2.87	4.78
1,400	3.26	0.43	1.34	1.18	2.07	3.14	3.14	1.49	2.44	3.64	2.60	4.40
1,200	2.79	0.38	1.09	0.94	1.84	2.71	2.71	1.23	2.01	3.08	2.25	4.03
0	0.00	0.00	0.00	0.00	0.00	0.00	0.00	0.00	0.00	0.00	0.00	0.00

Figure C-5 and Table C-5 compare effect of thermal integration on turbine cycle efficiency ( $\eta_{cycle}$ ) relative to the baseline (no CO<sub>2</sub> capture). As  $q_{Reb}$  decreases, increase in  $\eta_{cycle}$  associated with the post-combustion CO<sub>2</sub> capture decreases. For the state-of-the-art amines, thermal integration reduces increase in  $\eta_{cycle}$  by 1.82%-points (from 6.22 to 4.40%). For the  $q_{Reb}$  value, determined for the MEA in this study, thermal

integration reduces increase in  $\eta_{\text{cycle}}$  associated with post-combustion CO<sub>2</sub> capture by 2.00%-points (from 8.30 to 6.30%).

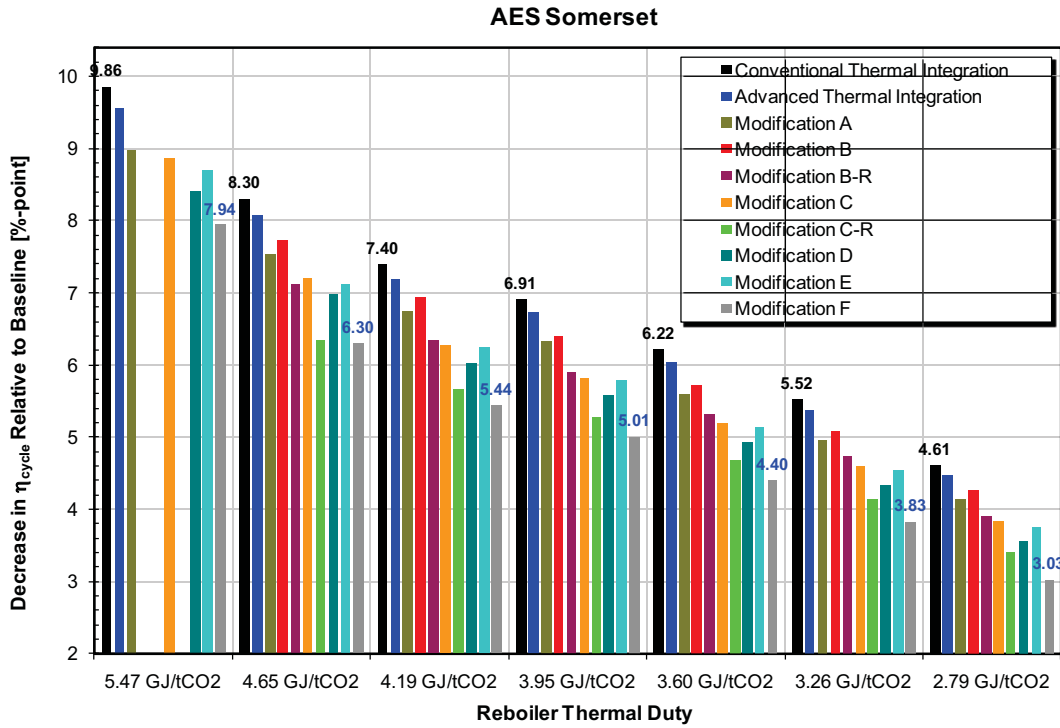


Figure C-5. Decrease in Turbine Cycle Efficiency Relative to Baseline (no CO<sub>2</sub> capture) vs.  $q_{\text{Reb}}$ .

Table C-5. Reduction in Turbine Cycle Heat Rate Relative to Baseline (no CO<sub>2</sub> capture) vs.  $q_{\text{Reb}}$ .

Reboiler Heat Duty		Conventional Integration	Advanced Integration	Modification B	Modification B	Modification B-R	Modification D	Modification D	Modification A	Modification C	Modification R	Modification E	Modification F	
		Decrease in Turbine Cycle Efficiency Relative to Baseline												
BTU/lb CO <sub>2</sub>	GJ/t CO <sub>2</sub>	% -point												
2,350	5.47	9.86	9.56	8.30	8.08	7.63	7.74	7.12	8.41	8.41	8.98	8.86	8.71	7.94
2,000	4.65	8.30	8.08	7.63	7.74	7.12	7.12	7.12	6.98	6.98	7.54	7.20	6.34	6.30
1,800	4.19	7.40	7.20	6.84	6.95	6.33	6.02	6.02	6.74	6.28	5.67	6.25	5.44	5.44
1,700	3.95	6.91	6.72	6.32	6.40	5.90	5.58	5.58	6.32	5.81	5.29	5.79	5.01	5.01
1,550	3.60	6.22	6.04	5.66	5.73	5.31	4.94	4.94	5.61	5.19	4.69	5.15	4.40	4.40
1,400	3.26	5.52	5.36	5.02	5.09	4.74	4.33	4.33	4.97	4.60	4.13	4.54	3.83	3.83
1,200	2.79	4.61	4.47	4.20	4.25	3.91	3.56	3.56	4.14	3.84	3.41	3.74	3.03	3.03
0	0.00	0.00	0.00	0.00	0.00	0.00	0.00	0.00	0.00	0.00	0.00	0.00	0.00	0.00

The percentage-point improvement in  $\eta_{\text{cycle}}$  relative to the conventional thermal integration is presented in Figure C-6 and Table C-6. The improvement in  $\eta_{\text{cycle}}$  relative to the conventional thermal integration is highest for Modifications F and C-R. For the state-of-the-art amines Modification F improves  $\eta_{\text{cycle}}$  relative to the conventional thermal integration by 1.82%-points. For the  $q_{\text{Reb}}$  value, determined for the MEA in this study and Modification F, improvement in  $\eta_{\text{cycle}}$  relative to the conventional thermal integration is 2.00%-points. These results are consistent with the results presented in Figure C-5.

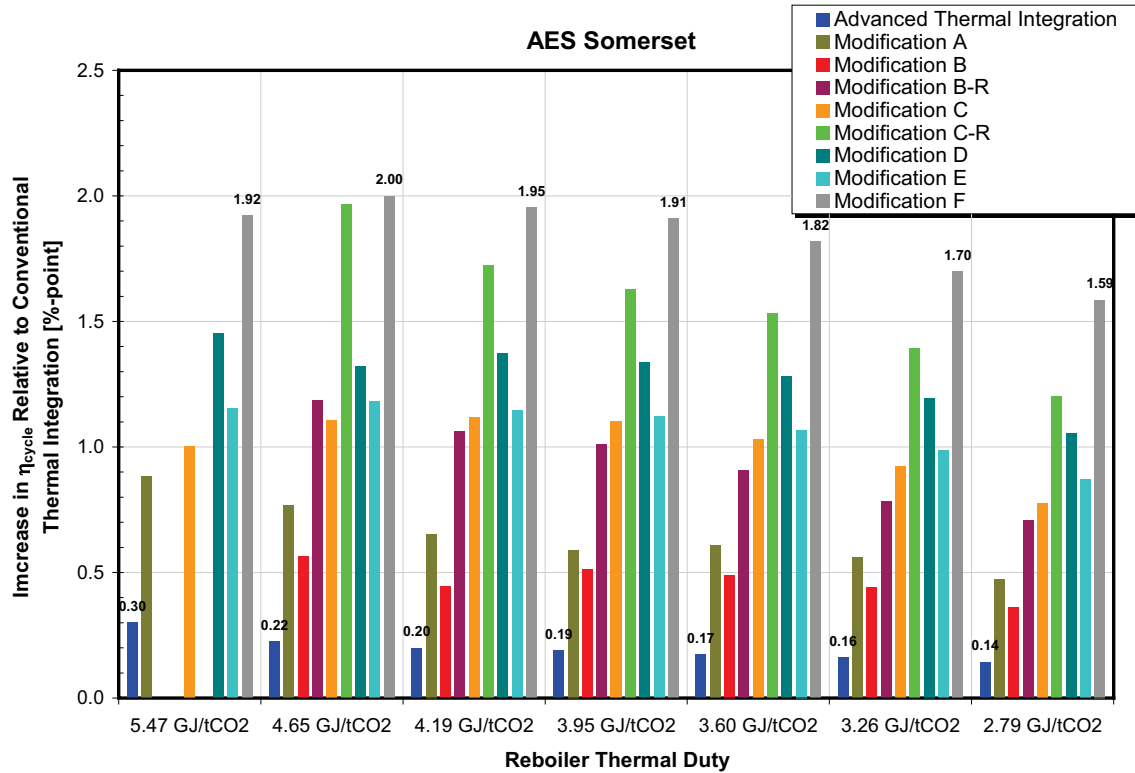
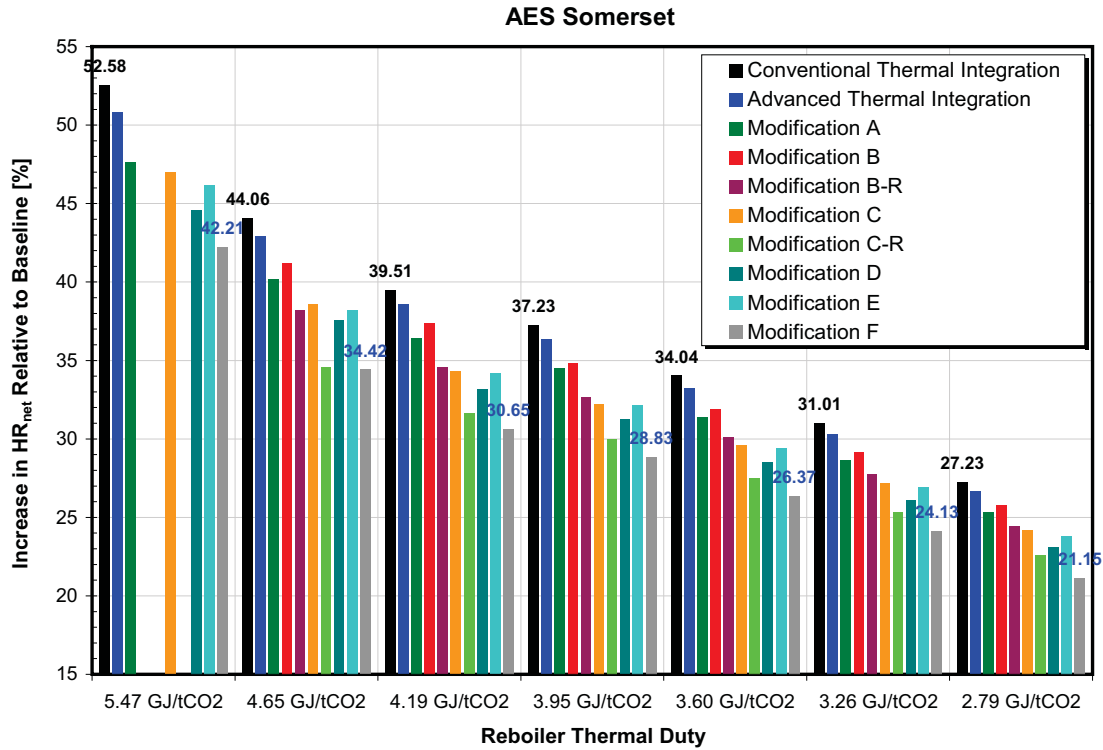


Figure C-6. Improvement in Turbine Cycle Efficiency Relative to Conventional Thermal Integration vs.  $q_{Reb}$ .

Table C-6. Improvement in Turbine Cycle Efficiency Relative to Conventional Thermal Integration vs.  $q_{Reb}$ .

Reboiler Heat Duty		Advanced Thermal Integration	Modification B	Modification B	Modification B-R	Modification D	Modification D	Modification A	Modification C	Modification C-R	Modification E	Modification F
Improvement in Turbine Cycle Efficiency Relative to Conventional Thermal Integration (Case 1)		% -point										
BTU/lb CO <sub>2</sub>	GJ/tCO <sub>2</sub>											
2,350	5.47	0.30				1.45	1.45	0.88	1.00		1.15	1.92
2,000	4.65	0.22	0.67	0.56	1.19	1.32	1.32	0.77	1.10	1.97	1.18	2.00
1,800	4.19	0.20	0.56	0.45	1.06	1.37	1.37	0.65	1.12	1.72	1.15	1.95
1,700	3.95	0.19	0.59	0.51	1.01	1.34	1.34	0.59	1.10	1.63	1.12	1.91
1,550	3.60	0.17	0.56	0.49	0.91	1.28	1.28	0.61	1.03	1.53	1.07	1.82
1,400	3.26	0.16	0.50	0.44	0.78	1.20	1.20	0.56	0.92	1.39	0.98	1.70
1,200	2.79	0.14	0.42	0.36	0.71	1.05	1.05	0.47	0.78	1.20	0.87	1.59
0	0.00	0.00	0.00	0.00	0.00	0.00	0.00	0.00	0.00	0.00	0.00	0.00

Figure C-7 and Table C-7 compare effect of thermal integration on net unit heat rate ( $HR_{net}$ ) relative to the baseline (no CO<sub>2</sub> capture). As  $q_{Reb}$  decreases, increase in  $HR_{net}$  associated with the post-combustion CO<sub>2</sub> capture decreases. For the state-of-the-art amines, thermal integration reduces increase in  $HR_{net}$  by 7.67%-point (from 34.04 to 26.37%). For the  $q_{Reb}$  value, determined for the MEA in this study, thermal integration reduces increase in  $HR_{net}$  associated with post-combustion CO<sub>2</sub> capture by 9.64%-point (from 44.06 to 34.42%).



**Figure C-7. Increase in Net Unit Heat Rate Relative to Baseline (no CO<sub>2</sub> capture) vs.  $q_{Reb}$ .**

**Table C-7. Increase in Net Unit Heat Rate Relative to Baseline (no CO<sub>2</sub> capture) vs.  $q_{Reb}$ .**

Reboiler Heat Duty		Conventional Integration	Advanced Integration	Modification B	Modification B	Modification B-R	Modification D	Modification D	Modification A	Modification C	Modification C-R	Modification E	Modification F
		Increase in Net Unit Heat Rate Relative to Baseline											
BTU/lb CO <sub>2</sub>	GJ/t CO <sub>2</sub>	%											
2,350	5.47	52.58	50.85				44.60	44.60	47.63	46.97		46.18	42.21
2,000	4.65	44.06	42.91	40.67	41.21	38.18	37.55	37.55	40.20	38.57	34.57	38.21	34.42
1,800	4.19	39.51	38.56	36.88	37.39	34.55	33.17	33.17	36.42	34.30	31.63	34.17	30.65
1,700	3.95	37.23	36.34	34.52	34.86	32.65	31.24	31.24	34.52	32.25	30.00	32.17	28.83
1,550	3.60	34.04	33.26	31.60	31.88	30.10	28.55	28.55	31.37	29.59	27.52	29.43	26.37
1,400	3.26	31.01	30.33	28.90	29.16	27.75	26.09	26.09	28.66	27.18	25.32	26.93	24.13
1,200	2.79	27.23	26.66	25.57	25.80	24.44	23.13	23.13	25.36	24.18	22.57	23.81	21.15
0	0.00	0.00	0.00	0.00	0.00	0.00	0.00	0.00	0.00	0.00	0.00	0.00	0.00

The improvement in  $HR_{net}$  relative to the conventional thermal integration is summarized in Figure C-8 and Table C-8. The improvement in  $HR_{net}$  relative to the conventional thermal integration is highest for Modifications F and C-R. For the state-of-the-art amines Modification F improves  $HR_{net}$  relative to the conventional thermal integration by 5.72%. For the  $q_{Reb}$  value, determined for the MEA in this study and Modification F, improvement in  $HR_{net}$  relative to the conventional thermal integration is 6.69%.

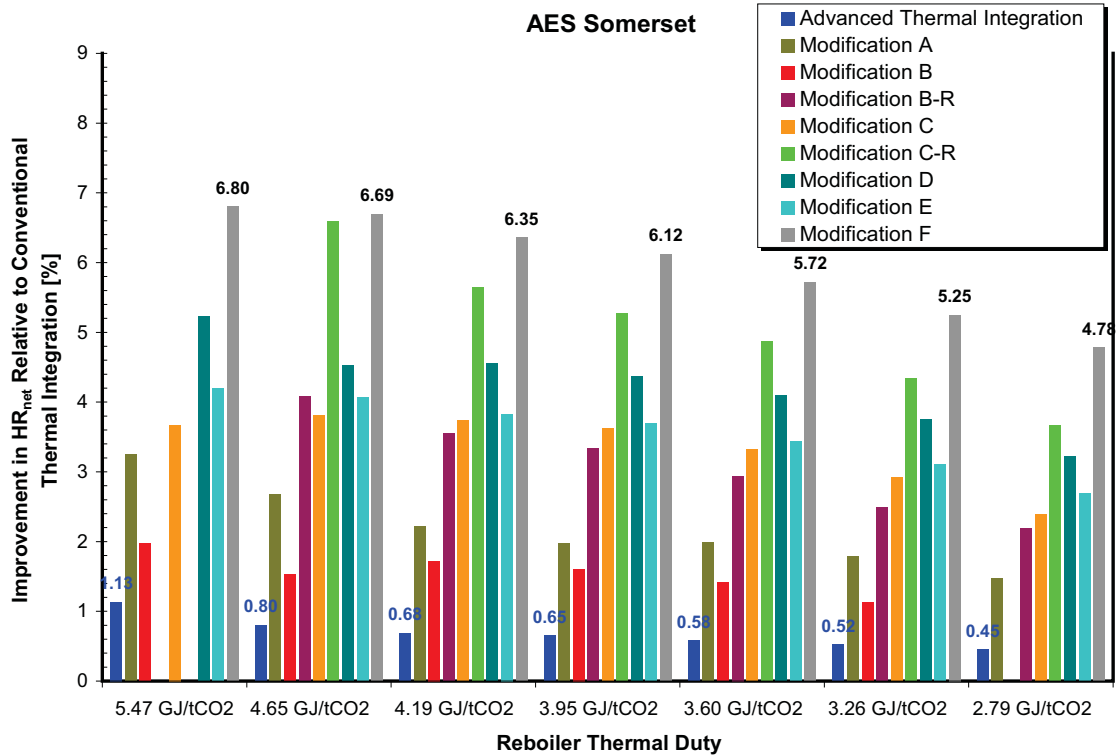
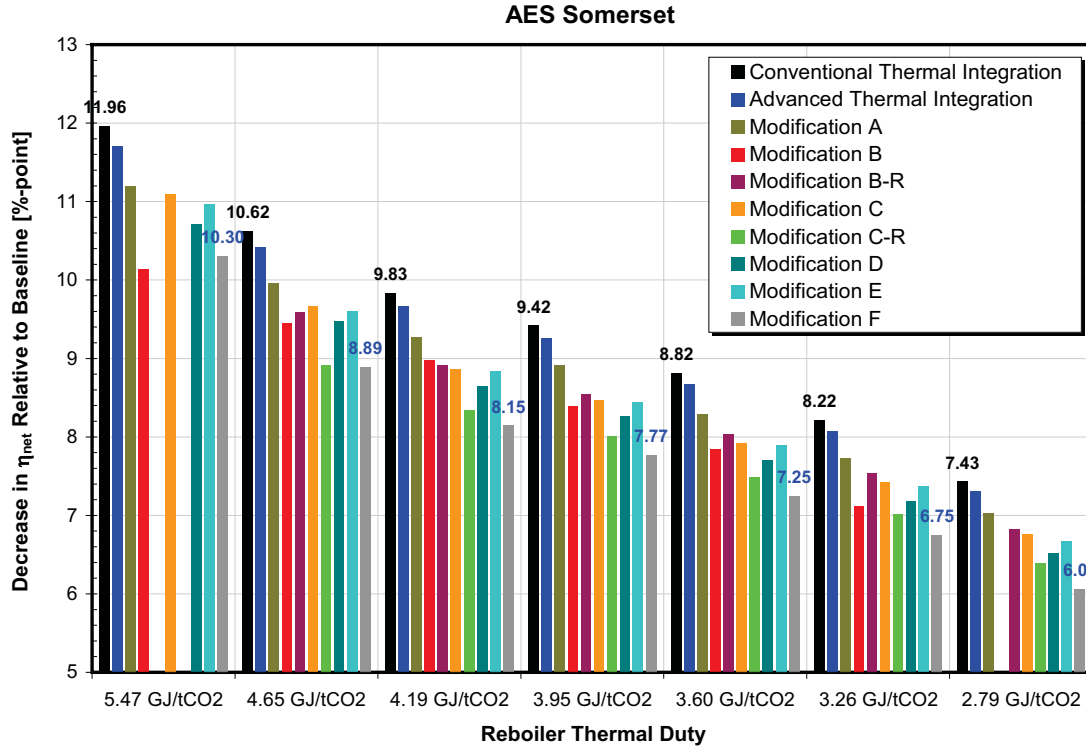


Figure C-8. Improvement in Net Unit Heat Rate Relative to Conventional Thermal Integration vs.  $q_{Reb}$ .

Table C-8. Improvement in Net Unit Heat Rate Relative to Conventional Thermal Integration vs.  $q_{Reb}$ .

Reboiler Heat Duty	Advanced Integration	Modification B	Modification B	Modification B-R	Modification D	Modification D	Modification A	Modification C	Modification C-R	Modification E	Modification F
	Improvement in Net Unit Heat Rate Relative to Conventional Thermal Integration										
BTU/lb CO <sub>2</sub> / GJ/t CO <sub>2</sub>	%										
2,350 / 5.47	1.13				5.23	5.23	3.25	3.67		4.20	6.80
2,000 / 4.65	0.80	2.36	1.98	4.08	4.52	4.52	2.68	3.81	6.59	4.06	6.69
1,800 / 4.19	0.68	1.89	1.52	3.56	4.55	4.55	2.22	3.74	5.65	3.83	6.35
1,700 / 3.95	0.65	1.98	1.72	3.33	4.36	4.36	1.97	3.63	5.26	3.69	6.12
1,550 / 3.60	0.58	1.82	1.61	2.94	4.09	4.09	1.99	3.32	4.86	3.44	5.72
1,400 / 3.26	0.52	1.61	1.41	2.48	3.75	3.75	1.79	2.92	4.34	3.11	5.25
1,200 / 2.79	0.45	1.31	1.12	2.19	3.22	3.22	1.47	2.39	3.66	2.68	4.78
0 / 0.00	0.00	0.00	0.00	0.00	0.00	0.00	0.00	0.00	0.00	0.00	0.00

Figure C-9 and Table C-9 compare effect of thermal integration on net unit efficiency relative to the baseline (no CO<sub>2</sub> capture). Similar to other performance parameters, the quantity  $q_{Reb}$  has a major effect on net unit efficiency; the penalty in  $\eta_{net}$  decreases as  $q_{Reb}$  is reduced. For the state-of-the-art amines Modification F reduces penalty in net unit efficiency relative to the baseline by 1.57%-points (from 8.82 to 7.25%-point). For the  $q_{Reb}$  value, determined for the MEA in this study, Modification F reduces penalty in net unit heat rate by 1.73%-points (from 10.62 to 8.89%-points) relative to the baseline.



**Figure C-9. Decrease in Net Unit Efficiency Relative to Baseline vs.  $q_{Reb}$ .**

**Table C-9. Decrease in Net Unit Efficiency Relative to Baseline vs.  $q_{Reb}$ .**

Reboiler Heat Duty		Conventional Integration	Advanced Integration	Modification B	Modification B	Modification B-R	Modification D	Modification D	Modification A	Modification C	Modification C-R	Modification E	Modification F
		Decrease in Net Unit Efficiency Relative to Baseline											
GJ/t CO <sub>2</sub>	BTU/lb CO <sub>2</sub>	% -point											
5.47	2,350	11.96	11.70				10.71	10.71	11.20	11.10		10.97	10.30
4.65	2,000	10.62	10.42	10.04	10.13	9.59	9.48	9.48	9.96	9.66	8.92	9.60	8.89
4.19	1,800	9.83	9.66	9.35	9.45	8.92	8.65	8.65	9.27	8.87	8.34	8.84	8.15
3.95	1,700	9.42	9.25	8.91	8.98	8.55	8.26	8.26	8.91	8.47	8.01	8.45	7.77
3.60	1,550	8.82	8.67	8.34	8.39	8.03	7.71	7.71	8.29	7.93	7.49	7.89	7.25
3.26	1,400	8.22	8.08	7.78	7.84	7.54	7.19	7.19	7.73	7.42	7.02	7.37	6.75
2.79	1,200	7.43	7.31	7.07	7.12	6.82	6.52	6.52	7.02	6.76	6.39	6.68	6.06
0.00	0	0.00	0.00	0.00	0.00	0.00	0.00	0.00	0.00	0.00	0.00	0.00	0.00

The percentage-point improvement in net unit efficiency relative to the conventional thermal integration is summarized in Figure C-10 and Table C-10. The improvement relative to the conventional thermal integration is highest for Modifications F and C-R. Consistent with the results presented in Figure C-9, for the state-of-the-art amines Modification F improves net unit efficiency relative to the conventional thermal integration by 1.57%-points. For the  $q_{Reb}$  value, determined for the MEA in this study and Modification F, improvement in net unit efficiency relative to the conventional thermal integration is 1.73%-points.

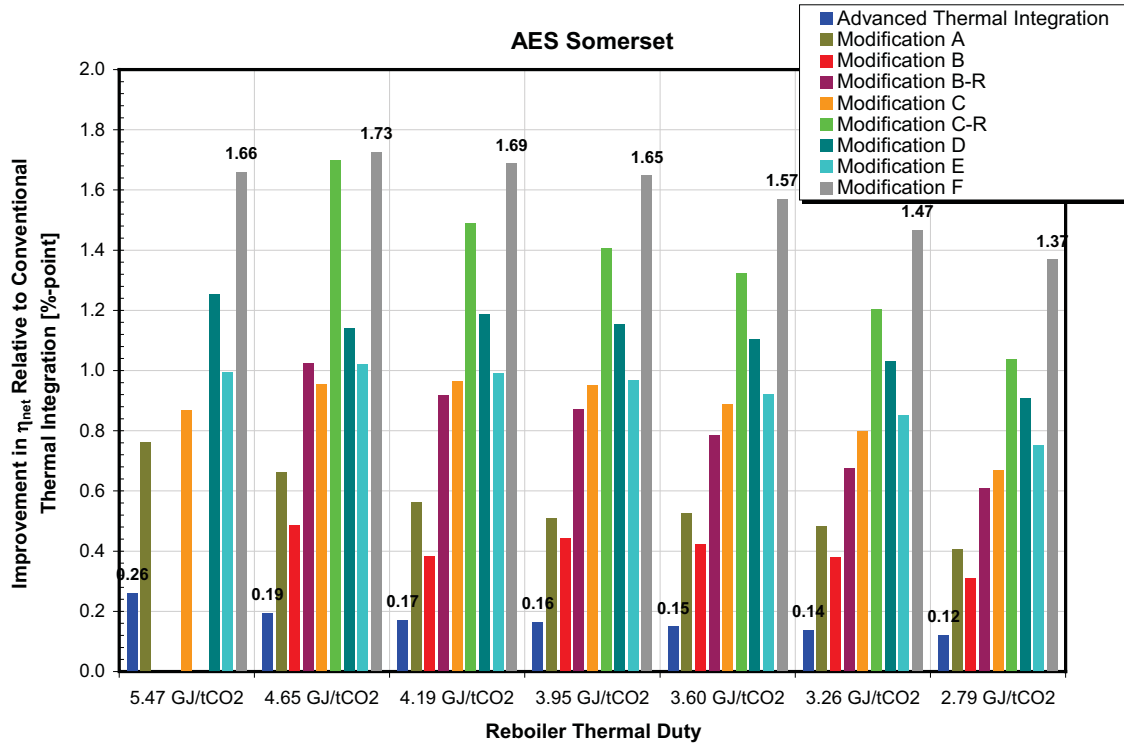


Figure C-10.Improvement in Net Unit Efficiency Relative to Conventional Thermal Integration vs.  $q_{Reb}$ .

Table C-10.Improvement in Net Unit Efficiency Relative to Conventional Thermal Integration vs.  $q_{Reb}$ .

Reboiler Heat Duty		Advanced Integration	Modification B	Modification B	Modification B-R	Modification D	Modification D	Modification A	Modification C	Modification C-R	Modification E	Modification F
		Improvement in Net Unit Efficiency Relative to Conventional Thermal Integration (Case 1)										
GJ/tCO <sub>2</sub>	BTU/lb CO <sub>2</sub>	% -point										
5.47	2,350	0.26				1.26	1.26	0.76	0.87		1.00	1.66
4.65	2,000	0.19	0.58	0.49	1.03	1.14	1.14	0.66	0.95	1.70	1.02	1.73
4.19	1,800	0.17	0.48	0.39	0.92	1.19	1.19	0.56	0.97	1.49	0.99	1.69
3.95	1,700	0.16	0.51	0.44	0.87	1.15	1.15	0.51	0.95	1.41	0.97	1.65
3.60	1,550	0.15	0.48	0.42	0.78	1.11	1.11	0.53	0.89	1.32	0.92	1.57
3.26	1,400	0.14	0.43	0.38	0.68	1.03	1.03	0.48	0.80	1.20	0.85	1.47
2.79	1,200	0.12	0.36	0.31	0.61	0.91	0.91	0.41	0.67	1.04	0.75	1.37
0.00	0	0.00	0.00	0.00	0.00	0.00	0.00	0.00	0.00	0.00	0.00	0.00

NYSERDA, a public benefit corporation, offers objective information and analysis, innovative programs, technical expertise and funding to help New Yorkers increase energy efficiency, save money, use renewable energy, and reduce their reliance on fossil fuels. NYSERDA professionals work to protect our environment and create clean-energy jobs. NYSERDA has been developing partnerships to advance innovative energy solutions in New York since 1975.

*To learn more about NYSERDA programs and funding opportunities visit [nyserda.ny.gov](http://nyserda.ny.gov)*

**New York State  
Energy Research and  
Development Authority**

17 Columbia Circle  
Albany, New York 12203-6399

**toll free:** 1 (866) NYSERDA  
**local:** (518) 862-1090  
**fax:** (518) 862-1091

[info@nyserda.ny.gov](mailto:info@nyserda.ny.gov)  
[nyserda.ny.gov](http://nyserda.ny.gov)



State of New York  
Andrew M. Cuomo, Governor

# Use of Waste and CO<sub>2</sub> Compression Heat to Reduce Penalty Due to Post-Combustion CO<sub>2</sub> Capture

Final Report No. 12-11  
March 2012

New York State Energy Research and Development Authority  
Francis J. Murray, Jr., President and CEO